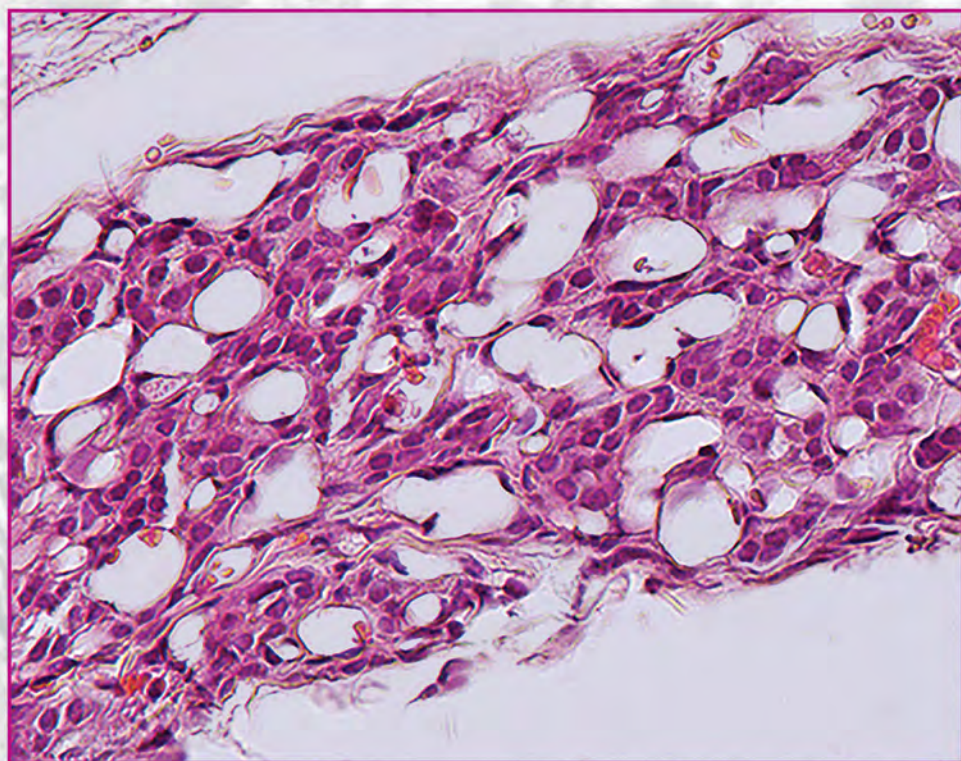


Acta Morphologica et Anthropologica **29** (3–4)



**Prof. Marin Drinov Publishing House
of Bulgarian Academy of Sciences**

Acta Morphologica et Anthropologica

is the continuation of Acta cytobiologica et morphologica

Indexed in:



WEB OF SCIENCE



Editorial Correspondence

Institute of Experimental Morphology, Pathology and Anthropology with Museum
Bulgarian Academy of Sciences
Acta Morphologica et Anthropologica
Acad. Georgi Bonchev Str., Bl. 25
1113 Sofia, Bulgaria

E-mail: ygluhcheva@hotmail.com, iempam@bas.bg
Tel.: +359 2 979 2344

Издаването на настоящия том 29, книжки 3 и 4 е осъществено с финансовата подкрепа на Фонд „Научни изследвания“

©БАН, Bulgarian Academy of Sciences, Institute of Experimental Morphology, Pathology and Anthropology with Museum, 2022

Prof. Marin Drinov Publishing House of Bulgarian Academy of Sciences
Bulgaria, 1113 Sofia, Acad. Georgi Bonchev Str., Bl. 6

Graphic designer .Veronika Tomcheva.

Format 70×100/16 Printed sheets 12,75

Printing Office of Prof. Marin Drinov Publishing House of Bulgarian Academy of Sciences
Bulgaria, 1113 Sofia, Acad. Georgi Bonchev Str., Bl. 5

Acta Morphologica et Anthropologica

Editorial Board

Editor-in-Chief: Prof. Nina Atanassova (Institute of Experimental Morphology, Pathology and Anthropology with Museum, Bulgarian Academy of Sciences, Sofia, Bulgaria)

e-mail: ninaatanassova@bas.bg; ninaatanassova@yahoo.com

+359 2 979 2342

Deputy Editor-in-Chief: Prof. Dimitar Kadiysky (Institute of Experimental Morphology, Pathology and Anthropology with Museum, Bulgarian Academy of Sciences, Sofia, Bulgaria)

e-mail: dimkad@bas.bg; dkadiysky@yahoo.com

+359 2 979 2340

Managing Editor: Assoc. Prof. Yordanka Gluhcheva (Institute of Experimental Morphology, Pathology and Anthropology with Museum, Bulgarian Academy of Sciences, Sofia, Bulgaria)

e-mail: ygluhcheva@hotmail.com

+359 2 979 2344

Web Management: Assoc. Prof. Ivelin Vladov (Institute of Experimental Morphology, Pathology and Anthropology with Museum, Bulgarian Academy of Sciences, Sofia, Bulgaria)

e-mail: iepparazit@yahoo.com

+359 2 979 2326

Members

Prof. Doychin Angelov (Center of Anatomy, University of Cologne, Germany)

Prof. Radostina Alexandrova (Institute of Experimental Morphology, Pathology and Anthropology with Museum, Bulgarian Academy of Sciences, Sofia, Bulgaria)

Prof. Osama Azmy (National Research Centre, Cairo, Egypt)

Prof. Barbara Bilinska (Jagiellonian University, Krakow, Poland)

Prof. Alexandra Buzhilova (Research Institute and Museum of Anthropology, Moscow State University, Russia)

Assoc. Prof. Alexandra Comsa („Vasile Pârvan” Institute of Archaeology, Romanian Academy, Bucharest, Romania)

Assoc. Prof. Natasha Davceva (Institute of Forensic Medicine and Criminalistics, Ss. Cyril and Methodius University, Scopje, North Macedonia)

Prof. Michail Davidoff (University Medical Center Clinic Hamburg-Eppendorf, Medical History Museum, Hamburg, Germany)

Prof. Valentin Djonov (Institute of Anatomy, University of Bern, Switzerland)

Prof. Mashenka Dimitrova ((Institute of Experimental Morphology, Pathology and Anthropology with Museum, Bulgarian Academy of Sciences, Sofia, Bulgaria)

Prof. Milena Fini (Rizzoli Orthopedic Institute, Bologna, Italy)

Prof. Mary Gantcheva ((Institute of Experimental Morphology, Pathology and Anthropology with Museum, Bulgarian Academy of Sciences, Sofia, Bulgaria)

Prof. Volodia Georgiev (Department of Biology, Manhattanville College, New York, USA)

Prof. Elena Godina (Research Institute and Museum of Anthropology, Moscow State University, Russia)

Assoc. Prof. Manana Kakabadze („Alexandre Natishvili“ Institute of Morphology, Tbilisi State University, Georgia)

Acad. Vladimir Kolchitsky (Institute of Physiology, National Academy of Sciences, Minsk, Belarus)

Prof. Dimitri Kordzaia („Ivane Javakhishvili“ Tbilisi State University, Georgia)

Prof. Nikolai Lazarov (Medical University Sofia, Bulgaria)

Prof. Tsvetanka Marinova (Faculty of Medicine, Sofia University “St. Kliment Ohridski”, Bulgaria)

Prof. Ralf Middendorff (Institute of Anatomy and Cell Biology, Justus Liebig University, Gießen, Germany)

Prof. Modra Murovska (Institute of Microbiology and Virology, Riga Stradins University, Latvia)

Acad. Wladimir Ovtscharoff (Medical University Sofia, Bulgaria)

Prof. Svetlozara Petkova ((Institute of Experimental Morphology, Pathology and Anthropology with Museum, Bulgarian Academy of Sciences, Sofia, Bulgaria)

Assoc. Prof. Marina Quartu (University of Cagliari, Monserrato, Italy)

Prof. Gorana Rancic (School of Medicine, University of Niš, Serbia)

Prof. Stefan Sivkov (Medical University Plovdiv, Bulgaria)

Assoc. Prof. Racho Stoev ((Institute of Experimental Morphology, Pathology and Anthropology with Museum, Bulgarian Academy of Sciences, Sofia, Bulgaria)

Assoc. Prof. Katja Teerds (Wageningen University, Netherlands)

Prof. Angel Vodenicharov (Faculty of Veterinary Medicine, Trakia University, Stara Zagora, Bulgaria)

C o n t e n t s

MORPHOLOGY 29 (3)

Editorial

- N. Atanassova** – 8th National Conference with International Participation
“Morphological Days”, 10-12 June, 2022 7

Original Articles

- N. Manchorova, M. Guenova, D. Keskinova** – Regulation of Apoptosis in Odontoblasts
in Ageing Dental Pulp by NFkB and JAK1-STAT3 Signaling Pathway. 11
- D. Molander, Y. Sbirkov, I. Bodurov, D. Dikov, V. Sarafian** – Comparative Analysis of
Bioinks in 3D Bioprinted Organoids of Colorectal Cancer. 17
- R. Ivanov, R. Pankov** – Exploring Senescence Reversal Potential of Antioxidants in
Human Foreskin Fibroblasts. 22
- M. Dimitrova, K. Todorova, I. Iliev, I. Sulikovska, L. Kirazov, I. Ivanov** – Effects of
Geranium sanguineum Ethanol Extract After i.p. Application in a Mouse Model of
Ehrlich’s Breast Cancer. 29
- K. A. Iteire, F. U. Enemali, E. I. Odokuma** – Neuroprotective Role of Caffeic Acid in
Lipopolysaccharide-Induced Neurodegeneration in Mice 33
- F. Gerginska, S. Delchev, V. Vasilev, K. Georgieva, N. Boyadjiev** – The Selective
Androgen Receptor Modulator Ostarine Increases the Extracellular Matrix in the
Myocardium without Altering it in the EDL Muscle. 44

D. Krushovlieva, S. Georgiev, P. Ivanova, Z. Petkova, T. Stoyanova, J. Tchekalarova – Age-Dependent Differences in Behavioral Responses: the Impact of Hsp70 and Hsp90 in the Frontal Cortex	49
M. Markova, A. Kolarov, I. Chakarova, V. Hadzhinesheva, R. Zhivkova, S. Delimitreva, M. Mourdjeva, V. Nikolova – Preliminary Observations on Apoptotic Fragmentation of Cultured Mouse Oocytes	53
V. Broshtilova, T. Vuteva, V. Kantardjiev, M. Gantcheva – Interstitial Granulomatous Dermatitis Associated with Systemic Lupus Erythematosus	57

Review Articles

N. Lazarov, D. Atanasova – The Human Carotid Body and its Role in Ventilatory Acclimatization to Hypoxia.	63
S. Delimitreva – The Odd Behavior of the Nuclei in Maturing Mammalian Oocytes and Zygotes.	69

ANTHROPOLOGY AND ANATOMY 29 (4)

Original Articles

S. A. Tineshev, A. G. Baltadjiev – Somatotype Characteristics of Bulgarian Children from the Region of the Eastern Rhodope Mountains.	73
L. Manoilova, V. Russeva – Results from the Anthropological Investigation of the Material from Tomb from Antique Apolonia Pontica.	83
N. Atanasova, L. Ovnarska – Anthropological Data about the Buried in a Christian Necropolis (from the Ottoman Period), Situated near the Town of Dimovo, Vidin District, Northwestern Bulgaria.	88
V. Russeva, Y. Meshekov, I. Borissova, V. Panchev – Defects on Cranial Bones from Tomb №1, Sofia, Janko Sakazov Str.	93
M. R. Schneider, D. Stoyanov, M. Angelova, D. Marinova, V. Mihaleva – Multi-Tendon M. Abductor Pollicis Longus and its Clinical Significance.	99
G. Aytac, S. Tunali – Virtual Reality in Anatomy Instruction: a Preliminary Study.	103
D. Marinova, M. Angelova, V. Zhekova – M. sternalis: a Case Report and Literature Review.	109

Review Articles

A. Comşa – Some Dental Problems of the Romanian Bronze Age.	115
E. Georgieva, R. Stoyanova, V. Yancheva, I. Velcheva, S. Petrova, S. Stoyanova, S. Tomov – A Review on Impaired Sperm Quality and Overweight/Obesity: Basic Mechanisms.	120
In Memoriam – Professor Yordan Yordanov, Corresponding Member of the Bulgarian Academy of Sciences.	129

**SUPPLEMENT – PROCEEDINGS OF THE 8TH NATIONAL
CONFERENCE WITH INTERNATIONAL PARTICIPATION
“MORPHOLOGICAL DAYS”**

S. Zapryanova, E. Pavlova, N. Atanassova – Impact of Diabetes Mellitus Induced in Early Postnatal Life on Bax Protein Expression in Rat Testes.	133
D. Barbutska, A. Petrova, Y. Koeva, K. Georgieva, J. Tchekalarova, G. Nanov – Testicular Steroidogenesis after Pinealectomy: The Role of BDNF Signaling System.	137
E. Hristova, N. Petrova, P. Todorov – Cryopreservation of Gametes, Embryos and Ovarian Tissue as a Method for Fertility Preservation in Oncological Patients.	141
A. Kolarov, I. Chakarova, V. Hadzhinesheva, V. Nikolova, S. Delimitreva, M. Markova, R. Zhivkova – Oocyte Morphology in a Mouse Model of Collagenase-Induced Osteoarthritis.	146
M. Gantcheva – Extragenital Lichen Sclerosis et Atrophicus.	151
A. Vodenicharov, I. Stefanov, N. Tsandev, G. Kostadinov – Mast Cells Distribution in the Domestic Swine Urinary Bladder’s Wall.	157
G. Nenkova, G. Yaneva, T. Dimitrova, E. Kovachev, S. Anzhel, D. Ivanov – Quality of Intact and Artificially Collapsed Human Blastocysts after Vitrification.	161
B. Blagova, D. Krastev, L. Malinova – Thermal Changes in Human Bone Following Osteotomy by Three Different Devices – a Histological Analysis Using Different Staining Protocols.	165
V. Kolyovska, D. Drenska, D. Maslarov – Can Serum IgG Antiganglioside Antibodies to GM1, GM3 and GD1a be Used as Markers in Patients with Ischemic Stroke?.	170
V. Nanev, I. Vladov, E. Dencheva, M. Gabrashanska, A. Katsarov – Profile of Manganese Accumulation in the Host-Parasite (<i>Rattus norvegicus</i> - <i>Fasciola hepatica</i>) System after Manganese Treatment.	174
S. Naudi, R. Raimets, M. Jürison, E. S. Liiskmann, M. Mänd, D. Salkova, R. Karise – Effect of <i>Nosema apis</i> and <i>N. ceranae</i> on Honey Bee <i>Apis mellifera</i> Queen Development.	178
R. Stoev, Z. Mitova – Age at Menarche in Sofia Girls /2014-2018/.	183
V. Iliev, L. Malinova, L. Jelev – Avariation of the Third Common Palmar Digital Artery.	188
A. Gradev, N. Vulova, L. Jelev, L. Malinova – A Rare Variation of the Digastric Muscle Anterior Belly Related to False Submandibular Triangle.	191
M. Kanarev, N. Petrova, A. Petrova, S. Sivkov – Functional Aspects of the Human Claustrium.	195

MORPHOLOGY 29 (1)

Editorial

VIII National Conference with International Participation “Morphological Days”, Sofia, 10-12 of June, 2022

*Nina Atanassova**

Institute of Experimental Morphology, Pathology and Anthropology with Museum, Bulgarian Academy of Sciences, Sofia, Bulgaria

*Corresponding author e-mail: ninaatanassova@yahoo.com

The traditional 8th National Conference with International Participation “Morphological Days” was held on 10th – 12th of June, 2022 in Sofia. The organizer of this event was the Institute of Experimental Morphology, Pathology and Anthropology with Museum at the Bulgarian Academy of Sciences. Co-organizer was Bulgarian Anatomical Society. The venue of the Conference was the National Anthropological Museum of the Institute.

The opening of the conference started by welcome addresses from Professor Svetlozara Petkova – Director of the Institute, Professor Nina Atanassova – President of the Organizing Committee and Professor Nikolai Lazarov – President of the Bulgarian Anatomical Society.

The main topics of the conference included all the fields of anatomy, cell biology, histology, embryology, pathology and anthropology. The conference was attended by more than 150 participants of which 46 young scientists and 13 students – from USA, Switzerland, Netherlands, Germany, Latvia, Estonia, Romania, Slovenia, North Macedonia, Turkey, Egypt and Bulgaria. In national aspect, the meeting integrated scientists from biomedical institutes of the Bulgarian Academy of Sciences, Sofia University “St Kliment Ohridski”, Plovdiv University

“Paisii Hilendarski”, Southwestern University “Neofit Rilski” – Blagoevgrad, Bourgas University “Prof. Asen Zlatarov”; scientists and lecturers from all Medical Universities – in Sofia, Plovdiv, Varna, Pleven, Trakia University in Stara Zagora, University of Forestry – Faculty of Veterinary Medicine, as well as clinical specialists from University Hospitals.

The conference was organized in 14 scientific sessions with 133 presentations, as follow: 7 plenary sessions with 17 lectures, 5 sessions for oral presentations with 34 talks and 2 poster session presentations with 82 posters. Plenary lectures were given by Prof. Valentin Djonov from the University of Bern in Switzerland, Prof. Katja Teerds from Wageningen University in Netherlands, Prof. Modra Murovska from Riga Stradins University, Latvia, Prof. Osama Azmy from the National Research Centre in Cairo, Egypt, Prof. Volodia Georgiev from New York Manhattanville College, USA, Prof. Crtomir Podlipnic from the University of Ljubljana, Slovenia, Assoc. Prof. Natasha Davcheva from the University “Sv. Kiril i Metodij” Skopje, Alexandra Comsa from the Institute of Archaeology, Romanian Academy of Sciences, Bucharest, Romania.

During the conference, a meeting of the Bulgarian Anatomical Society was held, opened with a lecture by Professor Nina Atanassova in memoriam to Professor Yordan Yordanov – former Director of the Institute and the founder of the National Anthropological Museum and one of the founders of the “Morphological Days” Conference.

Compared to the previous 7th National Conference “Morphological Days” in 2018, the number of participants in the current 8th Conference was higher, which indicated that the morphological community/society in Bulgaria has increased.

The conference was distinguished by a high level of presented scientific results. It is evident that morphological science has spread beyond the classical macroscopic and microscopic morphology by developing multidisciplinary and interdisciplinary research with molecular and cellular biology, chemistry, computer sciences and modelling, archaeology and national identity. The presentations showed the modern trends in the development of morphological science and its application in medicine for more precise diagnosis and treatment of socially significant diseases.

At the end of the scientific forum, Prof. Nikolai Lazarov announced two awards of the Bulgarian Anatomical Society – for the best oral presentation and the best poster presentation. Two oral presentations were awarded – by Dr. Toma Spiriev (Faculty of Medicine of Sofia University “Kliment Ohridski”) and co-authors and by Prof. Neshka Manchorova (Medical University-Plovdiv). Two poster presentations were awarded – by Assistant Professor Kristina Malinova (Institute of Molecular Biology “Academician Rumen Tsanev”) and co-authors and by Assistant Professor Dimo Stoyanov (Medical University-Varna) and co-authors.

The conference was funded by the National Scientific Fund of the Ministry of Education and Science in Bulgaria (Grant КП06-МНФ/22). Sponsorship was provided by the Bulgarian Anatomical Society, FOT Ltd, SAVIMED and Microoptica Ltd.

The venue of the conference – The National Anthropological Museum provided nice and lovely atmosphere around the museum expositions and anthropological reconstructions of the head of great Bulgarians as Tzar Kaloyan, Tzar Samuil, Thracian Princess, Georgi Rakovski, Luben Karavelov, Zahari Stoyanov, Bacho

Kiro created by Prof. Yordan Yordanov. All the participants enjoyed the meeting and later the Organizing Committee received letters of acknowledgements and high recognition by the participants.



Original Articles

Regulation of Apoptosis in Odontoblasts in Ageing Dental Pulp by NFkB and JAK1-STAT3 signaling pathway

Neshka Manchorova^{1*}, Margarita Guenova², Donka Keskinova³

¹ Department of Operative Dentistry and Endodontics, Faculty of Dental Medicine, Medical University – Plovdiv, Bulgaria

² Laboratory of Haematopathology and Immunology, National Specialized Hospital for Haematological Diseases, Sofia, Bulgaria

³ Applied and Institutional Sociology, University of Plovdiv “Paisii Hilendarski”, Faculty of Philosophy and History, Plovdiv, Bulgaria.

*Corresponding author e-mail: Neshka.Manchorova@mu-plovdiv.bg

The aim of the study was to examine and compare the immunohistochemical distribution of NFkB, JAK1 and STAT3 in human odontoblastic cells depending on age, gender, tooth type, and cell topography. Ninety intact teeth of healthy individuals were enrolled in the study and arranged in three groups (n=30) regarding the patients' age. Immunohistochemistry of paraffin-embedded sections was performed using mouse monoclonal antibody NFkB p65, JAK1, and STAT3. Statistical analysis were applied ($p<0.05$) by IBM SPSS Statistics 25. In aged dental pulp, odontoblasts expressed statistically significant more NFkB ($p<0.05$). A greater expression of JAK1 and STAT3 was shown in cells ageing ($p<0.05$). The signaling pathway JAK1-STAT3 was significantly immunopositive in women, frontal teeth and root pulp ($p<0.05$). In conclusion, the activity of signaling pathway JAK1-STAT3 in dental pulp in ageing presented a direct pathway of regulation of apoptosis, however NFkB maintained the inhibitory threshold.

Key words: ageing, dental pulp, apoptosis, regulation

Introduction

The JAK-STAT signal pathway provides a fast, direct flow of information to the cell nucleus. The JAK-STAT pathway operates in the cell not only through cytokine receptors such as IL-6, but also uses other alternative receptors such as GPCRs, Toll-receptors (TLRs) and microRNA, especially in carcinogenesis [6]. Growth hormone can activate the signaling pathway JAK-STAT and the result brings a new course to its

functionality and plays an important role in ageing and carcinogenesis. Many of the signals associated with stress (oxidative, radiation, etc.), inflammation and congenital immune response work through the NF κ B-dependent signaling pathway. Odontoblastic cells of the dental pulp express Toll receptors, receptors for TNF α , IL1 and other that belonged to superfamily of cytokine receptors. Pulpal odontoblast cells have a different set of adaptor proteins inside the cell, which are associated with different signaling pathways for activation of NF κ B and JAK-STAT signaling pathway [7]. Transcription factor NF κ B sets the inhibitory threshold in pulp odontoblasts, the effect of which it realizes anti-apoptotic effects and protects cellular life. Our available specialized literature lacks studies related to the roles of NF κ B, JAK1-STAT3 in pulp odontoblasts. There are no data on the influence of ageing on the activity of NF κ B, JAK1-STAT3 in human pulp cell lines, as well as in isolated human cells from bone or dental pulp. A full understanding of the gender-dependant activity of NF κ B, JAK1-STAT3 signaling path remains unclear, and cells topography as well. The aim of the study is to examine and compare the immunohistochemical distribution of NF κ B, JAK1 and STAT3 in human odontoblastic cells depending on the age, gender, tooth type and cell topography.

Material and Methods

Ninety intact teeth of healthy individuals were enrolled in the study and arranged in three groups (n=30) regarding the patients' age: dental germs with young pulp and dentin up to 17 years old patients, mature pulp and dentin up to 40 years old patients, and adult pulp and dentin over 41 years old patients. All teeth were freshly extracted by dental indications and the study was approved by Ethical Committee of Medical University of Plovdiv (protocol 1/13.02.2020). Immediately after extraction the molars were fixed overnight in 10% buffered paraformaldehyde. The specimens were reduced in size by trimming the enamel, superficial coronal dentin and the roots up to 2 mm below the Cemento-enamel junction (CEJ). The coronal dentin-pulp specimens were decalcified in a 3% hydrochloric acid (HCl) for 6 hours and dehydrated using graded ethanol and acetone, embedded in paraffin, serially sectioned, and stained with hematoxylin and eosin. For immunohistochemistry, paraffin sections were dewaxed in xylene, rehydrated with distilled water, and then subjected to antigen retrieval (sodium citrate buffer, pH 6.0) and incubated with mouse monoclonal antibodies NF κ B p65 (F-6), JAK1 (A-9), and STAT3 (F-2) (Santa Cruz Biotechnology Inc., USA). The microscopic observation of immunolabeling was done in the peripheral odontoblastic layer and in the subodontoblastic zone including 0-immunonegative, 1-weak immunopositive, 2-strong immunopositive reactions. Statistical analysis including Kruskal-Wallis and Mann-Whitney tests was performed ($p < 0.05$).

Results

The expression of the biomarkers studied is presented in **Figure 1**.

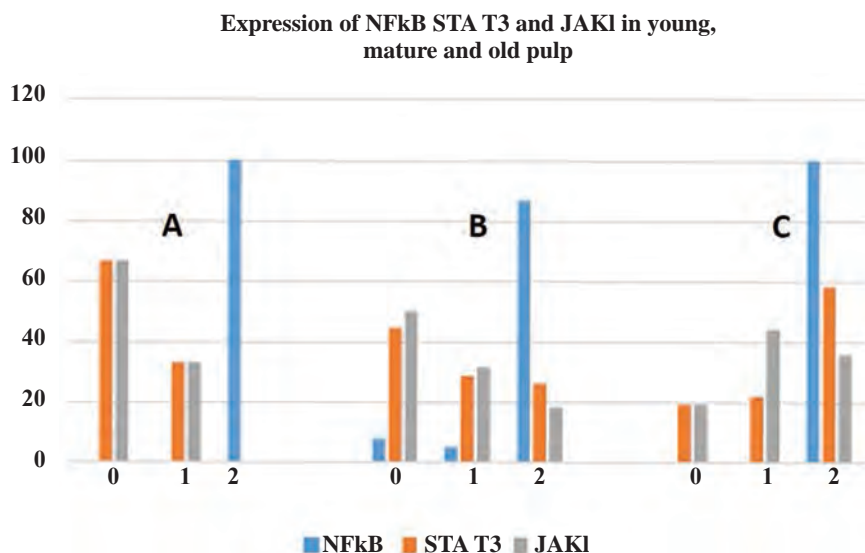


Fig. 1. Expression of biomarkers in odontoblasts in young (A), matured (B) and adult (C) pulp (0-immunonegative, 1-weak immunopositive, 2-strong immunopositive).

Age-dependant changes

The results for the expression of biomarkers in pulp odontoblasts from the three age groups studied are illustrated in **Figs. 2-4**.

The analysis of the results obtained for the expression of NFκB from odontoblasts in different ages showed that the marker was positive in all the samples studied. Only in cuts of mature pulp there was NFκB-immunonegative odontoblasts. The expression of JAK1 and STAT3 showed dynamics. The young pulp of dental germs (**Fig. 2**) was statistically significant immunonegative for STAT3 compared to an old pulp ($p < 0.05$). A similar pattern was observed in the expression of JAK1.

Samples of young and mature pulp showed a negative immune reaction for the STAT3 with statistical significance ($p < 0.05$) comparing to old odontoblastic cells. Our results showed that cell ageing of pulp odontoblasts increased the expression of JAK1 and STAT3, and the signaling path for the initiation of apoptosis was characterized by age-dependant activity (**Fig. 3** and **Fig. 4**).

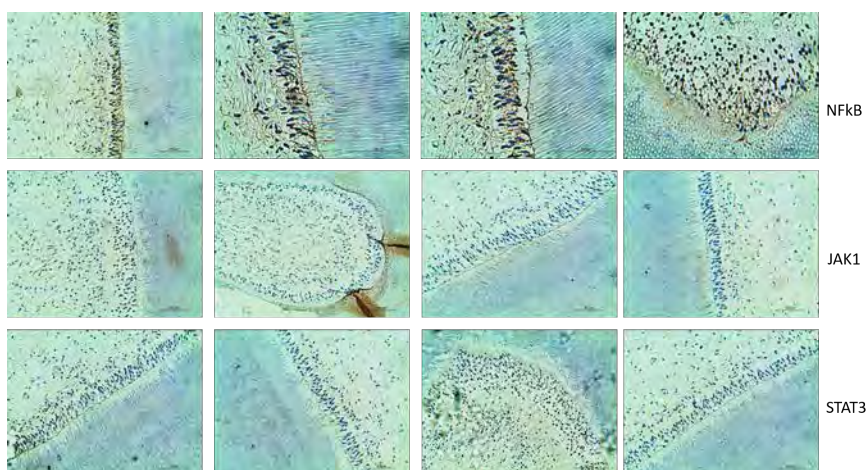


Fig. 2. Expression of NFκB, JAK1 and STAT3 from young pulp odontoblasts. Immunopositive marking for NFκB was observed in the area of the pulp horn of the young pulp tissue of dental germ 38 of a 16-year-old patient. Immune reactions for JAK1 and STAT3 were negative.

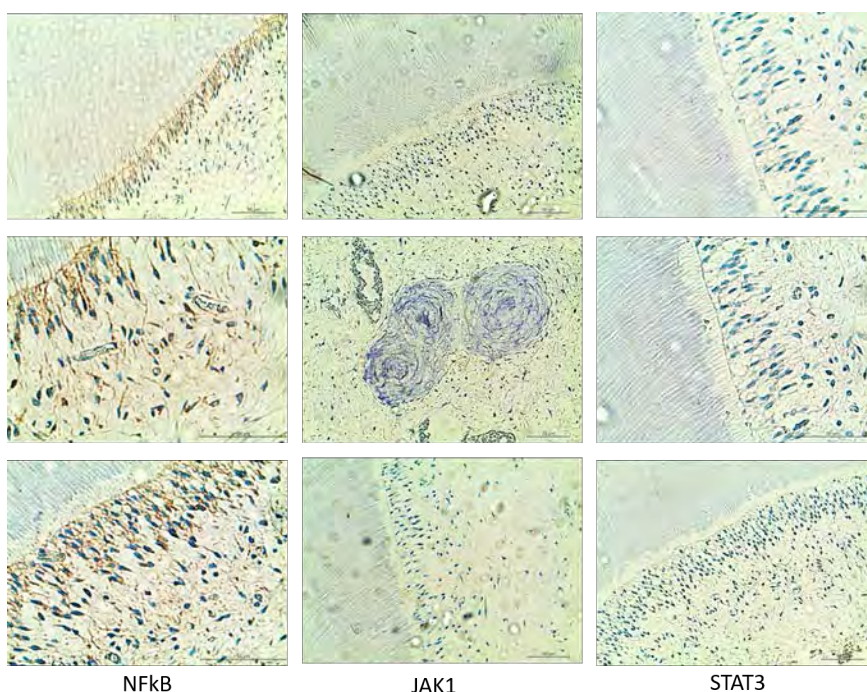


Fig. 3. Expression of NFκB, JAK1 and STAT3 from mature pulp odontoblasts in the proximal part of the pulp chamber of mature pulp tissue of a sample tooth 18 of a 20-year-old patient. Immunolabeling for NFκB was positive. Freely spaced denticle in the pulp chamber was visualized, which was immunonegative for all the markers studied. Odontoblastic cells did not express JAK1 and STAT3, objectified by the immunonegative finding.

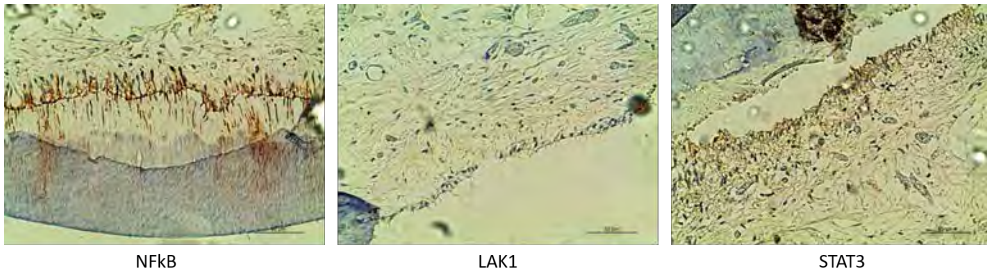


Fig. 4. Expression of NFκB, JAK1 and STAT3 from adult pulp odontoblasts of tooth 22 to 57 year-old patient. Immunopositive marking for NFκB and STAT3 and low-positive immune response for JAK1 were evident.

Gender-related changes

Analysis of results related to gender differences in the expression of biomarkers showed that the signaling route JAK1-STAT3 is significantly immunopositive in women ($p < 0.05$). Explaining this result is not easy, perhaps the activity may be related to the receptor function that starts the transfer of the signal inside the cell. The receptors that activate JAK1-STAT3 are tyrosinekinasis-like type, a subgroup of membrane cell receptors associated with enzymes. Their ligands are various growth factors, cytokines, hormones. Their activity can be modulated to the concentration of ligand, negative stimulation is not excluded when there is reduced or absent growth factors, which is part of the mechanism for negative initiation of apoptosis program. A full understanding of the gender-dependant activity of JAK1-STAT3 signaling path remains unclear.

Changes according to the type of tooth (frontal/posterior, upper/lower)

In frontal teeth there was a statistically significant greater immunoreactivity for JAK1 and STAT3 ($p < 0.05$). In sync with other objectives, the frontal teeth were representatives of the group of old pulp, confirming that cell ageing is the factor influencing the activity of the signaling path. The position of the tooth of the upper or lower jaw had no effect on the expression of NFκB, JAK1 and STAT3, which was confirmed in both primary and secondary data grouping.

Changes according to dental topography (crown/root)

In the analysis of the results for the expression of biomarkers according to dental topography, statistically significant immunonegative reactivity for STAT3 was revealed in the odontoblastic cells of the root pulp ($p < 0.05$). This indicates different activity in terms of STAT3 positive odontoblasts in the crown and root of the tooth.

Discussion

The signaling route JAK-STAT plays a key role in the regulation of cell proliferation, differentiation, inflammatory response and apoptosis [5]. In the signaling pathway JAK1-STAT3, significantly active in the ageing of the dental pulp, a key role is played by the receptor apparatus. Odontoblasts express receptors from all families

for activation of signaling pathway JAK1-STAT3, but the tyrosine-kinase-associated receptors in odontoblasts are of a particular importance [4]. Their ligands are various biologically active proteins including hormones. This may explain our findings that expression of JAK1-STAT3 is statistically significant immunopositive in women. The functions of NFkB are both pro-apoptotic and anti-apoptotic. Active NFkB in mouse cells leads to stimulation of their apoptosis and to proinflammatory cell status. [1, 2, 3]. Our results confirmed the link between NFkB expression in odontoblasts and ageing. The NFkB showed the strong regulatory effect in favor of cytoprotection and odontoblasts cells were defined as cells Type II with a potent inhibitory threshold.

Based on the limitations of this study, the high-differentiated long-lived pulp odontoblast cells also have a specific receptor function, intracellular information transfer and regulatory control of gene transcription in the nucleus. They have multilateral control over programmed cell death and use evolutionarily conservative regulation mechanisms. Clarifying the molecular map of odontoblasts would also reveal new strategies in a diagnostic and healing perspective.

Conclusion

In conclusion, the activity of signaling pathway JAK1-STAT3 in dental pulp in ageing presents a direct pathway of regulation of apoptosis, however NFkB maintains the inhibitory threshold.

References

1. Rawlings, J. S., K. M. Rosler, D. A. Harrison. The JAK/STAT signaling pathway. – *Journal of cell science*, 117, 2004, 1281-1283.
2. Roskoski, Jr R. Src protein-tyrosine kinase structure and regulation. – *Biochem. Biophys. Res. Commun.*, **324**, 2004, 1155-1164.
3. Sahin, M., P. L. Greer, M. Z. Lin, H. Poucher, J. Eberhart, S. Schmidt, T. M. Wright, S. M. Shamah, S. O'Connell, C. W. Cowan, L. Hu. Eph-dependent tyrosine phosphorylation of ephexin1 modulates growth cone collapse. – *Neuron*, **46**, 2005, 191-204.
4. Schlessinger, J. Cell signaling by receptor tyrosine kinases. – *Cell*, **103**, 2000, 211-225.
5. Teng, Y., J. L. Ross, J. K. Cowell. The involvement of JAK-STAT3 in cell motility, invasion, and metastasis. – *Jak-Stat*, **3**, 2014, e28086.
6. Yu, H., H. Lee, A. Herrmann, R. Buettner, R. Jove. Revisiting STAT3 signalling in cancer: new and unexpected biological functions. – *Nature reviews Cancer*, **14**, 2014, 736.
7. Wullschleger, S., R. Loewith, M. N. Hall. TOR signaling in growth and metabolism. – *Cell*, **124**, 2006, 471-484.

Comparative Analysis of Bioinks in 3D Bioprinted Organoids of Colorectal Cancer

Diana Molander^{1}, Yordan Sbirkov^{1,2}, Ilia Bodurov³, Dorian Dikov⁴,
Victoria Sarafian^{1,2}*

¹ Department of Medical Biology, Medical University of Plovdiv, Bulgaria

² Research Institute at Medical University of Plovdiv, Bulgaria

³ University Hospital Eurohospital, Plovdiv, Bulgaria

⁴ Department of General and Clinical Pathology, Medical University of Plovdiv, Bulgaria

*Corresponding author e-mail: diana.molander@mu-plovdiv.bg

Colorectal cancer (CRC) is the third most common and fourth deadliest cancer in Western countries. Despite treatment regimens, the number of deaths increases yearly, particularly among younger patients. Current therapies are insufficient due to the heterogenetic nature of CRC and demand new strategies for personalized treatment.

The aim of our pilot study was to develop 3D organoids utilizing bioinks suitable for extrusion 3D bioprinting of CRC cell lines. We focused on the characterization of 3D printed organoids based on bioink properties. We assessed cell viability and growth patterns by fluorescence microscopy. 3D CRC cells printed in different bioinks revealed 90 % viability up to seven days after printing showing various cell growth patterns.

In conclusion, our work demonstrates the immense opportunities of 3D bioprinting to generate tumor organoids. We proved that alginate and gelatin-based bioinks mixed with live cells are suitable for extrusion 3D bioprinting.

Key words: bioink, 3D bioprinting, colorectal cancer, tumor organoids

Introduction

3D bioprinting is defined as an innovative biofabrication strategy generating constructs through layer-by-layer deposition of cell-laden hydrogel materials, using computer-aided design. The technology allows easy reproducibility and ensures physiologically pertinent cell-cell and cell-matrix interactions by mimicking the 3D heterogeneity of real tumors. Major components of 3D bioprinting are multiple types of live cells, biopolymer gels (bioinks), and 3D design. Choosing the appropriate cell types and density helps to assess viability, growth pattern, integrity and morphology.

The term “bioink” describes the carrier material (biopolymer) where cells are embedded in and to which they attach. Bioinks are classified as natural or synthetic and differ in their ability to mimic cell microenvironments. They have mild cross-linking properties to preserve cells in the construct and to prevent degradation of the model [10]. Some bioinks require crosslinking with CaCl_2 while others need UV or blue radiation. All gels serve as 3D structural and mechanical support to the cells as they mimic extracellular matrix (ECM) and assist cell adhesion, differentiation and proliferation. The ideal bioink should possess biomechanical properties to allow easy extrusion during printing and to maintain construct shape after printing [9]. Natural and synthetic bioinks often combine to create the most functional model possible.

The choice of bioinks in 3D bioprinting is based on important characteristics. These include mechanical support (permeability, elasticity, degradation), gelation kinetics, bioprintability (encompassing viscosity) and biocompatibility with the chosen cell type supporting cell adhesion, migration, proliferation and ECM secretion [10].

In recent years, biomaterial engineering is improving to satisfy the need of mimicking *in vivo* tumor characteristics and preserving live cell functions. 3D bioprinted organoid models are equivalent of real tumors. They open new horizons in oncology, pharmaceutical screening, biological research and regenerative medicine [2, 3].

Organoids are three-dimensional novel model systems derived from numerous sources including differentiated pluripotent stem cells, adult primary tissue and primary or metastatic tumors [5]. The components are self-organized through cell-cell and cell-matrix interactions to recapitulate the architecture of real tumors *ex vivo* [6]. The ultimate goal of the 3D bioprinted organoid is to represent tumor structure closest to the actual *in vivo* tumor. They allow studying cancer processes including tumor cell behavior and testing of new personalized therapeutic combinations [7].

Our aim was to develop 3D bioprinting protocols and to create tumor organoids based on the utilization of different bioinks. We focused on identifying the mechanical integrity and cell viability of 3D bioprinted tumor models. In our algorithm, we applied extrusion-based 3D bioprinting technology and two different bioinks - RGD (composed of alginate with covalently bound RGD nanofibrillar cellulose) and GelMa (gelatin methacrylate). Previously, we successfully printed constructs using RGD bioink [8] and sought to compare it with other bioinks. GelMa was chosen because it is widely used in extrusion-based bioprinting [9]. We created cell-laden GelMa bioprints via a simple heating and cooling process. The constructs permit cell survival for over a week and enhance cells spreading.

Materials and Methods

Cell cultures

The human colorectal cell line Caco-2 was grown in DMEM/F12 supplemented with 10% FBS and 5% Pen/Strep (P04-41250, P40-37500, and P06-07100, PAN-Biotech, Germany) under standard cell culture conditions 5 % CO_2 and high humidity 37°C. 3D bioprinted organoids were cultured in the media described above for 7 days.

Bioinks

Two types of bioinks were applied. The CELLINK RGD bioink contains the ECM peptide motif RGD (R-arginine, G-glycine, and D-aspartic acid), (catalog # IK1020100301, CELLINK, Sweden). It is composed of alginate with covalently bound RGD and nanofibrillar cellulose with viscosity of 3–20,000 Pa/s and shear rate 0.002–500 1/sec. The second bioink -GelMa A (gelatin methacrylate), (catalog # IK352102, CELLINK, Sweden) is with 30-150 Pa/s and shear rate from 0.002 s⁻¹ to 500 s⁻¹, 22°C (parameters from the manufacturer's specification sheet).

3D bioprinting

Mini tumor organoids from the human colorectal cell line Caco-2 were printed. The process began by detaching Caco-2 cells using Accutase® (catalog # 423201, BioLegend, USA). Cells were then counted (30 million cells/ml), centrifuged and mixed with the CELLINK RGD or GelMaA bioink respectively. The cell-bioink mixture was placed in 3 ml cartridges (catalog # CSC010311101, CELLINK, Sweden) and extruded. We used a computer-generated disk-shape model with 2 mm of diameter and 0.82 mm of height. To preserve the tumor model, it was cross-linked for 1 min with CaCl₂, when using the RGD ink. Cross-linking agent was not applied to the GelMa model. We employed the extrusion technique to print CRC organoid models through a 410 µM (0.41 mm), high-precision nozzle (catalog # NZ3220005001, CELLINK, Sweden) at a pressure of 8-10 kPa, speed 10 ms in standard 24-well plates on an extrusion printer BioX Cellink, Sweden. The printed tumors were cultured in DMEM/F12 with 10% FBS and 0.5% Pen/Strep under standard condition at 37°C, 5% CO₂. The medium was replaced every 2 days over a period of 1 week.

Calcein AM/PI viability assay

To assess cell viability after printing we used calcein AM (cat. # 56,496, Sigma-Aldrich, USA) and propidium iodide (PI), (cat. #P4170, Sigma-Aldrich, USA). In short, 3D bioprints were incubated with calcein AM (at 5 ng/ml final concentration) for >10 min at 37°, 5% CO₂, staining metabolically active cells in green. Then PI (at 2 µg/ml final concentration) was added staining cells with destroyed membrane in red. Microscopic images were acquired and analyzed by fluorescent microscope (Nikon Eclipse Ni, Japan) at 10x magnification.

Morphological assay

3D bioprinted organoids using both bioinks RGD and GeLMA were fixed in 10% neutral buffered formaldehyde. Further processes include embedding the organoid models in paraffin and slicing in 4 µm thick sections. Pathomorphological assessment was performed with standard hematoxyline and eosin (H&E) staining, which revealed different cell growth patterns.

Results

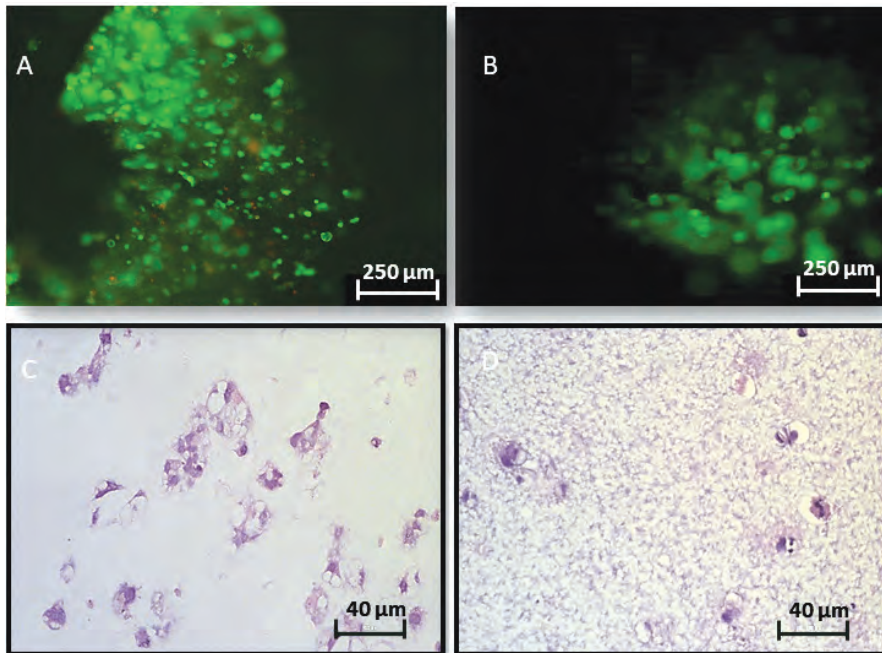
A simple two-layer cylindrical 3D organoid model was created using the human colorectal cell line Caco-2 embedded in two different commercially available bioinks. We employed extrusion-based technique and observed good extrudability and

biocompatibility with Caco-2 cells in both RGD and GelMa bioinks. We assessed the viability and distribution of cells in both prints at day 7. Post-printing cell viability of Caco-2 cells is demonstrated on **Fig. 1**. Both RGD and GelMA bioinks showed 90% viability as analyzed by the ImageJ software.

No significant cell death was registered during the 7day follow-up period (**Fig. 1A, B**).

The parallel morphological analysis revealed Caco-2 cells growing in large clusters. This started on day 3 (data not shown). Clusters resembled glandular-like structures as in the *in vivo* tumor when the RGD bioink was used. We observed no cluster formation in 3D organoids in GelMa ink but a wider distribution of cells throughout the print was noted.

Fig. 1. 3D organoids of Caco-2 cells using RGD and GelMa bioinks at day 7. (A)



Live/dead cell assay using Calcein AM/PI, (C) H&E in RGD ink prints. (B) Live/dead cell assay using Calcein AM/PI, (D) H&E in GelMA ink prints.

Discussion

3D preclinical models closely mimic the dynamics of the *in vivo* environment and serve as a powerful tool for studying different cell behavior particularly when bioinks possessing varying properties are being used. These innovative tumor organoids offer significant potential in oncology, pharmacology testing and biological research. 3D bioprinting enables the fabrication of a “bottom up” physiologically-relevant organoid, using live cells mixed with bioinks. 3D models closely mimicking native ECM environment with interconnected pores are ideal for nutrient and oxygen

delivery and intracellular communication [1, 4]. Overall, the usage of different bioinks revealed high cell viability exhibiting different growth patterns. Given the complexity of the 3D organoid architecture, it is important to analyze the correlation between characteristics and properties of the bioinks and cell behavior. Diverse bioinks provide useful information in the development of complex organoids and in tissue modeling. Creating organoid models using various bioinks can be applied as screening platforms to identify novel antitumor drug candidates. The present 3D CRC model utilizing these specific bioinks (RGD and GelMa) provides unconventional drug testing strategy for personalized medicines.

In conclusion, we present a novel, simple 3D bioprinted construct of Caco-2 colorectal cancer cells encapsulated in RGD and GelMa bioinks. We validated our algorithm as a platform for studying cell viability and morphology. Therefore, 3D bioprinted organoid models have potential in preclinical studies as a platform for identifying new therapeutic regimens.

Acknowledgements: The study is funded by MU-Plovdiv (Project ДП/ДП-01/2020) and the National University Complex for Biomedical and Applied Research, with participation in “BBMRI-ERIC” (NUCBPI-BBMRI.BG), within the national road map for research infrastructure (Contract No DO1-395/December 18, 2020).

References

1. Agarwal, S., S. Saha, K. V. Balla, A. Pal, A. Barui, S. Bodhak. Current developments in 3D bioprinting for tissue and organ regeneration – A Review. – *Front. Mech. Eng.*, **6**, 2020, Article ID 589171.
2. Datta, P., M. Dey, Z. Ataie, D. Unutmaz, I. T. Ozbolat. 3D bioprinting for reconstituting the cancer microenvironment. – *Precision Oncology*, **4**(18), 2020.
3. Decant, G., J. B. Costa, J. S. Correia, M. N. Collins, R. L. Reis, J. M. Oliveira. Engineering bioinks for 3D bioprinting. – *Biofabrication*, **13**(3), 2021.
4. Ersimo, N., Witherel, C. E., Spiller, K. L. Differences in time-dependent mechanical properties between extruded and molded hydrogels. – *Biofabrication*, **8**(3), 2016.
5. Kim, J., B. Kyoung-Koo, J. Knoblich. Human organoids: model systems for human biology and medicine. – *Nature Reviews Molecular Cell Biology*, **21**, 2020, 571–584.
6. Marsee, A., F. J. M. Roos, M. A. Monique, M. M. A. Versteegen. Building consensus on definition and nomenclature of hepatic, pancreatic, and biliary organoids HPB Organoid Consortium – *Cell Stem Cell*, **28**(5), 2021, 816-832.
7. Reidy, I., N. Leonard, O. Treacy, A. Ryan. A 3D View of colorectal cancer models in predicting therapeutic responses and resistance. – *Cancer (Basel)*, **13**(2), 2021.
8. Sbirkov, Y., D. Molander, M. Clement, I. Bodurov, A. Boykov, R. Penkov, N. Belev, N. Forraz, C. McGuckin, V. Sarafian. A Colorectal cancer 3D bioprinting workflow as a platform for disease modeling and chemotherapeutic screening. – *Frontiers in Bioengineering and Biotechnology*, **9**, 2021, Article ID 755563.
9. Shin H., B. Olsen, A. Khademhosseini. The mechanical properties and cytotoxicity of cell-laden double-network hydrogels based on photocrosslinkable gelatin and gellan gum biomacromolecules. – *Biomaterials*, **33** (11), 2012, 3143-3152.
10. Tarassoli, S. P., Z. M. Jessop, T. Jovic, K. Hawkins, I. S. Whitaker. Candidate bioinks for extrusion 3D bioprinting – a systematic review of the literature. – *Front. Bioeng. Biotechnol.*, **9**, 2021, Article ID 616753.

Exploring Senescence Reversal Potential of Antioxidants in Human Foreskin Fibroblasts

Rosen Ivanov^{1,2}, Roumen Pankov²

¹*Institute of Experimental Morphology, Pathology and Anthropology with Museum, Bulgarian Academy of Sciences, Sofia, Bulgaria*

²*Department of Cell Biology and Developmental Biology, Sofia University “St. Kliment Ohridski”, Sofia, Bulgaria*

*Corresponding author e-mail: rosen.lyubomirov.ivanov@gmail.com

Cell aging (senescence) is a process of irreversible blocking of the cell cycle and inability to perform normal replication. By blocking cell division, aging prevents the proliferation of damaged old cells and makes them resistant to apoptosis. In addition to reduced proliferative potential, aging cells are characterized by specific morphology, increased β -galactosidase activity, and changes in some important signaling pathways such as p53/p21. Aging cells have a typical secretory phenotype called SASP. Aging can be divided into two categories based on the mechanism involved – replicative aging and stress-induced aging. The latter is caused by accumulation of oxidative stress. The aim is to study the effectiveness of several antioxidants – resveratrol, quercetin, and vitamin C to slow down cell aging caused in cell culture of primary human foreskin fibroblasts (HFF), exposed to oxidative stress by treatment with high (25 mM) concentrations of glucose.

Key words: senescence, oxidative stress, glucose, p53, quercetin

Introduction

Senescence is an innate state of the cell. Often, it is the result of chronic stress exposure and is an alternative to the standard fate that is apoptosis. Cells opt for senescence to avoid potential oncogenesis, however by entering this state, in the long term they start to exude a plethora of pro-inflammatory molecules which is referred to as the SASP (senescence associated secretory phenotype). Accumulation of senile cells, emitting SASP elements throughout the life of an organism can lead to health complications. *In vitro* cultivated cells that have entered senescence exhibit a specific morphology characterized by flattening and enlargement of the cell. Additionally, a marker for such cells is the enzyme senescence-associated β -galactosidase (SA- β -gal) which is hardly expressed in any type of normal cell [5]. Even though ROS have a designated role, a

lack of balance between them and antioxidant systems results in their surplus which could lead to senescence. Evidence suggests that supraphysiological concentrations of glucose have the potential to generate ROS. Reactive oxygen species can influence the expression of GLUT transporters, their vesicular transport, as well as their behavior in the membrane. On the other hand, GLUT transporters mediate the transport of dehydroascorbic acid (DHA) into the cell and mitochondria, and it is an important tool in maintaining the balance of free radicals in the cell [7].

Materials and Methods

Cultivation

Primary human skin fibroblasts (Human Skin Fibroblasts, HSF) from the collection of the Department of Cytology, Histology and Embryology are used. Routinely, cells are grown in low glucose medium supplemented with 10% FBS/FCS and antibiotics. They were subsequently planted in 10 cm diameter petri dishes with low glucose medium (LG) as in physiological conditions (5.5 mM), high glucose (25 mM – HG) to mimic a diabetic state and low glucose, but with added artificial sweetener mannitol at a concentration of 25 mM (MN), comparable to the high glucose medium. They are grown under standard conditions – temperature 37°C and 5% CO₂. Every day, the medium of the cells is replaced with a new one. The experiment was conducted in a six-well plate where cells are inoculated at 5×10⁴ concentration.

Staining

A β-galactosidase stain was performed to quantitatively determine senescence where fixed cells from five consecutive days were incubated with the substrate X-gal which upon metabolization by SA-β-gal positive cells yields a blue-green color. HFF were cultivated in medium with 5,5 mM (control/LG), 25 mM glucose (HG) and 5,5 mM glucose + 25 mM mannitol (MN). Culture medium was removed, cells were washed with PBS followed by fixation with 3% formaldehyde for 5 min at room temperature. A freshly prepared staining solution is then added, and the plates or petri dishes are incubated for 24 h in the dark at a temperature of 37 °C. The development of staining was observed using an inverted microscope or binocular magnifier. Once sufficiently intense staining was obtained in the LG-grown control cells, the solution was removed, and the wells were rinsed three times with PBS and the plates were stored in a refrigerator at 4 °C.

Expression analysis

A Western blot analysis was conducted to evaluate the expression levels of p53 and caveolin-1. The transcription factor p53 plays a key role in the fate of a stressed cell – apoptosis, senescence, or carcinogenesis. Precast 8-16% Mini-PROTEAN TGX Stain-Free Gel gradient gel is used. Electrophoresis was carried out for 30 min at 200 V DC voltage. For the transfer of the electrophoretically separated proteins from the gel to the nitrocellulose membrane, a Trans-Blot Turbo Transfer Pack (BIORAD) and the Trans-Blot® Turbo™ Transfer System of the same company were used. The manufacturer's instructions were followed.

Once the proteins have been transferred, they should be treated with 5% dry milk dissolved in TBST for 30 min. Upon blockage, the membrane was treated with the first antibody (Upstate Biotechnology anti-P53, Santa Cruz rabbit anti-caveolin 1, Santa Cruz mouse anti-GAPDH) at 4°C for 24 hours. After washing three times with TBST to wash off the unbound first antibody, it was incubated with a second antibody for 1 h, anti-mouse and anti-rabbit, respectively, which are conjugated with peroxidase (HRP). This is followed by a final triple wash for 15 min each with TBST. For development, the membrane was incubated in the dark for 1 min with Clarity™ Western ECL Substrate. After development, the membranes were viewed on a ChemiDoc® Imaging System (BIORAD). ImageJ program was used for data analysis.

Visualization of ROS and lipid peroxidation

For visual assessment of the damage by ROS and to confirm its abundance in cells, exposed to higher glucose levels immunofluorescent microscopy methods were used. For quantitative measurement of ROS the DCFDA / H2DCFDA – Cellular ROS Assay Kit was used. For the purposes of the experiment, cells were grown on glass coverslips under standard conditions. Cells were washed once or twice with 1x buffer provided by the manufacturer and stained with diluted DCFDA solution. Incubate for 45 min in the dark at 37 °C. Wash again once or twice with 1x buffer. Live cells were mounted in Mowiol fluorescence microscopy medium (Sigma-Aldrich) and observed under a fluorescence microscope.

To assess the damage ROS inflicted on the cells was utilized the Image-iT® Lipid Peroxidation Kit. This methodology allows indirect observation of ROS because the active ingredient in the kit changes color when oxidized from red to green. For this purpose, cells are seeded on glass coverslips in medium with a low and high concentration of glucose and incubated overnight at 37°C. Add Image-iT Lipid Peroxidation Sensor in medium or buffer with a final concentration of 10 µM and incubate for 30 min at 37°C. The medium was removed and the cells were washed three times with PBS. It was embedded in Mowiol (Sigma-Aldrich) medium and observed under a fluorescence microscope.

Senolytic potential assessment

An experiment to explore the senescence reversal potential of different substances was designed. We tested the antioxidants Vit C 100 µM, resveratrol 10 µM, quercetin 5 µM and the senolytic and approved drug metformin 500 µM all of which were added to 25 mM glucose medium to establish whether the generated ROS by the high glucose would be neutralized by the antioxidants. In three six-well plates, 0.5×10^5 cells were seeded per well.

For five days, the medium is changed daily, preferably at the same time. The following concentrations of antioxidants are used – 100 µM vitamin C, 5 µM quercetin, 10 µM resveratrol and 500 µM metformin. The respective antioxidant was pre-added to 25 mM glucose medium. After five days, the steps to stain for β-galactosidase were followed, ending with counting and quantification of the stained cells as described above.

Statistical analysis

For statistical analysis Student's t-test was applied with significance at $P < 0.05$.

Results and Discussion

Staining

Generated data (**Fig. 1**) display a time-dependent increase in the percentage of senescent cells compared to all cells in the group treated with 25 mM glucose and no changes in other groups (5,5 mM and 5,5 mM glucose + 25 mM mannitol). The data resonate with the preliminary results of teams such as Wang et al., 2019 [8] and Ha & Lee, 2000 [4] and provide basis for further exploring the suspected connection between glucose and senescence.

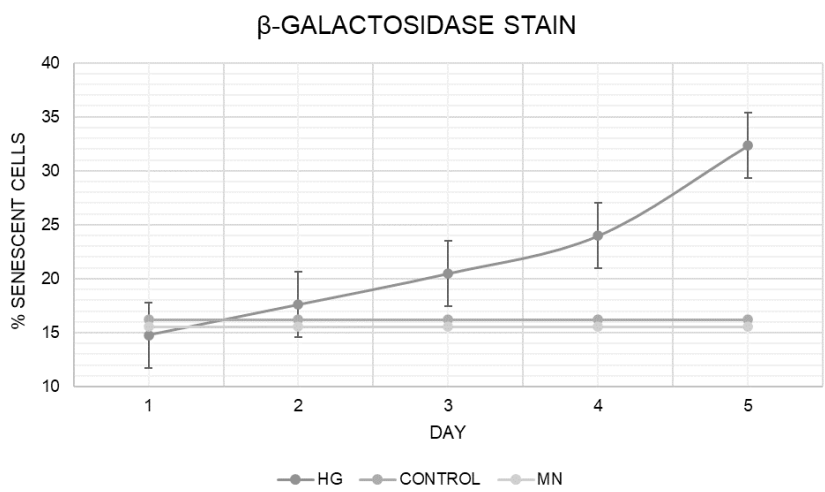


Fig.1. Time-dependent increase in the percentage of senescent cells after cultivation of human skin fibroblasts with 5,5 mM (control-LG), 25 mM glucose (HG) and 5,5 mM glucose + 25 mM mannitol (MN).

Expression analysis

Considering the typical morphological changes of senescent cells caveolin 1, a crucial membrane protein is a logical target for monitoring during those changes. Results from the experiment (**Fig. 2**) point toward a statistical rise in the expression of both molecules – caveolin 1 and p53. This provides a clear link between p53 and cellular aging and makes the molecule an object of interest for further study as well as a target for antiaging drugs. The data obtained are consistent with Atadja et al., 1995 [1], showing a similar increase in p53. Apart from that results open the possibility to use caveolin 1 not only as a marker for various cancers [3] and as a marker to detect senescent cells, similar to SA- β -gal.

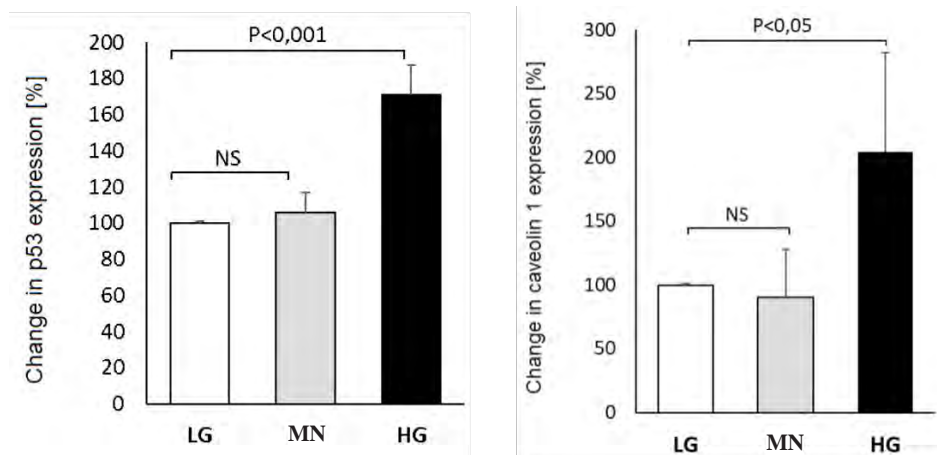


Fig. 2. Expression of p53 and calvelolin in cultivated human skin fibroblasts with with 5,5 mM (control-LG), 25 mM glucose (HG) and 5,5 mM glucose + 25 mM mannitol (MN).

Visualization of ROS and lipid peroxidation

The results in **Fig. 3** show a clear increase of fluorescence in the cells cultivated in 25 mM glucose. These data are in sync with those obtained by Buranasin et al., 2018 [2] demonstrating that exposure to high levels of glucose in human gingival fibroblasts leads to an increase in ROS levels in the cells. The produced images in **Fig. 4** depict that in the 5,5 mM group (LG) the red (showing all lipids in the cell) and green (showing oxidized lipids) channels have similar intensity. On the other hand, the higher glucose group depicts noticeable increase in intensity at the green channel corresponding to higher levels of lipid oxidation hence ROS. Similar experiment investigating the effect of high glucose on LDL oxidation found that treatment with 25 mM glucose (HG) induced increased levels of oxidized LDL. Although these are lipoprotein complexes, the data match with ours because in both cases we are talking about HSFs treated with 25 mM glucose [6].

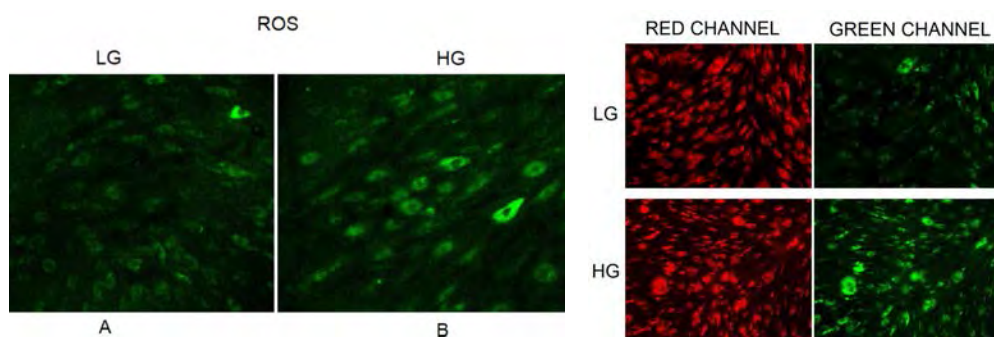


Fig. 3 and Fig. 4. Fluorescent images of cells cultivated human skin fibroblasts with 5,5 mM glucose (LG) or 25 mM glucose (HG)

Senolytic potential assessment

Initially, we explored the effect of treatments with antioxidants (Vit. C, quercetin-Q, resveratrol-Res and metformin-Met) on the levels of senescence through β -galactosidase stain (**Fig. 5**). After the treatments, Western blot analysis (**Fig. 6**) was repeated to unveil whether treatment with the explored substances affected the expression of p53 and caveolin 1. Both experiments point toward a significant reduction in the percentage of senescent cells, as well as the expression of caveolin 1 and p53. Quercetin (Q) appears to have to the most noticeable senolytic properties.

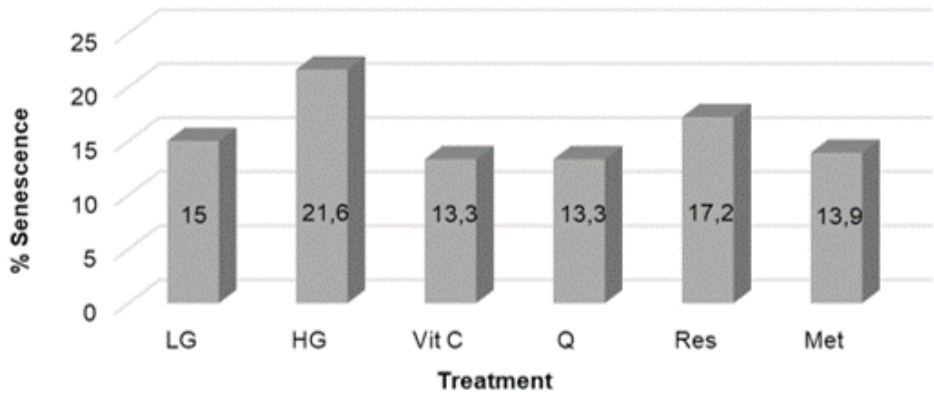


Fig. 5. Effect of treatments with antioxidants (Vit. C, quercetin, resveratrol and metformin) on the levels of senescence (through β -galactosidase stain) of human skin fibroblasts, cultivated with 25 mM glucose (HG). LG – low glucose (5,5 mM)

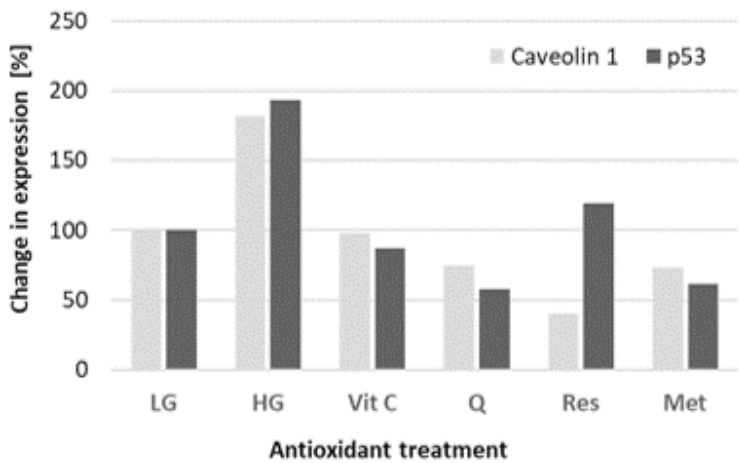


Fig.6. Effect of treatments with antioxidants (Vit. C, quercetin, resveratrol and metformin) on the expression of caveolin 1 and p53 in human skin fibroblasts cultivated with 25 mM glucose (HG). LG – low glucose (5,5 mM)

Conclusions

Based on the obtained results, the following conclusions can be suggested:

1. Cultivation of human skin fibroblasts in high glucose medium (25 mM) causes an increase in the percentage of senescent cells expressing β -galactosidase and this effect is not due to increased osmotic pressure of the medium.
2. High glucose induces an increase in the expression of the cellular senescence markers caveolin 1 and the transcription factor p53. A similar effect was not observed in control cells grown in medium with increased osmotic pressure (5.5 mM glucose + 25 mM mannitol).
3. Hyperglycemia causes an increase in cellular levels of reactive oxygen species (ROS) and lipid peroxidation.
4. The addition of antioxidants vitamin C (100 μ M), quercetin (5 μ M), resveratrol (10 μ M) and the senolytic metformin (500 μ M) effectively reduced senescent cells to and even below control levels, supporting the hypothesis that hyperglycemia induces cellular senescence by stimulating the production of reactive oxygen species (ROS).

Acknowledgements: This study was supported by grant ДН 11/7 by the Bulgarian National Science Fund.

References

1. Atadja, P., H. Wong, I. Garkavtsev, C. Veillette, K. Riabowol. Increased activity of p53 in senescing fibroblasts. – *Proceedings of the National Academy of Sciences*, **92**(18), 1995, 8348-8352.
2. Buranasin P., K. Mizutani, K. Iwasaki, C. Mahasarakham, D. Kido, K. Takeda, Y. Izumi. High glucose-induced oxidative stress impairs proliferation and migration of human gingival fibroblasts. – *PLoS One*, **13**(8), 2018.
3. Demirci N., M. Dogan, G. Erdem, S. Kacar, T. Turhan, S. Kilickap, L. Cigirgan, E. Kayacetin, Y. Bozkaya, N. Zengin. Is plasma caveolin-1 level a prognostic biomarker in metastatic pancreatic cancer? – *Saudi J. Gastroenterol.*, **23**(3), 2017, 183-189.
4. Ha H., H. B. Lee. Reactive oxygen species as glucose signaling molecules in mesangial cells cultured under high glucose – *Kidney International*, **58**, 2000, S19–S25.
5. Hernandez-Segura, A., J. Nehme, M. Demaria. Hallmarks of cellular senescence. – *J. Trends in Cell Biol.*, **28**(6), 2018, 436-453.
6. Kawamura M., J. Heinecke, A. Chait. Pathophysiological concentrations of glucose promote oxidative modification of low density lipoprotein by a superoxide-dependent pathway. – *J. Clin. Invest.*, **94**(2), 1994, 771-778.
7. Liemburg-Apers, D., P. Willems, W. Koopman, S. Grefte. Interactions between mitochondrial reactive oxygen species and cellular glucose metabolism. – *J. Arch. Toxicol.*, **89**(8), 2015, 1209-1226.
8. Wang, S., Q. Wang, H. Wang, C. Qin, X. Cui, L. Li, Y. Liu, H. Chang. Induction of ROS and DNA damage-dependent senescence by icaritin contributes to its antitumor activity in hepatocellular carcinoma cells. – *Pharmaceutical Biology*, **57**(1), 2019, 424-431.

Effects of *Geranium sanguineum* Ethanol Extract After i.p. Application in a Mouse Model of Ehrlich's Breast Cancer

Mashenka Dimitrova^{1*}, Katerina Todorova¹, Ivan Iliev¹, Inna Sulikovska¹,
Ludmil Kirazov¹, Ivaylo Ivanov²

¹Institute of Experimental Morphology, Pathology and Anthropology with Museum – Bulgarian Academy of Sciences

²Department of Medicinal Chemistry and Biochemistry, Medical University – Sofia

*Corresponding author e-mail: mashadim@abv.bg

Geranium sanguineum has a strong anti-oxidant and antitumor activity documented *in vitro* but less examined *in vivo*. Recently, we obtained 80% ethanol extract from the plant roots and showed that it is a valuable antitumor agent in *in vitro* studies. The aim of the present study was to evaluate the effects of the above extract used i.p. in a mouse model of Ehrlich's breast carcinoma, to compare it with the effect of oxaliplatin and to look for a possible synergistic action of the two agents. The results showed that *G. sanguineum* and oxaliplatin have no synergistic action but act similarly when applied alone. This activity included directing the ascites cells to apoptosis and preventing metastases in the liver. The results presume the *G. sanguineum* ethanol extract to be a possible alternative/auxiliary chemotherapeutic to oxaliplatin for this type of tumor.

Key words: *Geranium sanguineum*, oxaliplatin, Erlich's carcinoma, pathomorphology

Introduction

Geranium sanguineum (blood geranium) is a perennial herbaceous plant of the *Geraniaceae* family, which rhizomes and leaves are widely used in folk medicine for the regulation of blood pressure, as an anti-septic, anti-inflammatory and hemostatic agent, in gastrointestinal diseases, and others [2]. Polyphenol-rich extracts have strong antioxidant and antitumor activity [3]. Recently, we obtained 80% ethanol extract (composed mainly of anthocyanidins and their derivatives) from the plant roots and showed its antitumor activity in a panel of tumor cells (unpublished results).

The aim of the present study was to evaluate the effects of the above extract used i.p. in a mouse model of Ehrlich's breast carcinoma, to compare it with the effect of oxaliplatin and to look for a possible synergistic action of the two agents.

Materials and Methods

G. sanguineum ethanol extract (GSE). Dried and crushed roots of the herb were treated with 80% ethanol in a ratio 1g : 10 mL for 3 hours, then the solid residue was re-extracted overnight. The collected filtrates were concentrated on a vacuum evaporator. Acetonitrile was added, evaporated, and the residue was treated with diisopropyl ether, filtered and dried *in vacuo*.

Animals and treatment. Male ICR mice (20, 20g b.w.), were randomly allocated to four groups (5 mice each), as follows:

- Group 1 – inoculated with 1×10^6 Ehrlich's cells i.p. to develop ascites tumor (positive controls);
- Group 2 – like group 1 but treated daily i.p. with 30 mg/kg b.w. GSE;
- Group 3 – like group 1 but treated i.p. with a single dose of 10 mg/kg b.w. oxaliplatin on the third day of the experiment;
- Group 4 – like group 1 but treated i.p. with 15 mg/kg b.w. GSE (daily) and 10 mg/kg b.w. oxaliplatin on the third day of the experiment.

All the animals were fed and watered *ad libitum* during the testing period (10 days). The experiments were carried out in accordance with the national regulation Nr 20/01.11.2012 regarding laboratory animals and animal welfare. The animals from all groups were sacrificed by cervical dislocation on the 11th day. Tissue samples from liver were extracted, stained with H&E and examined microscopically (Leica DM 5000B, Germany). Ascites' smears were stained with DiaPath May-Gründwald-Giemsa Fast Method and examined as above.

Results and Discussion

Ehrlich's carcinoma is a rapidly developing, poorly differentiated tumor in mice, similar to the most sensitive to chemotherapy human breast cancers. It is used to study the therapeutic potential of various substances [1,4] also in our laboratory [5]. We tested the possibilities of i.p. application of the GSE and oxaliplatin, which allows direct contact of the agent with the ascites tumor cells. The pilot study was conducted using the scheme of Elkhawaga et al. [1] with healthy animals at doses 15 or 30 mg/kg b.w.(daily) GSE and 10 mg/kg b.w. oxaliplatin (a single dose) as 0.2 ml aqueous solution. The experience did not show any deviations from the norm which let us approve the above test scheme.

Ascites smears showed a number of giant tumor cells, cells in different stages of mitosis and leukocyte effusions in positive controls and animals treated with both extract and oxaliplatin (**Fig. 1A and C**). In the animals treated only with extract or oxaliplatin respectively, the number of leukocytes was visibly lower and a substantial formation of apoptotic blebs in tumor cells was observed (**Fig. 1B and D**). Obviously, the antitumor agents applied separately tend to direct the tumor cells to apoptosis.

In the liver of positive controls (group 1) and in group 4, signs of acute serous hepatitis were noticed. Extended sinusoidal capillaries with effusions of inflammatory cells and metastatic tissue (in some animals) were also visible (**Fig. 2A**). In groups 2 and 3 a perivascular inflammation was present but no metastases were seen (**Fig. 2B and D**).

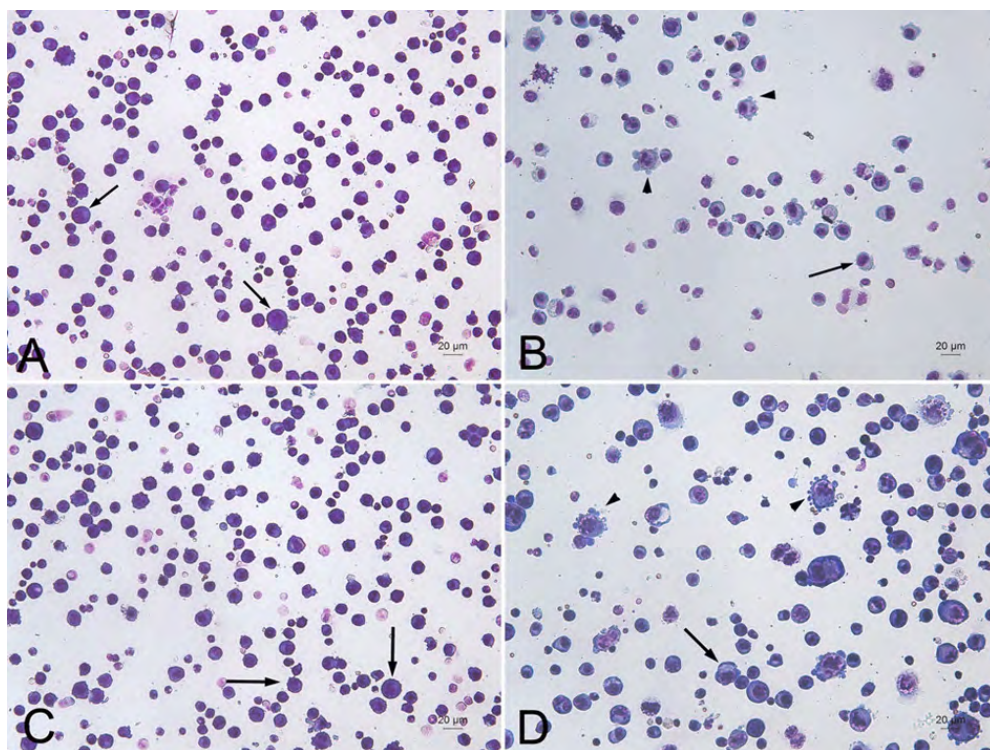


Fig. 1. Ascites form of Ehrlich's carcinoma. A – non-treated with anti-tumor agents positive control; B – mice treated only with GSE; C – mice treated with both GSE and oxaliplatin; D – treated only with oxaliplatin. Giant carcinoma cells (arrows). Only in groups 2 and 3 (treated with the extract or oxaliplatin respectively) – formation of apoptotic blebs (arrowheads). May-Gründwald-Giemsa staining, 200X

According to the above results it could be concluded that *G. sanguineum* ethanol extract has not a preventive effect on the development of Ehrlich's carcinoma in mice and has not a synergistic action with oxaliplatin. However, the extract applied alone has a very similar activity to that of oxaliplatin also applied alone: it prevents metastasizing of tumor cells and directs them to apoptosis in the ascites fluid. Those findings presume that *G. sanguineum* ethanol extract deserves to be studied as a possible alternative/auxiliary chemotherapeutic to oxaliplatin for this type of tumor.

Acknowledgements: This work is financially supported by the Scientific Fund of the Bulgarian Ministry of Education and Science, Grant No KP-06-N31/1.

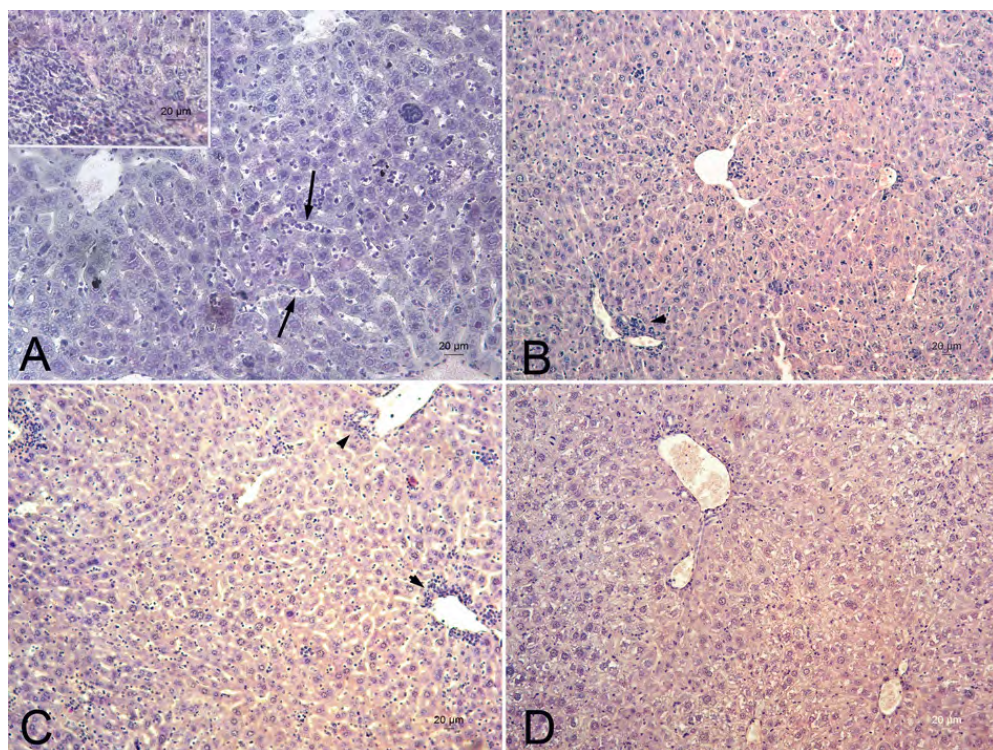


Fig. 2. Liver. A – non-treated with anti-tumor agents control; B – mice treated with GSE; C – mice, treated with both extract and oxaliplatin; D – mice, treated only with oxaliplatin. In controls – signs of acute serous hepatitis; extended sinusoidal capillaries with effusions of inflammatory cells (arrows); inclusion – metastatic tissue. Treated animals – no metastases but perivascular inflammation (arrowheads). H&E staining, 200X

References

1. Elkhawaga, O.-A., S. Gebril, N. Salah. Evaluation of anti-tumor activity of metformin against Ehrlich ascites carcinoma in Swiss albino mice. – *Egyptian Journal of Basic and Applied Sciences*, **6**(1), 2019, 116–123.
2. Ilic, M., S. Samardzic, J. Kotur-Stevuljevic, D. Uslak, M. Milenkovic, N. Kovacevic, M. Drobac. Polyphenol rich extracts of *Geranium* L. species as potential natural antioxidant and antimicrobial agents. – *European Review for Medical and Pharmacological Sciences*, **25**, 2021, 6283–6294.
3. Leucuta, S., L. Vlase, S. Gocan, L. Radu, C. Fodorea. Determination of phenolic compounds from *Geranium sanguineum* by HPLC. – *Journal of Liquid Chromatography & Related Technologies*, **28**, 2005, 3109–3117.
4. Ozaslan, M., I. D. Karagoz, I. H. Kilic, M. E. Guldur. Ehrlich ascites carcinoma. – *Afr. J. Biotech.*, **10**, 2011, 2375–2378.
5. Todorova K., I. Ivanov, I. Iliev, L. Kirazov, M. Dimitrova. Biological activity of orally given ethyl acetate extract from *Cotinus coggygria* in albino mice with solid and ascites forms of Ehrlich's tumor. – *Acta Morphol. Anthropol.*, **28**(3-4), 2021, 3–9.

Neuroprotective Role of Caffeic Acid in Lipopolysaccharide-induced Neurodegeneration in Mice

Kingsley Afoke Iteire^{1*}, Enemali Felix Udawnojo¹, Emmanuel Igho Odokuma²

¹Department of Anatomy, Faculty of Basic Medical Sciences, Ondo State University of Medical Sciences, Ondo City, Nigeria

²Department of Anatomy, Faculty of Basic Medical Sciences, Delta State University, Abraka Delta State, Nigeria

*Corresponding author e-mail: aiteire@unimed.edu.ng

This study aimed to investigate the anti-inflammatory role of Caffeic acid (CFA) on Lipopolysaccharide (LPS)-induced neurotoxicity by quantifying astrocyte and microglial activation. Mice were randomly divided into Groups A-D (n=8). Group A, the Control group, received water; B (Neurotoxicity model) received LPS for seven days and sacrificed; C (Neurotoxicity and anti-inflammatory model) received LPS and caffeic acid concurrently, D (Positive control) received caffeic acid. All administrations were through oral gavage once daily at 08:00 hours, and the experiment lasted 14 days. An open field test (OFT) was used to assess the effect of LPS and other treatments on the exploratory behavior of the animals. LPS-induced neurotoxicity reduced mice's motor activities, significant degeneration of cerebral neurons, and increased cerebral GFAP (glial fibrillary acidic protein) and Iba1 (ionized calcium-binding adapter molecule 1) immuno-reactivity. The study also establishes the ameliorating effect of CFA on LPS-induced neurotoxicity by restoring cerebral histoarchitecture, improving motor activities, and reducing cerebral GFAP and Iba1 expression.

Key words: Caffeic acid; Lipopolysaccharide; Neurodegeneration; Cerebral cortex; Mice

Introduction

Neurodegenerative disorders (ND) constitute a heterogeneous group of age-related disorders characterized by a slow but irreversible deterioration of brain functions [24]. Over two decades, evidence has implicated calcium-related homeostatic mechanisms, giving rise to the Ca²⁺ hypothesis of brain aging and cell death [28]. Neurodegenerative diseases have become a global problem affecting mostly older adults. Parkinson's disease (PD), a type of ND, is major motor disorder, and the second most common neurodegenerative age-related disorder [19]. This disease is of great clinical and

economic importance due to its effect on mobility in the elderly. The primary locus of PD, comprised of pigmented, dopaminergic neurons inside the substantia nigra pars compacta (SNpc) and attendant projections to the putamen, is characterized clinically by resting tremor, bradykinesia, rigidity, and postural instability. Even though the pathogenesis and differential diagnosis of PD is poorly understood, however, a multifactorial process appears to initiate dopaminergic neuron degeneration in PD. Moreover, several inflammatory responses have been suggested to play a key role in dopaminergic neuron degeneration and hence progression of the disease. The two most common inflammatory models of PD are those involving the use of polyinosinic polycytidylic acid (poly (I: C) and lipopolysaccharide (LPS), which activate toll-like receptors 3 and 4, respectively [21]. Toll-like receptors (TLR) recognize pathogen-associated molecular patterns, initiating an immune response and promoting the production of pro-inflammatory cytokines, chemokines, and oxidative factors [21]. The earliest duration of LPS-induced PD studied was 3 days, and it led to robust activation of substantia nigra (SN)-microglial cells. Between 1 and 2 weeks after starting LPS infusion, SN microglia became fully activated, exhibiting the characteristic amoeboid morphology [10].

Animal PD models have improved our knowledge of the disease and have played a critical role in developing neuroprotective drugs. Although much funding has been earmarked for the development of drugs or technology for the cure or treatment of ND, unfortunately, up till now, there is less effective management currently available for the amelioration of these elderly-related diseases. This has led to the advent of complementary means of control, including the use of Caffeic acid (CFA), a polyphenol produced through the secondary metabolism of vegetables [25], including olives, coffee beans, fruits, potatoes, carrots, and propolis, and constitutes the main hydroxycinnamic acid found in the diet of humans [27]. The phenolic acid constituents of coffee, such as CFA, have also been reported to possess antioxidants, anti-inflammatory, anti-apoptotic, and neuroprotective properties [27]. A study has disclosed that Caffeic acid can protect the blood-brain barrier (BBB) in a rodent model of traumatic brain injury [32], preventing neonatal hypoxic-ischemic brain injury. Another study also postulates that CFA attenuated dopaminergic neuronal loss in 6-OHDA Parkinson's model [3], and this could be due to its dihydroxy atom, which easily makes CFA a potent antioxidant molecule [26]. Furthermore, CFA has been proven to be a potent 5-lipoxygenase (LOX) inhibitor, and has subsequently demonstrated an ability to down-regulate NF- κ B, IL-6, and IL-1 β in inflammatory reactions [13]. These benefits of CFA have been captured in a large prospective epidemiological study which documented a reduced risk of developing PD with a relative risk ranging from 0.45 to 0.80 in coffee drinkers versus non-coffee drinkers [14]. Therefore, the index study was designed to evaluate the neuro-ameliorative role of caffeic acid on anxiety-like (anxiolytic or anxiogenic) behavior and how these dietary constituents modulate the general behavior, including the normal locomotion and depressive symptoms when presented with stressors like Lipopolysaccharides.

Materials and Methods

Experimental Animals

Thirty-two (32) young male Swiss mice weighing 20 g and 30 g were obtained from the Animal House of the University of Medical Sciences, Ondo City. They were kept and housed in plastic cages at room temperature and 12:12 h light-dark cycle, and fed with a balanced rodent pellet diet and water ad libitum. Mice were acclimatized for fourteen days before the commencement of experiments. The NIH Guideline on experimental procedures for the Care and Use of Laboratory Animals for research was strictly adhered during our experiment.

Drugs and Chemicals

Caffeic acid, lipopolysaccharide – LPS (*Escherichia coli* serotype, 055: B5), acetylthiocholine, Ellman Reagent [5', 5'-Dithiobis- (2-nitrobenzoate) DTNB] and thiobarbituric acid (TBA) were obtained from Sigma-Aldrich, St. Louis, USA. Trichloroacetic acid (TCA) was obtained from Burgoyne Burbidge & Co., Mumbai, India. Primary antibodies (Anti-Iba 1, GFAP), Polymer Anti-mouse igG Reagent, DAB peroxidase (HRP) Substrate kit (Vector®) were purchased from Vector Labs, Burlingame, CA, USA, Elite Vectastain ABC kit), visualization was with diaminobenzidine (DAB) (Vector Labs, peroxidase substrate kit, SK-4100).

Experimental Procedure

The animals were randomly assigned into four experimental Groups (A-D), n=8. Group A serves as the Control group and received water and vital pellet feed only for 14 days; Group B (LPS) received water, vital pellet feed, and 5 mg/kg of LPS for seven days to induce neurodegeneration [4, 12]; Group C (CFA + LPS) received water, Vital pellet feed, 5 mg/kg of LPS, and 40 mg/kg of caffeic acid for 14 days to determine the protective potential of caffeic acid; Group D (CFA) received water, Vital pellet feed and caffeic acid only for 14 days. All administrations were done via oral gavage using an improvised oral cannula once a day at 08:00 hours, and the whole experiment lasted for 14 days.

Behavioral paradigms

Open field test

An open field test (OFT) was used to assess the effect of LPS and other treatment groups on the exploratory behavior of the animals. Locomotor activity (LMA) was assessed in mice individually placed into a clean, novel glass arena (30×30×60 cm) that was divided into nine virtual quadrants (10×10 cm each). Locomotor activity was measured by counting the number of crossings, the number of rearing, centre square entries and time in the centre, and grooming over a 5 min period. Between the experiments, the apparatus was cleaned with 70% ethanol [29].

Animal Sacrifice and Tissue Excision

The mice were sacrificed 24 hours after the last administration. Animals were sacrificed via cervical dislocation, carried out by a skilled personnel. The brain was exposed by a sagittal incision of the skull, and the brain harvested and fixed in 10% neutral buffered formalin before processing for histology. The recommended procedure of Drury and Wallington was adopted [6].

Histological and Immunohistochemical Procedure

The brain samples were processed for routine histological processing for hematoxylin and eosin (H&E) staining technique. Brain sections for immunohistochemistry were stained for astrocyte and microglia with GFAP and IBA, as described by Gray and Hand [9].

Photomicrography and Image Analysis

The histological and Immunohistochemical slides were viewed under a Digital Light microscope, and an attached camera took digital photomicrographs at $\times 400$, $\times 100$, and $\times 40$ magnifications using OMAX software. The cell counter plug-in, NIH-sponsored Image J software, was used to digitally analyze photomicrographs with a resultant quantification of protein expression [11].

Data Analysis

One-way ANOVA was carried out to analyze data from behavioral tests, GFAP, and Iba1 immunoreactivity, followed by the Tukey test for multiple comparisons. A GraphPad Prism 8 was utilized for statistical analysis. A significant difference was set at $p < 0.05$.

Results

Open Field Test

Behavioral activity data from the LPS mice group, control mice group, LPS + CFA group, and caffeic only group were collected on the 3rd, 5th, 7th, 10th, 12th, and 14th day of the experiment. The days chosen for the test were for convenience and to allow for enough time for drug actions. However, the data recorded for day 5, 7, and 12 were used for general presentation of our data analysis (**Fig. 1**).

Total Distance Traveled

The mice' total distance travelled on the open field test over the three days was calculated as a graphical representation shown in **Fig. 1 (chart 1)**. The control group mice had a mean total distance travelled of 449.00 ± 14.43 (cm), which was significantly reduced to 126.90 ± 5.17 ($P < 0.0001$) in the LPS-only group. LPS + Caffeic acid increased the mean total distance travelled to 307.90 ± 6.14 ($P = 0.0001$) compared to LPS-group mice. Similarly, caffeic acid-group mice increased the mean distance travelled to 424.30 ± 15.53 ($P = 0.0001$) across the 5th, 7th, and 12th day of the open field experiment.

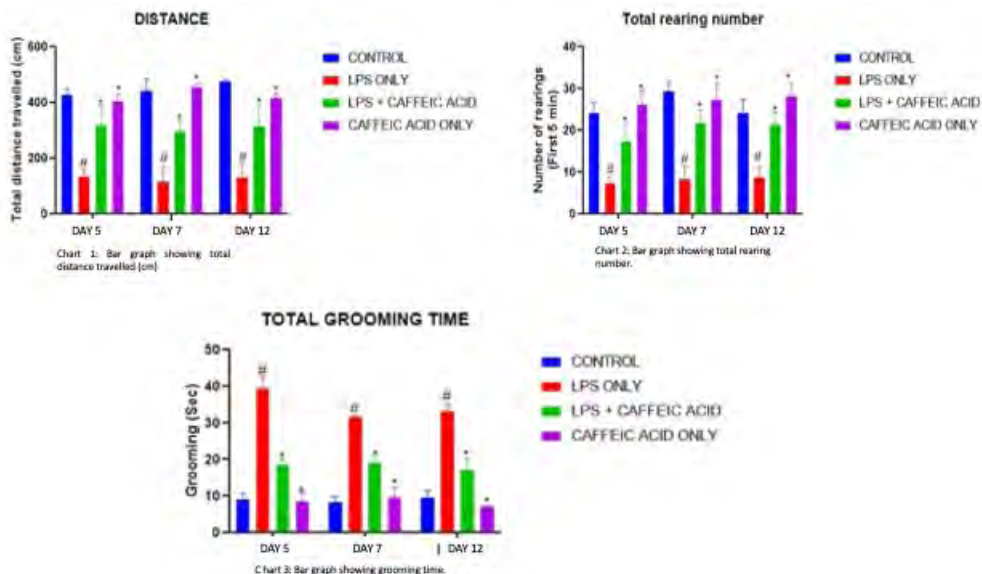


Fig 1: Bar charts showing behavioral assessment using Open Field Test

Fig. 1. Behavioral assessment using Open Field Test. Chart 1. Total distance of mice travelled on the open field test; Chart 2. Total rearing number; Chart 3. Grooming time in the open field test.

Total Rearing Number

The mean total rearing number in the control mice was 26.33 ± 3.48 , 25.33 ± 1.20 , and 25.67 ± 2.03 on the 5th, 7th, and 12th day, respectively (**Fig. 1, chart 2**). LPS-group significantly reduced the mean total rearing number on the 5th, 7th, and 12th day to 7.33 ± 1.86 ($P < 0.0001$), 9.00 ± 0.00 ($P < 0.0001$), 8.00 ± 1.53 ($P < 0.0001$) compared to the control group. LPS + CFA-group increased the mean total rearing number to 21.67 ± 2.33 ($P = 0.0022$) 16.33 ± 1.667 ($P < 0.0001$) and 22.33 ± 0.33 ($P = 0.0002$) compared to LPS-group. CFA-group also increased the mean total rearing number to 27.33 ± 1.20 , 25.67 ± 0.67 , 28.33 ± 3.18 ($P < 0.0001$).

Total Grooming Time

The grooming time in the open field test of control-group mice was 8.33 ± 2.33 , 8.00 ± 0.58 , 10.67 ± 0.88 sec on days 5, 7, and 12 (**Fig. 1, chart 3**). LPS-group significantly increased mean grooming time to 35.67 ± 5.24 ($P < 0.0001$) on the 5th day, 34.67 ± 1.45 ($P < 0.0001$) on the 7th day and 33.67 ± 1.76 ($P < 0.0001$) on the 12th day. Treatment of LPS-group mice with caffeic acid consequently significantly reduced this means grooming time to 18.33 ± 1.86 ($P = 0.0022$), 18.33 ± 3.712 ($P < 0.0001$), 18.00 ± 0.58 ($P = 0.0002$) compared to LPS-group. For the CFA-group, there was no significant difference in the mean grooming time [7.33 ± 0.33 ($P > 0.05$), 8.67 ± 2.186 ($P > 0.05$), and 9.33 ± 2.85 ($P > 0.05$)] when compared to the control-group, suggesting no major adverse effect of CFA in the mice.

Demonstration of histologic features with hematoxylin and eosin staining

The hematoxylin and eosin staining of the cerebrum shows distinct pyramidal neurons and oligodendrocytes (**Fig. 2**). Control (**Fig. 2A**) and CFA (**Fig. 2D**) groups show normal cerebral histology. LPS-group (**Fig. 2B**) shows obvious degenerative features in neurons characterized by cellular shrinking, loss of nuclear constituent, and cytoplasmic vacuolations. Treatment with CFA helped restore cerebral histology in the LPS+CFA-group (**Fig. 2C**). However, some visible cytoplasmic vacuolations are still present compared to control and CFA-group.

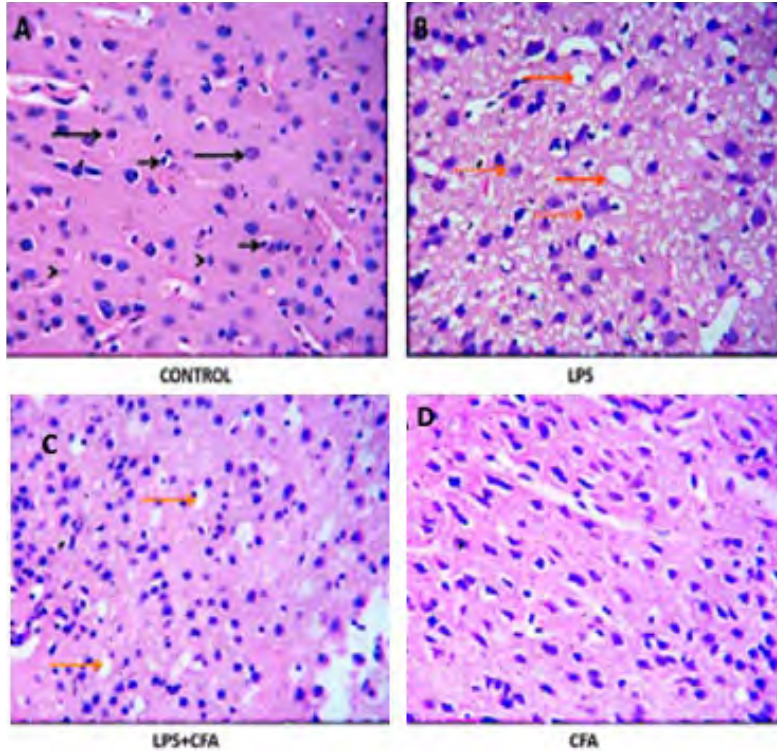


Fig. 2. Photomicrographs of H&E staining of the cerebrum of control, LPS, CFA, and LPS+CFA groups (H&E, $\times 400$). Black arrows – pyramidal neurons; Short arrows – oligodendrocytes; Arrowhead – astrocytes; Brown arrows – cytoplasmic vacuolations; Dashed arrows – degenerating neurons

Quantification of immuno-expressed GFAP

The present study shows increased GFAP immunoreactivity in the LPS-group (15.00 ± 1.77) compared to the control-group (1.00 ± 0.21), CFA-group (4.00 ± 0.77), and LPS + CFA group (6.25 ± 1.61). The CFA group (4.00 ± 0.77) and LPS + CFA group (6.25 ± 1.61) showed no significant difference in immunoreactivity when compared to the control group (1.00 ± 0.21) (**Fig. 3**).

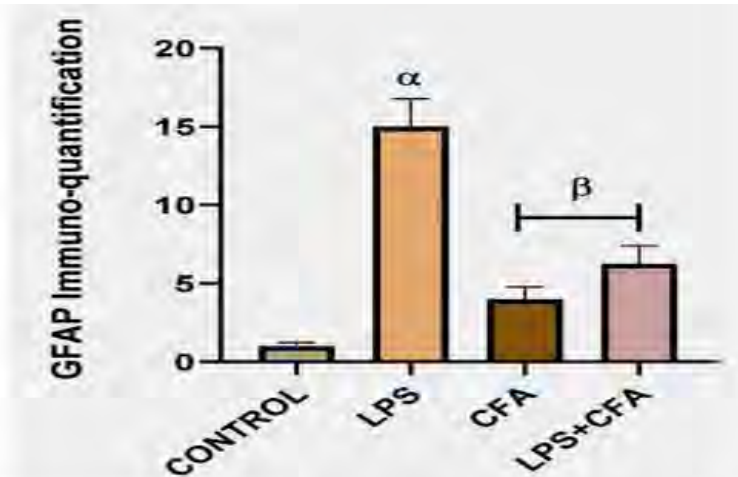


Fig 3: The bar chart depicts the number of GFAP immunoreactivity in control and treated groups, Bars are Mean \pm SE. α denotes significant increase ($p < 0.05$) compared to control group. β denotes significant decrease ($p < 0.05$) compared to LPS only treated group. One-way ANOVA followed by Tukey test .

Quantification of immuno-expressed IBA1

The present study shows increased Iba1 immunoreactivity in the LPS-group (7.17 ± 0.18) compared to the control group (3.09 ± 0.59), CFA-group (4.00 ± 0.47), and LPS + CFA-group (4.14 ± 0.39). The CFA-group (4.00 ± 0.47) and LPS + CFA-group (4.14 ± 0.39) showed no significant difference in immunoreactivity when compared to the control-group (3.09 ± 0.59) (**Fig. 4**).

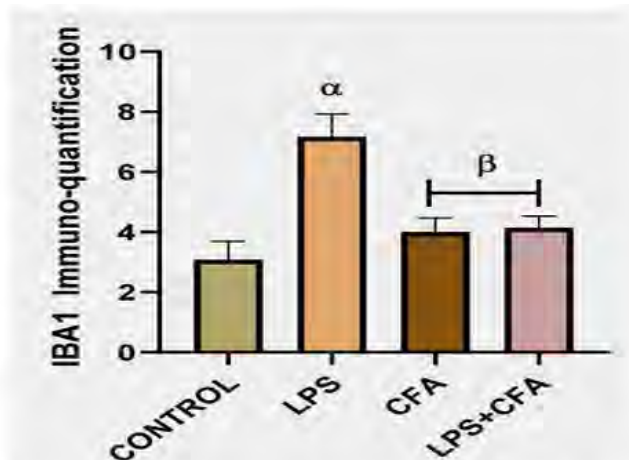


Figure 4: The bar chart depicts the number of IBA1 immunoreactivity in experimental groups, Bars are Mean \pm SE. α denotes significant increase ($p < 0.05$) compared to control group. β denotes significant decrease ($p < 0.05$) compared to LPS only treated group. One-way ANOVA followed by Tukey test.

Discussion

The current study examines the anti-inflammatory effect of caffeic acid (CFA) on LPS-induced cerebral neuroinflammation by quantifying astrocyte and microglial cell activation. Lipopolysaccharide (LPS) is the polysaccharide component of the gram-negative bacterial cell wall. Once recognized by the immune system, LPS elicits a proinflammatory response [31] and has thus become extensively used in research to induce neuroinflammation [16]. Neuroinflammation plays an important role in the etiology and progression of neurodegenerative diseases, including Parkinson's disease [8]. However, CFA possesses unique biological characteristics, including antioxidant, anti-inflammation, and immune regulation [20]. It also exerts strong antioxidant effects by blocking reactive oxygen species [5]. CFA's anti-inflammatory and antioxidant activity have been demonstrated in many cells [7]. In addition, CFA was shown to exert direct neuronal protection through up-regulation of endogenous antioxidants and modulation of inflammatory homeostasis [17]. While several studies have used osmotin [2] and dihydrotestosterone [30], among other anti-inflammatory agents, to mitigate the neuroinflammatory effect of LPS, none have reported the anti-inflammatory activity of CFA in LPS-induced cerebral neuroinflammation. Therefore, this study aims to demonstrate that CFA can attenuate cerebral neuroinflammation following LPS-induced neurotoxicity in experimental mice.

Neuronal loss in the cortex is closely related to cognitive and behavioral dysfunction. Accumulating evidence indicates that systemic LPS injection in mice induces cognitive deficits, including spatial learning and memory impairment, as measured by the open field test (OFT), which is the most popular test of cerebral-dependent cognitive functions. The current study utilizes OFT to measure locomotive activity in experimental mice. The reported data indicate that LPS treatment decreased distance travelled, total rearing number, and increased total grooming time in mice, suggesting decreased locomotor activity, a clinical symptom of Parkinson's disease [8]. Previous studies have shown that LPS administration in mice affects locomotors and motor activity [1]. Herein, our results showed that locomotors' activity was improved by CFA, as indicated by increased distance travelled and total rearing time, and reduced total grooming time in the LPS + CFA-group. Previous studies indicate that the cerebral cortex undergoes neurodegenerative changes following LPS induction [1]. In the present study, the light microscopic examination of H&E-stained cerebral sections of the LPS-treated group revealed marked neurodegenerative changes in the pyramidal neurons of the cerebral cortex. The pyramidal cells were undergoing karyolysis and had no visible nuclei. Also, there are several visible cytoplasmic vacuoles. Due to the anti-inflammatory role of CFA in previous works, this study hypothesizes that treatment with CFA could help rescue the neurodegenerative changes observed in the cerebral cortex following LPS exposure. This study demonstrated restorative changes in the histological features of LPS-treated mice following CFA administration.

Chronic neuroinflammation mediates neuronal damage and apoptosis in the pathogenesis of neurodegenerative diseases, including Parkinson's disease [15]. Aberrant glial activation and neuroinflammation play a prominent role in the pathogenesis of neurodegenerative diseases [30]. This study presents data that supports neuroinflammation in the cerebral cortex following LPS-induced neurotoxicity. To quantify the extent of neuroinflammatory changes in the cerebral cortex, GFAP and Iba1 was demonstrated via immunohistochemistry [24].

Astrocytes participate in the generation and control of inflammatory mediators. The activation states of astrocytes are determined based on increased GFAP immunolabeling [24]. GFAP is a key component of the astrocyte's cytoskeleton that maintains cell integrity and resilience. There was a significant increase in GFAP expression following LPS exposure in mice cortex, consistent with Khan et al. findings [12]. CFA attenuated cerebral inflammation by down-regulating GFAP activation. As resident macrophages in the brain, microglia, typically marked by Iba1, can be activated and trigger the innate immune response by sensing exogenous neurotoxic substances, such as LPS and proinflammatory stimuli. Rapid microglial activation and associated inflammatory reactions are responses to combat the effect of insults and contribute to immune defense and tissue repair in the central nervous system (CNS) [22]. This acute activation is considered protective. By contrast, persistent microglial activation will ultimately result in the vast production of proinflammatory mediators, chemokines, and the recruitment of peripheral immune cells [18] to the brain that characterizes chronic neurodegenerative diseases, including Parkinson's disease and Alzheimer's disease [23]. In this study, over-expression of cerebral Iba1 was established following LPS-induced neurotoxicity, consistent with other findings [12, 24]. In addition, there was a significant reduction in Iba1 expression in treatment with CFA. Therefore, CFA-induced down-regulation of microglia and astrocytes, as evident by reduced Iba1 and GFAP levels, respectively, shows that CFA could be a potential therapeutic agent to mitigate cerebral neurotoxicity.

Conclusion

In conclusion, this study presents novel evidence that CFA can mitigate LPS-induced neuroinflammation and neurodegeneration in the cerebral cortex of experimental mice via reduced astrocyte and microglia activation, consequently rescuing LPS-induced locomotive impairment. In summary, the study results provide evidence that the anti-inflammatory property of CFA can enable it to exert neuroprotection on the cerebral cortex. Therefore, CFA should be extensively studied as it may be a therapeutic agent against neuroinflammation and neurodegenerative diseases, such as Parkinson's.

References

1. Arab, Z., M. Hosseini, F. Mashayekhi, A. Anaeigoudari A. Zataria multiflora extract reverses lipopolysaccharide-induced anxiety and depression behaviors in rats. – *Avicenna J. Phytomed.*, **10**(1), 2020, 78-88.
2. Badshah, H., T. Ali, M. O. Kim. Osmotin attenuates LPS-induced neuroinflammation and memory impairments via the TLR4/NFκB signaling pathway. – *Sci. Rep.*, **6**, 2016, 24493.
3. Barros Silva, R., N. A. Santos, N. M. Martins, D. A. Ferreira, F. Jr. Barbosa, V. C. Oliveira Souza, A. Kinoshita, O. Baffa, E. Del-Bel, A. C. Santos. Caffeic acid phenethyl ester protects against the dopaminergic neuronal loss induced by 6-hydroxydopamine in rats. – *Neuroscience*, **233**, 2013, 86-94.
4. Beier, E. E., M. Neal, G. Alam, M. Edler, L-J. Wu, J. R. Richardson. Alternative microglial activation is associated with cessation of progressive dopamine neuron loss in mice systemically administered lipopolysaccharide. – *Neurobiol. Dis.*, **108**, 2017, 115-127.

5. Cao, C., L. Wang, X. Lin, M. Mamcarz, C. Zhang, G. Bai, J. Nong, S. Sussman, G. Arendash. Caffeine synergizes with another coffee component to increase plasma GCSF: Linkage to cognitive benefits in Alzheimer's mice. – *J. Alzheimers Dis.*, **25**(2), 2011, 323-335.
6. Drury, R. A., E. A. Wallington, R. Cancerson (Eds.). *Carlton's histopathological techniques*, London, Oxford University Press, 1976, 435, 25-28.
7. Fontanilla, C., Z. Ma, X. Wei, J. Klotsche, L. Zhao, P. Wisniewski, R. C. Dodel, M. R. Farlow, W. H. Oertel, Y. Du. Caffeic acid phenethyl ester prevents 1-methyl-4-phenyl-1, 2, 3, 6-tetrahydropyridine induced neurodegeneration. – *Neuroscience*, **188**, 2011, 135-141.
8. Glass, C. K., K. Saijo, B. Winner, M. C. Marchetto, F. H. Gage. Mechanisms underlying inflammation in neurodegeneration. – *Cell*, **140**(6), 2010, 918-934.
9. Gray, T., N. Hand. Enzyme histochemistry. – In: *The science of laboratory diagnosis* (Eds. D. Burnett, J. Crocker), Chichester, John Wiley & Sons Ltd, 2005, 27-30.
10. Iravani, M. M., K. Kashefi, P. Mander, S. Rose, P. Jenner. Involvement of inducible nitric oxide synthase in inflammation-induced dopaminergic neurodegeneration. – *Neuroscience*, **110**(1), 2002, 49-58.
11. Iteire, K. A., A. T. Sowole, B. Ogunlade. Exposure to pyrethroids induces behavioral impairments, neurofibrillary tangles and tau pathology in Alzheimer's type neurodegeneration in adult Wistar rats. – *Drug Chem. Toxicol.*, **45**(2), 2022, 839-849.
12. Khan, M. S., T. Ali, M. W. Kim, M. H. Jo, J. Chung, M. O. Kim. Anthocyanins improve hippocampus-dependent memory function and prevent neurodegeneration via JNK/Akt/GSK3 β signaling in LPS-treated adult mice. – *Mol. Neurobiol.*, **56**(1), 2019, 671-687.
13. Kinra, M. D., J. Arora, K. Mudgal, C. M. Pai, M. Rao. Nampoothiri effect of caffeic acid on ischemia-reperfusion-induced acute renal failure in rats. – *Pharmacol.*, **103**(5-6), 2019, 315-319.
14. Kouli, A., K. M. Torsney, W.-L. Kuan. Parkinson's Disease: Etiology, Neuropathology, and Pathogenesis. – In: *Parkinson's disease: pathogenesis and clinical aspects* (Eds. T. B. Stoker, J. C. Greenland), Brisbane, Codon Publications, 2018, 3-26.
15. Lei, Y., Z. Renyuan. Effects of androgens on the amyloid- β protein in Alzheimer's disease. – *Endocrinology*, **159**(12), 2018, 3885-3894.
16. Lopes, P. C. LPS and neuroinflammation: a matter of timing. – *Inflammopharmacology*, **24**(5), 2016, 291-293.
17. Lu, D. Y., B.-R. Huang, W.-L. Yeh, H.-Y. Lin, S.-S. Huang, Y.-S. Liu, Y.-H. Kuo. Anti-neuroinflammatory effect of a novel caffeine derivative, KS370G, in microglial cells. – *Mol. Neurobiol.*, **48**(3), 2013, 863-874.
18. Maa, M.-C., T.-H. Leu. Activation of Toll-like receptors induces macrophage migration via the iNOS/Src/FAK pathway. – *BioMedicine*, **1**(1), 2011, 11-15.
19. Myers, D., E. Allen, A. Essa, M. Gbadamosi-Akintele. Rapidly growing squamous cell carcinoma of the tongue. – *Cureus*, **12**(3), 2020, e7164.
20. Ning, X., Y. Guo, X. Ma, R. Zhu, C. Tian, Z. Zhang, X. Wang, Z. Ma, J. Liu. Design, synthesis and pharmacological evaluation of (E)-3,4-dihydroxy styryl sulfonamides derivatives as multifunctional neuroprotective agents against oxidative and inflammatory injury. – *Bioorg. Med. Chem.*, **21**(17), 2013, 5589-5597.
21. Olsen, L. K., A. G. Cairns, J. Aden, N. Moriarty, S. Cabre, V. R. Alamilla, F. Almqvist, E. Dowd, D. P. McKernan. Viral mimetic priming enhances alpha-synuclein-induced degeneration: implications for Parkinson's disease. – *Brain Behav. Immun.*, **80**, 2019, 525-535.
22. Olson, J. K., S. D. Miller. Microglia initiate central nervous system innate and adaptive immune responses through multiple TLRs. – *J. Immunol.*, **173**(6), 2004, 3916-3924.

23. **Politis, M., N. Pavese, Y. F. Tai, L. Kiferle, S. L. Mason, D. J. Brooks, S. J. Tabrizi, R. A. Barker, P. Piccini.** Microglial activation in cognitive function regions predicts onset of Huntington's disease: a multimodal imaging study. – *Hum. Brain Mapp.*, **32**(2), 2011, 258-270.
24. **Shah, M.-A., D.-J. Park, J.-B. Kang, M.-O. Kim, P.-O. Koh.** Baicalin attenuates lipopolysaccharide-induced neuroinflammation in the cerebral cortex of mice via inhibiting nuclear factor kappa B (NF- κ B) activation. – *J. Vet. Med. Sci.*, **81**(9), 2019, 1359-1367.
25. **Silva, T., C. Oliveira, F. Borges.** Caffeic acid derivatives, analogs, and applications: a patent review (2009-2013). – *Expert Opin. Ther. Pat.*, **24**(11), 2014, 1257-1270.
26. **Son, S., B. A. Lewis.** Free radical scavenging and antioxidant activity of caffeic acid amide and ester analogs: structure-activity relationship. – *J. Agric. Food Chem.*, **50**(3), 2002, 468-472.
27. **Szwajgier, D., K. Borowiec, K. Pustelniak.** The neuroprotective effects of phenolic acids: molecular mechanism of action. – *Nutrients*, **9**(5), 2017, 477.
28. **Thibault, O., J. C. Gant, P. W. Landfield.** Expansion of the calcium hypothesis of brain aging and Alzheimer's disease: minding the store. – *Aging Cell*, **6**(3), 2007, 307-317.
29. **Van Der Heyden, J. A., T. J. Zethof, B. Olivier.** Stress-induced hyperthermia in singly-housed mice. – *Physiol. Behav.*, **62**(3), 1997, 463-470.
30. **Yang, L., R. Zhou, Y. Tong, P. Chen, Y. Shen, S. Miao, X. Liu.** Neuroprotection by dihydrotestosterone in LPS-induced neuroinflammation. – *Neurobiol. Dis.*, **140**, 2020, 104814.
31. **Zhang, G., S. Ghosh.** Molecular mechanisms of NF- κ B activation induced by bacterial lipopolysaccharide through Toll-like receptors. – *J. Endotoxin Res.*, **6**(6), 2000, 453-457.
32. **Zhao, J., S. Pati, J. B. Redell, M. Zhang, A. N. Moore, P. K. Dash.** Caffeic acid phenethyl ester protects blood-brain barrier integrity and reduces contusion volume in rodent models of traumatic brain injury. – *J. Neurotrauma*, **29**(6), 2012, 1209-1218.

The Selective Androgen Receptor Modulator Ostarine Increases the Extracellular Matrix in the Myocardium Without Altering it in the EDL Muscle

Fanka Gerginska^{1}, Slavi Delchev¹, Veselin Vasilev², Katerina Georgieva², Nikolay Boyadjiev²*

¹*Department of Anatomy, Histology and Embryology, Faculty of Medicine, Medical University-Plovdiv, Plovdiv, Bulgaria;*

²*Department of Physiology, Faculty of Medicine, Medical University-Plovdiv, Plovdiv Bulgaria*

*Corresponding author e-mail: Fanka.Gerginska@mu-plovdiv.bg

The selective androgen receptor modulators (SARMs) are androgen receptor (AR) ligands that bind to AR and exhibit a pronounced anabolic effect. They are used in sports to improve physical performance. Their adverse side effects are not well studied. The aim of this study was to investigate the effect of SARMs on the myocardium and a skeletal muscle. Male Wistar rats were divided into 2 groups: control (SARM–) and group receiving SARM (Ostarine for 8 weeks) (SARM+). At the end of the experiment, Azan staining on sections of myocardium and extensor digitorum longus muscle (EDL) was applied to account for the collagen distribution. The heart weight in SARM+ group was higher than controls. The amount of extracellular matrix (ECM) in the SARM+ myocardium was increased, while in EDL it was not altered. The observed increase of the heart weight and the amount of ECM can be taken as an indication for side effect of SARM.

Key words: SARM, collagen, myocardium, EDL, side effects

Introduction

SARMs are characterized by predominant anabolic effects and relatively limited androgenic ones. SARMs accomplish their effects by genomic mechanism. They are widely used in sports to improve physical performance and athletic achievements [7]. In addition, they have potential use in patients with a number of diseases – amyotrophic lateral sclerosis (Lou Gehrig's disease), dermatomyositis, osteoporosis, breast cancer, sarcopenia, various types of cachexia, benign prostatic hyperplasia and hypogonadism [2, 3, 11]. Some of the most commonly used SARMs include Ostarine and Andarine [6]. Their adverse side effects are not well studied. The aim of this study was to investigate

the effect of SARMs on the extracellular matrix (ECM) of myocardium and skeletal muscles.

Material and Methods

Young, sexually mature male Wistar rats, weighing 140-200 g, aged three to four months, were used in the experiment. The animals were divided into two groups: a control group without SARM (SARM–, $n = 6$) and a group receiving SARM (SARM+, $n = 6$). Throughout the experiment, rats were housed in individual metabolic cages, which made it possible to determine the amount of food eaten and the amount of SARM (Ostarine) consumed, taken orally once daily 5 times a week at a dose of 0.4 mg / kg with supplemental food. Water and food were given ad libitum. A light/dark cycle and a temperature of $23 \pm 1^\circ \text{C}$ were maintained for 12 h. The experimental protocol was approved by the Ethical Committee on Human and Animal Experimentation of the Medical University-Plovdiv, and the Commission for Ethical Treatment of Animals at the Bulgarian Food Safety Agency. The rats were reared and all experimental procedures were performed according to the recommendations of the European Commission for the protection and humane treatment of laboratory animals. At the end of the experiment, all rats were decapitated after anaesthesia with Ketamine at a dose of $180 \text{ mg} \times \text{kg}^{-1}$ i.p. and Xylazine at a dose of $15 \text{ mg} \times \text{kg}^{-1}$ i.p., having previously measured their body weight. A guillotine for small experimental animals (HUGO SACHS ELECTRONIC D-79232 March F.R., Germany) was used for decapitation.

After dissection, heart and muscles of each animal were weighed and the ratio of organ weight to body weight was calculated. Materials from the wall of the left ventricle of the heart and the whole EDLs were fixed in neutral formalin 10% for 24 hours and embedded in paraffin. Paraffin sections, 5 μm thick, after deparaffinization and rehydration were stained with Azan by Heidenhain (1915). With the help of image analysis software (“DP-Soft” 3.2, Olympus, Japan) using a measuring grid (19 \times 25 fields) at $\times 200$ magnification, the relative percentage distribution of collagen fibres in the ECM of muscles was calculated according to the formula $x = (n/475) \cdot 100$, where n is the number of squares containing collagen fibres and 475 is the total number of squares [9]. Student’s t-test was applied for statistical processing, and a P value ≤ 0.05 was considered statistically significant.

Results

Heart weights in the SARM+ group were higher than SARM– (strong tendency was found out, $P=0.06$), (**Fig. 1**). Statistical analysis of the heart/body weight ratio did not reveal an effect of the application of SARM ($P>0.05$). The weight of EDL didn’t show differences between the groups. In the myocardium of the control animals, collagen fibres of the endomysium were distributed in fine longitudinal stripes between the cardiomyocytes, and those of the perimysium were circularly arranged around the blood vessels in the perivascular spaces (**Fig. 2A, B**). A significant increase in the amount of collagen fibres between the cardiomyocytes and around the conducting coronary arteries and arterioles was found in the myocardium of animals receiving

SARM (**Fig. 2C, D**). Collagen fibres, which are missing in the control group, were also noted around smaller arterioles in myocardium of SARM+ animals. The amount of ECM in EDL of the SARM+ animals was not altered (**Fig. 2E, F**).

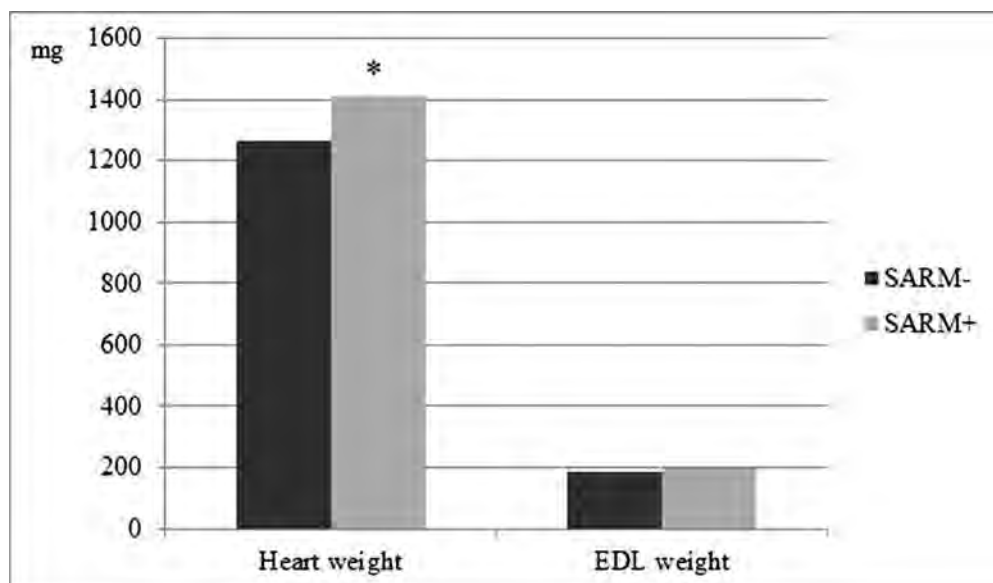


Fig. 1. Heart and EDL weight (mg) at the end of the experiment. * $P = 0.06$ v/s SARM-.

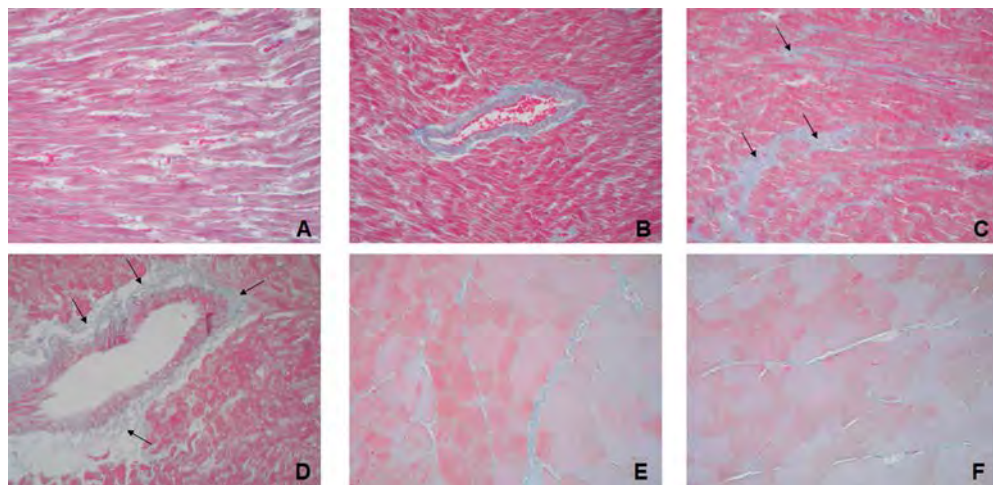


Fig. 2. Sections of myocardium (A-D) and EDL (E, F) of animals from the experimental groups. Arrows – collagen fibres in myocardium of SARM+ group (C, D). Azan staining (*Magn.* $\times 200$).

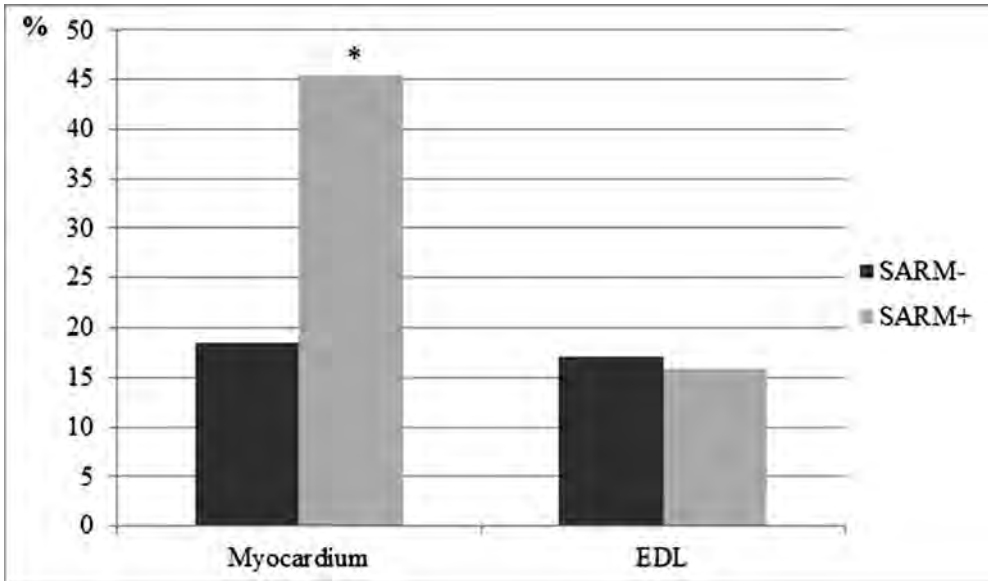


Fig. 3. Relative percentage distribution of collagen fibres in the myocardium and EDL of the experimental groups in Azan stained sections. *P < 0.001 v/s SARM-.

Discussion

Myocardial collagen is a complex three-dimensional matrix that surrounds and connects individual cardiomyocytes, thus facilitating their contraction and promoting normal systolic performance [1, 4]. The results of our experiment show that the application of SARM for an 8-week period affected the amount of collagen in the endomysium. Interstitial fibroblasts are mainly responsible for the synthesis of type I and type III collagen fibres present in the endomysium [4]. The dose and duration of Ostarine we used have activated processes of enhanced collagen synthesis by fibroblasts. The increase in collagen fibres around arterial vessels in the myocardium of SARM receiving animals would be difficult to assess according this duration of administration. Increases in perivascular collagen have also been reported in anabolic steroid treated rats [10].

As a potential mechanism to explain the predominant increase in collagen around conducting coronary arteries and arterioles, the ability of vascular smooth muscle cells to produce collagen (mainly type III) may be considered. The Ostarine administration probably activated AR in the nuclei of these cells [7]. If this trend persists with prolonged usage, then certainly the perivascular accumulation of collagen would lead to limited vasodilation, disorders of coronary blood flow and a reduced oxygen supply to cardiomyocytes. Similar changes are common in pathological myocardial hypertrophy [8]. Initial signs of hypertrophy were found in animals of the SARM-treated group, such as an increase in heart weight. Comparable data on cardiac hypertrophy after the use of anabolic steroid with SARMs like properties have been found by other authors [5].

Conclusion

The observed increase in heart weight and amount of the extracellular matrix in the myocardium after SARMs treatment can be considered as an initial myocardial fibrosis and potential side effect. Further research would help to clarify the nature of the side effects of these drugs.

Acknowledgements: The study was funded by project №: HO – 06/2021 by Medical University – Plovdiv.

References

1. Baicu, C. F., J. D. Stroud, V. A. Livesay, E. Hapke, J. Holder, F. G. Spinale, M. R. Zile. Changes in extracellular collagen matrix alter myocardial systolic performance. – *Am. J. Physiol. Heart Circ. Physiol.*, **284**, 2003, H122-H132.
2. Chen, J., J. Kim, J. T. Dalton. Discovery and therapeutic promise of selective androgen receptor modulators. – *Mol. Interv.*, **5**, 2005, 173-188.
3. Christiansen, A. R., L. I. Lipshultz, J. M. Hotaling, A. W. Pastuszak. Selective androgen receptor modulators: the future of androgen therapy? – *Transl. Androl. Urol.*, **9**, 2020, S135-S148.
4. De Souza, R. R. Aging of myocardial collagen. – *Biogerontology*, **3**, 2002, 325-335.
5. Diel, P., A. Friedel, H. Geyer, M. Kamber, U. Laudénbach-Leschowsky, W. Schänzer, M. Thevis, G. Vollmer, O. Zierau. Characterisation of the pharmacological profile of desoxymethyltestosterone (Madol), a steroid misused for doping. – *Toxicol. Lett.*, **169(1)**, 2007, 64-71.
6. Geyer, H., W. Schänzer, M. Thevis. Anabolic agents: recent strategies for their detection and protection from inadvertent doping. – *Br. J. Sports Med.*, **48(10)**, 2014, 820-826.
7. Machek, S. B., T. D. Cardaci, D. T. Wilburn, D. S. Willoughby. Considerations, possible contraindications, and potential mechanisms for deleterious effect in recreational and athletic use of selective androgen receptor modulators (SARMs) in lieu of anabolic androgenic steroids: A narrative review. – *Steroids*, **164**, 2020, 108753.
8. Morisco, C., J. Sadoshima, B. Trimarco, R. Arora, D. E. Vatner, S. F. Vatner. Is treating cardiac hypertrophy salutary or detrimental: the two faces of Janus. – *Am. J. Physiol. Heart Circ. Physiol.*, **284**, 2003, H1043-H1047.
9. Sun, J., L. Fu, X. Tang, Y. Han, D. Ma, J. Cao, N. Kang, H. Ji. Testosterone modulation of cardiac β -adrenergic signals in a rat model of heart failure. – *Gen. Comp. Endocrinol.*, **172(3)**, 2011, 518-525.
10. Trifunovic, B., A. J. Woodiwiss, M. Duffield, G. R. Norton. Novel attributes of an androgenic steroid-mediated increase in cardiac end diastolic stiffness in rats. – *Can. J. Physiol. Pharmacol.*, **76(6)**, 1998, 657-664.
11. Zhang, X., Z. Sui. Deciphering the selective androgen receptor modulators paradigm. – *Expert Opin. Drug Discov.*, **8(2)**, 2013, 191-218.

Age-Dependent Differences in Behavioral Responses: the Impact of Hsp70 and Hsp90 in the Frontal Cortex

Desislava Krushovlieva, Simeon Georgiev, Petja Ivanova, Zlatina Petkova, Tzveta Stoyanova, Jana Tchekalarova*

Institute of Neurobiology, Bulgarian Academy of Sciences, Sofia, Bulgaria

*Corresponding author e-mail: d.krushovlieva@inb.bas.bg

Age-related neurological complications are common and affect the quality of life. The present study was designed to investigate age-dependent changes in behavioral responses and the role of protective heat shock proteins (Hsp)s 70 and Hsp 90, which expression in the frontal cortex (FC) might be vulnerable to aging processes in rats. We report that 3-month-old rats exhibited the highest motor activity and lowest anxiety (increased distance, time and number of entries in the open arms of the elevated plus maze) compared to 14- and 18-month-old rats. Moreover, old rats showed a decreased level of Hsp 70 and Hsp 90 in the FC compared to young adult rats. These findings suggest that the aging process is accompanied by changes in emotional status that might be associated with a decreased function of protective chaperone proteins in the FC.

Key words: aging, behavioral responses, Hsp70, Hsp 90, rat

Introduction

Ageing is a natural phenomenon that involves many biological changes, including increased oxidative stress, DNA damage and protein misfolding, mitochondrial dysfunction, impaired immune responses, and vascular abnormalities [8]. Literature studies show altered chaperone (Hsp) activity, which in turn leads to oxidative status disturbances, is key to aging-related processes [3,5]. The reduction of inducible Hsp 70 can be a biomarker of altered oxidative status and ROS toxicity [4]. Hsp 90 also has a cellular protective effect as a key molecular chaperone involved in the cytoprotection of eukaryotic cells during stress [2]. In the present study, we aimed to evaluate the role of Hsp 70 and Hsp 90 expression in the frontal cortex (FC) and their link with presumed age-dependent changes in behavioral responses related to anxiety.

Materials and Methods

The procedures used in this study agree with the European Communities Council Directives of 24 November 1986 (86/609/EEC). The experimental design was approved by BFSA (contract # D-65/02.05.2017).

Experimental animals

The experiments were performed on male Wistar rats (Breeding vivarium at INB, BAS), at three ages: 1) young adults, 3-6 months, n= 10; 2) middle-aged, 14-17 months, n= 10; 3) old, 18-21 months, n= 10, kept in standard conditions: temperature: 21 °C, 50-60% humidity.

Behavioural tests

The Elevated plus maze (EPM) test is used to assess anxiety-related behavior. The apparatus consists of a central area, two closed arms and two open arms, positioned perpendicularly to each other. The preference for being in open arms over closed arms (expressed as count of entries, distance and time spent in the open arms) is calculated to measure anxiety-like behavior.

Biochemical analysis of brain homogenates

The frontal cortex was rapidly dissected, inserted in liquid nitrogen and stored at -20 °C until biochemical analysis by ELISA Kit (Rat HSP70, Rat HSP90, Cat: ELK8411) according to the manufacturer's instructions.

Statistical analysis

Data are given as mean \pm S.E.M. One-way ANOVA followed by Duncan post hoc test was used. SigmaStat®, GraphPad Prism 6 software were applied for statistical analyses.

Results and Discussion

Total motor activity was significantly decreased with aging. Young adult 3-month-old rats demonstrated the highest motor activity (total distance in closed and open arms) compared to the 18-month-old rat (**Fig. 1A**). Moreover, age-related elevation of the level of anxiety was detected (distance in open arms, time in open arms and number of entries) (**Fig. 1 B, C, D**).

The age-related behavioral changes are reported in animal models and in humans [1,6,7]. Our data confirmed previous reports revealing that aging is associated with decreased motor activity and elevated anxiety level [1,7].

Age-dependent changes in the expression of Hsp 70 and Hsp 90 was detected in the FC. The youngest 3-month-old rats and middle aged rats exhibited the higher expression of Hsp 70 compared to the 18-month-old rats (**Fig. 2A**). In addition, the drop in the level of Hsp 90 was demonstrated in the oldest rat group (**Fig. 2B**). *Post hoc* test confirmed that 3- and 14-month old rats had elevated Hsp 90 compared to 18-month old rats.

The aging process is associated with vulnerability to neurodegeneration and decreased brain activity that neurons should cause misfolded proteins over time. Recently, Yang et al. [9] reported that Hsp70 expression in the brain was closely related to the aging process in mice, while its recovery could alleviate mutant protein toxicity. Our results confirmed previous reports that decreased levels of Hsp 70 and Hsp 90 in the FC are closely associated with rats' aging. Moreover, the age-related changes in emotional responses in rats are suggested to be mediated by decreased function of the Hsp70 and Hsp90 in the FC.

Acknowledgements: This work was supported by the National Science Fund of Bulgaria (research grant # KP-06-H41/4, 2020).

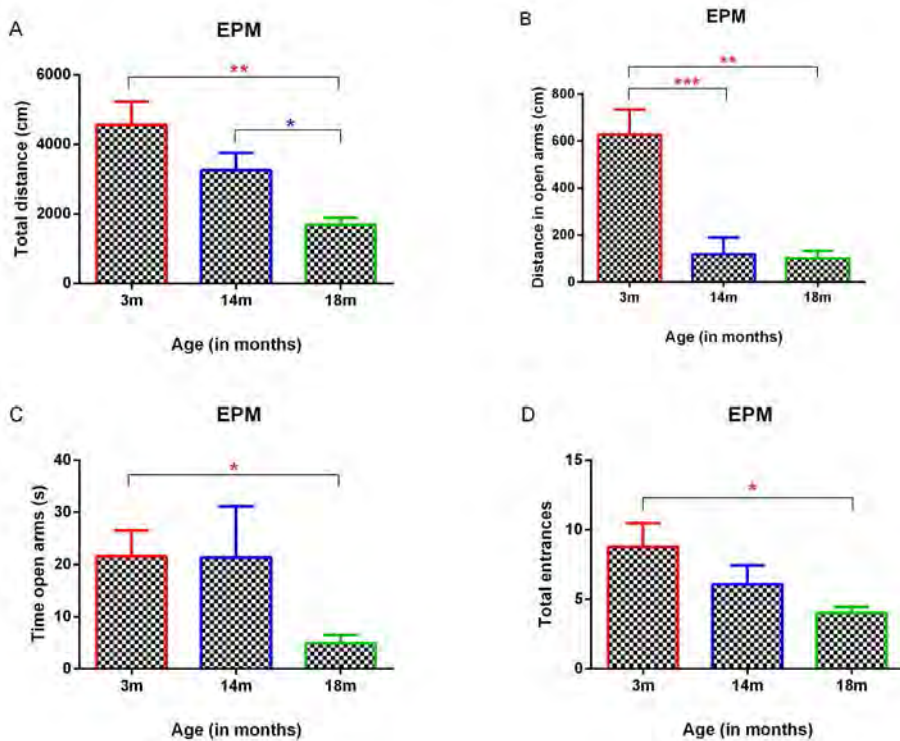


Fig. 1. Effects of aging on motor activity and anxiety parameters in the elevated plus maze test (A) total distance; (B) distance in the open arms (cm); (C) time in the open arms (s); (D) number of entries in the open arms. Data are given as mean±SEM. ($F = 4.956$, $p = 0.0147$). Young adult rats demonstrated the highest motor activity (total distance in closed and open arms) compared to aged rat ($p = 0.0091$, 18-month-old rats vs 3-month-old rats ; $p = 0.0458$, 18-month-old rats vs 14-month-old rats) (Fig. 1A). Moreover, age-associated elevation of the level of anxiety was detected (distance in open arms: $F = 13.33$, $p = 0.0002$; $p = 0.0011$, 18-month-old rats vs 3-month-old rats ; $p = 0.0009$, 14-month-old rats vs 3-month-old rats; time in open arms: $p = 0.0295$, 18-month-old rats vs 3-month-old rats; number of entries: $p = 0.0426$, 18-month-old rats vs 3-month-old rats) (Fig. 1 B, C, D).

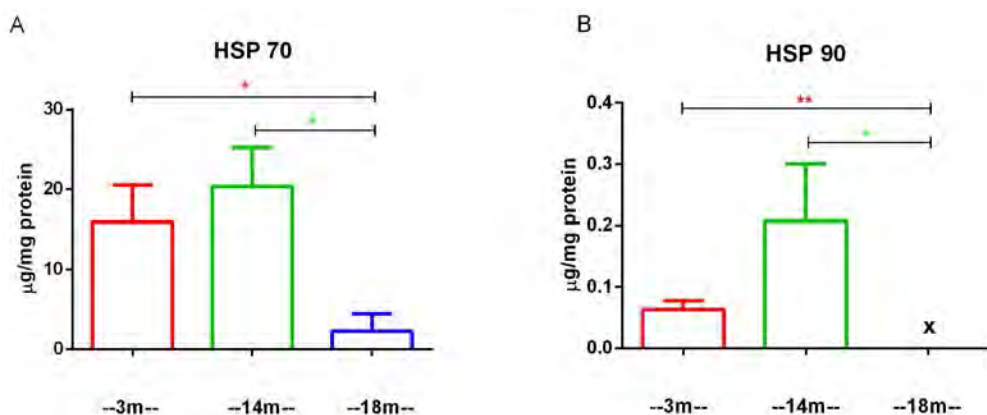


Fig. 2. The aging process affects the expression and function of the chaperone proteins Hsp70 and Hsp 90 in the frontal cortex. Data are given as mean \pm SEM. $p = 0.0333$, 3-month-old rats vs 18-month-old rats; $p = 0.0106$, 14-month-old rats vs 18-month-old rats (**A**). $p = 0.0073$, 3-month-old rats vs 18-month-old rats; $p = 0.0391$, 14-month-old rats vs 18-month-old rats (**B**).

References

1. Emerich, D. F., P. McDermott, P. Krueger, M. Banks, J. Zhao, J. Marszalowski, B. Frydel, S. R. Winn, P. R. Sanberg. Locomotion of aged rats: Relationship to neurochemical but not morphological changes in nigrostriatal dopaminergic neurons. – *Brain Res. Bull.*, **32**, 1993, 477-486.
2. Ghadban, T., J. L. Dibbern, M. Reeh, J. T. Miro, T. Y. Tsui, U. Wellner, J. R., Izbicki, C. Güngör, Y. K. Vashist. HSP90 is a promising target in gemcitabine and 5-fluorouracil resistant pancreatic cancer. – *Apoptosis*, **22**, 2017, 369-380.
3. Hoehn, R., M. Monse, E. Pohl, S. Wranik, B. Wilker, S. Keitsch, M. Soddemann, J. Kornhuber, M. Kohnen, M. J. Edwards, H. Grassméc, E. Gulbins. Melatonin acts as an antidepressant by inhibition of the acid sphingomyelinase/Ceramide System. – *Neurosignals*, **24**, 2016, 48-58.
4. Moniruzzaman, M., P. Midday, A. Dhara, D. Das, I. Ghosal, D. Mukherjee, S. Chakraborty. Change in redox state and heat shock protein expression in an Indian major carp Cirrhinus cirrhosus exposed to zinc and lead. – *J. Toxicol. Sci.*, **42**, 2017, 731-740.
5. Moniruzzaman, M., I. Ghosal, D. Das, S. Chakraborty. Melatonin ameliorates H₂O₂-induced oxidative stress through modulation of Erk/Akt/ NFkB pathway. – *Biol. Res.*, **51** (1), 2018, 17.
6. Murray, A. M., J. L. Waddington. Age-related changes in the regulation of behavior by D-1: D-2 dopamine receptor interactions. – *Neurobiol. Aging*, **12**, 1991, 431-435.
7. Sudakov, S. K., E. V. Alekseeva, G. A. Nazarova, V. G. Bashkatova. Age-related individual behavioural characteristics of adult wistar rats. – *Animals*, **2021**, *11*, 2282.
8. Sun, M., S. J. McDonald, R. D. Brady, L. Collins-Praino, G. R. Yamakawa, M. Monif, T. J. O'Brien, G. Cloud, C. G. Sobey, R. Mychasiuk, D. J. Loane, S. R. Shultz. The need to incorporate aged animals into the preclinical modeling of neurological conditions. – *Neurosci. Biobehav. Rev.*, **109**, 2020, 114-128.
9. Yang, S., S. Huang, M. A. Gaertig, X. J. Li, S. Li. Age-dependent decrease in chaperone activity impairs MANF expression, leading to Purkinje cell degeneration in inducible SCA17 mice. – *Neuron*, **81**, 2014, 349-65.

Preliminary Observations on Apoptotic Fragmentation of Cultured Mouse Oocytes

Maya Markova^{1*}, Anton Kolarov¹, Irina Chakarova¹, Valentina Hadzhinesheva¹, Ralitsa Zhivkova¹, Stefka Delimitreva¹, Milena Mourdjeva², Venera Nikolova¹

¹Department of Biology, Medical Faculty, Medical University of Sofia, Sofia, Bulgaria

²Department of Molecular Immunology, Institute of Biology and Immunology of Reproduction, Bulgarian Academy of Sciences, Sofia, Bulgaria

*Corresponding author e-mail: mayamarkov@gmail.com

We studied apoptotic fragmentation in ovulated mouse oocytes. Some cells were fixed immediately after isolation, while others were cultured for 3 hours with or without prostaglandin F2 alpha. Membrane organelles, fibrillar actin and DNA were stained with DiOC6, TRITC-phalloidin and Hoechst 33342, respectively. While fragmented cells were generally rare, most of them were in samples treated with prostaglandin F2 α , revealing it as a potential inducer of apoptosis. The chromatin had interphase appearance, indicating exit from meiosis or arrest at germinal vesicle stage. Fragmentation tended to be more pronounced in the vicinity of chromatin, which could be explained with the concentration of actin in the cap region. These preliminary data confirm the active participation of cytoplasm in oocyte apoptosis, and suggest that this process could be induced by mediators of inflammation.

Key words: Oocytes, apoptosis, fragmentation, postovulatory aging, prostaglandin F2 α

Introduction

The morphology of programmed cell death (apoptosis) is characterized by fragmentation of the cell [6]. So far, few studies have addressed this process in mature ovulated oocytes where it is complicated by their metaphase II arrest. After induced apoptosis in ovulated oocytes, cytoplasmic fragmentation reportedly requires activation and exit from meiosis [3]. In line with this, ovulated eggs undergoing degeneration known as postovulatory aging are often activated and exit metaphase II [7], and apoptosis of dividing somatic cells (a.k.a. mitotic catastrophe) typically includes formation of nuclear envelopes around chromosome clusters [9]. Postovulatory aging and apoptosis of oocytes can be influenced by culture conditions such as presence of signaling

molecules. The inflammation-associated signal prostaglandin F2 α has been reported to induce both cell survival [1] and apoptosis [8] in different cell types, and even in the same cell type [2]. We have investigated the impact of prostaglandin F2 α on ovulated mouse oocytes, and the main effect observed was degeneration of the cytoskeleton [4]. In the present study, untreated and prostaglandin F2 α -treated ovulated oocytes were examined for cytoplasmic fragmentation indicating apoptotic cell death.

Materials and Methods

All experiments conformed to legislature and ethical guidelines concerning animal research. Oocytes were obtained as described in [4] and stained as in [5] with small modifications. Briefly, female ICR mice were stimulated with follicle-stimulating hormone and luteinizing hormone, 7.5 IU each. After 48 h, ovulation was induced by 10 IU of human chorionic gonadotropin, and oocytes were collected on the next day. Some of them were immediately fixed in 2% paraformaldehyde, while others were cultured for 3 hours in α -MEM medium with or without prostaglandin F2 α (50 or 100 ng/ml) before fixation. Membrane organelles, fibrillar actin and DNA were visualized using the lipophilic dye DiOC6, TRITC-phalloidin and Hoechst 33342, respectively. Cells were observed by epifluorescence and confocal microscopy.

Results and Discussion

Apoptotic fragmentation was observed in a small proportion of oocytes. It was absent in freshly isolated oocytes and very rare in those cultured without prostaglandin. Though the vast majority of prostaglandin-treated cells also showed no fragmentation, most fragmented cells were prostaglandin-treated, indicating its possible pro-apoptotic action.

Fragmented oocytes had condensed interphase chromatin, indicating either exit from meiosis or arrest at germinal vesicle stage, in accordance with literature data [3]. In some cells, nucleolus-like bodies could be seen (**Fig. 1A**).

When fragmentation was limited to a part of the cell, it tended to be more pronounced in the vicinity of chromatin, which could be explained with the concentration of fibrillar actin in the cap region. In some oocytes, membrane staining was particularly strong in the zona pellucida (**Fig. 1B**). This was most likely due to membrane material released from the fragmenting cell and captured in the zona matrix. These morphological peculiarities of the process, and the role of prostaglandin F2 α as its potential inducer, are not discussed in the literature available to us and so provide new details about apoptosis of ovulated mammalian oocytes.

Conclusions

Our preliminary study confirms the active participation of cytoplasm in oocyte apoptosis, and suggests that apoptotic fragmentation could be induced by mediators of inflammation such as prostaglandin F2 α .

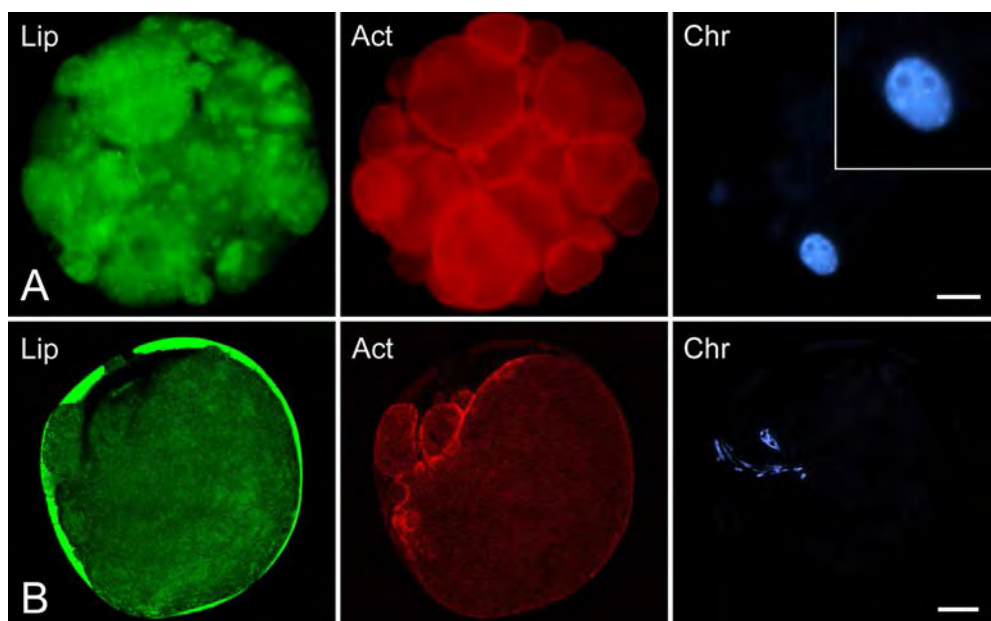


Fig. 1. Apoptotic fragmentation in mouse ovulated oocytes cultured for 3 h, staining for membranes (Lip), fibrillar actin (Act) and DNA (Chr). **A.** Complete fragmentation in a cell treated with 50 ng/ml prostaglandin F2 α , epifluorescence. The main nuclear fragment, shown magnified in the inset, has two nucleolus-like bodies. **B.** Partial fragmentation in the chromatin-containing region of a cell treated with 100 ng/ml prostaglandin F2 α , confocal microscopy. Zona pellucida is brightly stained for membrane material. Bars = 20 μ m.

Acknowledgements: This work was supported by Grant No. D-97/24.06.2020 of the Medical University of Sofia and by the Bulgarian Ministry of Education and Science under the National Program for Research “Young Scientists and Postdoctoral Students”.

References

1. Cheng, Y., L. Peng, X. Deng, T. Li, H. Guo, C. Xu, T. Fang, X. Liu, B. Sun, L. Chen. Prostaglandin F2 α protects against pericyte apoptosis by inhibiting the PI3K/Akt/GSK3 β / β -catenin signaling pathway. – *Ann. Transl. Med.*, **9**, 2021, 1021.
2. Jonezyk, A. W., K. K. Piotrowska-Tomala, D. J. Skarzynski. Effects of prostaglandin F2 α (PGF2 α) on cell-death pathways in the bovine corpus luteum (CL). – *BMC Vet. Res.*, **15**, 2019, 416.
3. Jurisicova, A., H. J. Lee, S. G. D’Estaing, J. Tilly, G. I. Perez. Molecular requirements for doxorubicin-mediated death in murine oocytes. – *Cell Death Differ.*, **13**, 2006, 1466-1474.
4. Kolarov, A. I., V. P. Hadzhinesheva, I. V. Chakarova, R. S. Zhivkova, S. M. Delimitreva, M. D. Markova, M. S. Mourdjeva, V. P. Nikolova. Prostaglandin F2 α causes fast degenerative changes in ovulated mouse oocytes. – *Folia Biol. (Praha)*, **67**, 2021, 208-212.
5. Kolarov, A., N. Mladenov, I. Chakarova, N. Ishkitiev, M. Markova, R. Zhivkova, S. Delimitreva, V. Nikolova. Fast, easy staining method to visualize cell morphology and apoptosis. – *Acta Morphol. Anthropol.*, **27**, 2020, 3-7.

6. **Perez, G. I., X. J. Tao, J. L. Tilly.** Fragmentation and death (a.k.a. apoptosis) of ovulated oocytes. – *Mol. Hum. Reprod.*, **5**, 1999, 414-420.
7. **Prasad, S., M. Tiwari, B. Koch, S. K. Chaube.** Morphological, cellular and molecular changes during postovulatory egg aging in mammals. – *J. Biomed. Sci.*, **22**, 2015, 36.
8. **Sharma, A. K., R. K. Sharma.** Effect of prostaglandins E2 and F2 α on granulosa cell apoptosis in goat ovarian follicles. – *Iran. J. Vet. Res.*, **21**, 2020, 97-102.
9. **Vakifahmetoglu, H., M. Olsson, B. Zhivotovsky.** Death through a tragedy: mitotic catastrophe. – *Cell Death Differ.*, **15**, 2008, 1153-1162.

Interstitial Granulomatous Dermatitis Associated with Systemic Lupus Erythematosus

Valentina Broshtilova¹, Tsvetomila Vuteva¹, Vessel Kantardjiev¹,
Mary Gantcheva^{2, 3 *}

¹Department of Dermatology and Venereology, Military Medical Academy, Sofia, Bulgaria

²Institute of Experimental Morphology, Pathology and Anthropology with Museum,
Bulgarian Academy of Science, Sofia

³Acibadem City Clinic Mladost, Sofia

* Corresponding author e-mail: mary_gant@yahoo.com

Interstitial granulomatous dermatitis is a rare skin condition that presents with erythematous violaceous plaques mostly associated with pruritus and pain. The etiopathogenesis remains obscure, hence, it is often associated with autoimmune systemic diseases and systemic infections. Herein, we present an anecdotal case of interstitial granulomatous dermatitis in a male patient with immune constellation of systemic lupus erythematosus. A comprehensive review of the literature on the possible pathogenetic pathways and clinical peculiarities is also highlighted.

Key words: interstitial granulomatous dermatitis, connective tissue disease, lupus erythematosus

Introduction

Interstitial granulomatous dermatitis (IGD) is a rare disease that clinically presents with a symmetric, erythematous, and violaceous plaques over the lateral trunk, buttocks, and thighs [11]. Fewer than 70 cases have been documented in the literature [6]. Diagnosed via skin biopsy, it is characterized by the infiltration of the mid-to-deep reticular dermis with palisadic histiocytes, linearly distributed among the thick collagen bundles. Variable evidence of phagocytosis may be seen. Neutrophils and eosinophils may also be present in the infiltrate [3].

A clinical entity of unknown etiology, IGD is associated with autoimmune triggers, which include connective tissue disease (lupus erythematosus (LE), rheumatoid arthritis), vitiligo, thyroiditis, and diabetes [4]. It has been hypothesized that the deposition of immune complexes in the dermal vessels induce complement

and neutrophil activation, which leads to dermal collagen damage and evokes palisading granulomatous inflammation in response to the insult [12]. Various medications, particularly calcium channel blockers, lipid-lowering agents, angiotensin-converting enzyme inhibitors, antihistamines, anticonvulsants, and antidepressants have been claimed to induce IGD. Most recently, anti-TNF agents such as etanercept, infliximab, and adalimumab are also implicated [4,7,8,11]. We report a case of histologically verified IGD, associated with systemic lupus erythematosus.

Case report

A 47-year-old man presented to our dermatology department with a history of asymptomatic, symmetric, erythematous plaques with annular configuration, distributed over his inner parts of the arms and lateral trunk with a 8-month duration (**Fig. 1**). He also suffered from photosensitivity, malaise, arthralgia, and non-specific myalgia since the onset. There was no history of drug intake or malignancy. His mother was diagnosed with systemic lupus erythematosus five years ago. A history of a tick bite one year ago in the area of the left thigh was also reported. Due to persistently positive IgM *Borrelia burgdorferi* titers, the patient experienced a series of beta-lactam antibiotics therapeutic courses, which did not alleviate his symptoms and did not affect the dermatological status. The *Borrelia burgdorferi* IgG antibodies showed constant negative trend. In the last two weeks, topical tacrolimus reduced the intensity of the erythema, but did not succeed to resolve the skin changes.



Fig. 1. Erythematous plaques with annular configuration over his left lateral part of trunk.

The laboratory results were in normal values except the increased levels of antinuclear screening titer and dsDNA antibodies. The level of *Borrelia burgdorferi* IgM was also positive 2.63 (value <1.1) in contrast to IgG level that was proved negative. A punch biopsy specimen taken from a skin lesion on the trunk showed deep dermal inflammation presented by palisading of lymphocytes and histiocytes along the collagen fibres (**Fig. 2**) and around foci of necrobiosis with mucin deposition (**Fig. 3**). Edematous endothelial cells with subsequent lumen obturation of small-to-middle-sized vessels in the deep dermis and leukocytoclasia as an epi-phenomenon was also demonstrated (**Fig. 4**). The histological picture was consistent with IGD.

Taken in consideration the patient's photosensitivity, arthralgia, positive antinuclear, and dsDNA antibody titers, we coined the diagnosis of systemic lupus erythematosus in association with IGD.

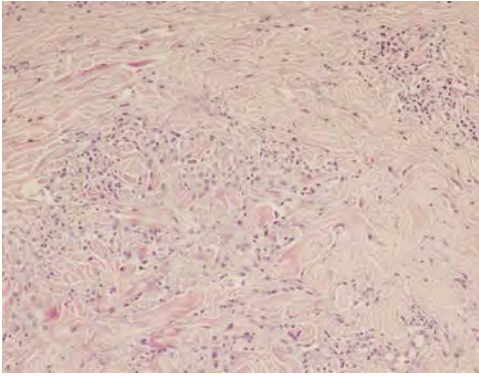


Fig. 2. Deep dermal interstitial granulomatous inflammation, presented with large epithelioid cells, lymphocytes and a few eosinophils around foci of necrobiosis and along the parallel orientated thick and edematous collagen bundles (H&E, ×200).

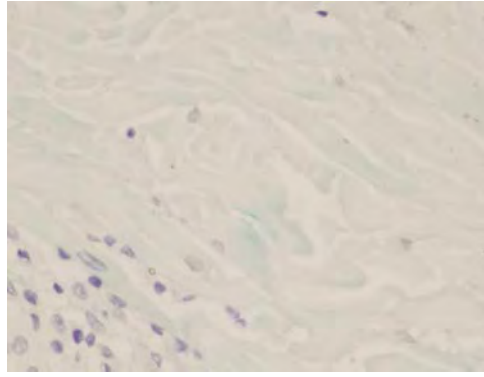


Fig. 3. Deposits of mucin in the deep dermal necrobiotic foci (Alcian blue staining, ×400).

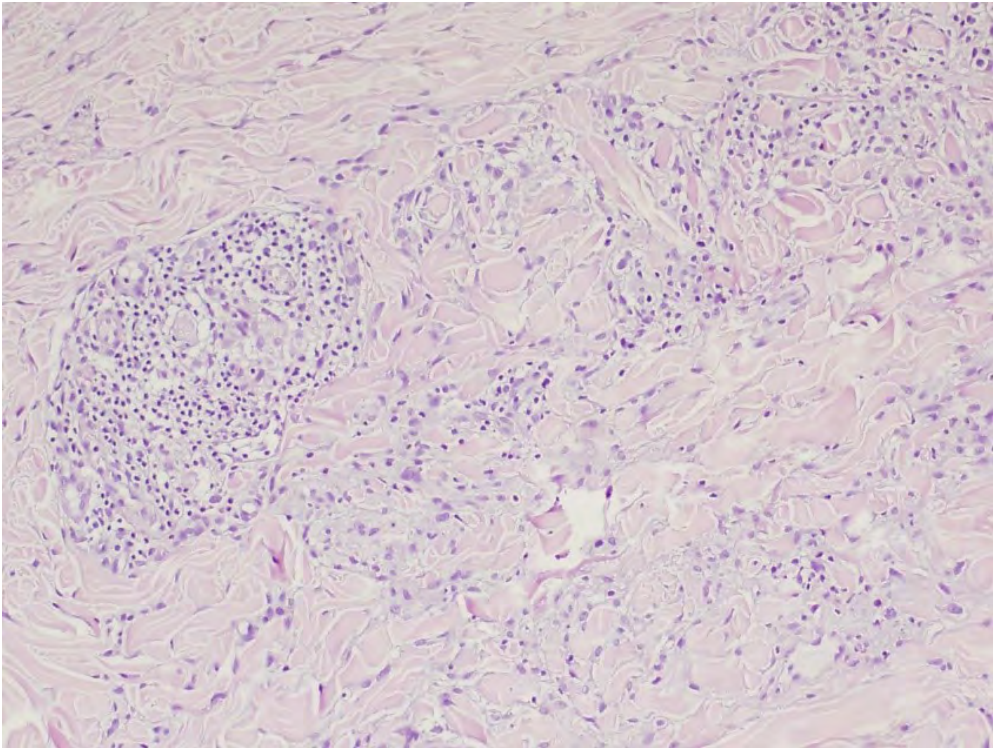


Fig. 4. Mixed perivascular inflammatory infiltrate with leukocytoclasia and nuclear dust surround the small-to-middle sized vessels in the deep dermis. Edematous endothelial cells with lumen obliteration is also presented (H&E, ×100).

Discussion

IGD is a rare skin disorder, presented with asymptomatic skin coloured or erythematous lesions, varying from linear cords, typically seen in patients with rheumatoid arthritis, to patches, papules and plaques, symmetrically distributed on the trunk and proximal extremities [10]. The morphological heterogeneity encompasses its histological characteristics [2]. The most typical findings reveal lower dermis perivascular and interstitial infiltrate of epithelial cells, lymphocytes and neutrophils with a variability of leukocytoclasia and nuclear dust. Foci of necrobiosis with mucin deposition are often present. Inflammation may extend to the hypodermis. Late stages show fibrosis and parallel orientation of collagen bundles [3]. The diagnosis of IGD relies on typical histological findings, corresponding to suggestive skin changes. Our patient showed erythematous annular plaques with elevated margins and pityriasisiform desquamation located to the trunk and upper extremities, a characteristic clue to IGD. The pathology skin findings of interstitial palisading inflammation with mucin deposits coined the diagnosis.

The etiology of IGD remains obscure. Most commonly, it occurs in patients with underlying immune-reactive predisposition and various forms of humoral autoimmune dysregulation, which easily initiate a profound formation of circulating immune complexes [9]. Thus, enhanced neutrophilic hemotaxis and complement activation evoke dermal collagen damage and final granulomatous responses, forming the classic clinic-pathological constellation of IGD. The key player that induces and perpetuates the granulomatous inflammation is a subtype of human macrophages, which belongs to M2b, expressing CD163 [14]. These cells are inducible by the circulating immune complexes and suppress lipopolysaccharide-regulated immune responses by inducing cell apoptosis. They inhibit tissue repair progression and remodeling to form permanent fibrosis and tumor progression. Remarkably, the same cell clone is over activated in patients with systemic lupus erythematosus and is the dominant subpopulation in lupus nephritis. The predominance of CD163-positive M2b human macrophages in the pathogenesis of both IGD and systemic lupus erythematosus proves common autoimmune humoral dysregulation in the two diseases, and finally give some light to their often clinical associations.

The persistent elevation of IgM *Borrelia burgdorferi* titer in our patient can also correspond to the enhanced immune complex formation under the influence of M2b macrophages. The negative seroconversion trend indirectly proves the lack of active Lyme disease, which is also supported by the therapeutic irresponsiveness towards specific antibiotic treatment. Our empiric observations on patients with undifferentiated connective tissue diseases often demonstrate high levels of IgM *Borrelia burgdorferi* antibodies in the absence of other clinical or laboratory clues to Lyme disease. We believe this phenomenon is immunologically defined and requires a thorough scientific exploration.

IGD treatment is not well established. The majority of documented cases have been treated with systemic and topical glucocorticoids [6, 8, 2]. In cases of drug-induced IGD, the withdrawal of the offending agent can resolve the cutaneous lesions [13, 9]. Narrow-band ultraviolet B phototherapy in conjunction with topical steroids has also been used successfully [10]. Alghamdi et al. described treatment with IVIG therapy [1]. Gerbing et al. and Wollina et al. reported treatment with

hydroxychloroquine and cyclosporine, respectively [5,13]. In conjunction with the underlying pathogenesis, biological agents have been the topic of recent discussion for the treatment of IGD.

Conclusions

We present an anecdotal case of IGD in association with systemic lupus erythematosus in a male patient. Interstitial granulomatous inflammatory reaction should always evoke a specific diagnostic interest since it can serve as a clinical clue to underlying immunological disorders. This suggestion relies on the dominant role of CD163 – positive M2-like macrophages in the pathogenesis of both diseases and gives some insights on the future therapeutic modalities that can be introduced. A high index of suspicion for connective tissue disease is needed at any case of interstitial granulomatous dermatitis.

References

1. **Alghamdi, R., C. Bejar, M. Steff, L. Deschamps, E. Marinho, B. Crickx, V. Descamps.** Intravenous immunoglobulins as a treatment of interstitial granulomatous dermatitis with arthritis. – *Br. J. Dermatol.*, **167**, 2012, 218–220.
2. **Blaise, S., D. Salameire, P. H. Carpentier.** Interstitial granulomatous dermatitis: a misdiagnosed cutaneous form of systemic lupus erythematosus? – *Clin. Exp. Dermatol.*, **33**, 2008, 712–714.
3. **Coutinho, I., N. Pereira, M. Gouveia.** Interstitial granulomatous dermatitis: a clinicopathological study. – *Am. J. Dermatopathol.*, **37**, 2015, 614–619.
4. **Deng, A., V. Harvey, B. Sina, D. Strobel, A. Badros, J. M. Junkins-Hopkins, A. Samuels, M. Oghilikhan, A. Gaspari.** Interstitial granulomatous dermatitis associated with the use of tumor necrosis factor alpha inhibitors. – *Arch. Dermatol.*, **142**, 2006, 198–202.
5. **Gerbing, E. K., D. Metze, T. Luger, S. Stander.** Interstitial granulomatous dermatitis without arthritis: successful therapy with hydroxychloroquine. – *J. Dtsch. Dermatol. Ges.*, **1**, 2003, 137–141.
6. **Leloup, P., H. Aubert, S. Causse, B. Le Goff, S. Barbarot.** Ustekinumab therapy for severe interstitial granulomatous dermatitis with arthritis. – *JAMA Dermatol.*, **149**, 2013, 626–627.
7. **Martín, G., J. Cañueto, Á. Santos-Briz, G. Alonso, P. Unamuno, J. Cruz.** Interstitial granulomatous dermatitis with arthritis associated with trastuzumab. – *J. Eur. Acad. Dermatol. Venereol.*, **24**, 2010, 493–494.
8. **Martínez-Morán, C., L. Nájera, A. Ruiz-Casado, A. Romero-Maté, P. Espinosa, C. Meseguer-Yebra, S. Córdoba, J. Borbujo.** Interstitial granulomatous drug reaction to sorafenib. – *Arch. Dermatol.*, **147**, 2011, 1118–1119.
9. **Olmes, G., M. Buttner-Herold, F. Ferrazzi.** CD163-positive M2c-like macrophages predominate in renal biopsies from patients with lupus nephritis. – *Arthritis Res. Ther.*, **18**, 2016, 90.
10. **Peroni, A., C. Colato, D. Schena, P. Gisondi, G. Girolomoni.** Interstitial granulomatous dermatitis: a distinct entity with characteristic histological and clinical pattern. – *Br. J. Dermatol.*, **166**, 2012, 775–783.

11. **Rosenbach, M., J. C. English.** Reactive granulomatous dermatitis: a review of palisaded neutrophilic and granulomatous dermatitis, interstitial granulomatous dermatitis, interstitial granulomatous drug reaction, and a proposed reclassification. – *Dermatol. Clin.*, **33**, 2015, 373–387.
12. **Sanguenza, O., M. Caudell, Y. Mengesha, L. Davis , C. Barnes, J. Griffin, A. Fleischer, J. Jorizzo.** Palisaded neutrophilic granulomatous dermatitis in rheumatoid arthritis. – *J. Am. Acad. Dermatol.*, **47**, 2002, 251–257.
13. **Wollina, U., J. Schönlebe, L. Unger, K. Weigel, E. Köstler, H. Nüsslein.** Interstitial granulomatous dermatitis with plaques and arthritis. – *Clin. Rheumatol.*, **22**, 2003, 347–349.
14. **Zizzo, G., B. A. Hilliard, M. Monestier.** Efficient clearance of early apoptotic cells by human macrophages requires M2c polarization and MerTK induction. – *J. Immunol.*, **189**, 2012, 3508–3520.

Review Articles

The Human Carotid Body and its Role in Ventilatory Acclimatization to Hypoxia

Nikolai Lazarov^{1,2,}, Dimitrinka Atanasova^{2,3}*

¹*Department of Anatomy, Histology and Embryology, Medical University of Sofia, Sofia, Bulgaria*

²*Department of Synaptic Signaling and Communications, Institute of Neurobiology, Bulgarian Academy of Sciences, Sofia, Bulgaria*

³*Department of Anatomy, Faculty of Medicine, Trakia University, Stara Zagora, Bulgaria*

*Corresponding author e-mail: nlazarov@medfac.mu-sofia.bg

The carotid body (CB) is a paired neural crest-derived small ovoid mass of tissue that registers the changes in the arterial blood levels of oxygen, carbon dioxide as well as hydrogen ion concentration and reacts to these changes by the initiation of an appropriate respiratory and cardiovascular response. The human CB shows remarkable structural plasticity and this plasticity underlies the so-called ventilatory acclimatization to hypoxia. The CB morphological changes to high-altitude adaptation include glomus cell hypertrophy and hyperplasia, marked vasodilation and vascular remodeling. The hypoxic CB also shows extraordinary plasticity in different neurotransmitter systems. The altered neurochemical profile of the chemosensory cells comprises elevated catecholamine contents, changes in purinergic mechanisms, up-regulation of nitric oxide metabolism, a marked reduction in peptide levels and production of neurotrophic factors. The structural changes and complex interactions among transmitters markedly influence hypoxia-induced responses in the human CB, thus implying its essential role in ventilatory acclimatization.

Key words: carotid body, high altitude, oxygen homeostasis, structural and neurochemical plasticity, ventilatory acclimatization to hypoxia

Introduction

The carotid body (CB) is the main peripheral arterial chemoreceptor in humans that registers the levels of gases in the blood, eliciting reflex responses to their changes. It is a conglomerate of two juxtaposed cell types: neuron-like glomus cells, which are considered chemosensory cells, and glial-like sustentacular cells, which play a role

in the metabolic support, and have recently been assumed stem cells that behave as glomus cell precursors [6, 8]. The CB is strategically located at the bifurcation of the common carotid artery to monitor blood chemicals just before they reach the brain and thereby to initiate respiratory, cardiovascular, and humoral responses to maintain blood gas homeostasis [for a recent review, see 12]. The phenomenon that helps the body to maintain oxygen homeostasis is called ventilatory acclimatization to hypoxia (VAH), an adaptive process to high altitudes. Certainly, low oxygen levels in blood known as hypoxemia are detected by peripheral arterial chemoreceptors, which accordingly accelerate the frequency and depth of breathing.

There is a large body of current evidence suggesting that the CB plays an important role in the physiological adaptation to high altitude [2, 3, 7, 14, 24]. Specifically, VAH that occurs in humans and several animal models exposed to chronic deficiency in tissue oxygenation called hypoxia [17] is characterized by enhanced CB chemosensory responses [22]. Moreover, the chemosensory transduction and transmission of the hypoxic stimulus, underlying the adaptive process to high altitudes, evoke considerable plasticity of the CB structure and function, as well as modify the neurochemical profile of its cell subpopulations [14].

Structural plasticity of the human CB at high altitude

The vast majority of humans dwell at or slightly above sea level, where the oxygen availability is sufficient. However, at 4000 m the oxygen concentration is only 60% of that at sea level and it gradually decreases with altitude ascent. In addition, when ascending to high altitude atmospheric pressure drops, resulting in a decreased partial pressure of inspired oxygen and saturation of arterial haemoglobin [21]. Globally, it has been estimated that more than 140 million people, i.e. approximately 1.1% of the world's human population, live permanently at altitudes above 2500 meters, defined as high altitude, thus putting these populations at risk of developing chronic mountain sickness. In fact, only three human populations have lived at high altitude for millennia: Andeans on the Andean Altiplano, Tibetans on the Tibetan Plateau, and Ethiopians on the Semian Plateau without apparent life-threatening complications. Obviously, these populations have evolved adaptive physiological phenotypes that aim to increase oxygen delivery into the body.

It has been shown that morphological and functional alterations in the CB occur in people during their acclimatization to sustained hypoxia [3] or pathologically in sea-level patients with emphysema [2]. Initially Arias-Stella and Valcarcel [1] report an increase in the CB size and weight in high-altitude dwellers in the Peruvian Andes at 4330 m and later Heath et al. [11] describe a similar CB enlargement in sea-level patients with emphysema. Heath and Smith [10] have subsequently demonstrated that the CBs of Quechua Indians born and living in the Peruvian Andes are larger than those of mestizos living on the coast [10]. Thus, the physiological acclimatization to high altitude in native highlanders includes a CB augmentation mainly due to glomus cell hypertrophy and hyperplasia, marked vasodilation and vascular remodeling. The increase in vascularity of the hypoxic CB may be a mechanism to increase blood flow and thus of oxygen transport to a hypoxic organ with elevated metabolic activity.

On the other hand, such structural CB adaptation responses to prolonged hypoxia occur in humans not only during long-term acclimatization to high altitudes (**Fig. 1**) but

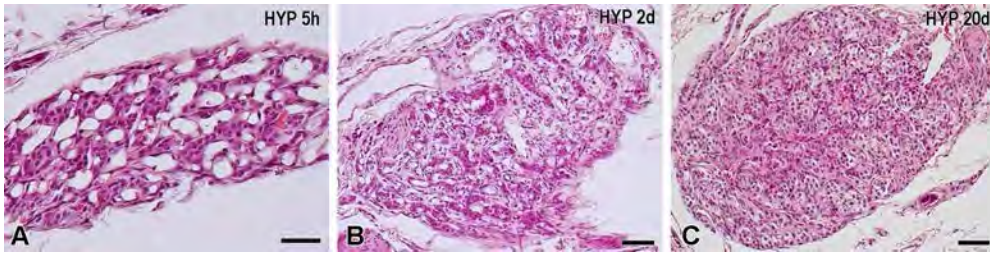


Fig. 1. Hematoxylin and eosin-stained tissue sections showing structural plasticity in the carotid body at (A) 5 hours of hypoxia (HYP 5h), (B) 2 days of hypoxia (HYP 2d), and (C) 20 days of hypoxia (HYP 20d). Note the marked vasodilation of blood vessels and hypertrophy of glomus cells. Scale bars = 50 μ m.

also in patients suffering from systemic hypertension and/or cardiopulmonary diseases with concomitant hypoxemia [9]. Indeed, our experiments have revealed that the hypertensive CB in rats could slightly enlarge its parenchyma with no apparent vascular expansion and/or dilation, and increase in extracellular matrix (**Fig. 2**) [4]. Similar CB hyperplasia has also been described in patients with essential hypertension [18]. However, the results of Kato et al. [13] suggest that the CB morphology under hypertensive conditions is rather altered by the effect of sympathetic nerves, and in this way, these structural changes could be secondary to hypertension.

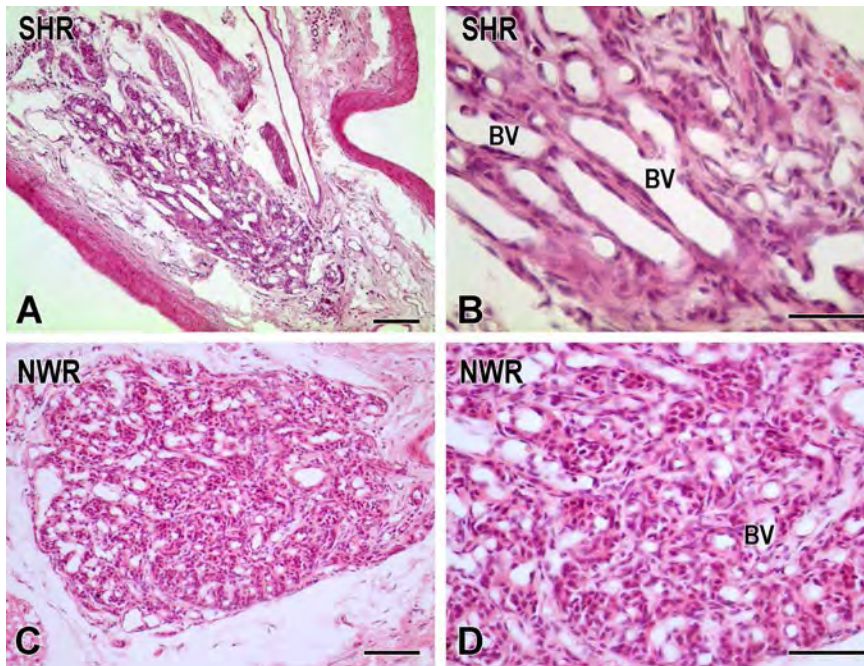


Fig. 2. Structural plasticity of the carotid body under hypertensive conditions in (A, B) spontaneously hypertensive rats (SHR) and their comparison with (C, D) age-matched normotensive Wistar rats (NWR) in hematoxylin and eosin-stained sections. Note the insignificant enlargement of its parenchyma with an apparent dilation of blood vessels (BV) in SHRs. Scale bars = 50 μ m.

It has lately been revealed that the CB structural plasticity depends on the existence of a population of multipotent adult neural crest-derived stem cells, which are quiescent in normoxia and activated during hypoxia to proliferate and differentiate into new glomus cells, as well as smooth muscle and endothelial cells [19].

Neurochemical plasticity of the human CB at high altitude

There is a growing consensus that in addition to the significant cellular rearrangement that culminates in structural plasticity, chronic hypoxia induces neurochemical changes in the chemosensory cells of the CB. It is well established that hypoxia causes glomus cells to depolarize and release both excitatory and inhibitory transmitters, which bind to autoreceptors or postsynaptic receptors on apposed chemoafferent nerve terminals [8]. Furthermore, upon exposure to hypoxia neurotransmitters and neuromodulators released by glomus cells act as paracrine signals that induce proliferation and differentiation of multipotent stem cells and progenitors, thus causing CB hypertrophy and an increased sensory output to the respiratory center in order to correct the condition [20].

Given the central role of ATP and adenosine in CB chemoexcitation, it is not surprising that alterations in purinergic neurotransmitter mechanisms, and particularly in adenosine signaling, have been implicated in VAH [16]. Chronic hypoxia also induces profound changes in other neurochemical systems within the CB such as catecholaminergic, peptidergic and nitrergic systems [23]. Our recent data have indicated that the nitrergic and neurotrophic profile of the CB cell population is also altered in hypertension and this may activate its chemosensitivity [5].

Taken together, current data suggest that complex interactions among transmitters markedly influence hypoxia-induced transmitter release from the CB. It is likely that the up- or down-regulation of these systems may contribute to increased ventilatory and chemoreceptor responsiveness to hypoxia at high altitude.

Conclusion

In conclusion, sustained high-altitude hypoxia induces apparent morphofunctional and neurochemical changes within the human CB, thus implying the plasticity in the cellular and molecular mechanisms of CB chemoreception. It is largely determined as functional changes resulting in increased glomus cell excitability and by neurochemical interactions between a variety of neurotransmitter systems and their receptors in the glomus cells. The CB tends to maintain oxygen homeostasis by marked morphological and neurochemical alterations in animal models of human hypertension as well, so most of the latter may be explained by the altered transmitter phenotype of CB chemoreceptor cells. Knowledge of the mechanisms of CB dysregulation is essential to understand the role of this tiny structure in the human body in various physiological and pathophysiological conditions, including VAH and sympathetically-mediated diseases [15].

Acknowledgements: This research is financially supported by the Faculty of Medicine at Trakia University – Stara Zagora (Grant No. 5 /2022).

References

1. **Arias-Stella, J., J. Valcarcel.** Human carotid body at high altitude. – *Amer. J. Pathol.*, **55**, 1969, 82a-83a.
2. **Arias-Stella, J., J. Valcarcel.** The human carotid body at high altitudes. – *Pathol. Microbiol. (Basel)*, **39**(3), 1973, 292-297.
3. **Arias-Stella, J., J. Valcarcel.** Chief cell hyperplasia in the human carotid body at high altitudes; physiologic and pathologic significance. – *Hum. Pathol.*, **7**(4), 1976, 361-373.
4. **Atanasova, D. Y., N. E. Lazarov.** Expression of neurotrophic factors and their receptors in the carotid body of spontaneously hypertensive rats. – *Respir. Physiol. Neurobiol.*, **202**, 2014, 6-15.
5. **Atanasova, D. Y., A. D. Dandov, N. E. Lazarov.** Neurochemical plasticity of the carotid body in hypertension. – *Anat. Rec.*, 2022, 1-12.
6. **Atanasova, D. Y., M. E. Iliev, N. E. Lazarov.** Morphology of the rat carotid body. – *Biomed. Rev.*, **22**, 2011, 41-55.
7. **Bisgard, G. E.** Carotid body mechanisms in acclimatization to hypoxia. – *Respir. Physiol.*, **121**(2-3), 2000, 237-246.
8. **González, C., L. Almaraz, A. Obeso, R. Rigual.** Carotid body chemoreceptors: from natural stimuli to sensory discharges. – *Physiol. Rev.*, **74**(4), 1994, 829-898.
9. **Heath, D., P. Smith.** *The pathology of the carotid body and sinus*. London, Edward Arnold, 1985.
10. **Heath, D., P. Smith.** The carotid bodies at high altitude. In: *Diseases of the Human Carotid Body* (Eds. D. Heath, P. Smith), London, Springer-Verlag, 1992, pp 91–100.
11. **Heath, D., C. Edwards, P. Harris.** Post-mortem size and structure of the human carotid body. – *Thorax*, **25**(2), 1970, 129-140.
12. **Iturriaga, R., J. Alcayaga, M. W. Chappleau, V. K. Somers.** Carotid body chemoreceptors: physiology, pathology, and implications for health and disease. – *Physiol. Rev.*, **101**(3), 2021, 1177-1235.
13. **Kato, K., J. Wakai, H. Matsuda, T. Kusakabe, Y. Yamamoto.** Increased total volume and dopamine β -hydroxylase immunoreactivity of carotid body in spontaneously hypertensive rats. – *Auton. Neurosci.*, **169**(1), 2012, 49-55.
14. **Kumar, P., N. R. Prabhakar.** Peripheral chemoreceptors: function and plasticity of the carotid body. – *Compr. Physiol.*, **2**(1), 2012, 141-219.
15. **Lazarov N., D. Atanasova.** The human carotid body in health and disease. – *Acta Morphol. Anthropol.*, **19**, 2012, 135-140.
16. **Leonard, E. M., S. Salman, C. A. Nurse.** Sensory processing and integration at the carotid body tripartite synapse: neurotransmitter functions and effects of chronic hypoxia. – *Front. Physiol.*, **9**, 2018, 225.
17. **Powell, F. L., W. K. Milsom, G. S Mitchell.** Time domains of the hypoxic ventilatory response. – *Respir. Physiol.*, **112**(2), 1998, 123-134.
18. **Smith, P., R. Jago, D. Heath.** Anatomical variation and quantitative histology of the normal and enlarged carotid body. – *J. Physiol.*, **137**(4), 1984, 287-304.
19. **Sobrinho, V., V. Annese, R. Pardal.** Progenitor cell heterogeneity in the adult carotid body germinal niche. – In: *Stem Cells Heterogeneity – Novel Concepts* (Ed. A. Birbrair), Adv. Exp. Med. Biol., Vol. 1123, Springer Nature Switzerland AG, 2019, pp 19-38.
20. **Sobrinho, V., A. Platero-Luengo, V. Annese, E. Navarro-Guerrero, P. González-Rodríguez, J. López-Barneo, R. Pardal.** Neurotransmitter modulation of carotid body germinal niche. – *Int. J. Mol. Sci.*, **21**(21), 2020, 8231.
21. **Tymko, M. M., J. C. Tremblay, D. M. Bailey, D. J. Green, P. N. Ainslie.** The impact of hypoxaemia on vascular function in lowlanders and high altitude indigenous populations. – *J. Physiol.*, **597**(24), 2019, 5759-5776.

22. **Vizek, M., C. K. Pickett, J. V. Weil.** Increased carotid body hypoxic sensitivity during acclimatization to hypobaric hypoxia. – *J. Appl. Physiol.*, **63**(6), 1987, 2403-2410.
23. **Wang, Z.-Y., G. E. Bisgard.** Chronic hypoxia-induced morphological and neurochemical changes in the carotid body. – *Microsc. Res. Tech.*, **59**(3), 2002, 168-177.
24. **Wilson, D. F., A. Roy, S. Lahiri.** Immediate and long-term responses of the carotid body to high altitude. – *High Alt. Med. Biol.*, **6**(2), 2005, 97-111.

The Odd Behavior of the Nuclei in Maturing Mammalian Oocytes and Zygotes

Stefka Delimitreva

Department of Biology, Medical Faculty, Medical University of Sofia, Bulgaria, Sofia, Bulgaria

Corresponding author e-mail: s.delimitreva@medfac.mu-sofia.bg

Meiosis in the ovary has some important differences both from mitosis and from meiosis in the testis. The main reason for this is the extremely large cytoplasm of the oocyte. Meiotic maturation is related to global chromatin rearmament. In that huge volume, the chromatin division requires cooperative support by nuclear and cytoplasmic factors. That is why, the oocyte nucleus (known as germinal vesicle), is unusual in many respects: the nuclear envelop in oocytes is not a real border between the nucleus and cytoplasm; the nucleolus does not function as real nucleolus; the centrioles are destroyed during prophase and meiotic spindle is constructed by smaller microtubule organizers; the chromosomes possess autonomy; the pronuclei in the zygote and the nuclei in the very first blastomeres also have unusual behavior – the multiple nucleoli in the male and female pronuclei are not real nucleoli; paternal and maternal genomes possess their own territory and autonomy.

Key words: meiosis, oocyte, zygote, karyosphere, germinal vesicle

In most vertebrates and in a number of invertebrates, the mature oocyte is arrested at the metaphase stage of the second meiotic division. Hence, at that moment the oocyte has no nucleus but a meiotic spindle. The onset of anaphase is not triggered, and meiosis does not finish if the contact with a spermatozoon did not occur. The organization of the genetic material in mature oocytes is really odd and that oddness has its roots in the oogenesis.

Traditionally, the oocyte nucleus is not called nucleus. The maturing oocytes are arrested initially at prophase I. In mammals, this sleeping period can be several years long, or even decades. The meiosis awakes after hormonal signals and continues to the metaphase II arrest in the oocytes that are ready for ovulation and fertilization. During the long prophase I arrest, waking, and till the metaphase II arrest, the oocyte chromatin is organized in an unusual nucleus. This nucleus is also known as germinal vesicle (GV). This traditional name was introduced by Jan Evangelista Purkyně in 1825, who used it for the nucleus of the hen egg. Several years later, his doctoral student

A. Bernhardt used “germinal vesicle” as a name for the nucleus in mammalian oocyte. Somehow, the name “germinal vesicle” survived and even now the embryologists use that name instead of “nucleus”. Perhaps the reason to keep the strange old name is that the researchers always intuitively knew that this structure is not an ordinary cell nucleus. Now we know – it was a good decision.

What is the karyosphere. During the total chromatin rearrangement, the typical nucleolus is transformed into a transcriptionally inactive sphere (nucleolus-like body). In the end of meiotic prophase I, a rim of heterochromatin is accumulated around the original nucleolus. The result is an absolutely spherical structure. In different papers it is referred to as “surrounded nucleolus”, “rimmed nucleolus” or “karyosphere”. Its border is made of the most compact parts of the chromosomes. Hence, at that moment all chromosomes are located in a limited nuclear volume around the karyosphere. The construction of the karyosphere starts with relocation of several centromeric and pericentromeric regions towards the nucleolus [5]. The process continues till the creation of full and bold heterochromatin rim. Curiously, at that time the general level of chromatin condensation increases, but the pericentromeric regions undergo partial decondensation. That makes them able to spread around the nucleolus. Together with this, the nucleolar organizer regions, that normally are in the nucleolus, move out of it and become condensed.

The karyosphere is a protected room. It seems that the heterochromatin border around the karyosphere very effectively isolates its interior. According to our observations [3], at late GV stages the nuclear envelope is not an effective barrier between the nucleus and the cytoplasm – cytoplasmic proteins can enter the nucleus, but they are not detected inside the karyosphere. The interior of the karyosphere contains proteins which are involved in the typical nucleolar functions – rRNA processing and ribosome construction. It contains also small amount of RNA, but the nature of this RNA is still not clear.

The karyosphere keeps the chromosomes in a limited volume. The construction of the karyosphere keeps the chromosomes clustered in a limited volume. That facilitates their transfer and positioning in the meiotic spindle. Also, the clustering reduces the risk to have chromosomal bivalents outside the spindle. The microfilaments are involved in the chromosome clustering that keep the bivalents together in a limited volume. That is in accordance with the fact that at metaphase I, the microfilaments organize an additional spindle-like structure around the tubulin meiotic spindle [7].

The nuclear envelop in oocytes is not a border between the nucleus and cytoplasm. The volume of GV is dramatically reduced after the appearance of the karyosphere, immediately before the germinal vesicle breakdown. That is the moment to start construction of the meiotic spindle. This process totally changes the nuclear architecture. During these steps of oocyte maturation, the behavior of cytoskeletal fibers is very specific. That is related to the following facts: the oocytes are extremely large cells, even in mammals (human oocyte diameter is 100-120 μm); the nucleus occupies very large territory (up to 40 μm); several hours before the nuclear envelope breakdown, nuclear pores lose their function to be checkpoints for the transport through the nuclear envelope; large openings (up to 800 nm in diameter) appear in the envelope; their function is to provide access of cytoplasmic proteins, including cytoskeletal elements, to the chromatin.

Our investigations revealed that at this moment the shape of the nucleus remains visibly normal, but in fact it stops being a separate compartment of the cell. When the karyosphere is constructed, the nuclear envelope gradually loses its integrity; cytoplasmic cytoskeletal elements enter the nucleus; GV stage is transformed into GVBD stage (germinal vesicle breakdown). During this transformation, the nucleus becomes positive for alpha-tubulin and fibrillar actin [4]. Only the interior of the karyosphere stays free of actin and tubulin. Outside the karyosphere, the most intensive reaction for actin and tubulin we detected at the places with the most condensed chromatin.

There are no centrioles in the oocyte. The fact that the maturing oocytes lose their centrosomes makes the probability to start development without egg-sperm fusion nearly zero. The oocyte centrioles are destroyed at prophase I. The chromatin takes the responsibility to arrange the spindle by itself – the chromosomes serve as platforms for creation of multiple microtubule asters that later fuse to construct a bipolar spindle. An additional problem here is the distance. The microtubules are unable to bind effectively chromosomes if the cells diameter exceeds 30 μm . In the oocytes, the chromosome relocation is mediated by the other types of cytoskeletal fibers – microfilaments and intermediate filaments. That is why, they must enter the GV.

Every chromosome is able to create its own spindle-like structure and its own nuclear envelope. The fact that the chromosomes are responsible to organize the microtubules has some unusual consequences. First, a small group of chromosomes, even single chromosomes separated from the main chromosomal set, are able to arrange microtubules into a small spindle-like structure around themselves. Second, the sperm chromosomes can use that autonomy to create a spindle for themselves. In this case, in the oocyte cytoplasm together with the oocyte spindle that is arrested at metaphase II, another spindle can be observed – a spindle with a sperm tail [2]. Third, the autonomy of the chromosomes is used to facilitate integration-disintegration cycle of the nuclei during the first divisions of the huge zygote – for example: in fish and amphibian embryos, single chromosomes are surrounded by their own nuclear envelopes; these structures are referred to as karyomeres; later the karyomeres fuse to form a common nucleus [1].

Paternal and maternal genomes possess autonomy. It was previously thought that a single microtubule spindle is responsible to combine the male and female genomes and then to create a two-cell embryo. In fact, in the mouse zygote two bipolar spindles are formed. They look like a single structure, but the maternal and paternal genomes are located in two independently arranged parts which must align to each other perfectly before the anaphase onset [6]. If the alignment fails, after the first zygote division blastomeres with more than one nucleus will be created. The two halves of the first mitotic spindle in the zygote hold the two parental genomes separated, so the maternal and paternal chromosomes do not mix. They do that in the subsequent developmental stages. This mechanism of dual-spindle assembly is a probable explanation for the relatively high level of morphological and chromosomal abnormalities in human embryos observed in the fertility clinics.

References

1. **Abrams, E. W., H. Zhang, F. L. Marlow, L. Kapp, S. Lu, M. C. Mullins.** Dynamic assembly of brambleberry mediates nuclear envelope fusion during early development. – *Cell*, **150**, 2012, 521-532.
2. **Delimitreva, S., O. Y. Tkachenko, A. Berenson, P. L. Nayudu.** Variations of chromatin, tubulin and actin structures in primate oocytes arrested during in vitro maturation and fertilization--what is this telling us about the relationships between cytoskeletal and chromatin meiotic defects? – *Theriogenology*, **77**, 2012, 1297-1311.
3. **Markova, M., V. Nikolova, I. Chakarova, R. Zhivkova, R. Dimitrov, S. Delimitreva.** Intermediate filament distribution patterns in maturing mouse oocytes and cumulus cells. – *Biocell*, **39**, 2015, 1-7.
4. **Nikolova, V., M. Markova, R. Zhivkova, I. Chakarova, V. Hadzhinesheva, S. Delimitreva.** Karyosphere, the enigmatic “Surrounded nucleolus” of maturing oocytes. – *Acta Morphol. Anthropol.*, **24**, 2017, 1-2, 78-84.
5. **Parfenov, V., G. Potchukalina, L. Dudina, D. Kostyuchek, M. Gruzova.** Human antral follicles: oocyte nucleus and the karyosphere formation (electron microscopic and autoradiographic data). – *Gamete Res.*, **22**, 1989, 219-231.
6. **Reichmann, J., B. Nijmeijer, M. J. Hossain, M. Eguren, I. Schneider, A. Z. Politi, M. J. Roberti, L. Hufnagel, T. Hiiragi, J. Ellenberg.** Dual-spindle formation in zygotes keeps parental genomes apart in early mammalian embryos. – *Science*, **361**, 2018, 189-193.
7. **Verlhac, M. H.** An actin shell delays oocyte chromosome capture by microtubules. – *J. Cell Biol.*, **217**, 2018, 2601-2603.

ANTHROPOLOGY AND ANATOMY 29 (4)

Original Articles

Somatotype Characteristics of Bulgarian Children from the Region of the Eastern Rhodope Mountains

Slavi Tineshev¹, Atanas Baltadjiev²

¹*Department of Human Anatomy and Physiology at Plovdiv University "Paisii Hilendarski", Plovdiv, Bulgaria*

²*Department of Anatomy, Histology, and Embryology, Faculty of Medicine, Medical University-Plovdiv, Bulgaria*

*Corresponding author e-mail: stineshev@abv.bg

Abstract

The purpose of the present study is to investigate the age and sex-related changes that occur in the somatic typological characteristics in children and adolescents from the Eastern Rhodope Mountains /Bulgaria/. Anthropometrically measured 1481 clinically healthy children and adolescents aged 7 to 17 years. The contingent is divided into 11 (for each year) age groups.

The result analysis show that there are age and sex-related changes in both the mean values of the three somatotype components and in the mean somatotype. In both sexes, changes in the average somatotype occurred mainly during prepuberty and puberty ages. The distribution according to somatotype categories showed that mesomorphic types predominate in both sexes, followed by mixed and ectomorphic ones.

Key words: Heath-Carter somatotype, children, somatotype components, somatotype categories

Introduction

The somatotype is an integral characteristic of the morphological status of an individual. It gives a complex assessment of body shape and structure. During the growth period, there are changes in physique and many specialists believe that there is a pronounced dependence between the characteristics, which determine the somatotype, the sex, the age of an individual, and the specific climate-geographical and socio-economic factors [1, 3, 6, 9, 10, 11, 12, 14, 19, 20, 21, 22, 23, 24]. The results of such research are of great practical importance in a number of directions, especially in medicine, as they are related to the prevention of a number of diseases.

The purpose of the present study is to investigate the age and sex-related changes that occur in the somatotype characteristics of children and adolescents from the Eastern Rhodope Mountains, and to contribute to the formation of the overall morphological picture of the adolescent generation in Bulgaria.

Material and Methods

The study involved 1481 /782 girls and 699 boys/ clinically healthy children and adolescents, aged 7-17, from the region of the Eastern Rhodope, Bulgaria. They were divided into 11 age groups, for each year of age. The study was conducted in the period 2007-2008 according to the classical methodology of Martin-Saller [7], after prior parents' information and their signed consent, in accordance with the „International Helsinki Federation for Human Rights” 1976, re-signed as „International Partnership for Human Rights” 2013. The somatotype of each child was determined according to the methodology of Heath & Carter [3, 4], which gives reliable data on the manifestation of the three components – endomorphic, mesomorphic, and ectomorphic. The values of the three components represent the somatotype in numerical form using somatotype units /SU/.

Directly measured were the main anthropological parameters for determining the somatotype: height, weight; biepicondylar diameters of humerus and femur; the circumferences of the arm and forearm, and the skin folds of the triceps, calf, subscapular and suprailiac skin folds. Toteva and Nacheva's graphic model was applied to represent the somatotype characteristics [24].

The data were analyzed using the statistical package “Statistica 6.0”, and the reliability of gender and age differences were verified by the ANOVA test ($p \leq 0.05$).

Results

The results of the variational analysis (X, SD) of somatotype components in each age period, in both sexes, are presented in **Tables 1-2**. Gender and age differences in the mean values are also given.

In boys, the endomorphic component varies between 3.05 SU at 7 years of age and 1.97 at 17, with the highest values reported at 8 years of age – 3.53 SU. During the growth period studied, the endomorphism changed by 1.08 SU. The second component, mesomorphic, had values ranging from 4.90 SU at the age of 7 to 4.24 SU at the age

of 17, or it decreased by 0.66 SU on average. The lowest mean values were reported for 16-year-old boys – 4.00 SU, while the highest – in 12-year-olds – 4.91 SU. The ectomorphic component at 7 years of age was 1.98 SU, and at 17 years – 3.08 SU, an increase of 1.10 SU was observed.

The endomorphic component in girls at the age of 7 is 3.25 SU, and after 11 up to 17 years of age a permanent decrease to 2.41 SU are observed. The highest values were reported for 8-year-old girls – 3.99 SU. In the growth period researched, there was a reduction in endomorphism by 0.84 SU. The mesomorphic component also showed a decrease after the age of 11. It ranges from 4.33 SU at the age of 7 to 3.17 SU at the age

Table 1. Descriptive statistics of somatotype components in boys

Age	N	Boys					
		Endomorphism		Mesomorphism		Ectomorphism	
		mean	SD	mean	SD	mean	SD
7	52	3.05	1.00	4.90	1.10	1.98	1.27
8	59	3.53	1.48	4.70	1.15	2.20	1.24
9	93	3.28	1.60	4.73	1.21	2.53	1.86
10	60	3.17	1.70	4.75	1.48	2.40	1.58
11	68	2.93*	1.30	4.79	1.47	2.43	1.52
12	58	3.08	1.25	✓ 4.91	1.33	2.30	1.49
13	63	2.69	1.27	✓ 4.69	1.73	2.72	1.59
14	81	2.37	1.34	4.37	1.54	✓ 3.22*	1.56
15	61	2.13	1.08	✓ 4.24	1.58	✓ 3.38	1.70
16	52	2.25	0.69	✓ 4.00	1.17	✓ 3.15	1.30
17	52	1.97*	0.46	✓ 4.24	1.37	✓ 3.08	1.43

Table 2. Descriptive statistics of somatotype components in girls

Age	N	Girls					
		Endomorphism		Mesomorphism		Ectomorphism	
		mean	SD	mean	SD	mean	SD
7	52	3.25	1.02	4.33	1.17	2.19	1.10
8	57	3.99	1.60	4.66	1.41	2.10	1.29
9	76	3.25	1.19	4.23	2.10	2.80	1.44
10	84	3.49	1.23	4.39	1.60	2.41	1.55
11	74	3.17	1.22	4.14	1.41	2.63	1.66
12	60	✓ 2.87*	0.95	3.76*	1.46	2.96	1.57
13	57	✓ 2.97	0.74	3.78	1.33	2.71	1.36
14	84	✓ 2.76	0.81	✓ 3.50	1.42	2.98	1.52
15	82	✓ 2.87	0.79	3.75	1.50	2.72	1.34
16	88	✓ 2.99	0.87	3.14*	1.92	2.16	1.29
17	68	✓ 2.41	0.66	3.17*	1.37	2.16	1.36

✓ – inter-sex differences / $p \leq 0.05$ /

* – inter-age differences / $p \leq 0.05$ /

of 17. The reduction in mesomorphism averaged 1.16 SU. For the eleven-year period, the mean values of the ectomorphic component showed relative stability – from 2.19 SU at 7 to 2.16 SU at 17. The highest values of this component were reported for the 12th and 14th years, respectively 2.96 and 2.98 SU.

In both sexes, the mean values of the endomorphic component decreased after the age of 11, and the gender differences were statistically significant / $p \leq 0.05$ /. Throughout the growth period, the mesomorphic component had higher values in boys, with significant differences observed after the age of 12. The differences in the ectomorphic component between the sexes, up to 13, were insignificant, and after this age, boys were significantly more ectomorphic than girls.

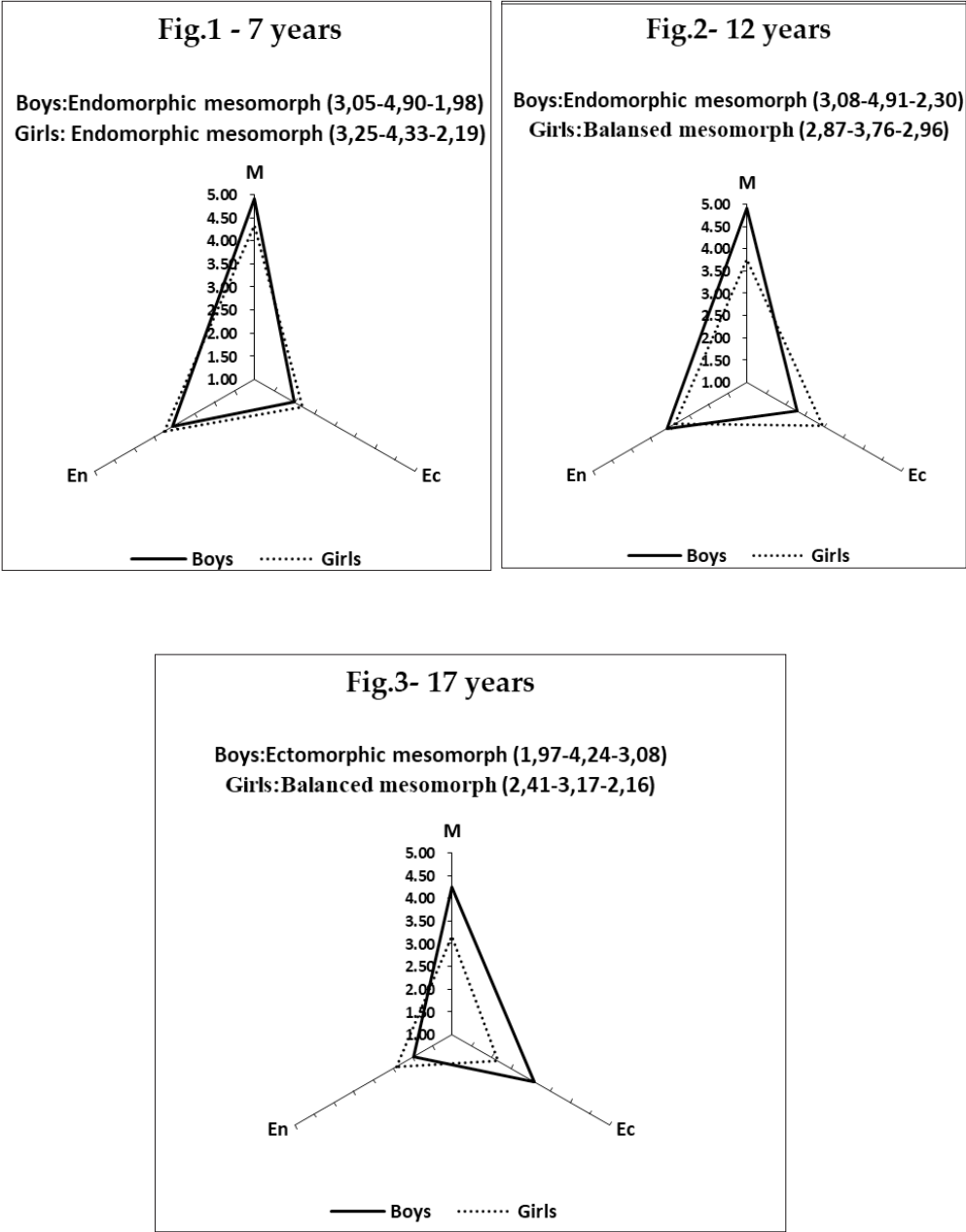
Table 3 shows that in boys up to 11 years of age, the mean somatotype was an endomorphic mesomorph. During this period, mesomorphism is predominant and endomorphism is the second component, which indicates a predominance of body weight. At the age of 11 and 13, the mean somatotype is a balanced mesomorph, characterized by a predominance of the mesomorphic component, and the other two do not differ by more than 0.5 SU. At all the other ages, the mean somatotype in boys is an ectomorphic mesomorph, representing good muscle-skeletal development.

Table. 3 Average somatotype in boys and girls by age

Somatotype	Boys			Age	Girls			Somatotype
	En	Me	Ec		En	Me	Ec	
Endomorphic mesomorph	3,05	4,90	1,98	7	3,25	4,33	2,19	Endomorphic mesomorph
Endomorphic mesomorph	3,53	4,70	2,20	8	3,99	4,66	2,10	Endomorphic mesomorph
Endomorphic mesomorph	3,28	4,73	2,53	9	3,25	4,23	2,80	Endomorphic mesomorph
Endomorphic mesomorph	3,17	4,75	2,40	10	3,49	4,39	2,41	Endomorphic mesomorph
Balanced mesomorph	2,93	4,79	2,43	11	3,17	4,14	2,63	Endomorphic mesomorph
Endomorphic mesomorph	3,08	4,91	2,30	12	2,87	3,76	2,96	Balanced mesomorph
Balanced mesomorph	2,69	4,69	2,72	13	2,97	3,78	2,71	Balanced mesomorph
Ectomorphic mesomorph	2,37	4,37	3,22	14	2,76	3,50	2,98	Balanced mesomorph
Ectomorphic mesomorph	2,13	4,24	3,28	15	2,87	3,75	2,72	Balanced mesomorph
Ectomorphic mesomorph	2,25	4,00	3,15	16	2,99	3,14	2,16	Mesomorph-endomorph
Ectomorphic mesomorph	1,97	4,24	3,08	17	2,41	3,17	2,16	Balanced mesomorph

In girls up to 12 years of age, the average somatotype is an endomorphic mesomorph. From the age of 12 to 16, the average somatotype is a balanced mesomorph, at the age of 16 it is an mesomorph-endomorph, and at the age of 17, it is a balanced mesomorph again. The illustration in the age changes of the average somatotype at 7, 12 and 17 years old are presented in **Figs. 1 – 3**.

Graphic somatotype models illustrating age changes



The percentage distribution of the 13 somatotype categories was brought together by us into four major groups: **Endomorphic type** – endomorphy is dominant and mesomorphic and ectomorphic components are more than one-half somatotype unit lower (meso-endomorphic and ecto-endomorphic types). **Mesomorphic type** – dominant is mesomorphy and endomorphic and ectomorphic components are more than one-half somatotype unit lower (endo-mesomorphic and ecto-mesomorphic types). **Ectomorphic type** – ectomorphy is dominant and endomorphic and mesomorphic components are more than one-half somatotype unit lower (endo-ectomorphic and meso-ectomorphic types). The remaining 7 body types (including the **central type**) are united in the group **other category** in which there are equal shares of two or three somatotype components.

The data are presented in **Table 3** and **Figures 4** and **5**.

As it can be seen in **Fig. 4**, the tendency for the leading role of the mesomorphic body structure in boys stays the same throughout the growth period, as its relative share is highest at 7, 11, and 12 years, on average about 70%. By the age of 13, the share of mixed and central types is relatively high. After the 12th year, there is a clear tendency to increase the frequency of occurrence of ecto- types at the expense of others, and at the end of the growth period, their relative share is almost equal to meso- types. Endomorphism plays an important role in the formation of body structure up to the 12th year, and its relative share is highest in the 8th and 10th years. After the age of 11, there are no boys of endomorphic type.

In girls, the leading role of the mesomorphic component remains again, with its relative share being the highest at the beginning of the growth period, about 60% – **Fig. 5**. With the exception of 11, 12, and 17-year-olds, the share of mixed and central types is relatively high. During puberty, there is a clear tendency to increase the frequency of occurrence of ectomorphic type at the expense of others, with the relative share being highest at 12- and 17-year-olds. In terms of body building, endomorphism is crucial until the age of 11, and after this age, there are no girls of endomorphic type. The highest relative share of endomorphism was recorded in 8-year-old girls.

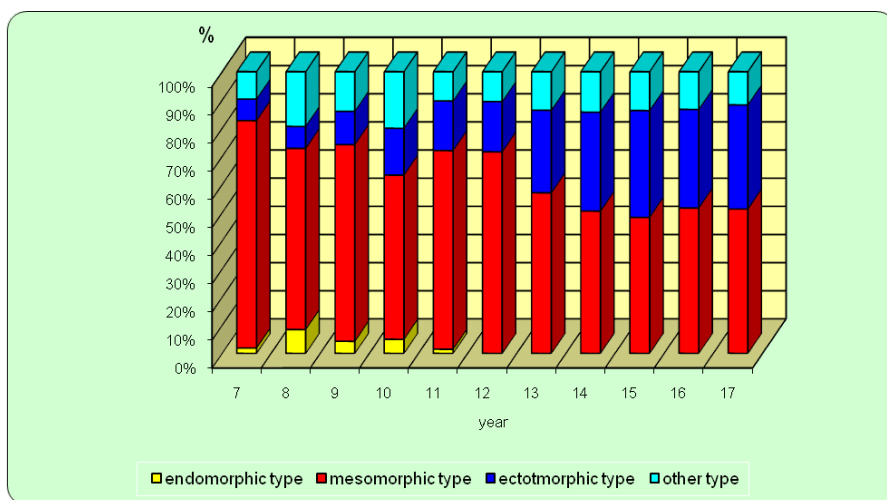


Fig. 4. Percentage distribution of somatotype categories in boys.

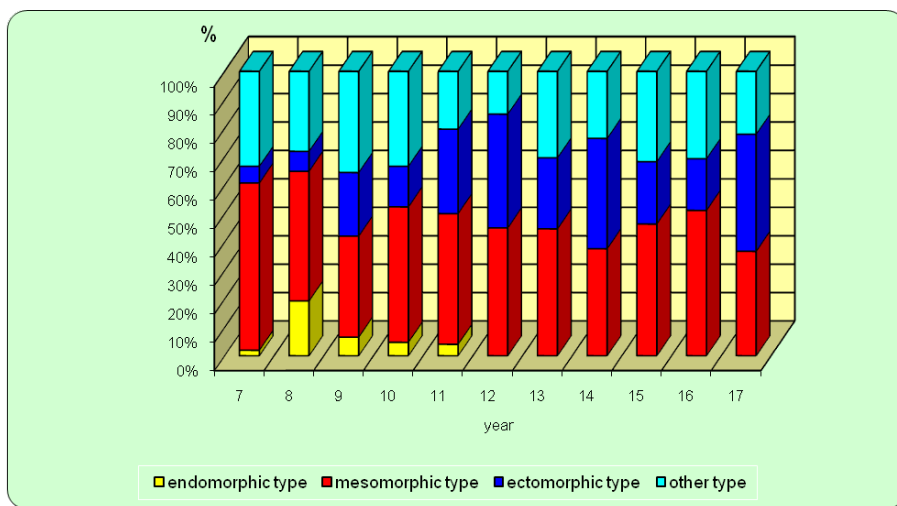


Fig. 5. Percentage distribution of somatotype categories in girls.

Discussion

In the process of growth, gender-specific changes in the individual somatotype components occur. Our results show that in both sexes in the prepubertal and pubertal periods the mean values of endomorphic component decrease, and they are the lowest in 17-year-olds, which is probably due to the pubertal growth spurt in height. At all ages, girls are more endomorphic than boys, except for 12-year-olds, with gender differences statistically significant after the age of 11. This shows a stronger development of subcutaneous adipose tissue and a relatively higher proportion of it in body composition compared to boys, which is particularly pronounced in 8-, 16- and 17-year-olds.

Many other authors report a better development of the endomorphic component in girls than in boys. [1, 6, 9, 10, 11, 14, 21, 24, 26]

In boys, during and after puberty, the amount of subcutaneous adipose tissue in the upper and lower limbs, back, and lower torso decreases, while the increase in height per unit of body mass explains the low values of endomorphism at these ages, especially in 17-year-olds. A similar decrease in the values of the endomorphic component in boys during puberty was found by several authors [8, 12, 13, 15, 16, 18, 25, 27]. For girls, significant age differences are observed between the ages of 11 and 12, and for boys in two age ranges – between 10 and 11 years and between 16 and 17 years.

The mesomorphic component is very well expressed in the boys in the initial age periods – 7-8 years and reaches its peak of development in the 12th year. Then the importance of this component for determining the somatotype decreases until the age of 17. The changes are similar for girls. These results do not differ from the results for children from Plovdiv, Sofia, and Smolyan [8, 14, 15, 18, 24]. It is noteworthy, however, that in the population of Smolyan boys mesomorphism has high values at the end of the growth period. This is probably due to the specific genetic characteristics of the population, modified under the influence of environmental living conditions. In this

regard, a higher hereditary conditionality of mesomorphism in boys has been reported in the literature, followed by ecto- and endomorphism [5], as well as the influences of hereditary factors and the environment on the individual somatotype components and the average somatotype [6, 18, 21, 23].

For boys, the ectomorphic component has the lowest values at the age of 7, and the highest – at 15. The age differences are significant between 13 and 14 years of age, and the gender differences after 13 years of age. Ectomorphism up to 13 years is higher, although insignificant, in girls, i.e., they have more elongated body shapes. After this age, the values of the ectomorphic component are significantly higher in boys, which reflects the process of forming a longer proportionality in them.

A matter of interest is the analysis of changes, with age advancing, in the ratio between the sizes of the three somatotype components. Up to the age of 11, girls somatotype is endomorphic mesomorph, from 12 to 15 years of age the mesomorphic component continues to dominate, the endo- and ecto- components are equally and less expressed, and the type turns into a balanced mesomorph. Girls' somatotype switches to the mixed mesomorphic-endomorphic type not before the age of 16, because of the harmonious development of adipose tissue, bone skeleton, and muscles.

In boys, throughout the growth period, the average somatotypes are of the mesomorphic group. Until the age of 13, the average somatotype is an endomorphic mesomorph, with the exception of the 11th and 13th years, when the average somatotype is a balanced mesomorph. After the age of 14, when the pubertal height acceleration occurs, the somatotype becomes an ectomorphic mesomorph and remains such until the end of the growth period.

Changes in the average somatotype of Bulgarian children during growth have been reported by several authors [8, 10, 12, 18, 21]. Similar changes in the average somatotype during growth have been found in Hungarian children [6]; in Czech children [20]; and in Slovenian children [26].

The percentage distribution and the frequency of occurrence of the different somatotype categories in the different age periods show that in both sexes the relative share of somatotypes with dominant mesomorphism occurs throughout the growth period and during puberty, the percentage of ectomorphic type increases. It is noteworthy that the frequency of somatotypes with a predominant endomorphic component, in both sexes, is low, and after 11 years of age, such body types are not found.

Literature analyses done on the frequency of occurrence of the 13 somatotype categories, according to Heath & Carter, in the various territorial and age groups, showed the highest percentage of mesomorphic types, similarly to our data about Smolyan and Plovdiv boys throughout the growth period. In girls, however, the mesomorphic forms predominate throughout the growth period in Smolyan girls, while, in girls from Plovdiv, they are predominant at the beginning of the period [8, 12]. During and after puberty, in girls from Smolyan, the percentage of endomorphic type increases, while in girls from Plovdiv – the percentage of ectomorphic type. These comparisons confirm the fact that each population has its own unique somatic typological profile, which can be determined by specific genetic and environmental factors.

The results of this study show:

1. Age and sex-related changes occur in both the mean values of the three somatotype components and the average somatotype.

2. The skeletal and muscular systems play the leading role in the formation of the body structure of the children, followed by the linearity and proportionality of the body.
3. In both sexes, changes in the average somatotype are observed mainly in the period of prepuberty and puberty, as well as in the post-pubertal period in girls.
4. The distribution in somatotype categories shows that mesomorphic types predominate in both sexes at different age stages of growth, followed by mixed and ectomorphic body types. Endomorphic forms are the rarest.

References

1. **Andreenko, E., M. Nikolova.** Anthropological and somatotype characteristics of certain professional categories. – *Glasnik ADJ*, **32**, 1996, 41-45.
2. **Andreenko E., M. Nikolova.** Bioelectrical impedance analysis assessment of body composition of children and adolescents from Plovdiv (Bulgaria). – *Glasnik, ADS*, **46**, 2011, 59-65.
3. **Carter, L., B. Heath.** Somatotyping: Development and applications. Cambridge studies in biological anthropology, Cambridge University Press, Cambridge, 1990.
4. **Carter, L.** The Heath – Carter anthropometric somatotype. Instruction manual (Revised by J.E.L. Carter), San Diego, USA, 2002.
5. **Chovanova, E., P. Bergman, R. Stukovsky.** Genetic aspects of somatotypes in twins. Modern man and his biological evolution. – *Anthropos*, **22**, 1982, pp.19
6. **Eiben, O.** The Körmend growth study: Somatotypes. – *Humanobiologia Budapestinensis*, **16**, 1985, pp. 37-53.
7. **Martin, R., K. Saller,** Lehrbuch der Anthropologie in sistematischer Darsellung. Stittgart, Gustav Fisher Verlag, 1957, pp. 308-385.
8. **Mladenova, S., M. Nikolova, A. Andreenko, D. Boyadjiev.** Somatotypological characterization of bulgarian children and adolescents (Smolyan Region). – *Collegium Antropologicum*, **34**, 2010, 3, 963-971.
9. **Nikolova, M.** Somatotype of girls and boys from various sports groups. Biology, Univ. of Plovdiv “P. Hilendarski”, **22**, 1984, 2, 321-333. [In Bulgarian]
10. **Nikolova, M.** Somatotype characteristics of adolescents from the town of Plovdiv. Biology, Univ. of Plovdiv “P. Hilendarski”, **27**, 1989, 6, 253-264 [In Bulgarian].
11. **Nikolova, M.** Morphological configurations in women and ther relation to certain factors. – *Mankind Quarterly*, **37**, 1997, 4, 373-401.
12. **Nikolova, M., V. Akabaliev, S. Sivkov, S. Mladenova.** Body composition of children and adolescents from Plovdiv. – *Proceedings of the Balkan scientific conference of biology in Plovdiv, Bulgaria*, 2005, 150-158.
13. **Nikolova, M., D. Bojadjiev.** Age changes in body composition in children and adolescents. – *Homo, Univ. of Plovdiv “P. Hilendarski”*, 2007, 5-10.
14. **Nikolova, M., I. Petrov.** Typology of male and female students from the city of Plovdiv. – *Glasnik ADJ*, **23**, 1986, 61-68.
15. **Nacheva, A., Y. Zhecheva, I. Yankova, Z. Filcheva, Z. Mitova, Y. Yordanov.** *Physical development of children and youths in Bulgaria on the borderline between 20th and 21st century.* – Prof. Marin Drinov Academic Publishing House, Sofia, 2012, pp. 1-419. [In Bulgarian]
16. **Özener, B., I. Duyar.** Somatotype of labouring and non-labouring children and youths. – *Abstracts from 14th Congress of EAA*, 2004, 37.
17. **Panasiuk, T. V., S. I. Izaak.** Somatotype and the human body development during first childhood. – *Morfologia*, **118**, 2000, 64-67.

18. **Petrov, I., M. Nikolova.** The somatotypology of students. The Mankind, XXIII, 1983, pp. 279-297.
19. **Petrov, I., M. Nikolova, L. Popova, L.** Relationship between somatotype and some functional parameters of psychological efficiency of the students attending Plovdiv's higher institutes – *Biology, Univ.of Plovdiv "P. Hilendarski"*, **25**, 1987, 205-213. [in Bulgarian]
20. **Procopec, M., A. Stehlik.** Somatotypes at 6, 12 and 18 years of age; A longitudinal study. – *Humanobiologia Budapestinensis*, **25**, 1988, 425-434.
21. **Stoev, R.** Somatotype in students-adolescent in Smolyan. Book with paper from II national conference of anthropology with International participation, Plovdiv, Bulgaria, 1990, 160-163.
22. **Stoev, R.** Somatic development and sexual maturation in adolescents in Sofia and Smolyan. – *Journal of Anthropology*, **3**, 2000, 62-68.
23. **Toteva, M.** Age changes in somatotype of young football players. – *Journal of Anthropology*, **3**, 2000, 68-77.
24. **Toteva, M., A. Nacheva.** Grafical method for assessment of ecosensibility in component of human somatotype. – *Acta Morphol. Anthropol.*, **12**, 2007, 151-160.
25. **Toteva, M.** Somatotypology in the sport. NSA, Sofia, 1992. [In Bulgarian].
26. **Tomazo-Ravnik, T.** Juvenile somatotypes in Slovenia. – In: *Studies in human biology* (eds. E. Bodzsar, C. Susanne), Budapest, Eötvös University press, 1996, pp. 335-342.
27. **Walker, R., J. Tanner.** Prediction of adult Sheldon somatotypes I and II from ratings and measurements at childhood ages. – *Ann. Hum. Biol.*, **7**, 1980, 213.

Results from the Anthropological Investigation of the Material from a Section of the Necropolis of the Ancient Apollonia Pontica

Lyuba Manoilova, Victoria Russeva*

Institute of Experimental Morphology, Pathology and Anthropology with Museum, Bulgarian Academy of Sciences, Sofia, Bulgaria

*Corresponding author e-mail: l.manoilova@gmail.com

During 2020 archaeological season rescue excavations in a sector of the ancient necropolis of Apollonia Pontica (UPI 8173) are unearthed five graves, dated in 360-340 BC up to the end of the IV-beginning of III c. BC, four of which contain human remains. The anthropological investigation aims ascertaining of the number of individuals buried in the graves, their demographic distribution and identification of pathological changes on bones. Remains from nine individuals are recognized, seven males, incl. one adult and six matures, a grown up female and a child of ca. 10 years. Left parietal of a male, grave N 5, presents traces of trauma after incomplete trepanation, or accidental injury. Frontal bone from a male, grave N 3, presents a big osteoma. The individual from grave N 4 suffered from developing spondylosis of spine and advanced toothloss. Possible invalidisation could have caused changes of right femur from grave N 2.

Key words: skeletal remains, Apollonia Pontica, classical period

Introduction.

During 2020 archaeological season rescue excavations in a sector of the ancient necropolis of Apollonia Pontica (site UPI 8173) are unearthed five graves, four of which contain human remains. Grave structures, materials and reconstructed rituals date the structures in 360-340 BC up to the end of the IV-beginning of III c. BC [7].

The anthropological investigation aims to ascertain of the number of individuals buried in the graves, their demographic distribution and identification of possible pathological changes on bones.

Material and Methods

The number of individuals buried in the graves is obtained in most cases by documented repetition of bones. In some cases for recognition of a different individual are used clear differences in age, sex and other anthropological features of skeletal remains. The latter are used also in association of bones to skeletons, which lacked anatomical order on field, after reburial rituals. The age and sex of the individuals is ascertained based on classical methods after macroscopic features [1, 2, 11, 12, 13, 14, 16] (**Table 1**). In one case is used the method for age assessment based on the dental attrition of first to third molars, developed by Brothwell, included later in the study of Bass [4]. Measurements of bones are performed after standard methods [9] and used for additional data in sex assessment after standardized tables [4] and for stature reconstruction, performed, based on the formulae of Trotter-Gleser and Pearson-Lee in V. Alekseev [2].

The examined skeletal remains present also different pathological changes, which are compared to published finds for further interpretation [3, 8, 10].

Table 1. Age and sex identification. Used features in age and sex identification

N	Position	Identification		Age					Sex				
		Sex	Age, years	Dental development	Dental attrition	Skeletal development	Cranial sutures obliteration	Pubic symphyseal surface	Pelvic bones	Cranial bones	Mandible	Measurements	Massiveness, relief development
2	primary	M	40-50/60				●	●	●	●			
	reburial	M	50-60				●			●			
	reburial	M	50-60				●			●			
	reburial	M	20-25				●			●			
	reburial	F	20+			●							●
	reburial	0	Ca. 10	●									
3	primary	M	40-50				●		●	○		○	○
4	primary	M	50-60				●	●	●	●	●		
5	Single fragments	M	35-45		●						●		

M – male; F – female; 0 – undefined (child); ● – feature used in identification; ○ – feature with controversial data for identification

Results and Discussion

In the examined material are recognized skeletal remains from nine individuals. Graves N 3-5 contain remains of one individual each, those from graves N 3 and 4 being relatively completely preserved and identified as males at ca. 40-50 and 50-60 years respectively. In grave N 5 are registered only single bones from a male.

Grave N 2 contains bones from six individuals. A skeleton of one male, at ca. 50-60 years is uncovered in primary position. The remaining individuals are presented by singular reburied bones, which defined other three males (**Fig. 1**), two matures (40-60 years) and a younger one at about 20-30 years, an adult female and a child at about 10 years of age.



Fig. 1. Grave N 2, skull fragments. 1.1. Frontal bone, fragments of both parietals, nose bones and right zygomatic, next to the pelvic girdle of the skeleton in primary position. 1.2. Fragment from calva, South-East corner. 1.3. Fragment from frontal bone, North-East corner

For the three males from grave N 2, skeleton in primary position and one of the reburials and from grave N 4 is possible the reconstruction of stature, which is calculated on average of 165.29 cm, 167.73 cm and 161.69 cm respectively, based on the formula of Trotter-Gleser and 158.71 cm, 162.14 cm and 159.23 cm, based on the Pearson-Lee formula.

Left parietal of the male, grave N 5, 20-30 years presents traces of trauma (**Fig. 2**) after possible incomplete trepanation, or with accidental etiology, as compared to other similar defects [5, 6, 15]. Frontal bone from a male at ca. 40-50 years from grave N 3 presents a big osteoma with a diameter of 13.5×9.5 mm and height of about 5 mm (**Fig. 3**). Being a benign tumor it shouldn't affect much the overall health condition of this individual, but it was quite prominent on the face view. The individual from grave N 4 suffered from developing spondylosis of spine and advanced toothloss, characteristic for the



Fig. 2. Grave N 2, fragment from the left parietal, arrow – defect



Fig. 3. Grave N 3, *calvaria*, arrow – osteoma

ascertained age in the period. Possible invalidisation could have caused the defect on the condyles of right femur of the individual in the primary position from grave N 2. Additionally, in movement difficulties in the knee joint and possible overloading of adductors, developed the myositis on the linea aspera.

Conclusions

In the studied burial complexes were placed mostly males at advanced age for the period. The bones present a relatively good health condition, but the stature remains relatively short, characteristic for the populations from the Black Sea coast in the period.

References

1. **Alekseev, V., G. Debets.** Craniometry, methods of anthropological study. Moscow, Nauka, 1964 [in Russian].
2. **Alekseev, V.** Osteometry, methods of anthropological study. Moscow, Nauka, 1966 [in Russian].
3. **Aufderheide, C., C. Rodriguez-Martin.** The Cambridge encyclopedia of human paleopathology. Cambridge University Press, 1998.
4. **Bass, W.** Human osteology: a laboratory and field manual of the human skeleton. University of Missouri, 1987.
5. **Bennike, P.** Ancient trepanations and differential diagnoses: A re-evaluation of skeletal remains from Denmark. – In: *Trepanation, history, discovery, theory*. (Eds. R. Arnot, S. Finger, C.U.M. Smith). Swets & Zeitlinger, 2003, 95-115.

6. **Boev P.** Symbolic orepanations from Bulgaria. – Bulletins of Institute of Morphology, Bulgarian Academy of Sciences, 9-10, 1964, 289-298. [in Bulgarian].
7. **Bogdanova, T., D. Nedev, N. Aleksandrov.** Graves and traces of agricultural activity in the necropolis of Apollonia Pontica. Budzaka/Solinaria Locality, Sozopol. *Archaeological discoveries and excavations in the 2020*. Sofia 2021, II, 585-588. [in Bulgarian].
8. **Lukacs, J.** Dental paleopathology: methodology standardized. – In: *Reconstruction of Life from Skeleton*. Alan Liss Inc., 1989, p. 261-279.
9. **Martin, R., K. Saller.** Lehrbuch der Anthropologie, Stuttgart, Gustav Fischer Verlag, 1959, Band 2.
10. **Ortner D.** Identification of pathological conditions in human skeletal remains. Elsevier, Sec. Ed., 2003.
11. **Black, S., L. Scheuer, L., Juvenile.** Osteology: a laboratory and field manual. Elsevier, 2009.
12. **Ubelaker, D.** Human skeletal remains: excavation, analysis, interpretation. Washington DC, Taraxacum, 1989.
13. **Walrath, D., P. Turner, J. Bruzek.** Reliability test of the visual assessment of cranial traits for sex determination. – *Am. J. Phys. Anthropol.*, **125**, 2004, 132-137.
14. **White T., P. Folkens.** The human bone manual. Elsevier. USA. 2005.
15. **Yordanov, Y., B. Dimitrova.** Data from the anthropological investigation of the buried in the medieval necropolis N 2 by the village Odartsi, Dobrich distr. – In: *Doncheva-Petkova, L. Odartsi – necropolises from XI c., B. 2*. Sofia, “Marin Drinov”, 2005, p. 415-460. [in Bulgarian].
16. **Zubov, A.** Odontology. Methods of anthropological study. Moscow, Nauka, 1968 [in Russian].

Anthropological Data about the Buried in a Christian Necropolis (from the Ottoman Period), Situated Near the Town of Dimovo, Vidin District, Northwestern Bulgaria

Nadezhda Atanassova, Lilia Ovnarska*

Dept. Anthropology and Anatomy, Institute of Experimental Morphology, Pathology and Anthropology with Museum, Bulgarian Academy of Sciences

*Corresponding author e-mail: naditimeva@gmail.com

The aim of this article is to present the results of detailed anthropological characteristics of bone remains from a Christian necropolis (18th – the beginning of the 19th Century) situated near the town of Dimovo, Vidin district, Northwestern Bulgaria. Standard anthropological methods of investigation are applied. The age-at-death identification of buried shows that the ratio of subadults to adults is almost equal, but nevertheless the most numerous (35%) is the age group of children under the age of 7 years (*Infans I*), which is a negative demographic trend typical for the European populations during this historical period. Sex reconstruction shows a predominance of females. For both sexes, the mean values for stature fall into the categories „Average“ and „Above average“.

Key words: paleoanthropology, Christian necropolis, Ottoman period, National Revival period

Introduction

In 2020 during the construction of a gas pipeline from the Turkish border to the border with Republic of Serbia, a necropolis (archaeological site A10/2) with 83 graves was discovered north of the town of Dimovo, Vidin district (Northwestern Bulgaria). The funeral ritual is inhumation. The burials were carried out according to the Christian canon – the burial pits were oriented west-east, and in several cases there were also reburials. Traces of wooden coffins were revealed. According to the archaeologists the necropolis is dated in the 18th c. – until the beginning of the 19th c. and belonged to a nowadays non-existent village [19].

This paper includes the results from detailed anthropological characteristics of bone remains discovered during the rescue archaeological excavations of the mentioned necropolis.

Material and Methods

The material in this study includes inhumated human bone remains from 83 graves. The authors identified totally 91 individuals. Standard anthropological methods of investigation are applied [1, 2, 3, 4, 5, 6, 8, 11, 12, 13, 17, 20]. The reconstruction of the stature [7, 9, 10], in the adults was carried out depending on the state of the preserved long limb bones.

Results and Discussion

The distribution of the investigated individuals by age groups is illustrated on **Fig. 1**. The age-at-death identification of buried shows that the ratio between subadults to adults is almost equal (1:1.22), but nevertheless the most numerous (35%) is the age group of children under the age of 7 years (*Infans I*), which is a negative demographic trend typical for the European populations during this historical period, when infant mortality between 0-7 years was 50% [15, 16]. Concerning adult individuals from the necropolis near Dimovo, those who died in *Maturus* (40-60 years) prevail, while only 1 individual falls into an elderly age group *Senilis*.

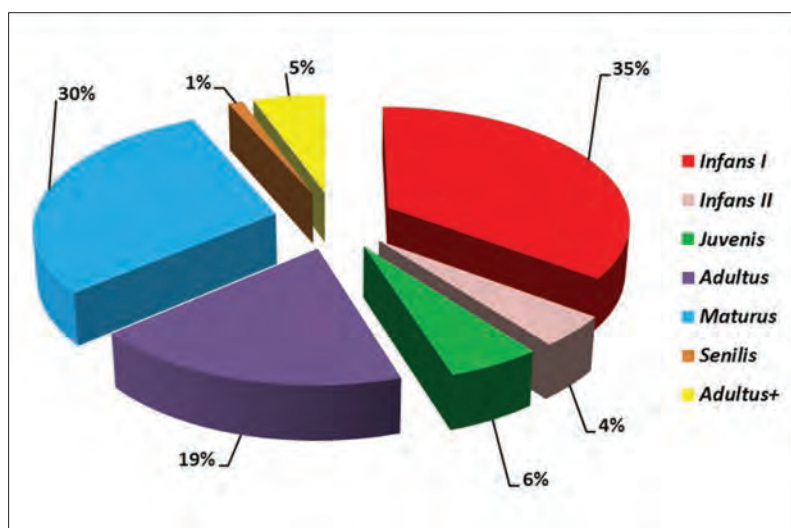


Fig. 1. Percentage distribution of the investigated individuals by age groups

Sexual reconstruction (**Fig. 2**) showed a significant predominance of females (ratio 1.5:1), which is not typical for the most necropolises in the territory of Europe in the Middle Ages. In adolescence the distribution between two sexes is almost equal, but in the age group *Adultus* (20-40 years) only 1 man was identified and women definitely prevail, which may be due to the fact that the entire necropolis was not excavated, because it did not fall into the servitude of the gas pipeline. Unfortunately, we still do not have data from the Ottoman registers about the settlement and the status of its inhabitants. We hope that in the future we will find the information we need to understand the reason for the lack of young men in the necropolis. In the maturity (40-60 years) the number

of males is higher, which is a specificity characteristic of most necropolises from the Ottoman period [14, 18].

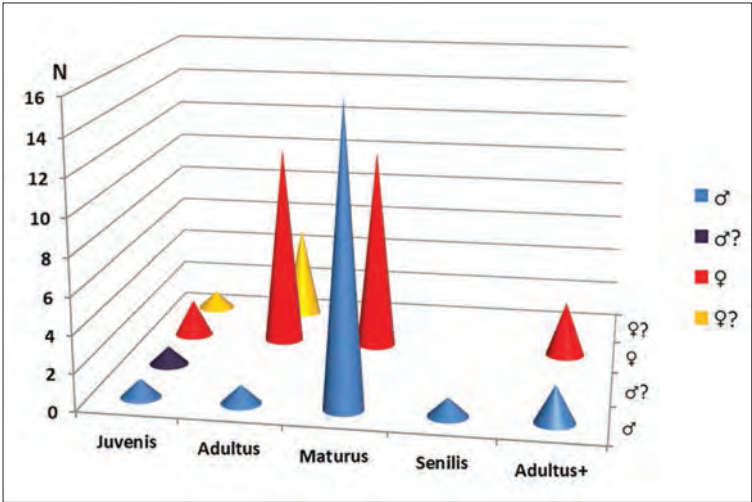


Fig. 2. Age and sex distribution of the investigated individuals

The diagrams (**Figs. 3A, 3B**) show that the majority of the studied males and females fall into the category “tall stature” according to the Trotter-Gleser formulas, while according to the Pearson-Lee formulas the cases in the category “below average stature” predominate in both sexes. The formulas of Trotter and Gleser [9, 10] are the most widely used worldwide for the estimating stature of buried individuals but anthropological investigations about the Ottoman period show that the Pearson-Lee formulas [7] are much more accurate concerning necropolises from nowadays Bulgarian lands [14].

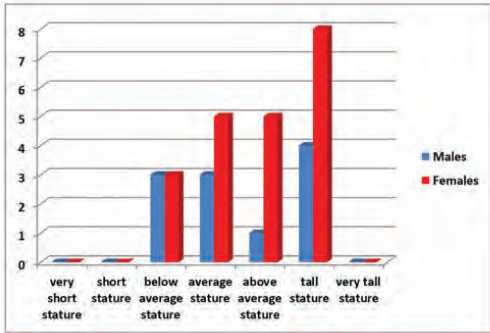


Fig. 3A

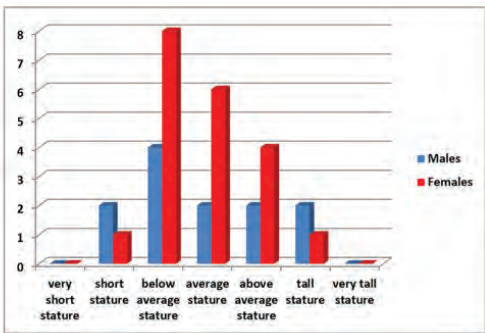


Fig. 3B

Fig. 3. Distribution of adult individuals by the stature categories (by Martin 1957): **A** – according Trotter-Gleser formulas (1952); **B** – according Pearson-Lee formulas (1935)

Conclusions

It should be emphasized that currently there are no other studied necropolises from the National Revival period in Northwestern Bulgaria. For this reason the results from the paleoanthropological investigation of the necropolis near the town of Dimovo are an important database for future studies and have a great importance for Bulgarian anthropology and archeology.

Acknowledgements: Thanks to the archeologists Vladislav Zhivkov, PhD and Svetlana Todorova from the National Archaeological Institute with Museum – Bulgarian Academy of Sciences for providing the human bone material, photographs and information about the necropolis!

References

1. **Bass, W.** Human osteology: A laboratory and field manual. – *Special publication no. 2 of the Missouri Archaeological Society*. Columbia, Mo, Missouri Archaeological Society 2005.
2. **Brothwell, D.** Digging Up Bones. London, British Museum of Natural History, 1965.
3. **Buikstra, J., D. Ubelaker.** Standards for data collection from human skeletal remains. Fayetteville, AK, Arkansas Archaeological Survey, 1994.
4. **Ferembach D., I. Schwidetzky, M. Stloukal.** Recommendations for age and sex diagnoses of skeletons. – *J. Hum. Evol.*, **9**, 1980, 517-549.
5. **Martin, R., K. Saller.** Lehrbuch der anthropologie in sistematischer Darstellung. Stuttgart, Gustav Fischer Verlag, 1957.
6. **Meindl, R., C. Lovejoy.** Ectocranial suture closure: a revised method for the termination of skeletal age at death based on lateral-anterior sutures. – *Am. J. Phys. Anthropol.*, **68**, 1985, 57-66.
7. **Pearson, K.** Mathematical contributions to the theory of evolution. V. On the reconstruction of the stature of prehistoric races. – *Phil. Trans. Royal Soc. A*, **193**, 1899, 169-244.
8. **Schaefer, M., S. M. Black, L. Scheuer.** Juvenile osteology: A laboratory and field manual. San Diego, CA, Academic Press, 2009.
9. **Trotter, M., G. Gleser.** Estimation of stature from long bones of American whites and Negroes. – *Am. J. Phys. Anthropol.*, **10**, 1952, 469–514.
10. **Trotter, M., G. Gleser.** A re-evaluation of estimation of stature based on measurements of stature taken during life and of long bones after death. – *Am. J. Phys. Anthropol.*, **16**, 1958, 79-123.
11. **White, T. D., P. A. Folkens.** *The human bone manual*. Burlington, Elsevier, 2005.
12. **Alexeev, V.P., G.F. Debetz.** Craniometry. Methods of anthropological research. Moscow, Science, 1964 [in Russian].
13. **Alexeev, V.P.** Osteometry. Methods of anthropological research. Moscow, Science, 1966 [in Russian].
14. **Atanassova, N.** Comparative characteristics of anthropological indicators of bone remains from the Ottoman period (15th – 19th Century). *PhD thesis*, Bulgarian Academy of Sciences, Sofia, 2018 [in Bulgarian].
15. **Georgieva, Ts.** *The world of the Bulgarians in the early centuries of the Ottoman rule 15th-17th Century*. Sofia, Mnemosina Publishing House, 1997 [in Bulgarian].
16. **Georgieva, Ts.** *Space and spaces of the Bulgarians 15th-17th Century*. Sofia, LIK Publishing House, 1999 [in Bulgarian].
17. **Gerasimov, M.** *Reconstruction of the face from the skull: (modern and fossil human)*. Moscow, Publishing house AN USSR, 1955 [in Russian].

18. **Russeva, V.** Anthropological data about changes in mortality and life expectancy on the territory of Bulgaria from the Neolithic to the Late Middle Ages. *PhD thesis*, Bulgarian Academy of Sciences, Sofia, 2003 [in Bulgarian].
19. **Zhivkov, V., S. Todorova.** Rescue excavations of a necropolis dated to the National Revival period, near Dimovo, Vidin district. – *Archaeological discoveries and excavations in 2020*, 2, 2021, 1197-1199 [in Bulgarian, with English summary].
19. **Zubov, A.** *Odontology. Methods of anthropological research.* Moscow, Science, 1968 [in Russian].

Defects on Cranial Bones from Tomb №1, Sofia, Janko Sakazov Str.

Victoria Russeva^{1*}, Yunian Meshekov², Iliana Borisova-Katsarova³,
Vanyo Panchev¹

¹*Institute of Experimental Morphology, Pathology and Anthropology with Museum, Bulgarian Academy of Sciences, Sofia, Bulgaria*

²*Regional History Museum - Sofia; Bulgaria*

³*Department of Archaeology, Sofia University "St. Kliment Ohridski", Sofia, Bulgaria*

* Corresponding author e-mail: victoria_russeva@yahoo.com

On a preliminary state of investigation two bone fragments out of 32 frontal and one out of 17 occipital bones present defects – pits, after trauma on the frontal fragments and perforation on the occipital. They could have been caused by a battle incident or could have been obtained after complete or incomplete trepanation/cauterization.

Key words: Middle Age, cranial trauma, trepanation

Introduction

A tomb from the Late Antiquity period is excavated in 2020 in the periphery of the East necropolis of Serdica (Yanko Sakasov Str., No 6, of modern Sofia). It is constructed with bricks, has a rectangular plan and possibly had a barrel vault. All four walls of the tomb bear disturbances from XX c. constructions [15].

The tomb was full with a thick layer of human skeletal remains of about 0,70 – 0,80 m, mixed with soil, fragments of bricks and stones (**Fig. 1**). Under the upper layer of bones and bone fragments, disarticulated and mixed, are discovered skeletal parts, which remained in primary anatomical order (**Fig. 2**). Most of the skulls and skull fragments are found at a lower position. Most convenient explication of the uncovered situation is that many dead bodies were placed one over another without soil layer in-between in the hollow area of the tomb. After decomposition of the soft tissues some parts of the skeletal remains became mixed, while others remained in partially anatomical position. Archaeological materials as well as AMS dating of four bone samples, proceeded in the Scottish Universities Environmental Research Centre place the date of the accumulation of skeletal remains in X-XI c AD.



Fig. 1. Tomb 1 with filling of human skeletal remains; stage of investigations



Fig. 2. Tomb 1, human skeletal remains, partially in anatomical position, lower limbs from three individuals, adults

Very reduced portion of uncovered human skeletal remains has been studied up to date. It provides fragments from 32 frontal and 17 occipital bones. Among them on two frontal and one occipital bones are recognized specific defects (**Figs. 3-5**).

Material and Methods

The two fragments from frontal and the one from the occipital bones are studied. Sex of the individuals is achieved after discrete traits of skull, preserved on the studied fragments [22], while age is assessed after the obliteration of preserved segments of cranial sutures based on the methods of Olivier-Simpson [1]. Defects are accurately measured, documented and compared to published materials.

Results and Discussion

The examined skull bones present two pits and a perforation, as follows:

Frontal bone, relatively completely preserved (**Fig. 3**). Right orbital margin reconstructs after fragmentation, only a small part on the right parietal border remains missing. The coronal suture is relatively completely preserved and small fragments of both parietals are also registered remaining on their places. The coronal and the first segment of the sagittal sutures obliteration ascertains the age of the individual at about 30-40 years at death. Based on the relief development of glabella region and superciliary arches and upper orbital margin the sex of the individual ascertains as male. On the outer table of the bone is found a pit, which intercepts the outer table and deepens into the diploe layer. The pit is situated on the sagittal plane above the

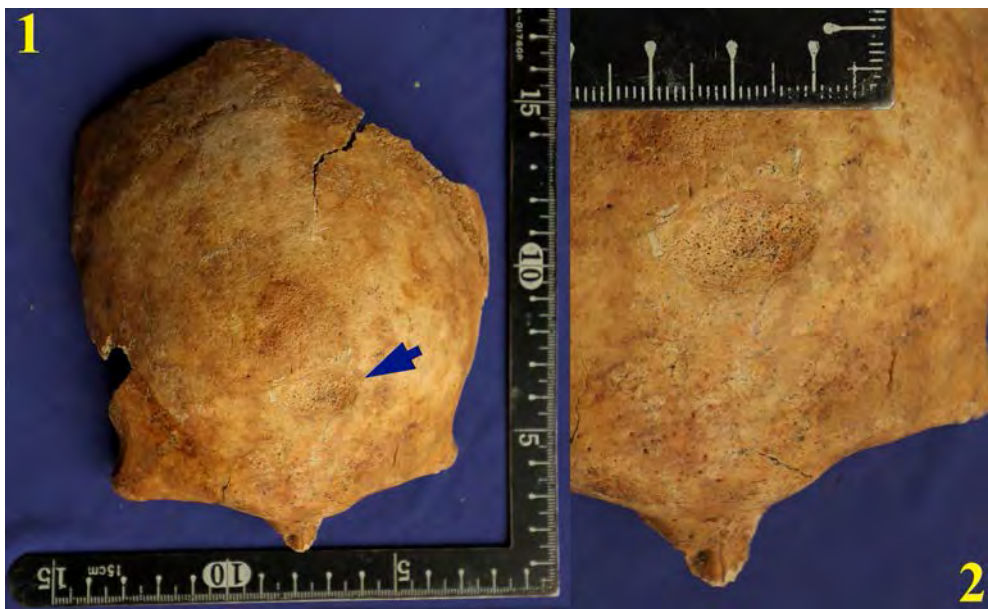


Fig. 3. Frontal bone, male, 30-40 years; defect on the sagittal plane, arrow

glabella. It has an oval form with diameters of 18,9 x 12,3 mm with bigger diameter, situated relatively horizontally. No bone reactions are found on the endo- or ectocranial surface, the defect presents a floor with smooth surface, after bone remodeling and only fair traces from the diploe can be recognized.

Frontal bone, relatively completely preserved (**Fig. 4**). A post-mortal destruction affects the glabella region and part from right orbital margin. The coronal suture is completely preserved, with no obliteration, ascertaining the age of the individual at about 18/20-25 years at death. After the development of the relief of superciliary arches and upper orbital margin (left side) the sex of the individual ascertains as male. On the outer table of the bone is found a pit, which intercepts the outer table and deepens into the diploe layer. The pit is situated on the right side, near to the center of the right frontal tuber. It has a form of a circle, or square with rounded angles, with diameter of 8,2 mm. No bone reaction is found on the endo- or ecto-cranial surface, the defect presents a floor with smooth surface after bone remodeling. The frontal sinus also presents a normal surface of bone.



Fig. 4. Frontal bone, male, 18/20-25 years; defect on the right side, arrow

Fragment from the occipital squama (**Fig. 5**). Poorly preserved endo and ectocranial surface after clear post-mortal destruction. No segments of cranial sutures are preserved and age of the individual ascertains generally as adult. Traces of relief of nuchal line makes it possible to be supposed a male sex of the individual. The fragment presents a round perforation, which intersects the whole breadth of the bone and reaches the occipital fossa. It has a diameter of 4,3 mm.

Similar defects to the ones found on both frontal bones are reported to get obtained after cuts with glancing directions, which affected the skull superficially and had been survived, documented in a sample from a mass grave of battle casualties from XIV c. in Naestved, Denmark [3]. On the other hand many similar defects to the studied ones are found in the materials from Middle Ages from South-East to Central Europe (Hungary), including North Black Sea Steppes and are interpreted as complete or incomplete trepanations [2, 4, 7, 10, 14, 16, 17, 21]. Such are also registered in Bulgarian material from XI-XII c. [6, 12, 19, 23, 24]. A case of complete trepanation, performed with round metal trepan is also known from V c. *Serdica*, [5].

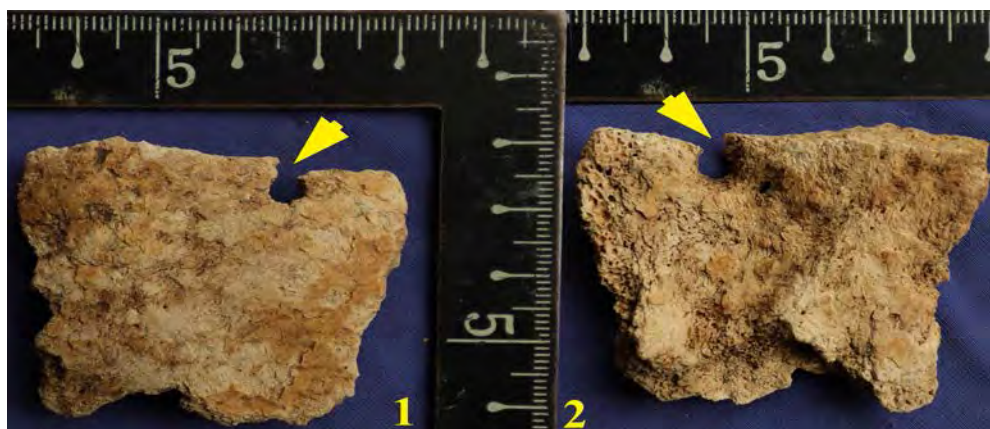


Fig. 5. Occipital squama, fragment, endo and ectocranial surface male, adult

Trepanation has been known in the medical practice of the ancient classical tradition from Hippocrates [9, 13, 18]. A method of cauterization, in some cases with removal of the bone plate on the place, which would leave traces similar to the defects from incomplete trepanation is also described [2, 6, 11].

In some cases a trepanation with boring technique is performed, as in the finding from Monte d'Argento [8], where possible reason for the manipulation could be a depression in the right cerebral fossa of the inner table of the occipital squama, regarded as a result of endocranial hypertension. The finding is very similar to the one, found on the occipital fragment in studied material. In Bulgarian material similar is found in the Early Medieval necropolis from Balchik [20]. The use of trepanation as a treatment of psychological disorders during the Crusades is attested by a letter of sheikh Shaizara [14].

Conclusions

The studied fragments present defects with traumatic etiology. They could have been caused by a battle incident or could have been obtained after complete or incomplete trepanation/cauterization.

References

1. **Alekseev, V., G. Debets.** *Craniometry, methods of anthropological study*. Moscow, Nauka, 1964, 228 p. [in Russian].
2. **Anda, T. 1951.** Anthropological investigations on the medical practice of the hungarians from the period of conquest of the state. Trepanation by scraping and drilling. – *Acta Archaeologica*, **34**, 1, 256-316. [in French]
3. **Bennike, P.** Ancient trepanations and differential diagnoses: A re-evaluation of skeletal remains from Denmark. – In: *Trepanation, History, Discovery, Theory*. (Eds R. Arnot, S. Finger, C.U.M. Smith). Swets & Zeitlinger, 2003, 95-115.
4. **Bereczki, Z., A. Marcsik.** Trephined skulls from ancient populations in Hungary. – *Acta Medica Lituanica*, **12**, 2005, 1, 65–69.
5. **Boev, P.** Trepanned skull from Sofia. – *Archaeologia*, **4**, 1961, 70-72. [in Bulgarian]

6. Boev, P. *Symbolic trepanations from Bulgaria*. Bulletins of institute of morphology, Bulgarian academy of sciences, **9-10**, 1964, 289-298. [in Bulgarian]
7. Boev, P. *Symbolic trepanations from SU*. Bulletins of institute of morphology, Bulgarian academy of sciences, **11**, 1965, 113-127. [in Bulgarian]
8. Capasso, L., G. di Totta. Possible treatment for headaches in ancient times. – *International Journal of Osteoarchaeology*, **6**, 1996, 316-319.
9. Dimopoulos, V., J. Robinson, K. Fountas. The pearls and pitfalls of skull trephination as described in the hippocratic treatise “On Head Wounds”. – *Journal of the History of the Neurosciences*, **17**, 2008, 2, 131-140.
10. Hinku I., V. Okushko. Burials with “Finger pits” on the skulls from necropolises from X-XIV c., by the village Hanska in Moldavia. – In: *Ethnography and Art of Moldavia*. Kishinew, 1972, 199-205. [in Russian]
11. Holck, P. Two ‘Medical’ cases from medieval Oslo. – *International Journal of Osteoarchaeology*, **12**, 2002, 166-172.
12. Jordanov, J. B. Dimitrova, S. Nikolov. Symbolic trepanations of skulls from the middle ages (IXth–Xth Century) in Bulgaria. – *Acta Neurochirurgica*, **92**, 1988, 1-4, 15-18.
13. Martin, G. Was hippocrates a beginner at trepanning and where did he learn? – *Journal of Clinical Neuroscience*, **7**, 2000, 6, 500-502.
14. Mednikova, M. Trepanations in the ancient world and head cult. Moscow 2004 [in Russian].
15. Meshekov, Y., I. Borisova-Katsarova. *New data on the eastern necropolis of Serdica. Archaeological discoveries and excavations in the 2020*. Sofia 2021, 907-910. [in Bulgarian]
16. Nemeskéri, J., K. Éry, A. Kralovānszky. Symbolically trepined skulls in Hungary. – *Anthropologiai Közlemények*, **4**, 1960, 3–32. [in Hungarian]
17. Nemeskeri, J., A. Kralovansky, L. Harsanyi. Trepined skulls from the tenth century. – *Acta Arch. Acad. Sci. Hung.*, **17**, 1965, 343-367.
18. Panourias, I., P. Skiadas, D. Sakas, S. Marketos. Hippocrates: a pioneer in the treatment of head injuries. – *Neurosurgery*, **57**, 2005, 1, 181-189.
19. Russeva, V. *Religion, magic or medicine?* New finds of trepaned skulls from southeastern Bulgaria, 11th-13th c. *archaeologica bulgariica* XVII, 2012, 77-95.
20. Russeva, V. Buried in the necropolis – anthropological evidences. [in Bulgarian]. – In: *The protobulgarian necropolis in Balchick*. (Eds L. Doncheva-Petkova, K. Apostolov, V. Russeva). Sofia, 2016.
21. Szathmáry, L., A. Marcsik. Symbolic trephinations and population structure. – *Memories from the Oswaldo Cruz Institute 101 (Suppl. II)*, 2006, 129-132.
22. Walrath, D., P. Turner, J. Bruzek. Reliability test of the visual assessment of cranial traits for sex determination. – *Am. J. Phys. Anthropol.*, **125**, 2004, 132-137.
23. Yordanov Y., N. Atanassova-Timeva, Y. Dimitrov, Y. Yordanov. *Anthropological study of two skeletons with trepanations from Pliska* (the End of X-XI c. – In: From Regional to National. (H. Haritonov), Veliko Tarnovo, 2010, 43-60. [in Bulgarian]
24. Yordanov, Y., B. Dimitrova. Data from the anthropological investigation of the buried in the medieval necropolis N 2 by the village Odartsi, Dobrich distr. – In: *Doncheva-Petkova, L. Odartsi – necropolises from XI c., B. 2*. Sofia, “Marin Drinov ”, 2005, p. 415-460. [in Bulgarian].

Multi-Tendon Abductor Pollicis Longus Muscle and its Clinical Significance

Marc R. Schneider, Dimo Stoyanov, Meglena Angelova, Desislava Marinova, Veselina Mihaleva*

Department of Human Anatomy and Cell Biology, Faculty of Medicine, Medical University Varna, Bulgaria

*Corresponding author e-mail: marcronaldschneider@gmail.com

Accessory tendons of the abductor pollicis longus muscle with variable insertions are a recurrent variation. Anatomical variations in this muscle group have profound clinical importance due to their significance during surgical intervention and correlation with wrist pathology. We are highlighting the importance of anatomical anomalies for the clinical operative setting with a rare case of a multi-tendon abductor pollicis longus insertion.

Key words: abductor pollicis longus, variations, deQuervain Syndrome

Introduction

Abductor pollicis longus muscle (APL), extensor pollicis brevis and extensor pollicis longus comprise the posterior antebrachial muscle group of the thumb. The latter executes movements in the carpal and the trapeziometacarpal joints and promotes their stability [1, 5, 6,7].

An APL tendon duplicity has been widely documented appearing in 56% to 98.5% of hands.

Classically the tendon of the APL attaches to the base of the first metacarpal bone. A relatively common anatomical variation of the APL is the presence of accessory tendons that have several major insertion patterns: 1. Insertion into abductor pollicis brevis, fascia or opponens pollicis 2. Insertion into the styloid process, trapezium or scaphoideum bone, variable areas of the 1st metacarpal bone or 1st phalanx, capsule of 1st carpometacarpal joint 3. Fusion with tendons of other muscles [1, 2, 3, 10]. We report a case of a multi-accessory tendon abductor pollicis longus muscle found during routine dissection and discuss the clinical significance of this anatomical variation.

Materials and methods

During routine dissection of the right upper limb of a cadaver in the dissection facility of the Medical University – Varna, we observed an anomalous muscle in the extensor compartment of the forearm. After the removal of the skin and superficial fascia of the forearm, we dissected the osteofibrous channels of the extensor retinaculum and exposed the musculature making up the “anatomical snuffbox”. All the muscles and tendons were inspected and it was observed that the APL has additional tendon slips. Cadaver material was obtained according to Regulation No 2 from 18.05.2012 of the Bulgarian Ministry of Health.

Results

Our dissection revealed three tendons arising from the body of the APL. The abductor pollicis longus muscle generally originates from the lateral part of the posterior surface of the body of the ulna, the interosseous membrane, and the middle third of the posterior surface of the radius. The muscle usually inserts on to the radial side of the base of the first metacarpal bone. In our case APL has normal origin but presents with two well-defined tendons arising from separated parts of the muscle belly (**Fig. 1A, B**). Two of the three tendons arise from the muscle body. The first is the main tendon and attaches at its normal anatomical position on the first metacarpal bone. The second is an accessory tendon, lies deeper to the main one and fuses with the body of the abductor pollicis brevis. The third is fairly small, splits off from the main tendon and inserts on the joint's capsule (**Fig. 1C**).

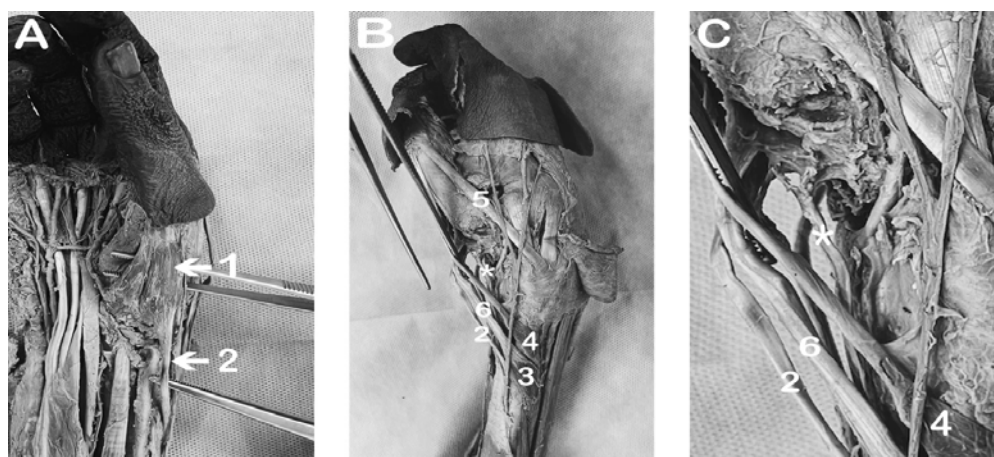


Fig. 1. A) The instruments display the accessory tendon of the APL with the insertion into abductor pollicis brevis muscle. B) Overview of the muscles around the joint and the multi-tendon APL. The instrument visualizes the relationship between the tendons. C) Insertion of the second accessory tendon in the the joint capsule. **Annotations:** 1. abductor pollicis brevis, 2. Accessory tendon, 3. abductor pollicis longus, 4. extensor pollicis brevis, 5. Tendon of extensor

pollicis longus, 6. Main tendon of APL, * Second accessory tendon, Arrow - the joint cavity of the 1st carpometacarpal joint.

Discussion

Posterior forearm muscle variations are common in routine dissections. A great variety of muscle bellies, tendons and insertion points have been described in the literature. In the case of thumb musculature, these variations may be explained by improvement of its movements. Some authors argue that the widespread area of attachments, ensured by the accessory tendons, could ensure better stability during movements of the 1st carpometacarpal joint or radial wrist deviation [9]. On the other hand, the distal third of the forearm and the posterior wrist area are places of closely related structures, covered by the extensor muscle retinaculum that forms narrow osteofibrous canals for the muscle's tendon. The presence of additional structures can lead to compression syndromes, tendovaginitis with limb overload, osteoarthritis and others. De Quervain syndrome, first carpometacarpal arthritis and trapeziometacarpal subluxation are examples of complications that may develop as a result of the described variations in the APL muscle [7, 10]. The knowledge of accessory muscle tendons can be used for the needs of plastic surgery. Accessory abductor pollicis longus (AAPL) tendon can be used as grafting material for reconstruction after chronic extensor pollicis longus ruptures, to treat osteoarthritis of the base of the thumb or other tendinous and ligamentous injuries of the hand [4].

Conclusion

Anatomical variations in this area and the APL respectively, are characteristic for a variety of pathology f.e De Quervain's Syndrome, first carpometacarpal arthritis, and trapeziometacarpal subluxation [7, 10]. They might influence joint functionality, which underlines the significance of upper limb anomalies in the operative clinical setting and eventually alter therapeutic outcomes [8].

Acknowledgements: We want to thank our dissection hall attendants for their general help in the dissection sector.

References

1. **Baba, M. A.** The accessory tendon of the abductor pollicis longus muscle. – *Anat. Rec.*, **119(4)**, 1954, 541-547.
2. **Bergman's Comprehensive Encyclopedia of Human Anatomic Variation.** 2016 John Wiley & Sons, Inc.
3. **Bharambe, V., D. Patel, P. R. Manvikar, S. Shevade, P. G. Bajpayee.** A study of extensor pollicis longus and brevis and abductor pollicis longus from the perspective of evolution. – *J. Med. Res.*, **3(3)**, 2017, 146-150.
4. **Bravo, E., R. B. Febopras, A. Febot.** Anatomic study of the abductor pollicis longus a source for grafting material of the hand. – *Clin. Orthop. Relat. Res.*, **468**, 2010, 1305-1309.

5. **El-Beshbishy, R. A., G. A. Abdel-Hamid.** Variations of the abductor pollicis longus tendon: an anatomic study. – *Folia Morphol.*, **72**(2), 2013, 161-166.
6. **Imaeda, T., K. N. An, W. P. Cooney** 3rd. Functional anatomy and biomechanics of the thumb. – *Hand Clin.*, **8**(1), 1992, 9-15.
7. **Karada, P., Ł. Olewnik, M. Podgórski, M. Polgaj, K. Ruzik, B. Szewczyk.** Anatomical variations of the abductor pollicis longus: a pilot study. – *Folia Morphol.*, **79**(4), 2020, 817-822.
8. **Nam, Y. S., G. H. Doh, K. Hong, S. Lim, S. Eo.** Anatomical study of the first dorsal extensor compartment for the treatment of de Quervain's disease. – *Annals of Anatomy*, **218**, 2018, 250-255.
9. **Oudenaarde, E. V.** Structure and function of Abductor pollicis longus muscle. – *J. Anat.*, **174**, 1991, 221-227.
10. **Tewari, J., P. R. Mishra, S. K. Tripathy.** Anatomical variation of abductor pollicis longus in Indian population: A cadaveric study. – *Indian J. Orthop.*, **49**(5), 2015, 549–553.

Virtual Reality in Anatomy Instruction: a Preliminary Study

Güneş Aytac^{1,2}, Selçuk Tunalı^{1,2*}

¹ Department of Anatomy, Faculty of Medicine, TOBB University of Economics and Technology, Ankara, Turkey.

² Department of Anatomy, Biochemistry and Physiology, John A. Burns School of Medicine, University of Hawaii, Honolulu, USA.

* Corresponding author e-mail: selcuk@hawaii.edu

Modern practical and theoretical instruction sessions need to be up-to-date, and nested with creativity and technology. Virtual reality (VR) is a state-of-the-art user interface interacting with multiple sensory channels and creating real-time simulations. In this study, we examined the effect of VR on the learning of the anatomy of the head and neck region. Seventeen students from 12 different medical schools in Turkey participated in this study. After one hour of theoretical training, the students were trained on cadavers for five hours. Then, a pre-test examination was given. After the pre-test, all students were given one-to-one virtual reality training and then a post-test. A statistically significant increase in the achievement of the students was found between the mean pre- and post-VR test scores ($p=0.003$). VR is considered as a rising trend in medicine when the skills and competencies of the generation Z on digital technologies are taken into consideration.

Key words: Medical education, virtual dissection, digital anatomy, virtual reality

Introduction

In 2018, the majority of students who are studying medicine are involved in the Generation Z. ‘Generation Z’ term describes the people born between 1995 and 2012 [4, 19], who were born and grown in advanced digital conditions. This makes them more susceptible to digital knowledge and skills without the need for extra training, unlike previous generations [16, 17]. The Generation Z is much more interested in technology; thus, expects practical and theoretical instruction media to be up-to-date, and lectures to be nested with creativity and technology [4, 18]. Therefore, traditional learning methods and environments do not appeal to the Generation Z.

Traditional techniques are well-established and have proven efficacy; however, up-to-date methods for differentiating and enriching education should be used to

attract the attention of these students [2]. The use of new technologies in medical education and practice requires special importance and priority. Virtual reality (VR), which is frequently used in flight and warfare simulators, architecture, engineering and industrial design, has also taken a remarkable place in medical education in recent years [9]. Parallel to the increase in the number of sensory organs involved in learning process, the learning becomes more permanent [5]. VR is a state-of-the-art user interface interacting with multiple sensory channels and creating real-time simulations. In VR, instead of the real world, a virtual world created by the computer is perceived [3]. VR has been used in the teaching of complex structures such as larynx [10] and temporal bone [6], in the experience of risky interventions such as endoscopic skull-base surgery [20] and kidney transplantation [14], in preoperative surgery planning of the congenital heart diseases [12], etc. All of these studies emphasized that VR is an effective tool for learning and practical applications. In this context, we conducted a preliminary study to test whether VR training is useful or not as an additional tool to classical anatomy instruction. The objective of this study was not to introduce a new method of instruction; however, we aimed to provide a statistical evidence to support the efficiency of a VR education tool.

Materials and Methods

Thirty students participated in the dissection course, organized by TOBB ETU Faculty of Medicine Students Scientific Research Association. Among these students, 17 volunteers were involved in the study. Informed consent was obtained from all participants. The content of this dissection course was “Head and Neck Region”.

Traditionally, students were given 1 hour of theoretical training and 5 hours of dissection. In addition to theoretical and dissection training, this course also included VR training. The seventeen students participating in this study, were 2nd and 3rd year medical students from 12 different medical schools in Turkey. The age range of the students was 19-21. After one hour of theoretical training, the students were trained in applied dissection on cadavers, in groups of five for five hours (**Fig. 1**). Following dissection, a pre-test examination was given to all students with 5 questions consisting of true-false questions, multiple choice questions and questions on anatomical models.



Fig. 1. Dissection set up of the study.

After the pre-test, students were given one-to-one virtual reality training using Vived Anatomy software (VIVED Inc., Coralville, IA, USA) on zSpace Desktop VR systems (zSpace Inc., Sunnyvale, CA, USA) for 15 minutes (**Fig. 2**). After the virtual reality training, all students were given post-test, which covered similar content with pre-test. Pre- and post-test scores were evaluated on 5 points and the results were recorded. Statistical analyzes were made using IBM SPSS Statistics 28 software.

Results and Discussion

The pre-VR and post-VR test scores of the 17 volunteers which involved in the study is presented in **Table 1**. The average pre-VR test score was 2.7059 ± 1.22382 while the average post-VR test score was 3.5647 ± 1.1418 . A statistically significant increase in the achievement of the students was noted when the averages of the pre- and post-VR test scores were compared ($p=0.003$).

Traditionally, textbooks and lecture presentations for theoretical education, cadavers and anatomical models for practical training, are used in anatomy lessons. One of the best methods for learning anatomy is observing cadavers, which provides better understanding of structure of the body, organs and limbs. Cadavers have been essential for students to have a thorough understanding of the human morphology, and have played a crucial role in medical education [2]. On the other hand, during the last decade cadaver supply got into a critical shortage level in Turkey. The developing technology and increasing expectations of students, led to numerous innovations in education. In recent years preliminary experiences have been carried out using simulations of diagnostic and treatment modalities, surgical operations, especially in faculties providing health education. Virtual classes, laboratories and operating rooms are being successfully tested by some universities and educational institutions [10, 13, 15]. VR offers possibilities to perform experiments in virtual environments where it is difficult to experience in live models, to see their results and to get their output. Although computer-based trainings could not compare with conventional anatomy teaching methods [8], they provide significant contributions to the anatomy education [11]. Some regions of the human body are much more complicated from anatomical point of view and have a difficult structure to learn. Liu et al. in their study on the larynx, which is a complex anatomic region, have transformed 2D images obtained from the database into 3D VR models. Then they used this model in the anatomy lessons of the students and received positive feedback [10]. Aebersold et al. showed that students who trained with VR for nasogastric tube implementation, were significantly more successful in this application than control



Fig. 2. Virtual reality set up of the study.

group [1]. Ha et al. obtained VR images from cadavers and they made measurements on these data. They indicated that VR can accurately simulate anatomical features, thus it could be used for planning of individual surgeries [7]. In our study, we provided a statistical evidence that VR training was effective in better understanding of the complex anatomy of head and neck.

Table 1. The pre-VR and post-VR test scores

Participant No	Pre-VR Test Score	Post-VR Test Score
1	3.50	5.00
2	3.50	4.50
3	2.00	3.00
4	2.00	2.00
5	3.50	3.50
6	3.00	3.80
7	1.00	3.00
8	3.00	3.80
9	1.50	1.50
10	4.50	4.50
11	2.00	4.50
12	1.00	1.00
13	2.00	3.50
14	3.50	4.00
15	1.00	4.00
16	4.50	4.50
17	4.50	4.50

Conclusion

In conclusion, VR should be considered as a rising trend in medical education, when the results of all the above studies, as well as the skills and competencies of the Generation Z on digital technologies, are taken into consideration.

References

1. Aebersold, M., T. Voepel-Lewis, L. Cherara, M. Weber, C. Khouri, et al. Interactive anatomy-augmented virtual simulation training. – *Clinical Simulation in Nursing*, **15**, 2018, 34-41.
2. Codd, A. M., B. Choudhury. Virtual reality anatomy: is it comparable with traditional methods in the teaching of human forearm musculoskeletal anatomy? – *Anatomical Sciences Education*, **4**(3), 2011, 119-125.
3. Cohen, A. R., S. Lohani, S. Manjila, S. Natsupakpong, N. Brown, et al. Virtual reality simulation: basic concepts and use in endoscopic neurosurgery training. – *Child's nervous system*, **29**(8), 2013, 1235-1244.
4. Eckleberry-Hunt, J., D. Lick, R. Hunt. Is medical education ready for generation Z? – *Journal of Graduate Medical Education*, **10**(4), 2018, 378-381.
5. Ekstrand, C., A. Jamal, R. Nguyen, A. Kudryk, J. Mann, et al. Immersive and interactive virtual reality to improve learning and retention of neuroanatomy in medical students: a randomized controlled study. – *CMAJ Open*, **6**(1), 2018, E103-109.
6. Fang, T. Y., P. C. Wang, C. H. Liu, M. C. Su, S. C. Yeh. Evaluation of a haptics-based virtual reality temporal bone simulator for anatomy and surgery training. – *Computer Methods and Programs in Biomedicine*, **113**(2), 2014, 674-681.
7. Ha, W., D. Yang, S. Gu, Q. W. Xu, X. Che, et al. Anatomical study of suboccipital vertebral arteries and surrounding bony structures using virtual reality technology. – *Medical Science Monitor*, **20**, 2014, 802-806.
8. Khot, Z., K. Quinlan, G. R. Norman, B. Wainman. The relative effectiveness of computer-based and traditional resources for education in anatomy. – *Anatomical Sciences Education*, **6**(4), 2013, 211-215.
9. Kuehn, B. M. Virtual and augmented reality put a twist on medical education. – *Journal of the American Medical Association*, **319**(8), 2018, 756-758.
10. Liu, K., B. Fang, Y. Wu, Y. Li, J. Jin, et al. Anatomical education and surgical simulation based on the Chinese Visible Human: a three-dimensional virtual model of the larynx region. – *Anatomical Science International*, **88**(4), 2013, 254-258.
11. Moro, C., Z. Štromberga, A. Raikos, A. Stirling. The effectiveness of virtual and augmented reality in health sciences and medical anatomy. – *Anatomical Sciences Education*, **10**(6), 2017, 549-559.
12. Ong, C. S., A. Krishnan, C. Y. Huang, P. Spevak, L. Vricella, et al. Role of virtual reality in congenital heart disease. – *Congenital Heart Disease*, **13**(3), 2018, 357-361.
13. Pan, J. J., J. Chang, X. Yang, H. Liang, J. J. Zhang, et al. Virtual reality training and assessment in laparoscopic rectum surgery. – *International Journal of Medical Robotics and Computer Assisted Surgery*, **11**(2), 2015, 194-209.
14. Pieterse, A. D., V. A. L. Huurman, B. P. Hierck, M. E. J. Reinders. Introducing the innovative technique of 360 degrees virtual reality in kidney transplant education. – *Transplant Immunology*, **49**, 2018, 5-6.
15. Schuster-Amft, C., K. Eng, I. Lehmann, L. Schmid, N. Kobashi, et al. Using mixed methods to evaluate efficacy and user expectations of a virtual reality-based training system for upper-limb recovery in patients after stroke: a study protocol for a randomised controlled trial. – *Trials*, **15**, 2014, 350.

16. **Shatto, B., K. Erwin.** Moving on from millennials: preparing for generation Z. – *Journal of Continuing Education in Nursing*, **47**(6), 2016, 253-254.
17. **Shatto, B., K. Erwin.** Teaching millennials and generation Z: Bridging the Generational Divide. – *Creative Nursing*, **23**(1), 2017, 24-28.
18. **Vogelsang, M., K. Rockenbauch, H. Wrigge, W. Heinke, G. Hempel.** Medical education for “Generation Z”: everything online?! – An analysis of Internet-based media use by teachers in medicine. – *GMS Journal for Medical Education*, **35**(2), 2018, Doc21.
19. **Wells, T., E. K. Fishman, K. M. Horton, S. P. Rowe.** Meet generation Z: Top 10 trends of 2018. – *JACR*, **15**(12), 2018, 1791-1793.
20. **Won, T. B., P. Hwang, J. H. Lim, S. W. Cho, S. H. Paek, et al.** Early experience with a patient-specific virtual surgical simulation for rehearsal of endoscopic skull-base surgery. – *International Forum of Allergy & Rhinology*, **8**(1), 2018, 54-63.

Sternalis Muscle: a Case Report and Literature Review.

Desislava Marinova, Meglena Angelova, Veselina Zhekova*

*Department of Human Anatomy and Cell Biology, Faculty of Medicine, Medical University
Varna, Bulgaria*

*Corresponding author e-mail: dmarinova81@abv.bg

Sternalis muscle is an anatomical variation of the anterior thoracic wall. Its incidence in white population is 4-7%. During a routine dissection of male cadaver, a long flat muscular structure was observed, crossing the anterior thoracic wall, which was composed of two bellies and intermediate tendon. It was located underneath the superficial thoracic fascia and superficially to pectoralis major. Superior belly was oriented parallel and merges with the fibers and fascia of right pectoralis major. Thin long intermediate tendon crossed the sternum. The inferior portion of the muscle was wider and longer than the upper one. Its fibers were oriented perpendicularly to the fibers of left pectoralis major and caudally fused with the anterior layer of the rectus abdominis sheath. The two bellies had different nerve supply by the pectoral nerve (superior belly) and anterior branches of the intercostal nerves (inferior belly). The knowledge of sternalis muscle is important for radiologists and surgeons.

Key words: sternalis muscle, pectoralis major muscle, rectus abdominis muscle, variation

Introduction

Sternalis muscle is an uncommon anatomical variant located on the human anterior thoracic wall, superficial to pectoralis major muscle [1]. This long and flat muscle usually extends from the inferior costal cartilages and rectus sheath to the upper part of the sternum or superiorly located costal cartilages or fuses with the fibers of sternal head of sternocleidomastoid muscle [21]. Sternalis muscle was reported for the first time by Cabrol (1604) in his book “Anatomes Elenchus Accuratissimus” and also described by Du Puy (1726) [12]. There are a lot of synonyms for this variable muscle: episternalis, presternalis, sternalis brutorum, rectus thoracis, rectus sterni, superficial rectus abdominis and they have also been used in the literature [4, 6, 11, 12, 14]. Nevertheless this muscle is often unknown even in clinical practice [2, 20].

The collected data shows that sternalis is a rare anatomical variation with different incidence in different populations. Its incidence in white population is 4-7%, in black population is 8,4% and in Asian population – 11% [17]. The first study and evaluation of the incidence of sternalis in Bulgaria and the first report on the frequency of the

muscle in Eastern Europe is performed by Jelev et al. [9]. They suggested a definition of sternalis muscle and also based on an extensive review of the literature they offer first classification of this rare variation [9].

The aim of this case report is to disseminate the awareness of this rare finding among clinicians, anatomists and medical students, as well as to expand data on the prevalence and morphology of sternalis in the Bulgarian population.

Materials and Methods

We present a case of a 90-year old male cadaver of Caucasian descent from the dissection hall of the department of Anatomy and Cell Biology, Medical University-Varna, Bulgaria. Routine dissection of the pectoral region was performed, according to the Vankov's standard dissection guideline. After removing the skin and superficial fascia of the dissected region, any muscular variation of the anterior chest-wall was carefully observed and followed for its details like origin, insertion and morphological features and photographs were taken. The length and breadth of the variable muscle were measured using a ruler. Cadaver material was obtained according to Regulation №2 from 18.05.2012 of the Bulgarian Ministry of Health.

Results

During routine dissection of the cadaver, a long muscular strip was observed under superficial fascia, over the anterior surface of the thoracic wall. It was a flat, double bellied muscle, oriented obliquely and located superficially to the pectoralis major on the right and left sides. Superior belly (1) was oriented parallel and merges with the fibers and fascia of right pectoralis major. It originated 4 cm laterally to the midline, at the level of second sternocostal junction and was about 1 cm wide. Thin flat 4 cm long tendon (2) crossed the sternum. The inferior portion of the muscle (3) was wider (about 2,5 cm) and longer (about 6,5 cm) than the superior one. Its fibers were perpendicularly oriented to the fibers of left pectoralis major and caudally fused with the anterior layer of the rectus abdominis sheath, medially to the attachment place of the left serratus anterior. The two bellies had different nerve supply by the pectoral nerve (superior belly) and anterior branches of the intercostal nerves (inferior belly) (**Fig. 1**).



Fig. 1. Anterior surface of thorax: 1-superior belly of m. sternalis, 2-tendon of m. sternalis, 3-inferior belly of m. sternalis.

Discussion

Although sternalis has been described for the first time in 17th century, it is still a mystery. There are a lot of theories for origination of this muscle. Some authors described it from sternocleidomastoid, rectus abdominis [4], pectoralis major [13], obliquus externus abdominis [18]. There are a number of theories about its phylogenetic origin. Although it has been described always superficially, some authors discuss it as a part of longitudinal ventral paramedian muscle sheet which disappears, leaving the hyoid muscles in the anterior cervical region and rectus abdominis of the anterior abdominal wall [16]. Sternalis is considered to be a remnant of panniculus carnosus, which is a thin sheet of skeletal muscles, located subcutaneously in lower mammals and acting to move the overlying skin [3]. Turner has described it as an atavistic form of *m. pectoralis cutaneous* of lower animal [19]. According to Ruge it is presented as rudimentary cuticular muscle in some mammals, which could be found as a subcutaneous muscular fibers of the anterior thoracic wall in humans [15]. Clemente considered it as misplaced portion of pectoralis major [7].

In our case report, the superior belly of sternalis was located in the left pectoral region, just superiorly to superficial pectoral fascia. It originated from aponeurosis of pectoralis major and the fibers direction was same as that of the pectoral muscles. Therefore we would exclude that it was a part of the ventral longitudinal column of muscles, and rather agree with authors who accept it as a part of atavistic thoracic subcutaneous muscle or a misplaced portion of pectoral muscles [7, 15, 19]. Inferior part of sternalis, in our opinion, probably has another origin. We can accept this because the muscle fibers run parallel to those forming *m. rectus abdominis* and are perpendicular to the fibers of the thoracic muscles on the right. For this part of the variant muscle we rather agree with Sadler [16] that it is a part of the ventral longitudinal column of muscles or as a part of panniculus carnosus in lower mammals [3].

Reported incidence of sternalis in the literature is between 4% and 11% in different populations. The variation is mostly one-sided, varying in shape and size. In Bulgaria the reported incidence is 2.9% [9]. Incidence of sternalis has been reported as 4.5% unilaterally and less than 1.7% bilaterally [22]. Unilateral sternalis is twice as common as bilateral one [2, 3]. Five cases of this rare variation have been reported in Bulgarian studies: three of them are unilateral and two of them are with bilateral localization [8, 9]. The sternalis muscle presented in our case can be classified as “crossed sternalis” [10].

Researchers are uncertain regarding innervations of sternalis. In 55% of the cases the innervation is by branches of pectoral nerves, in 43% by branches of intercostal nerves and 2% by both intercostal and pectoral nerves [3, 5]. Because the nerve supply corresponds to the myotomes of origin, we can make this assumption for the two-bellied sternalis in our case – each belly has a different embryonic origin. We can accept that there are two different muscles, which are located bilaterally and fused by intermediate tendon over body of the sternum.

Conclusions

The knowledge about the variations of sternalis helps in better interpretation of great number of mammography done every year. The presence of it may mimic focal densities in the medial breast on mammography, leading to suspicion of a neoplasm. It is necessary to document this unusual anatomical variants with the use of various diagnostic and therapeutic tools like mammography, CT or MRI as its presence may affect area of surgical excision and radiation dose in breast cancer. It also could be used in breast reconstruction or in the plastic and reconstructive surgery of the head and neck region. This shows the importance of this structure in everyday clinical practice.

Acknowledgements: We want to thank our dissection hall attendants for their general help in the dissection sector.

References

1. **Bailey, P. M., C. D. Tzarnas.** The sternalis muscle: a normal finding encountered during breast surgery. – *Plast. Reconst. Surg.*, **103**, 1991, 1189-1190.
2. **Bailey, P. M., C. D. Tzarnas.** The sternalis muscle: a normal finding encountered during breast surgery. – *Plast. Reconst. Surg.*, **103**, 1999, 1189-1190.
3. **Barlow, R. N.** The sternalis muscle in American whites and Negroes. – *Anat. Rec.*, **61**, 1935, 413-426.
4. **Blees, G.** A peculiar type of sternalis muscle. – *Acta Morphol. Neerl. Scand.*, **7**, 1968, 69-72.
5. **Bradley, F. M., H. C. Jr. Hoover, C. A. Hulka.** The sternalis muscle: an unusual normal finding seen on mammography. – *AJR Am. J. Roentgenol.*, **166**, 1996, 33-36.
6. **Calori, L.** About the episternal muscle and its anatomical interpretations. – *Memoirs of the Academy of Sciences of the Institute of Bologna*, **9**, 1888, 131-140. [in Italian]
7. **Clemente, C. D.** Muscle and fasciae. Gray's Anatomy, 30th Ed, Philadelphia: Lea and Febiger., 1985, 520.
8. **Georgiev, G., L. Jelev, V. Ovtsharov.** On the clinical significance of the sternalis muscle. – *Folia Medica*, **53** (3), 2009, 53-56.
9. **Jelev, L., G. Georgiev, L. Surchev.** The Sternalis muscle in the Bulgarian population: Classification of Sternalis. – *J. Anat.*, **199**, 2001, 359-363.
10. **Landzhov, B., L. Jelev.** The crossed sternalis muscle. – *International Journal of Anatomical Variations (IJAV)*, **6**, 2013, 107-108.
11. **Loukas, M., M. Bowers, J. Hullett.** Sternalis muscle: a mystery still. – *Folia Morphol.*, **63**(2), 2004, 147-149.
12. **Natsis, K., K. Vlasis, T. Totlis, G. Paraskevas, P. Tsikaras.** An unusual bilateral sternalis muscle. – *Chirurgia (Bucur)*, **103**(2), 2008, 231-2.
13. **Novakov, S. S., N. I. Yotova, T. D. Petleshkova.** Sternalis muscle – a riddle that still awaits an answer. – *Folia Med.*, **50**, 2008, 63-66.
14. **Pichler, K.** About the occurrence of the musculus sternalis after investigations in vivo. – *Anatomischer Anzeiger*, **39**, 1911, 115. [in German]
15. **Ruge, G.** The dermal muscle of the trunk in mammals: the sternalis muscle under the axillary arch of humans. – *Morph Jahrb.*, **33**, 1905, 379-531. [in French]
16. **Sadler, T. W.** *Langman's essential medical embryology.* Baltimore and Philadelphia. Lippincott Williams & Wilkins, 1995, 37.
17. **Sarikcioglu, L., B. M. Demirel, N. Ocuz.** Three sternalis muscles associated with abnormal attachments of the pectoralis major muscle. – *Exp. Clin. Anat.*, **2**, 2008, 67-71.

18. **Testut, L.** Muscular abnormalities in man, explained by comparative anatomy. – *Masson*, Paris 1884.
19. **Turner, W. M.** On the musculus sternalis. – *J. Anat. Physiol.*, **1**, 1867, 246-253.
20. **Vandeweyer, E.** The sternalis muscle in head and neck reconstruction. – *Plast. Reconst. Surg.*, **104**, 1999, 1578-1579.
21. **Williams, S. P. L., I. H. Bannister, M. M. Berry, M. Dyson, J. E. Dussek, M. W. Ferguson.** *Gray's Anatomy*, Edinburgh, Scotland, 38th Edition. Churchill Livingstone, 1995.
22. **Young, L. B., B. J. Young, K. H. Hee.** The sternalis muscles, incidence and imaging findings on MDCT. – *J. Thorac. Imaging*, **21**, 2006, 179-183.

Review Articles

Some Dental Problems of the Romanian Bronze Age

Alexandra Comşa

„Vasile Pârvan” Institute of Archaeology, Bucharest, Romania

*Corresponding author e-mail: alexcomsa63@yahoo.com

The evolution and history of past communities have shown us that the human body is in permanent change, meaning in a dynamic balance, in order to get adapted and compensate the environmental modifications, which occurred over time. Moreover, its pathology, both dental and skeletal, is also different, depending on the conditions of the natural, socio-economic and cultural environment in which those people had lived. This paper refers to the dental pathology in the Bronze Age Romania, which is obviously variable, depending upon the populations that we refer to and the food regime that they had. The most important aspect that we want to emphasize is that an obvious difference could have been observed between the dental pathology of the bearers of the tumular ochre burials (Yamnaya, Mnogovalikovaya and Katakombnaya cultures) compared to the other ethnic groups, existing during that time.

Key words: dental pathology, Bronze Age, skeletons, Romania

Introduction

Bronze Age was an epoch characterized by large population movements, which affected not only the territory of today Romania, but also the entire Europe. The larger, or smaller ethnic groups which migrated from one place to another, had interacted with the environment (which was a natural, socio-economic or cultural one) (**Fig. 1**) but also the local communities. Some consequences could be observed, either on one, or another of them. In Romania, for instance, the bearers of the tumular ochre burials had exerted an obvious influence upon the cephalic index of the local populations, which, during the Bronze Age, had decreased in the extra-Carpathian regions, but, they had also changed, at least in part, some of the dental pathology existing in the epoch, by their mixture with other communities from this region. As they were semi-nomadic steppe populations, they used to consume, besides meat, also milk and dairy products and

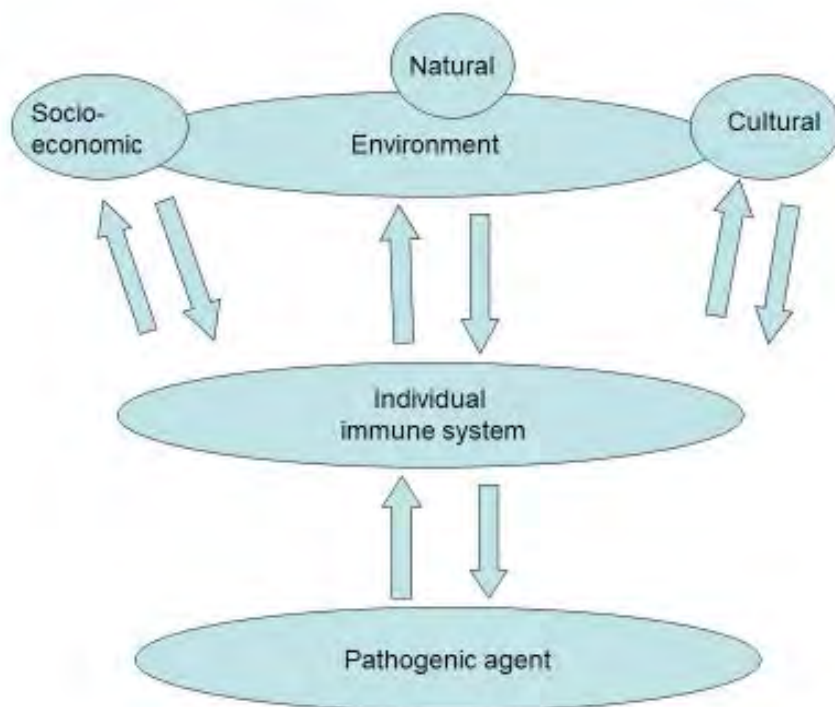


Fig. 1

this provided them with whiter and healthier dentition, compared with other people of those times. Moreover, the food regime initiated the formation of an alkaline milieu in the mouth of those people, which favored the appearance of tartar, also named dental calculus. Thus, they could be easily distinguished from other populations.

The other ethnic groups of the Bronze Age had consumed both products resulted from cattle breeding, but also from the practice of agriculture, the latter ones being richer in fibers and carbohydrates. These were not only more abrasive, but they also created acid conditions in the mouth of those individuals, which were favorable for the caries occurrence. As we could see, tartar and caries excluded each other, as they used to appear in distinct, different conditions (acid and alkaline). The poor mouth hygiene had also favored the existence of other pathologies, like parodontosis.

Materials and methods

We have studied the dental pathology existing in various skeletal series of the Romanian Bronze Age (Păuleni-Covasna County, Tureni-*La Furci*-Cluj County, Truşeşti-Botoşani County, Trestiana-Vaslui County, Leţcani-Iaşi County, Covurlui Plain-Galaţi County) we have used the macroscopic examination of the teeth, sometimes using also a magnifier.

The methodology is the one existing in the Dental Anthropology [4] practice and in the Human Paleopathology [6], in general.

Results

In a study of dental pathology that was done during the 6th decade of the past century, it was mentioned that the most important aspect of this kind was represented by caries, whose incidence had grown constantly, beginning since prehistory up to the recent times. In fact, during the Neolithic and metal ages, the caries frequency was similar, being situated between 20 and 30%, while a remarkable increase in its occurrence was noticed just later, in the pre-feudal series (53%) when, a significant change in the food regime of those communities must have appeared [3].

In present day Romania, there are no other similar complex analyses but, the general picture existing by now had shown that, during the Bronze Age, caries had remained on the first position as concerns dental pathology, in spite of exceptions, like bearers of the tumular ochre burials, mentioned above. Still, even in such communities, there were situations when caries existed, like in the series from Câmpia Covurlui (Galati County), comprising 39 skeletons. The caries had affected just the crown and root of the teeth in that series [1]. It is interesting to note that, also, in the populations that were mixtures between the local and steppe communities, the same healthier dentition could be found. We could mention here, as examples, the skeletal series from Trușesti (Botoșani County), comprising 127 skeletons, which had a small incidence of caries. Also, at Lețcani (Iași County) and Trestiana (Vaslui County), also with Noua skeletal finds, no caries could be found [5]. Of course, this diversity with regard to the presence, or absence of the caries could be explained by the food customs and habits of the people, which are very important and sometimes change the entire food regime of some individuals, or families. We should not forget that the caries is also connected with the absence of fluorine, that assures protection of the teeth enamel against the acid conditions in the mouth.

Dental abscess, is a complex problem, which might be a complication of a carious process, but it could be, also, the result of an injury or of an intense wear of the teeth, thus the dental pulp being exposed. Initially, a granuloma is created, after the spreading of infection (pulpitis) from the dental pulp towards the apex of the tooth. This is accompanied by an intense pain and pus accumulation that, finally, results in the formation of a dental abscess. In fact, this is a pus bag but, it is very dangerous for the life of the respective individual, as the pus might get disseminated through the blood stream and produce septicemia. A very large dental abscess could be found on a female skeleton discovered at Tureni-La Furci (Cluj County – **Fig. 2**), having the dimensions of 17,56x11,21 mm. As the bone structure around the respective molar was much affected, we could not say, for certain, which was the initial cause that produced this dental abscess. Such a pathological condition was not frequently found in other Bronze Age series, but some cases could be found in the sample from the Covurlui Plain (Galați County) [1].

Tartar, as already mentioned, was often present in the series belonging to the bearers of the tumular ochre burials but also in other skeletons of the Bronze Age, being an indicator of the food regime consisting in meat, milk and dairy products.



Fig. 2

based upon the receding position of the dental alveolus and often without taking into consideration the presence of inflammation signs upon it. Still, when we have already several teeth missing, like in a male mandible from Păuleni-Ciuc (inv. no. 7311), Harghita County, with the age of 40-45 years, we could be sure that this situation was determined by such a pathological condition [2].

Dicussion

Every new finding of dental paleopathology brings its contribution to a better knowledge, not only about the health conditions in past communities, but also, about their lifestyle and social organization, occupations, individual activities (when teeth are used as tools), as well as some rituals, in which teeth were involved (**Fig. 2**). This paper had referred strictly to the more usual interpretations related to teeth, which are the social-economical ones, that we have considered as being more appropriate for the topic of the Morpho-Days Conference, as their ritual, or symbolical meanings were closer to archaeology, the same like their use as tools. Therefore, this study of the teeth was somehow limited but, we hope it still brought some interesting information.

Conclusions

This paper had provided a glimpse into the importance of the teeth in the archaeological samples of the Bronze Age as, besides other aspects specific to a society, they reflected all types of living conditions in which those communities had lived. Of course, as expected, we could observe the lack of mouth hygiene, which favored the infections and their complications, beginning with the carious process which was more frequently found and dental abscess which was rarely documented and ending up with parodontosis. Tartar was not an infection but it facilitated such processes that would have affected the gums and surrounding tissues.

References

1. **Bălteanu, C., G. Miu, A. Tudose.** Contributions to the anthropological study of the skeletons in the complex of ochre burials from Cîmpia Covurlui, Galați County. (Contribuții la studiul antropologic al scheletelor din complexul mormintelor cu ocră din Cîmpia Covurlui, județul Galați). – *Studii și cercetări de antropologie*, **26**, 11-18. [in Romanian]
2. **Comșa, A.** Anthropological Data Regarding some of the Bronze Age Funerary Finds from Păuleni-Ciuc (Harghita County). (Date antropologice referitoare la unele dintre descoperirile funerare ale Epocii Bronzului de la Păuleni-Ciuc jud. Harghita). *Angustia* **23**, 2019, 109-186. [in Romanian]
3. **Firu, P., A. Negrea-Gherga.** Odontographic study of the ancient populations from Sărata Monteoru. – In: *Anthropological study Sărata Monteoru*. (Eds.: C. Maximilian, V. V. Caramelia, P. Firu, A. Gherga-Negrea). (Studiul odontografic al populațiilor vechi din Sărata Monteoru. Sărata Monteoru. Studiu antropologic). București. Editura Academiei Republicii Populare Române, 1962, 139-146.
4. **Hillson, S.** *Dental Anthropology*. Cambridge University Press, 1996.
5. **Necrasov, O., M. Cristescu, D. Botezatu, G. Miu.** Paleoanthropological research regarding the populations on the territory of Romania, Cercetări paleoantropologice privitoare la populațiile de pe teritoriul României (Romanian). – *Arheologia Moldovei*, **13**, 1990, 173-223.
6. **Ortner, D. J., W. G. J. Putschar.** *Identification of pathological conditions in human skeletal remains*. – Smithsonian Institution Press, 1981.

Is There a Correlation Between Impaired Sperm Quality and Overweight/Obesity?: A Review

Elenka Georgieva², Radoslava Stoyanova¹, Vesela Yancheva³, Iliana Velcheva³, Slaveya Petrova³, Stela Stoyanova², Stoil Tomov⁴

¹ Andrological laboratory, In vitro center „Selena“, Plovdiv, Bulgaria

² Department of Developmental Biology, Faculty of Biology, Plovdiv University “Paisii Hilendarski”, Plovdiv, Bulgaria

³ Department of Ecology and Environmental Conservation, Faculty of Biology, Plovdiv University “Paisii Hilendarski”, Plovdiv, Bulgaria

⁴ Department of General Medicine and Urology, Medical University-Plovdiv Plovdiv, Bulgaria

* Corresponding author e-mail: elenkageorgieva@uni-plovdiv.bg

Obesity is associated with significant disturbance in the hormonal status that can affect the reproductive system. In recent decades, an increasing interest in related to the association between high BMI levels, obesity and decreased sperm quality, which could also lead to a decrease in male reproductive potential. The aim of the present work is to identify the basic mechanisms of impaired sperm quality due to overweight and obesity. Sedentary lifestyle and work, as well as age of men are defined as possible ways to elevated BMI levels. Both inflammation and oxidative stress (as related pathophysiological processes) are considered as basic mechanisms, which could be found in the pathogenesis of male infertility caused by high BMI levels and obesity.

Key words: body mass index (BMI), sperm quality, sedentary lifestyle, age, inflammation, oxidative stress

Introduction

One of the most interesting periods in human ontogenesis is associated with the rapid processes of growth, development and sexual maturation. Thus, phenotypic traits are formed and the body reach the reproductive maturity.

The main goal of the experts in the biomedical sciences is to improve the system for assessment and prevention of adolescent health issues [23]. In this regard, for each new generation, the dynamics and completion of the physical and sexual maturation is associated with physical development during growth. Moreover, to achieve the correct

determination of the physical development it is not enough to take into consideration only the quantitative morphofunctional changes, but also the qualitative changes that occur at certain stages of development should be followed. Thus, these changes are the basis of the adult individual formation [4, 5].

It is therefore necessary to study the body composition and type. In this regard, different studies showed the physical development and indicators of the body composition and type [26, 27, 29].

The present review aims to study the pathophysiological mechanisms of male infertility associated with high BMI levels and obesity based on literature data.

Body weight and overweight – an important part of the processes of growth and sexual development: Many studies also report that various diseases and increased mortality in adulthood are associated with abnormalities in normal body weight, especially during the accelerated morphological development during the adolescence. Furthermore, body weight is measured as the main indicator of overweight, which could serve as environmentally sensitive indicator during the individual development. However, data on the body weight cannot be used alone as a direct indicator for determining overweight without considering its relationship to height. The most commonly used type of connection between the two traits is the body mass index (BMI). Thus, research is focused on this integral physical characteristic, which is related to the variations from healthy body weight [6, 24, 25, 28, 30, 43]. In this regard, in recent years studies indicate a deviation from healthy body weight with frequent achievement of high BMI levels ($BMI > 25.0 \text{ kg/m}^2$) and obesity ($BMI \geq 34.9 \text{ kg/m}^2$). In addition, the obesity is becoming a global health problem, reaching epidemic levels in recent years [1, 18]. In general, the obesity impairs the body health and the potential to maintaining the balance in metabolic processes and homeostasis. As a result, the obesity could lead to pathophysiological processes in the organism, which affect the cardiovascular, nervous and endocrine systems, as well as reproductive system and sperm quality. Obesity-induced high levels of BMI can also be due to various factors, such as sedentary lifestyle and work, men age, etc.

Association between elevated BMI levels and sperm quality: In recent decades, there has been an increasing interest in research related to the association between elevated BMI levels and decreased sperm quality, which could also lead to a decrease in male reproductive potential. Studies published in databases such as PubMed, Embase, Scopus, Web of Science, and Wanfang are related to the impact of the overweight and obesity on sperm quality. In parallel, opposite data are found regarding the relationship between elevated levels of BMI and decreased sperm quality [1, 17, 21, 40].

Hammoud et al. [15] and Sermondade et al. [39, 40] reported that overweight and obesity were associated with an increased prevalence of azoospermia or oligozoospermia. In addition, Ramaraju et al. [34] found oligozoospermia and asthenozoospermia in men with obesity. Jensen et al. [17] established that men with $BMI < 20.0 \text{ kg/m}^2$ and $BMI > 25.0 \text{ kg/m}^2$ had reduced sperm concentration and total sperm count, respectively, compared to men with BMI between $20.0 - 25.0 \text{ kg/m}^2$. Moreover, the percentage of normal spermatozoa was also reduced, among men with high levels of BMI. According to the authors, sperm volume and percentage of motile spermatozoa were not affected by elevated BMI levels. Kort et al. [19] studied 520 men and found significant ($p < 0.05$) and negative relationship between BMI and the total number of normal-motile sperm cells. In addition, a significant difference ($p < 0.05$) was

found in the total number of normally motile sperm among the different BMI groups. According to a new retrospective study of 9 464 patients, Ramírez et al. [35] found that elevated BMI levels affect first sperm concentration and total sperm count, which is confirmed by applying logistic predictions analysis.

Ramaraju et al. [34] conducted a retrospective cohort of 1 285 men with CASA analysis. The authors found that obesity ($\text{BMI} \geq 30 \text{ kg/m}^2$) was associated with lower volume, sperm count and concentration, progressive motility and total. After an analysis of 30 publications and a total of 115 158 participants, we can conclude that obesity is associated with reduced reproductive potential. As a proof of the statement, Campbell et al. [8] found that the obesity-induced male infertility ($\text{OR} = 1.66$, 95% CI 1.53-1.79) and the rate of live birth per cycle of Assisted Reproduction Technology (ART) was reduced ($\text{OR} = 0.65$, 95.0% CI 0.44-0.97). In addition, according to the authors men had an increased percentage of spermatozoa with low mitochondrial membrane potential (MMP), DNA fragmentation and abnormal morphology.

Many studies showed changes in the main sperm parameters, along with the sperm chromatin, DNA fragmentation, mitochondrial damage, apoptosis processes, serum reproductive hormone levels, etc. Oliveira et al. [31] investigated 1 824 men and found that elevated BMI levels negatively affected the sperm concentration, motility and morphology ($p < 0.05$). In contrary, elevated BMI levels were not associated with impaired sperm DNA integrity, which was assessed by DNA fragmentation using TUNEL assays test, sperm chromatin protamination using chromomycin A3 staining and apoptosis of the spermatozoa using annexin V staining ($p < 0.05$). However, elevated BMI levels were associated with increased mitochondrial damage in the sperm cells detected by applying Mito Tracker Green test ($p < 0.05$). Chavarro et al. [9] found that BMI was positively related to estradiol levels and inversely related to total testosterone and sex hormone-binding globulin (SHBG) levels. The authors also found a strong inverse relationship between BMI and inhibin B levels and a lower testosterone: LH ratio among men with a $\text{BMI} > 35 \text{ kg/m}^2$, as well as between BMI and inhibin B levels and a lower testosterone: LH ratio among men with a $\text{BMI} > 35 \text{ kg/m}^2$. In addition, the authors found that men with obesity had a lower total sperm count (concentration \times volume) than men with normal weight. Chavarro et al. [9] stated that sperm cells with elevated DNA damage were significantly increased in men with obesity.

High BMI levels and impaired sperm quality related to sedentary lifestyle and work: The relationship between overweight, obesity and sedentary occupations, as well as sedentary lifestyles in the male population were also studied. Sedentary jobs, such as long-haul driving, desk work, call center operators, computer-based work lead to immobilization and weight gain. That suggests elevated BMI levels and obesity, which in turn affects spermatogenesis. According to Brownson et al. [7] and Stamatakis et al. [42] the sedentary behavior became an increasing part of modern life, including transportation, work and leisure time. Sharpe [41] also proved the negative effects of the sedentary lifestyle and obesity on testicular function (testosterone levels and sperm production). According to Magnúsdóttir et al. [22] poor sperm quality was associated with sedentary work and obesity but not with plasma levels of persistent organochlorines. Priskorn et al. [33] found that men who watch television more than 5 hours/day had total sperm count 104 million and an adjusted sperm concentration of 37 million/mL versus 158 million and 52 million/mL, among men who did not watch

television that long on a regular basis. Furthermore, an increase in follicle-stimulating hormone and decreases in testosterone and the testosterone/luteinizing hormone ratio were detected in men who watched television for a long time.

After the analysis of spermograms (according to the WHO, 2010) of 159 men who visited a clinic for ART, we found the highest levels of overweight and obesity in the group of men who work in a sitting position and at the same time they had reduced sperm quality (unpublished data). Further research is needed to clarify the importance of a sedentary lifestyle, obesity and sperm quality.

High BMI levels and impaired sperm quality related to men age: Concerning man age and fertility, some evidence showed a decrease in reproductive potential with increased age, as presented in assisted reproductive technology outcomes. Nevertheless, further consensus remains to be achieved regarding male aging impact on sperm quality. In addition, some studies showed an association between age and sperm quality, others reported no relationship between them [44]. According to Sallmén et al. [36], the association between BMI and infertility was similar regarding men of different ages.

Based on our study (unpublished data), BMI showed a significant correlation only with the age of the patients regarding to the conventional sperm parameters. Moreover, impaired sperm parameters due to obesity factors were more significant in younger men (25-30 years).

WHO [45] reported worldwide obesity has nearly tripled since 1975. In 2016, more than 1.9 billion adults, 18 years and older, were overweight. Of these over 650 million were obese. 39.0% of adults aged 18 years and over were overweight in 2016, and 13.0% were obese. Most of the world's population lives in countries where overweight and obesity kill more people than underweight. Approximately 39 million children under the age of 5 were overweight or obese in 2020. Over 340 million children and adolescents aged 5-19 were overweight or obese in 2016.

Association between elevated BMI levels and sperm quality - basic mechanisms: Based on the studied literature concerning the mechanisms of reduced reproductive potential caused by obesity and high BMI levels, we could conclude that these mechanisms are mainly related to the expression of inflammation and oxidative stress. Impaired sperm quality in men is furthermore associated with the impact of endogenous and exogenous factors. Multifarious male infertility impair male reproductive functions via the common mechanisms of inflammation and oxidative stress, where both are related pathophysiological processes. Moreover, occurrence of one the above processes induced the other. Inflammation and oxidative stress could be found in the pathogenesis of male infertility. Inflammatory mechanisms activate specific pattern recognition receptors (PRRs) in testicular and epididymal cells, leading to activation of transcription factors. On the other hand, reactive oxygen species (ROS) production cause oxidation of membrane phospholipids and intracellular proteins, which can activate the PRRs-inflammatory pathway as well. In addition, according to Dutta et al. [13] the activated transcription factors supported the expression of inflammatory mediators, which caused exaggerated inflammation and could also act as oxidative stress, creating a vicious feedback loop.

However, the relation between the obesity and sperm parameters is not sufficiently studied, as well as its mechanism of action and the expression of the impaired sperm parameters. Sengupta et al. [38] found that obesity caused systemic inflammation

associated with a chronic inflammation dependent on T-helper 1 (TH-1) T-lymphocytes. Several pro-inflammatory mediators, including the cytokines [16], interacted with the complex reproductive regulations of the hypothalamic-pituitary-gonadal (HPG) axis, resulting in changes in the spermatogenesis [11]. According to the authors, impaired steroidogenesis or spermatogenesis resulted in hypogonadotropic hypogonadism, as well as decreased sperm parameters. In addition, inflammation could result in the excessive production of ROS and induced oxidative stress [12]. As stated Sengupta et al. [37] oxidative stress caused disruption of the functions and morphology of the sperm cells. Sperm DNA damage, deformation, and compromised plasma membrane integrity were observed by Alahmar et al. [2, 3]. ROS induced sperm motility led to altered sperm mitochondrial activities and reduced energy production in the spermatozoa.

According to Du Plessis et al. [10], Liu and Ding [20] changes, such as induced sleep apnea, alterations in the hormonal profiles (reduced inhibin B and androgen levels, elevated estrogen levels) and increased scrotal temperatures were expressed as impaired sperm parameters (decreased total sperm count, concentration and motility; increased DNA fragmentation index). Hakonsen et al. [14] and Palmer et al. [32] stated that that weight loss, lifestyle changes or bariatric surgery, can efficiently result in increased serum testosterone levels and sperm count, suggesting benefits for a possible weight loss on male fertility. Moreover, clinicians should consider the men obesity before applying assisted reproduction. More exercise is recommended, as well as increased movement in order to reduce the body weight and to therefore improve sperm parameters and have better performance in ART.

Conclusion

Based on the present review, we could conclude that obesity and high BMI levels could possibly lead to male infertility. Sedentary lifestyle and work, as well as age of men are defined as possible ways to elevated BMI levels and obesity, which induced basic mechanisms such as inflammation and oxidative stress. Such experiments need to be further performed in order to gain more thorough knowledge on the pathophysiological mechanisms of male infertility associated with high BMI levels and obesity.

References

1. Aggerholm, A. S., A.M. Thulstrup, G. Toft, C. H. Ramlau-Hansen, J. P. Bonde. Is overweight a risk factor for reduced semen quality and altered serum sex hormone profile? – *Fertility and Sterility*, **90**(3), 2008, 619-626.
2. Alahmar, A. T., A. E. Calogero, R. Singh, R. Cannarella, P. Sengupta, S. Dutta. Coenzyme Q10, oxidative stress, and male infertility: A review. – *Clinical and Experimental Reproductive Medicine*, **48**, 2021a, 97-104.
3. Alahmar, A. T., P. Sengupta. Impact of Coenzyme Q10 and Selenium on seminal fluid parameters and antioxidant status in men with idiopathic infertility. – *Biological Trace Element Research*, **199**, 2021b, 1246-1252.
4. Andreenko, E., M. Nikolova. Age features in the development of the subcutaneous fat tissue, muscularity and muscle-fat rations in men with different physical activity. – *Glasnik, Antropološkog društva Srbije*, **43**, 2008, 478-487.

5. **Andreenko, E., M. Nikolova.** Topical distribution of the subcutaneous fat tissue on some parts and regions of the body in children and adolescents from south Bulgaria. – *Biotechnology and Biotechnological Equipment*, **24**, 2010, 342-346.
6. **Boukov, Y., M. Nikolova, G. Baltadgiev, T. Matev.** Basic somatometric indices in three generations of children from Plovdiv. – *Journal of Anthropology*, **3**, 2000, 41-49.
7. **Brownson, R. C., T. K. Boehmer, D. A. Luke.** Declining rates of physical activity in the United States: what are the contributors? – *Annual Review of Public Health*, **26**, 2005, 421-443.
8. **Campbell, J. M., M. Lane, J. A. Owens, H. W. Bakos.** Paternal obesity negatively affects male fertility and assisted reproduction outcomes: a systematic review and meta-analysis. – *Reproductive BioMedicine Online*, **31(5)**, 2015, 593-604.
9. **Chavarro, J. E. , Th. L Toth, D.L Wright, J. D Meeker, R. Hauser.** Body mass index in relation to semen quality, sperm DNA integrity, and serum reproductive hormone levels among men attending an infertility clinic. – *Fertil. Steril*, **93(7)**, 2010, 2222-2231.
10. **Du Plessis, S. S., S. Cabler, D. A. McAlister, E. Sabanegh, A. Agarwal.** The effect of obesity on sperm disorders and male infertility. – *Nature Reviews Urology*, **7**, 2010, 153-161.
11. **Dutta, S., A. Biswas, P. Sengupta.** Obesity, endocrine disruption and male infertility. – *Asian Pacific Journal of Reproduction*, **8**, 2019a, 195-201.
12. **Dutta, S., A. Majzoub, A. Agarwal.** Oxidative stress and sperm function: A systematic review on evaluation and management. – *Arab Journal of Urology*, **17**, 2019b, 87-97.
13. **Dutta, S., P. Sengupta, P. Slama, S. Roychoudhury.** Oxidative stress, testicular inflammatory pathways, and male reproduction. – *International Journal of Molecular Sciences.*, **22**, 2021, Article ID10043.
14. **Hakonsen, L. B., A. M. Thulstrup, A. S. Aggerholm, J. Olsen, J. P. Bonde, C. Y. Andersen, M. Bungum, E. H. Ernst, M. L. Hansen, E. H. Ernst, C. H. Ramlau-Hansen.** Does weight loss improve semen quality and reproductive hormones? Results from a cohort of severely obese men. – *Reproductive Health*, **8**, 2011, 24.
15. **Hammoud, A. O., N. Wilde, M. Gibson, A. Parks, D. T. Carrell, A. W. Meikle.** Male obesity and alteration in sperm parameters. – *Fertility and Sterility*, **90(6)**, 2008, 2222-2225.
16. **Irez, T., S. Bicer, S. Sahin, S. Dutta, P. Sengupta.** Cytokines and adipokines in the regulation of spermatogenesis and semen quality. – *Chemistry and Biology Letters*, **7**, 2020, 131-139.
17. **Jensen, T. K., A.-M. Andersson, N. Jørgensen, A.-G. Andersen, E. Carlsen, J. H. Petersen, N. E. Skakkebaek.** Body mass index in relation to semen quality and reproductive hormones among 1,558 Danish men. – *Fertility and Sterility*, **82(4)**, 2004, 863-870.
18. **Kasman, A., F. Del Giudice, E. Shkolyar, A. Porreca, G. M. Busetto, Y. Lu, M. L. Eisenberg.** Modeling the contribution of the obesity epidemic to the temporal decline in sperm counts. – *Archivio Italiano Di Urologia E Andrologia*, **92(4)**, 2020.
19. **Kort, H. I., J. B. Massey, C. W. Elsner, D. Mitchell-Leef, D. B. Shapiro, M. A. Witt, W. E. Roudebush.** Impact of body mass index values on sperm quantity and quality. – *Journal of Andrology*, **27(3)**, 2006, 450-452.
20. **Liu, Y., Ding Z.** Obesity, a serious etiologic factor for male subfertility in modern society. – *Reproduction*, **154(4)**, 2017, 123-131.
21. **MacDonald, A. A., G. P. Herbison, M. Showell, C. M. Farquhar.** The impact of body mass index on semen parameters and reproductive hormones in human males: a systematic review with meta-analysis. – *Human Reproduction Update*, **16**, 2010, 293-311.

22. **Magnusdottir, E. V., T. Thorsteinsson, S. Thorsteinsdottir, M. Heimisdottir, K. Olafsdottir.** Persistent organochlorines, sedentary occupation, obesity and human male subfertility. – *Human Reproduction*, **20(1)**, 2005, 208-215.
23. **Mitova, Z.** Distribution of subcutaneous fat tissue in 9-15 year-old schoolchildren from Sofia. – *Acta Morphol. et Anthropol.*, **10**, 2005, 234-238.
24. **Mladenova, S., M. Nikolova, D. Boyadzhiev.** Body mass index, some circumference indices and their ratios for monitoring of physical development and nutritional status of children and adolescents. – *Acta Morphol. et Anthropol.*, **10**, 2005, 226-229.
25. **Mladenova, S., M. Nikolova.** Components of body mass and their relations during the growth period of the boys. – *Proceedings from Balkan Scientific Conference of Biology, Plovdiv University Press*, 2005, 138-150.
26. **Nikolova, M., S. Mladenova.** Anthropometric indicators for assessment of body composition. – *Acta Morphol. et Anthropol.*, **10**, 2005, 218-225.
27. **Nikolova, M., S. Sivkov, V. Akabaliev, S. Mladenova.** Body composition of children and adolescents in Plovdiv. – *Proceedings from Balkan Scientific Conference of Biology, Plovdiv University Press*, 2005, 150-159.
28. **Nikolova, M., E. Godina, D. Mollova.** A comparison of Plovdiv and Moscow children's height, weight and BMI values. – *Acta morphologica et anthropologica*, **15**, 2010, 212-216.
29. **Nikolova, M., D. Mollova, Sl. Tineshev.** Peculiarities in body composition of children. Comparison of Anthropometric and Bioelectrical impedance methods. – *Journal of Biomedical & Clinical Research*, **2**, 2009, 121-126.
30. **Nikolova, M., S. Tineshev.** Comparison of the body mass index to other methods of body fat assessment in bulgarian children and adolescent. – *Biotechnology and Biotechnological Equipment*, **24**, 2010, 329-337.
31. **Oliveira, J. B. A., C. G. Petersen, A. L. Mauri, L. D. Vagnini, A. Renzi, B. Petersen, M. Mattila, F. Dieamant, R. L. R. Baruffi, J. G. Franco Jr.** Association between body mass index and sperm quality and sperm DNA integrity. A large population study. – *Andrologia*, **50(3)**, 2018.
32. **Palmer, N. O., H. W. Bakos, J. A. Owens, B. P. Setchell, M. Lane.** Diet and exercise in an obese mouse fed a high-fat diet improve metabolic health and reverse perturbed sperm function. – *American Journal of Physiology-Endocrinology and Metabolism*, **302**, 2012, 768-780.
33. **Priskorn, L., T. K. Jensen, A. K. Bang, L. Nordkap, U. N. Joensen, T. H. Lassen, I.A. Olesen, S. H. Swan, N.E. Skakkebaek, N. Jørgensen.** Is sedentary lifestyle associated with testicular function? A cross-sectional study of 1,210 Men. – *American Journal of Epidemiology*, **184(4)**, 2016, 284-294.
34. **Ramaraju, G. A., S. Teppala, K. Prathigudupu, M. Kalagara, S. Thota, M. Kota, R. Cheemakurthi.** Association between obesity and sperm quality. – *Andrologia*, **50(3)**.
35. **Ramírez, N., G. Estofán, A. Tissera, R. Molina, E. M. Luque, P. J. Torres, A. Mangeaud, A. C. Martini.** Do aging, drinking, and having unhealthy weight have a synergistic impact on semen quality?. – *Journal of Assisted Reproduction and Genetics*, **38(11)**, 2021, 2985-2994.
36. **Sallmén, M., D. P Sandler, J. A Hoppin, A. Blair, D. D. Baird.** Reduced fertility among overweight and obese men. – *Epidemiology*, **17(5)**, 2006, 520-523.
37. **Sengupta, P., K. Bhattacharya, S. Dutta.** Leptin and male reproduction. – *Asian Pacific Journal of Reproduction*, **8**, 2019, 220-226.
38. **Sengupta, P., S. Dutta, U. D'Souza, A. Alahmar.** Reproductive tract infection, inflammation and male infertility. – *Chemistry and Biology Letters*, **7**, 2020, 75-84.

39. Sermondade, N., C. Faure, L. Fezeu, A. G. Shayeb, J. P. Bonde, T. K. Jensen, M. Van Wely, J. Cao, A. C. Martini, M. Eskandar, J. E. Chavarro, S. Koloszar, J. M. Twigt, C. H. Ramlau-Hansen, E. Borges Jr, F. Lotti, R. P. M. Steegers-Theunissen, B. Zorn, A. J. Polotsky, S. La Vignera, B. Eskenazi, K. Tremellen, E. V. Magnusdottir, I. Fejes, S. Herberg, R. Lévy, S. Czernichow. BMI in relation to sperm count: an updated systematic review and collaborative meta-analysis. – *Human Reproduction Update*, **19**(3), 2013, 221-231.
40. Sermondade, N., C. Faure, L. Fezeu, R. Lévy, S. Czernichow. Obesity and increased risk for oligozoospermia and azoospermia. – *Archives of Internal Medicine*, **172**(5), 2012, 440-442.
41. Sharpe, R. M. Environmental/lifestyle effects on spermatogenesis. – *Philosophical Transactions of the Royal Society B*, **365**, 2010, 1697-1712.
42. Stamatakis, E., N. Coombs, R. Jago, A. Gama, I. Mourão, H. Nogueira, V. Rosado, C. Padez. Type-specific screentime associations with cardiovascular risk markers in children. – *American Journal of Preventive Medicine*, **44**(5), 2013, 481-488.
43. Tineshev, S., M. Nikolova. Anthropological characteristics of body composition in children and adolescents from Plovdiv. – *Biotechnology and Biotechnological Equipment*, **24**, 2010, 338-341.
44. Veron, G. L., A. D. Tissera, R. Bello, F. Beltramone, G. Estofan, R. I. Molina, M. H. Vazquez-Levin. Impact of age, clinical conditions, and lifestyle on routine semen parameters and sperm kinematics. – *Andrology*, **110**(1), 2018, 68-75.
45. World Health Organization. Obesity and overweight, 2021. <https://www.who.int/news-room/fact-sheets/detail/obesity-and-overweight>



IN MEMORIAM

Professor Yordan Alexiev Yordanov

Corresponding member of the Bulgarian Academy of Sciences

On the 22th of February 2022 Professor Yordan Yordanov, Corresponding Member of the Bulgarian Academy of Sciences passed away.

Yordan Yordanov was born on the 6th November, 1938 in the village of Dragomirovo, Svishtov county, Veliko Tarnovo region in a teacher's family. He lived, studied and worked in the village of Strahilovo, Veliko Tarnovo region, the town of Polski Trambesh and in the city of Sofia.

Yordanov Yordanov graduated Faculty of Dentistry at Higher Medical Institute in Sofia (1963) with excellent score. After graduating he worked in a rural health department (1963-1965). In 1965 he was appointed an intern-research associate in the Department of Orthopedic Dentistry at the Higher Medical Institute in Sofia. There he acquired a degree in orthopedic dentistry with orthodontics (1967). From 1967 til 1968 he worked in the Ministry of Interior in Sofia. In July 1968 he was appointed as a researcher in the Department of Anthropology and Human Anatomy at the Institute of Morphology, Bulgarian Academy of Sciences, where in March 1971 he was promoted into assistant professor. In 1973 he acquired a degree in human anatomy and PhD degree after defence of dissertation on "Anatomical and anthropological characteristics

of the hard palate in humans”. In 1982 he acquired degree “Doctor of Medical Sciences” after defence of dissertation on “Restoration of the head on the skull”. In 1984 Yordan Yordanov was promoted to Associate professor and in 1990 – to full Professor. Professor Yordanov was promoted in Corresponding Member of BAS in 2004.

Professor Yordanov was founder (1980) and Head of the “Laboratory of Plastic Anthropological Reconstruction of the Head of the Skull” in the Institute of Morphology. For 25 years Yordan Yordanov was Head of the Department of Anthropology in the same Institute (1987-2012). He was Director of the Institute of Experimental Morphology and Anthropology with Museum (1991-2010). He was Coordinator of the National Program “Anthropological Characteristics of the Bulgarian People”.

Professor Yordanov specialized in anthropology in Poland (1973/74), USSR (Russia and Armenia – 1981). Then followed a specialization in Germany (1982/83) and in USA (1987).

With his great expertise and experience Professor Yordanov was a member and chairman of many scientific councils and commissions as follow: member of Specialized Scientific Council for Normal and Pathological Morphology at the Higher Attestation Commission (1991-2010) and its chairman (1993-1997); Chairman of the Scientific Council of the Institute of Experimental Morphology and Anthropology (1993-2010), Chairman of the Board of Directors of the Biological Institutes at the Bulgarian Academy of Sciences (1998-2010), Chairman of the Expert Council for Publishing Activity of the Academy (2003-2010), member of the General Assembly of the Academy, Mandate Commission and its chairman (1990-2010); member of the Legislation Committee and the Expert Council for DNA – Polymorphic Analysis of the Academy; member of the National Advisory Museum Council at the Ministry of Culture.

He was also the founder and Chairman of the Bulgarian Anthropological Society, a member and Chairman of the Bulgarian Anatomical Society; Editor-in-Chief of “Acta morphologica et anthropologica” and “Journal of Anthropology”; member of the Board of European Anthropological Association (Representative for Bulgaria); member of the International Identification Association, based in the United States.

Professor Yordanov was dedicated in teaching students from Sofia University “St. Kliment Ohridski”, University of Veliko Tarnovo “St. St. Cyril and Methodius”; New Bulgarian University – Sofia, Southwestern University “Neofit Rilski” – Blagoevgrad, Slavic University – Sofia. He was supervisor of many post-graduate student.

Yordan Yordanov’s remarkable scientific activity was in different fields of: physical anthropology (paleoanthropology, paleopathology, paleodemography), morphology of the human skeletal system, craniology, gemelology, morphology, dentistry, medical and applied anthropology, museum work. He created original methods for determining the biological age of man, for the quantitative assessment of the manifestations of asymmetry in the human face. He also established new relationships between individual facial sizes. He is the author of the invention “Model of the human head”. His main fundamental and applied scientific achievements are:

1. He introduced in Bulgaria, modified and updated the method for plastic anthropological reconstruction of the head on the skull, introduced new indices and methods in physical anthropology.

In 1982/83 in Germany he demonstrated the method of plastic anthropological reconstruction on a female skull of a Hun princess from the V century – exhibited

in the museum in Braunschweig. In 1987, in the city of Atlanta (USA), the method was demonstrated on a male Indian skull from the 14th century (Etowah culture). The reconstruction was presented in three museums in the state of Georgia (USA).

2. Professor Yordanov is author of more than 70 plastic anthropological reconstructions from archeological excavations from the Neolithic to the Renaissance in the territory of Bulgaria. Among them are the anthropological reconstructions of great Bulgarians and revivalists, activists of the liberation movement as Tzar Kaloyan and Tzar Samuil, Thracian Princess, Bacho Kiro, Georgi Rakovski, Luben Karavelov, Zahari Stoyanov, etc. Many of them are presented in the museum expositions in the country and abroad – in Japan, USA, France, Germany, Russia.

3. He was founder of the Anthropological exhibition “The Man in the Past”, registered by the Ministry of Culture. Later, the exposition grew into National Anthropological Museum that was opened on 21.03.2007 and registered by ICOM and Ministry of Culture.

4. His contributions to the characteristics of the human masticatory apparatus – hard palate, teeth, dental arches, thickness of the tooth walls are published for the first time in the literature.

5. He worked on the anthropological characteristics of the people who lived in our lands from the Neolithic to the Renaissance as well as on the modern population of the Republic of Bulgaria in the late twentieth century.

Professor Yordanov is the author of about 360 publications and 26 books and handbooks for medical students. The most famous book “Anthropology of the population of Bulgaria in the late twentieth century” is published in Bulgarian and in English by Professor Marin Drinov Publishing House of Bulgarian Academy of Sciences, Sofia.

Prof. Yordanov was the initiator of many scientific events. As a member and chairman of the Board of Bulgarian Anatomical Society, he worked very hard in organizing the National Congresses of the Society. On his idea, a conference began to be held, for the first time in 2004 in the city of Koprivshtitsa, known as Koprivshtitsa Morphological Days. Since 2012, the conference has been held in Sofia, in the National Anthropological Museum.

Recognition for Professor Yordanov’s contribution are several prestigious awards by the Bulgarian Academy of Sciences and the President of the Republic of Bulgaria.

Professor Yordanov is remembered by his colleagues as an erudite and talented person with unique sense of humour, elegant style and glamour. He was patriot with active public position and humanism. He was beloved teacher, a scientist with wide interests not only in the field of anthropology and biomedicine, but also in the field of history and archaeology, literature, art, music, etc. He was famous with numerous interviews in the press and on TV on wide-ranging topics - from cultural and historical heritage and the origin of man to the trends in the development of the modern population of Bulgaria and demographic problems.

Professor Yordanov was an epoch of the development of physical anthropology in Bulgaria! With his death Bulgarian Academy of Sciences as well as Bulgarian Morphological School lost a great scientist.

Racho Stoev and Nina Atanassova

**SUPPLEMENT – PROCEEDINGS
OF THE 8TH NATIONAL CONFERENCE
WITH INTERNATIONAL PARTICIPATION
“MORPHOLOGICAL DAYS”**

**Impact of Diabetes Mellitus Induced in Early Postnatal
Life on Bax Protein Expression in Rat Testes**

Silvina Zapryanova¹, Ekaterina Pavlova^{2}, Nina Atanassova²*

¹ *Institute of Biology and Immunology of Reproduction, Bulgarian Academy of Sciences, Sofia, Bulgaria*

² *Institute of Experimental Morphology, Pathology and Anthropology with Museum, Bulgarian Academy of Sciences, Sofia, Bulgaria*

*Corresponding author e-mail: e_bankova@yahoo.com

The aim of our study was to investigate the impact of experimentally induced hyperglycemia on Bax expression in the testes of pubertal and mature rats. Diabetes mellitus (DM) was induced by single i.p. streptozotocin injection at dose of 100 mg/kg b.w. on day 1 (neonatally, NDM) or day 10 (prepubertally, PDM). Treated animals were sacrificed on day 18 or day 50 and testes and blood were sampled. Serum glucose was evaluated. Testis lysates were used to determine expression of pro-apoptotic Bax protein by SDS-PAGE followed by Western blot. Our results revealed prominent expression of pro-apoptotic Bax protein with most intensive reaction in adult PDM testes. Experimentally induced DM in early life increased pro-apoptotic Bax expression in pubertal and mature rat testes that is probably involved in mechanisms underlying reproductive disorders in diabetic males.

Key words: Diabetes mellitus, streptozotocin, testis, apoptosis, Bax

Introduction

Diabetes mellitus (DM) can lead to male infertility via action at multiple levels including altered sperm count and quality, degeneration and apoptosis of germ cells,

impaired glucose metabolism in Sertoli cells, compromised testosterone production and secretion [6, 8]. Investigation of apoptotic protein expression in conditions of hyperglycemia would contribute to elucidate the mechanisms underlying reproductive disorders in diabetic males. Bax is a multidomain, pro-apoptotic member of the Bcl-2 family that is required for normal spermatogenesis in different mammalian species. The ratio of Bax/Bcl-2 family members is a critical determinant of cell fate: elevated Bcl-2 favors extended survival of cells whereas increasing levels of Bax expression accelerates cell death [2]. Bax is found in all mouse and human testicular cell types [1]. In this regard the aim of our study was to investigate the Bax protein expression in pubertal and mature rat testes after experimentally induced hyperglycemia in early postnatal life of rats.

Materials and Methods

Diabetes mellitus was induced by single intraperitoneal injection of streptozotocin at dose of 100 mg/kg body weight on day 1, to induce neonatal DM (NDM) or on day 10, to induce prepubertal DM (PDM) in male rat pups. Animals were sacrificed at day 18 (early puberty) or day 50 (maturity) and testes and blood were sampled. Serum glucose was evaluated. Testis lysates were used to detect changes in expression of the pro-apoptotic Bax protein (1:1000) by SDS-PAGE followed by Western blot. As internal reference control α -smooth muscle actin (1:5000) was used. The experiment was carried out in accordance with guidelines EU Directive 2010/63/EU for animal experiments.

Results

Diabetic status of rats was validated by elevation of serum glucose in both ages. More pronounced increase was detected in prepubertal diabetic rats than in neonatal DM. On day 18 glucose was 75% and 6% higher than control, respectively. On day 50 fasting glucose was 69% and 26% higher than control, in PDM and NDM respectively. In early puberty Western blotting revealed increased but not consistent reaction of antibody against pro-apoptotic Bax protein. In the control group Bax expression was not detected. In most of the NDM and PDM samples bands on the membrane correspond to 21 kDa Bax protein and protein levels in both diabetic groups increased compared to control. On day 50 Bax expression in NDM and PDM was increased compared to controls but reaction in PDM testes was more intensive than in NDM lysates (**Fig. 1**). In both diabetic groups on day 50 Bax reaction was stronger compared to early pubertal diabetic testes.

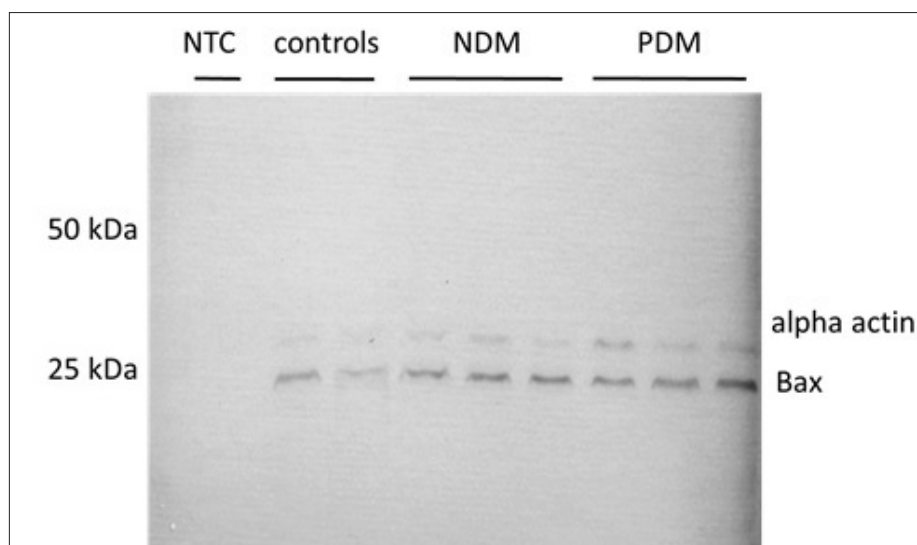


Fig. 1. Western blot expression of Bax in adult (day 50) control and diabetic testis homogenates. NDM – Neonatally induced diabetes mellitus; PDM – Prepubertally induced diabetes mellitus; NTC – negative control; α -smooth muscle actin as internal reference control.

Discussion

The high proliferative capacity of the seminiferous epithelium is accompanied by spontaneous apoptosis during development. Germ cell apoptosis can be induced under stress caused by radiation, hormonal imbalance, temperature and chemical toxicants [6]. Glucose metabolism is an important factor for normal proceeding of spermatogenesis. In this study we provide new data that high glucose levels at adulthood due to DM induced in early life, caused elevated testicular expression of proapoptotic Bax protein in 50 day old rats, more pronounced in PDM than in NDM animals. Koh et al. and Zha et al. [3, 7] reported increased apoptosis (phosphorylation of JNK, elevated Bax expression and TUNEL positive cells, decreased Bcl-2 expression) in diabetic condition induced in adult animals. The results from current study correspond to our previous data for significant reduction of serum testosterone levels and gonadosomatic index (testis weight to body weight ratio) in mature rats [4]. According to Zha et al. [7] hyperglycaemia induced in adulthood is associated by lower testosterone production. At day 18 we did not find any increase in testosterone levels (unpublished data) in both PDM and NDM animals that could explain why increase in testicular Bax protein expression is not consistent at that age. It is well known that elevated germ cell apoptosis can be responsible for reduced germ cell number that in turn is directly related to lower testis weight. Summarizing our observations it seems that prepubertally induced diabetes significantly increased glucose levels in mature animals that is associated with reduced testosterone levels and elevated germ cell apoptosis (evidenced by increased Bax expression) in the testis.

Conclusions

Our results indicate that Diabetes mellitus exerts more adverse impact on the testis if induced at the beginning of puberty manifested by increased expression of pro-apoptotic Bax protein in pubertal and adult rat testes.

Acknowledgements: This study was supported by Grant No KP-06-M21/3 for Junior Basic Researchers and Postdocs from the Bulgarian National Science Fund.

References

1. Beumer, T. L., H. L. Roepers-Gajadien, I. S. Gademan, T. M. Lock, H. B. Kal, D. G. De Rooij. Apoptosis regulation in the testis: Involvement of Bcl-2 family members. – *Mol. Rep. Dev. Incorpor. Gam. Res.*, **56**(3), 2000, 353-359.
2. Kale, J., E. Osterlund, D. Andrews. BCL-2 family proteins: changing partners in the dance towards death. – *Cell Death Differ.*, **25**, 2018, 65-80.
3. Koh, P. O. Streptozotocin-induced diabetes increases apoptosis through JNK phosphorylation and Bax activation in rat testes. – *J. Vet. Med.Sci.*, **69**(9), 2007, 969-971.
4. Pavlova, E., E. Lakova, I. Vladov, S. Zapryanova, Y. Gluhcheva, I. Ivanov, K. Svechnikov, N. Atanassova. Experimental approach for metabolic disorders as a tool to investigate impact of environment on human health. – *Proc. 16th Int. Conf. Environ. Sci. Tech.*, Rhodes, Greece, 2019.
5. Rato, L., M. G. Alves, A. I. Duarte, M. S. Santos, P. I. Moreira, J. E. Cavaco, P. F. Oliveira. Testosterone deficiency induced by progressive stages of diabetes mellitus impairs glucose metabolism and favors glycogenesis in mature rat Sertoli cells. – *Int. J. Biochem. Cell Biol.*, **66**, 2015, 1-10.
6. Singh, B., G. Gupta. Testicular germ cell apoptosis and spermatogenesis. In: *Molecular Signaling in Spermatogenesis and Male Infertility* (Ed. Rajender Singh), CRC Press, UK, 2019, 31-40.
7. Zha, W., Y. Bai, L. Xu, Y. Liu, Z. Yang, H. Gao, J. Li. Curcumin attenuates testicular injury in rats with streptozotocin-induced diabetes. – *BioMed. Res. Int.*, 2018, 7468019.
8. Zhong, O., L. Ji, J. Wang, X. Lei, H. Huang. Association of diabetes and obesity with sperm parameters and testosterone levels: a meta-analysis. – *Diabetol. Metab. Syndr.*, **13**, 2021, 109.

Testicular Steroidogenesis after Pinealectomy - the Role of BDNF Signaling System

Darina Barbutska¹, Aneliya Petrova^{1}, Yvetta Koeva¹, Katerina Georgieva², Yana Tchekalarova³, Georgi Nanov⁴*

¹ Medical University of Plovdiv, Department of Anatomy, Histology and Embryology

² Medical University of Plovdiv, Department of Physiology

³ Institute of Neurobiology, Bulgarian Academy of Sciences

⁴ Student in Medicine, Medical University of Plovdiv, Faculty of Medicine

* Corresponding author e-mail: Anelia.Petrova@mu-plovdiv.bg

The relationship between melatonin and steroidogenesis in the male reproductive system has been confirmed in many studies. However, there is limited data on changes in testicular steroidogenesis as an age-related process in melatonin deficiency conditions. In this regard, the immunohistochemical localization of the neurotrophic factor BDNF and its corresponding TrkB receptor was investigated in the Leydig Cells (LCs) of 5-, 16- and 20-month-old Wistar rats, divided into two groups – animals with removed pineal glands and SHAM-group. The results showed more pronounced immunoreactivity for BDNF and its receptor in the LCs of animals with removed pineal glands, compared to the SHAM group, as the expression correlates with age-related changes in the three groups. The data obtained confirm the role of melatonin as a regulator of testicular function by influencing the hypothalamic-pituitary-gonadal axis, as well as the role of the BDNF-signaling system in auto- and paracrine control of testicular steroidogenesis.

Key words: Leydig cells, melatonin, neurotrophic factor, steroidogenesis

Introduction

The main secretory product of the pineal gland – melatonin – is the subject of research, not only for its role in the regulation of circadian rhythms, but also for its diverse anti-inflammatory, antioxidant and anti-apoptotic effects [2, 10]. Well known is its suppressive effect on the secretion of the two adenohypophyseal gonadotropic hormones – luteinizing hormone (LH) and follicle-stimulating hormone (FSH), affecting the male hypothalamic-pituitary-gonadal axis [1]. It has been established that by binding to its specific receptors, melatonin can directly regulate testosterone

secretion [13], and Frungieri et al., [1] demonstrated that melatonin can downregulate the expression of key steroidogenic enzymes.

Recently, an object of research has been the potential role of the BDNF-signaling system, consisting of the brain derived neurotrophic factor (BDNF) and its corresponding receptor TrkB, outside the development and proliferation of neurons, namely: in the autocrine and paracrine control of testicular steroidogenesis [11,12]. The expression of this signaling molecule and its corresponding receptor in testicular Leydig cells (LCs) supports the hypothesis that neurotrophins produced and/or acting on LCs are involved in the process of their differentiation and functional activity [3-8].

The immunohistochemical analysis of BDNF and its corresponding receptor TrkB, as markers of the differentiation status and activity of LCs in an experimental model of removed pineal gland makes it possible to clarify the action of melatonin on the processes of steroidogenesis in the male reproductive system during aging. In this regard, we aimed to investigate the immunoexpression of BDNF and its receptor TrkB in the LCs of rats in melatonin deficiency conditions.

Materials and Methods

Male Wistar rats, bred under standard conditions (Temp.: $21 \pm 1^\circ\text{C}$, humidity: 50-60% and artificial lighting mode) from three different age groups: 5 months (sexually mature), 16 months (adults) and 20 months (old), were divided into two groups: (n=8) – sham- and rats with removed pineal glands. The experimental model of pinealectomy was performed according to the methodology described by Hoffman and Reiter. Testicular fragments (4-5 mm thick) were gathered after decapitation of the animals and were fixed in Bouin's fluid for 24 h, embedded in paraffin and prepared for immunohistochemistry. The expression of BDNF and TrkB was monitored using the ABC method with the ImmunoCruz™ goat ABC Staining System kit (Santa Cruz Biotechnology, Inc., USA), with DAB as a chromogen and monoclonal primary anti-BDNF- and anti-TrkB antibody (1:100). Sections in which the primary antibody was substituted with phosphate buffered saline (PBS) were used as negative controls. The study was conducted in accordance with all accepted ethical guidelines for working with experimental animals and with the acknowledgement of the Scientific Ethics Committee at MU-Plovdiv No P-1583/2021.

Results

Our results demonstrate stronger immunoexpression of BDNF (**Fig. 1 A**) and its TrkB-receptor (**Fig. 1 B**) in 5-month-old rats with removed pineal glands, compared to the SHAM-group (**Fig. 1 C and 1 D**).

In 16-month-old rats, the immune response to BDNF in Leydig cells of the testicular interstitium was moderate. Again, the immune response is better expressed in animals with removed pineal gland (**Fig. 2**)

In 20-month-old animals, atrophic populations of LCs demonstrate relatively poor immunohistochemical reactivity for BDNF and TrkB in both groups – rats with removed pineal glands and SHAM – group (**Fig. 3**).

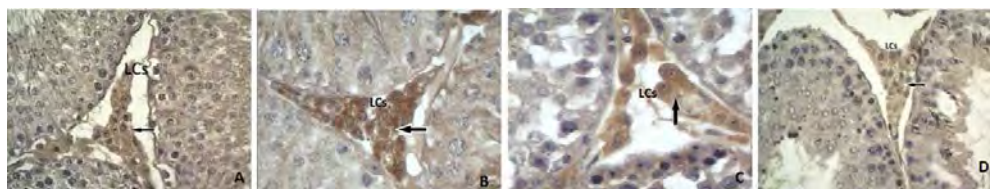


Fig. 1. Immunoreactivity for BDNF and TrkB in rat testis at 5 months postpartum. $\times 400$ A and B – rats with removed pineal glands; C and D – SHAM-group

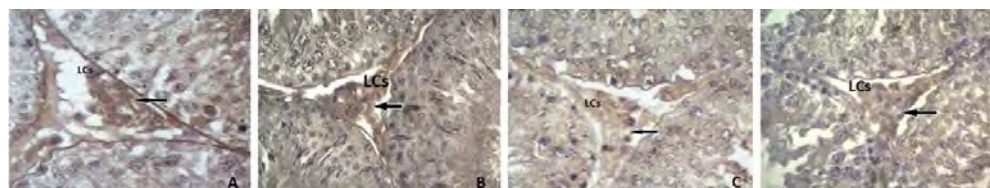


Fig. 2. Immunoreactivity for BDNF and TrkB in rat testis at 16 months postpartum. $\times 400$ A and B – rats with removed pineal glands; C and D – SHAM-group

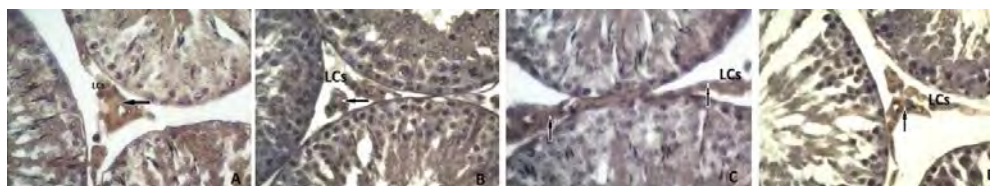


Fig. 3. Immunoreactivity for BDNF and TrkB in rat testis at 20 months postpartum. $\times 400$ A and B – rats with removed pineal glands; C and D – SHAM-group

Discussion

Our study showed strong immunoreactivity for BDNF and its corresponding receptor TrkB in LCs of 5-month-old rats and a significant reduction in immunoexpression in the atrophic LCs populations of adult rats. In all three age groups, the immune reaction was better manifested in the animals with removed pineal glands. The gathered experimental data demonstrate the role of melatonin as a regulator of testicular steroidogenesis by influencing the male hypothalamic-pituitary-gonadal axis [1, 13]. These observations define the BDNF signaling system primarily as a paracrine factor with a leading role in LCs differentiation and functional activity and suggest the role of melatonin in the control of the testicular steroidogenesis under the regulatory effect of the hypothalamic-pituitary axis [1,10].

Acknowledgements: The research was funded by a project of MU-Plovdiv NO-02/2021.

References

1. Frungieri, M., R. Calandra, S. P. Rossi. Local actions of melatonin in somatic cells of the testis. – *Int. J. Mol. Sci.*, **18**, 2017, 1170.
2. Gheban, A., A. Rosca, M. Crisan. The morphological and functional characteristics of the pineal gland. – *Medicine and Pharmacy Reports*, **92**, 2019, 3, 226-234.
3. Koeva, Y. Neuronal markers in the human Leydig cells- immunohistochemical study. – *Andrologiia*, 2002a; **11**, 10-12.
4. Koeva, Y. The Leydig cells of the human testis- site of the immunocytochemical expression of growth and neurotrophic factors. – *Andrologiia*, 2000a, **9**, 14-17.
5. Koeva, Y., M. Bakalska, M. Davidoff. Neurotrophic factors in rat Leydig cells after treatment with ethane dimethanesulphonate (EDS). – *Andrologiia*, 2001, **10**, 11-12.
6. Koeva, Y., M. Davidoff, L. Popova. Identification of BDNF, NT-3 and their receptors localized in Leydig cells of human testis. – *Comp. Rend. Acad. Bulg. Sci.*, **53**(2), 2000, 129-132.
7. Koeva, Y., M. Davidoff, L. Popova. Immunocytochemical expression of p75LNGFR and trkA in Leydig cells of the human testis. – *Folia Medica*, **4**, 1999, 53-58.
8. Koeva, Y., M. Davidoff. Brain derived neurotrophic factor (BDNF) and its receptor trkB in rat Leydig cells during the postnatal development. – *Acta Morphol. et Anthropol.*, **7**, 2002b, 23-27.
9. Müller, D., M. Davidoff, O. Bargheer, H. Paust, W. Pusch, Y. Koeva, D. Ježek, A. Holstein, R. Middendorff. The expression of neurotrophins and their receptors in the prenatal and adult human testis: evidence for functions in Leydig cells. – *Histochemistry and Cell Biology*, **126**, 2006, 199-211.
10. Patel, S., B. Rahmani, J. Gandhi, O. Seyam, G. Joshi, I. Reid, N. L. Smith, W. C. Waltzer, S. A. Khan. Revisiting the pineal gland: a review of calcification, masses, precocious puberty, and melatonin Functions. – *Int. J. Neurosci.*, **130**(5), 2020, 464-475.
11. Schultze, R., M. Metsis, T. Hokfelt, M. Parvinen, M. Pelto-Huikko. Expression of neurotrophin receptors in rat testis. Upregulation of TrkA mRNA with hCG treatment. – *Mol. Cell Endocrinol.*, **182**, 2001, 121-127.
12. Vidal, F., P. Lopez, L. Lopez-Fernandez, F. Ranc, J. Scimeca, F. Cuzin, M. Rassoulzagedan. Gene trap analysis of germ cell signalling to Sertoli cells: NGF-TrkA mediated induction of Fra1 and Fos by postmeiotic germ cells. – *J. Cell Sci.*, **11**, 2001, 4, 435-443.
13. Wu, C. S., S. F. Leu H. Y. Yang, B. M. Huang. Melatonin inhibits the expression of steroidogenic acute regulatory protein and steroidogenesis in MA-10 cells. – *J. Androl.*, **22**, 2001, 245-254.

Cryopreservation of Gametes, Embryos and Ovarian Tissue as a Method for Fertility Preservation in Oncological Patients

Elena Hristova, Nadya Petrova, Plamen Todorov

Institute of Biology and Immunology of Reproduction, Bulgarian Academy of Sciences, Sofia, Bulgaria

*Corresponding author e-mail: hristova.elena@gmail.com

Cancer is the second most common cause of death after the diseases of the cardio-vascular system. Due to the modern complex treatment methods, there are increasing survival rates of oncological patients. That puts forward the question for the quality of life of the recovered and respectively, their ability to have children. In large number of cases, the chemo-/radiotherapy leads to damage to oogenesis and spermatogenesis. For that reason, the patients are offered fertility preservation solutions before the start of the anti-tumour therapy. The basic approaches to fertility preservation in patients with pending chemo- or radiotherapy are presented in the current review.

Key words: fertility preservation, cryopreservation, gametes, embryos, ovarian tissue

Introduction

Worldwide, cancer diseases are the second most common reason for death after the disorders of the cardio-vascular system. At the same time, mortality is constantly decreasing, due to the contemporary complex treatment methods, and in a number of cases there is full recovery. For example, the five-year survival rates of the patients with haematological cancers, breast carcinoma, etc. is often above 90%. That brings up the question about the quality of life of the recovered and respectively, their ability to have children. It is known, that in many cases the chemo-/radiotherapy leads to damage of the gonadal functions – the oo- and spermatogenesis. Therefore, it is important that patients are offered options for their fertility preservation prior to the start of the anti-tumour treatment. The advances in the modern science of cryobiology provide opportunities for successful freezing of reproductive cells and tissues, which later can be used for transplantation or in the assisted reproductive technologies (ART).

Approaches for fertility preservation in male patients

Spermatogenesis starts in puberty and continues almost through the whole life of males. The duration of 1 complete cycle is a little more than 2 months, with 90 – 200 mln spermatozoa forming each day [3, 14]. Different disorders and exogenic factors influence the process and the quality of the resulting gametes. It is known that chemo- and radiotherapy in oncology have a negative effect: the quality of the semen deteriorates; the morphology worsens; DNA-fragmentation increases; the number of the spermatozoa is reduced and in some cases azoospermia is observed [11]. Surgery is also applied in certain types of cancer, sometimes with removal of the reproductive organs: orchiectomy, prostatectomy, radical cystectomy. The hormonal medication for prostate tumours effects the production of spermatozoa as well [2]. After treatment, many patients show remission or full recovery, but have lost or impaired reproductive abilities [7]. That suggests that fertility preservation opportunities should be offered to them before the beginning of the treatment. The cryopreservation of semen is most often used. The technology is well-established and routinely applied in the ART clinics. The semen is obtained by masturbation after 2 to 5 days of abstinence from sexual intercourse, and after liquification is diluted with cryopreservation medium and frozen with programme freezer or on liquid nitrogen vapour. Ready-to-use media are available on the market, with proven efficacy. The introduction of the vitrification method in clinical practice allows for the successful cryopreservation of low quality samples (insufficient number of spermatozoa) and gametes directly aspirated from the testes [13]. The storage period of the frozen semen (in liquid nitrogen, or its vapour or in low-temperature freezers) is practically indefinite.

The cases of pre-pubertal oncological patients, in which the spermatogenesis has not been initiated, are more challenging. The only available option for them is the cryopreservation of testicular tissue. Research shows that it contains spermatogonial stem cells [8]. Data exists, that after autologous transplantation of the frozen tissue the spermatogenesis can be recovered [6]. It is important to be noted that the method is still experimental and far from introduction into clinical practice. Protocols for collecting and cryopreservation of testicular tissue have been developed, but the techniques for the subsequent obtaining of spermatozoa from the thawed tissue are at research stage [5, 14].

Methods for fertility preservation of female patients

Different fertility preservation approaches are applied in women: selection of less invasive chemotherapeutics, ovary transposition, cryopreservation of reproductive cells and tissues. The strategy in every patient is individual and depends on her age, type and stage of the cancer, therapeutic plan, expected long-term results of the treatment, possibility to postpone the start of the therapy, presence of a partner of the patient, biology of the tumour and the potential risk of metastasis in the ovaries, etc [6]. In major part of the cases, cryopreservation of oocytes or zygotes/embryos is offered to the patients, and to lesser extent – of ovarian tissue. The main advantages and drawbacks of the methods are presented on **Table 1**.

Table 1. Main strategies for fertility preservation in female patients.

Strategy	Methodology description	Applicable in young children	Hormonal stimulation needed	Preservation of the ovarian functions	Limitating conditions
Embryo cryopreservation	Collection of oocytes, in vitro fertilization and freezing of the obtained embryos	No	Yes	No	10 – 14 days of stimulation; presence of a partner or donor sperm; price of the procedure; ethical problems in case of deceased patient
Oocyte cryopreservation	Pick-up and cryopreservation of unfertilized oocytes	No	Yes	No	10 – 14 days of stimulation; price of the procedure
Ovarian tissue cryopreservation	Freezing of ovarian tissue and transplantation post-treatment	Yes	No	Yes	Invasive procedure; risk of tumour cells transmission; price of the procedure

Some authors suggest a combination of approaches to preserve fertility in certain groups of patients, for example the simultaneous freezing of oocytes and ovarian tissue [1].

Oocyte Cryopreservation

The oocytes are a comparatively difficult object for cryopreservation due to their biological characteristics (size of the cell, high cumulative mass, presence of zona pellucida, membrane structure, the presence of the meiotic spindle, structure of the cytoskeleton) [6]. Unlike the freezing of spermatozoa and cell cultures, where the loss of certain quantity does not affect the outcome, the oocytes' number is limited, each of them is cryopreserved individually and the process should be approached carefully. It can be said that it is "all or nothing" principle. On the other hand, the recent developments in modern cryobiology and ART provide the techniques to successfully freeze and fertilize the female gametes. After the birth of the first baby in 1986 [4], worldwide at the moment hundreds of thousands of children have been born from cryopreserved oocytes [15]. On the market, cryobanks with frozen donor female gametes are functioning and there are ready-to-use media and devices for their cryopreservation. The freezing is performed by vitrification, and the fertilization with intracytoplasmic sperm injection (ICSI). The results in terms of fertilization and pregnancy rates after use of thawed oocytes practically do not differ significantly from fresh ones. Unfortunately, in certain groups of women – pre-pubertal girls, oncopatients to whom the hormonal stimulation is contraindicated etc. this approach is unsuited (Table 1).

Cryopreservation of pre-implantation embryos

In cases when the hormonal stimulation can be safely performed, the most successful method for fertility preservation is the freezing of pre-implantation embryos. It has to be noted, however, that it is applicable if the patient already has a partner or is agreeing to the use of donor sperm. The technology consists of the collection of oocytes, their in-vitro fertilization (IVF) and cryopreservation of the obtained embryos. They can be stored and after the finishing of the anti-tumour treatment thawed and transferred in the patient's uterus to achieve pregnancy. The method is well-established and routinely used in ART procedures. Two cryopreservation techniques are applied – programme freezing and vitrification, both showing good results. Again, this method cannot be used in young girls. Also, in certain countries, legal restrictions are forbidding the cryopreservation of embryos [12].

Cryopreservation of ovarian tissue

This technique can be applied in pre-pubertal girls or in patients with contraindication for hormonal stimulation. The establishment of ovarian tissue cryobanks is based on the principle of its cryoresistance. The ovarian cortex contains thousands of follicles, which unlike oocytes, can be frozen comparatively easy. Their relatively slow metabolism rate, the absence of zona pellucida and meiotic spindle are in the basis of the higher cryoresistance of primordial, compared to the growing follicles. Additionally, their small size facilitates the faster penetration of the cryoprotective agents.

The methodology includes laparoscopic collection of the ovarian tissue, which is cut into small fragments and cryopreserved most often with programme freezing with slow cooling rates. After thawing, the ovarian pieces are transplanted (ortho- or heterotopically). When the aim is to have a natural ovulation and conceptus, orthotropic transplantation is performed. The fragments are placed abdominally, close to the fallopian tube or to the remaining part of the ovary. In the heterotopic, the ovarian tissue is transplanted subcutaneously in the abdomen, in the hand between the elbow and the wrist, or other well-vascularized places. Practically, this is a less demanding procedure, but pregnancy can be achieved only after follicle puncture and IVF. Also critical is the fact that the women regain not only their reproductive functions, but their hormonal status as well [9]. Before cryopreservation, it is important to examine the tissue for the presence of tumour cells, to avoid their possible retransmission. Another approach is to culture the thawed primordial follicles, and fertilize *in vitro* the developed oocytes. Besides, the hypothesis for the presence of ovarian stem cells in the ovary is gaining further confirmation among scientists. Their possible differentiation into oocytes in the post-natal period is another consideration for freezing of ovarian tissue [10]. Up until now, over 300 babies have been born worldwide after cryopreservation of ovarian tissue.

Acknowledgements: The topic is investigated under the project grant KP-06-N51/11 „Cryopreservation, in vitro activation and culture of ovarian tissue and isolated follicles”, financed by NSF.

References

1. **Abir, R., I. Ben-Aharon, R. Garor.** Cryopreservation of in vitro matured oocytes in addition to ovarian tissue freezing for fertility preservation in paediatric female cancer patients before and after cancer therapy. – *Hum. Reprod.*, **31**, (4), 2016, 750-762.
2. **Brannigan, R. E., R. J. Fantus, J. A. Halpern.** Fertility preservation in men: a contemporary overview and a look toward emerging technologies. – *Fertil. Steril.*, **115**, (5), 2021, 1126-1139.
3. **Chen, C.** Pregnancies after human oocyte cryopreservation. – *Lancet*, **1**, 1986, 884-886.
4. **Chen, H., D. Mruk, X. Xiao, C. Y. Cheng.** Human spermatogenesis and its regulation. – In: *Male Hypogonadism. Contemporary Endocrinology*. Winters, S., Huhtaniemi, I. (Eds) Humana Press, Cham. 2017, Available at: https://doi.org/10.1007/978-3-319-53298-1_3
5. **Gassei, K., K. Orwig.** Experimental methods to preserve male fertility and treat male factor infertility. – *Fertil. Steril.*, **105**, 2016, 256-266.
6. **Grynberg, M., P. Patrizio.** Female and male fertility preservation. *Springer* 2022, 658p.
7. **Howlander, N., M. Krapcho, D. Miller, A. Brest, M. Yu, J. Ruhl.** SEER cancer statistics review, 1975-2017, National Cancer Institute. SEER Database 2020. Available at: https://seer.cancer.gov/csr/1975_2017/.
8. **Meachem, S.** Spermatogonia: stem cells with a great perspective. – *Reproduction*, **121**, 2001, 825-834.
9. **Oktay, K., F. Pacheco.** Current succes and efficiency of autologous ovarian transplantation with cryopreserved tissue: a meta-analysis. – *Fertil. Steril.*, **106**, (3), 2016, 131-132.
10. **Pacchiarotti, A. A., H. Selman, C. Valeri.** Perspective in infertility: the ovarian stem cells. – *Reproductive BioMedicine Online*, **8**, (1), 2015, 718-721.
11. **Qu, N., M. Itoh, K. Sakabe.** Effects of chemotherapy and radiotherapy on spermatogenesis: the role of testicular immunology. – *Int. J. Mol. Sci.*, **20**, 2019, 957p.
12. **Rebar, R.** Social and ethical implications of fertility preservation. – *Fertil. Steril.*, **105**, (6), 2016, 1449-1451.
13. **Spis, E., A. Bushkovskaia, E. Isachenko, P. Todorov, V. Isachenko.** Conventional freezing vs. cryoprotectant-free vitrification of epididymal (MESA) and testicular (TESE) spermatozoa: three live births. – *Cryobiology*, **90**, 2019, 100-102.
14. **Virant-Klun, I.** Stem cells in reproductive tissues and organs. From fertility to cancer. – *Humana press*, 2022, 368p.
15. **Walker, Z., A. Lanes, E. Ginsburg.** Oocyte cryopreservation review: outcomes of medical oocyte cryopreservation and planned oocyte cryopreservation. – *Reprod. Biol. Endocrinol.*, **20**, (1), 2022, 10.

Oocyte Morphology in a Mouse Model of Collagenase-Induced Osteoarthritis

*Anton Kolarov, Irina Chakarova, Valentina Hadzhinesheva, Venera Nikolova, Stefka Delimitreva, Maya Markova, Ralitsa Zhivkova**

Department of Biology, Medical Faculty, Medical University-Sofia, Sofia, Bulgaria

*Corresponding author e-mail: rzhivkova@yahoo.com

Investigation of the effect of collagenase-induced osteoarthritis (CIOA) on mouse oocyte diameter and meiotic spindle defects showed significantly larger size and higher proportion of spindle defects in CIOA oocytes compared to the control group: detached fibers or fully disorganized spindles and microtubule asters at the spindle poles were combined with a larger diameter of CIOA oocytes.

Key words: mouse model, osteoarthritis, oocytes, meiotic spindle, oocyte diameter

Introduction

Although osteoarthritis is thought to be the “wear and tear” disease of the elderly, recent investigations reveal that certain risk factors such as genetics, obesity, sport activities and joint injuries can lead to its development in younger and actively working people. The knee joint as well as many other joints (hip, foot, ankle, toe, elbow, wrist) could be affected at a younger age by repetitive movements, overload or traumas in active and retired athletes [11]. Common sports injuries can be risk factors for post-traumatic osteoarthritis in younger patients [5]. Some of these traumas endanger predominantly young females [4]. The higher risk of cartilage damage and degeneration in these younger individuals is related to repetitive impact and loading of the joint in athletes [2, 1]. Besides sports, the group of activities associated with osteoarthritic symptoms and injuries at a younger age includes arts such as dancing (especially ballet dancers) as well as ice skating [10, 3, 7] and even musicians [13]. Because of this subset of reproductive-age patients, studying the impact of osteoarthritis on oogenesis has not only theoretical but also practical relevance.

Material and Methods

Mouse model of collagenase-induced osteoarthritis was provided by the Institute of Microbiology, Bulgarian Academy of Sciences. The oocytes (193 from CIOA and 209 from control mice) were obtained after standard hormonal ovarian stimulation of the mice by intraperitoneal injection of FSH (follicle stimulating hormone, Meriofert, IBSA Farmaceutici, Italy), 12 IU/animal at day 31 post CIOA induction and hCG (human chorionic gonadotropin, Choriomon, IBSA Farmaceutici, Italy) – 14 IU/mouse, 48 h later. The oocytes were fixed in 2% paraformaldehyde, processed for immunocytochemistry, embedded in polyvinyl alcohol, mounted onto microscopic slides and covered by coverslip. Immunofluorescence was used to visualize the microtubule cytoskeleton (monoclonal mouse anti- α -tubulin antibody and FITC-labelled anti-mouse IgG antibody, Sigma-Aldrich) and chromatin (Hoechst 33258, Sigma-Aldrich). Laser-scanning confocal microscopy of selected images was performed for a precise measurement of the oocytes mounted under coverslips. Their diameter and spindle peculiarities were analyzed for all epifluorescent images. The collected data was analyzed using IBM SPSS Statistics for Windows (Version 27.0, IBM) and p-values under 0.05 were considered statistically significant.

Results

The average diameter of metaphase I and metaphase II (M I and M II) oocytes showed larger oocytes in the CIOA group compared to the controls: $113.28 \pm 9.57 \mu\text{m}$ for M I in CIOA versus $105.04 \pm 14.30 \mu\text{m}$ for M I in controls ($p < 0.01^{**}$) and $111.06 \pm 11.60 \mu\text{m}$ for M II in CIOA versus $107.70 \pm 15.71 \mu\text{m}$ for M II in controls ($p < 0.05^*$), shown in **Fig. 1**.

The oocytes of CIOA group had significantly more spindle defects: detached fibers or fully disorganized spindles were more frequent in the CIOA oocytes than in controls (46.76% for CIOA and 12.79% for controls in M I; 54.90% for CIOA and 31.90% for controls in M II), see **Fig. 2**.

CIOA group had twice more oocytes with microtubule asters at their spindle poles than the control group (48.92% for CIOA and 22.09% for controls in M I; 47.06% for CIOA and 17.24% for controls in M II), as shown in **Fig. 3**.

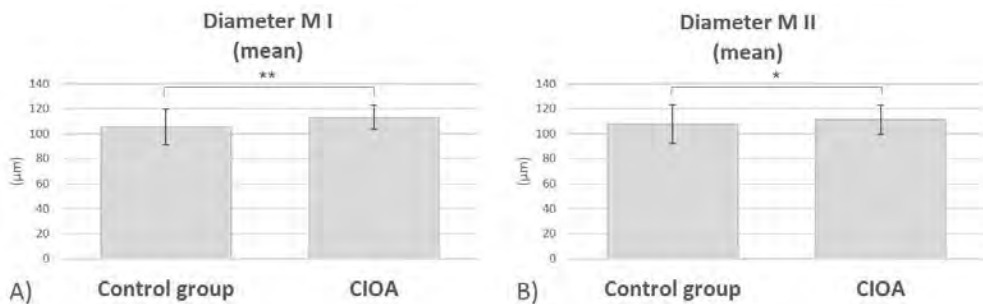


Fig. 1. Oocyte diameter in CIOA and controls: A – M I ($p < 0.01^{**}$); B – M II oocytes ($p < 0.05^*$).

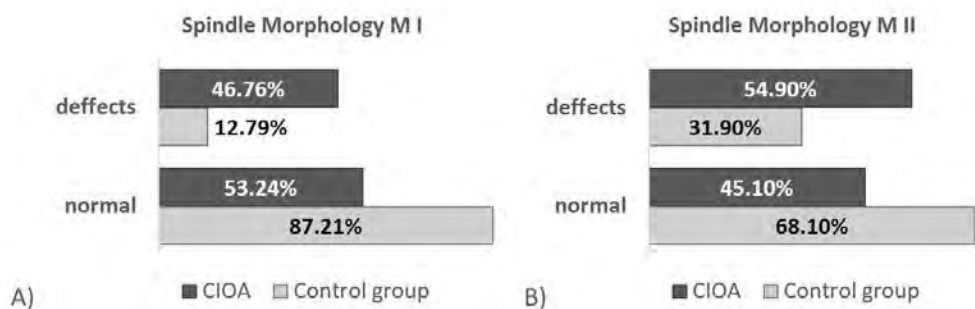


Fig. 2. Spindle normal / abnormal status of M I (A) and M II (B) – comparison of CIOA and controls.

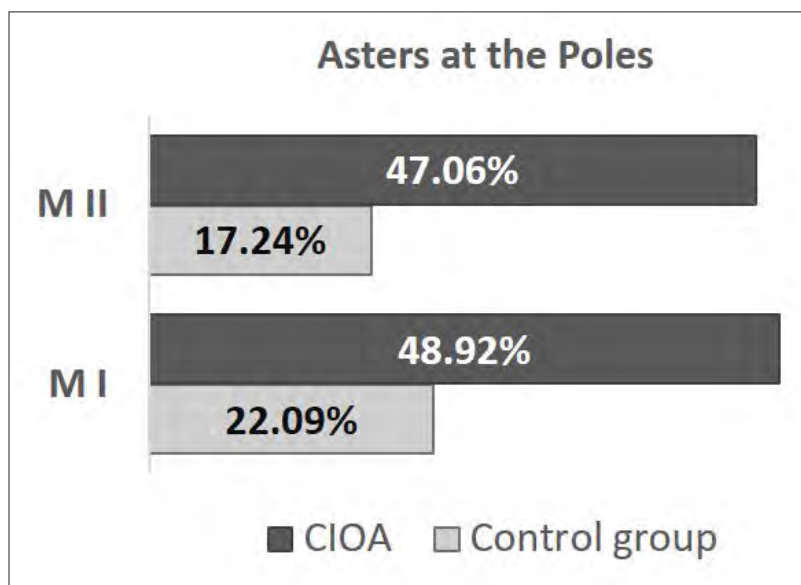


Fig. 3. Asters of microtubules at the spindle poles in M I and M II oocytes – CIOA and controls.

Discussion

Mammalian oogenesis is a complex process sensitive to its microenvironment. Osteoarthritis has recently been associated with systemic inflammation in addition to the local joint effect in both human [8] and the same mouse CIOA model [9], raising the question about its potential impact on oogenesis. In our study, the diameter of CIOA oocytes compared to controls showed an apparent enlargement, more pronounced for M I but statistically significant also for M II. It should be noted that diameters were measured when the oocytes were already under a coverslip, leading to a possibility that

any increase in observed size could be due to decreased mechanical properties of cells. The diameters of the controls were slightly larger but comparable to those reported for oocytes of outbred mice, about 100 μm [6]. Because CIOA oocytes had an increased diameter under the same coverslips, cytoplasmic factors affecting mechanical stability of the cell were supposed. We have found before cytoskeletal abnormalities in CIOA oocytes affecting the actin cap formation and spindle size [12]. These defects could provide an explanation for the supposed mechanical instability as well as the high proportion of abnormal spindles in CIOA oocytes (with detached fibers or fully disorganized, and microtubule asters at the spindle poles).

Conclusion

Osteoarthritis affects the apparent oocyte diameter and meiotic spindle formation: oocytes are significantly larger and spindle defects are significantly more frequent in CIOA mice than in controls.

Acknowledgements: We are grateful to Prof. Nina D. Ivanovska, Department of Immunology, Institute of Microbiology, Bulgarian Academy of Sciences, for providing the animals used in this study, and to Assoc. Prof. Milena Mourdjeva, Department of Molecular Immunology, Institute of Biology and Immunology of Reproduction, Bulgarian Academy of Sciences, for the Laser Scanning Confocal Microscopy imaging and measurements. The work was supported by the Bulgarian Ministry of Education and Science: National Science Fund [Grant Number DH13/6/15.12.2017] and the National Program for Research “Young Scientists and Postdoctoral Students”.

References

1. Ackerman, I. N., J. L. Kemp, K. M. Crossley, A. G. Culvenor, R. S. Hinman. Hip and knee osteoarthritis affects younger people, too. – *J. Orthop. Sports Phys. Ther.*, **47**, 2017, 67-79.
2. Amoako, A. O., G. G. Pujalte. Osteoarthritis in young, active, and athletic individuals. – *Clin. Med. Insights Arthritis Musculoskelet. Disord.*, **7**, 2014, 27-32.
3. Angioi, M., G. D. Maffulli, M. McCormack, D. Morrissey, O. Chan, N. Maffulli. Early signs of osteoarthritis in professional ballet dancers: a preliminary study. – *Clin. J. Sport Med.*, **24**, 2014, 435-437.
4. Bell, N. S., T. W. Mangione, D. Hemenway, P. J. Amoroso, B. H. Jones. High injury rates among female army trainees: a function of gender? – *Am. J. Prev. Med.*, **18**, 2000, 141-146.
5. Carbone A., S. Rodeo. Review of current understanding of post-traumatic osteoarthritis resulting from sports injuries. – *J. Orthop. Res.*, **35**, 2017, 397-405.
6. Dumont, J., S. Petri, F. Pellegrin, M. E. Terret, M. T. Bohnsack, P. Rassinier, V. Georget, P. Kalab, O. J. Gruss, M. H. Verlhac. A centriole- and RanGTP-independent spindle assembly pathway in meiosis I of vertebrate oocytes. – *J. Cell Biol.*, **176**, 2007, 295-305.
7. Gross, C., M. Rho, D. Aguilar, M. Reese. Self-reported hip problems in professional ballet dancers: The impact on quality of life. – *J. Dance Med. Sci.*, **22**, 2018, 132-136.
8. Hackney, A. J., N. J. Klinedinst, B. Resnick, M. Johantgen. Association of systemic inflammation and fatigue in osteoarthritis: 2007-2010 National health and nutrition examination survey. – *Biol. Res. Nurs.*, **21**, 2019, 532-543.

9. **Ivanovska, N., P. Dimitrova.** Bone resorption and remodeling in murine collagenase-induced osteoarthritis after administration of glucosamine. – *Arthritis Res. Ther.*, **13**, 2011, R44.
10. **Ko, E. H., S. F. Viegas.** Chronic wrist pain. – *Curr. Opin. Rheumatol.*, **9**, 1997, 155-158.
11. **Koh, J., J. Dietz.** Osteoarthritis in other joints (hip, elbow, foot, ankle, toes, wrist) after sports injuries. – *Clin. Sports Med.*, **24**, 2005, 57-70.
12. **Kolarov, A. I., I. V. Chakarova, V. P. Hadzhinesheva, V. P. Nikolova, S. M. Delimitreva, M. D. Markova, R. S. Zhivkova.** Osteoarthritis affects mammalian oogenesis: effects of collagenase-induced osteoarthritis on oocyte cytoskeleton in a mouse model. – *Int. J. Inflam.*, 2021, 8428713.
13. **Rietveld, A. B.** Dancers' and musicians' injuries. – *Clin. Rheumatol.*, **32**, 2013, 425-434.

Extragenital Lichen Sclerosis et Atrophicus

Mary Gantcheva^{1, 2}

¹ *Institute of Experimental Morphology, Pathology and Anthropology with Museum, Bulgarian Academy of Science, Sofia, Bulgaria*

² *Acibadem City Clinic Mladost, Sofia, Bulgaria*

*Corresponding author email: mary_gant@yahoo.com

Lichen sclerosus et atrophicus (LSA) is an uncommon chronic inflammatory dermatosis involving mainly the anogenital area in postmenopausal woman. Extragenital LSA is rare as an isolated form and is most commonly located on the neck, upper arms and flexor surfaces of the wrist. Only 6% of women and men with extragenital LSA do not have genital lesions.

This rare condition is cited in most of the cases as lichen sclerosis without the atrophic portion and is relevant to findings that lichen sclerosus can result in hypertrophic rather than atrophic epithelium. We report three patients – 2 men and 1 woman with solely extragenital involvement with multiple asymptomatic hyper and hypopigmented atrophic lesions on the trunk and discuss the histopathological and dermatoscopic data to achieve a proper diagnosis.

Key words: Lichen sclerosus et atrophicus, extragenital sites, unusual form, hypertrophic epithelium, histology

Introduction

Lichen sclerosus et atrophicus (LSA) is an acquired, inflammatory skin disease of unknown etiology. It usually involves the anogenital area – vulva, perineum and perianal skin with itching, soreness and sexual dysfunction. It could be also asymptomatic. The primary lesions are flat ivory-colored spots, which conflate into thin atrophic lesions or hyperkeratotic plaques. Women are more affected than men with a reported female: male ratio 10:1 [9]. This statistic might be influenced by male circumcision. Postmenopausal women are at higher risk to develop the disease, followed by girls between the age of 8 and 13 years, men and children. The course of LSA is usually chronic and is associated with an increased risk of squamous cell carcinoma of the affected area. In children the signs and symptoms may improve at puberty, but they need monitoring for disease activity.

LSA is most commonly localized only on the anogenital area with 85% to 98% of the cases. However, in some patients both genital and extragenital involvement is reported up to 15% [11].

Extragenital LSA is rare as an isolated form and the most often localization is on the neck, upper arms and flexor surfaces of the wrist. Only 6% of women and men with extragenital LSA do not have genital lesions.

We report three patients with solely extragenital form of LSA as two of them are men. One of the men has an uncommon presentation, which includes lesions on the scalp.

Case report

The first case is a 71-year old healthy man. He noticed white spots on the skin of his back three years ago. He had neither itching nor discomfort but because of the coalescence of the spots and thickening of the involved area decided to go to a dermatologist. On the physical examination we saw one large whitish-colored irregular plaque and numerous atrophic lesions around it with a diameter 2-3 mm up to 1 cm on the back. Linear and nummular violaceous brownish plaques with different sizes and slightly atrophic center were localized laterally on both sites on the truncus and both thighs symmetrically. A biopsy was taken from the lesion of the back showing hyperkeratosis and partial atrophy of the epidermis, oedema and hyalinization of the upper dermis, dilated vessels and slightly thickened hyalinized collagen in the lower dermis (**Fig. 1**).

The second case is a 52-year old woman. She suffered from mild itching on the back and several thick and dense plague on the back, which appeared six years ago. The treatment is with topical corticosteroids and emollients with no improvement. A month

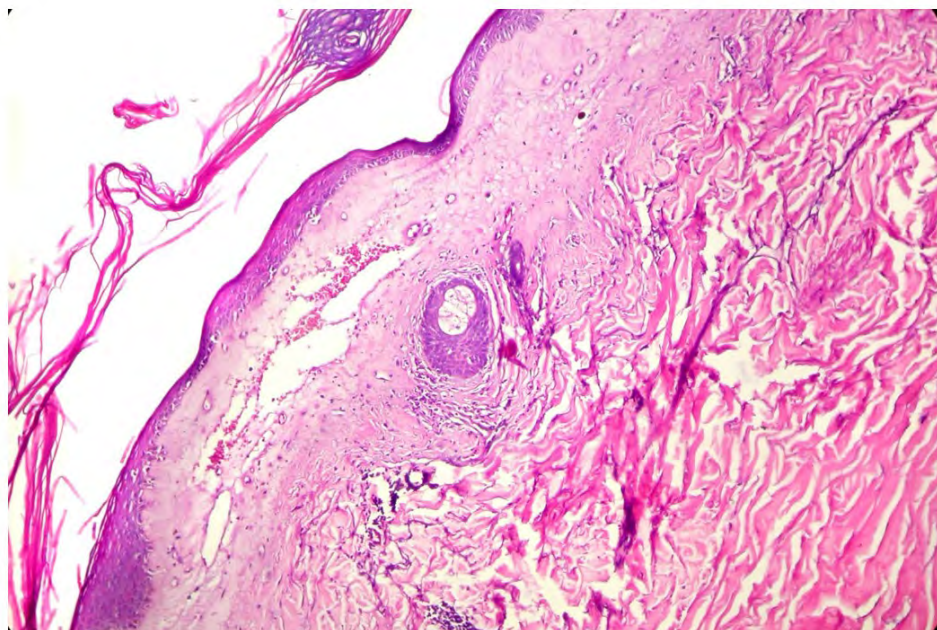


Fig. 1. Hyperkeratosis and partial atrophy of the epidermis, oedema and hyalinization of the upper dermis, dilated vessels and slightly thickened hyalinized collagen in the lower dermis (H&E, $\times 200$).

ago she noticed new plaques on the skin of her left inguinal fold and internal part of the left thigh. The histopathological findings from the new lesion showed hyperkeratosis, flattening of the dermoepidermal junction, oedema in the upper dermis and occasional perivascular infiltrates (**Fig. 2**). Fragmented white yellow structure – expression of atrophy, keratotic plugs and superficial desquamation were seen on dermatoscopy.

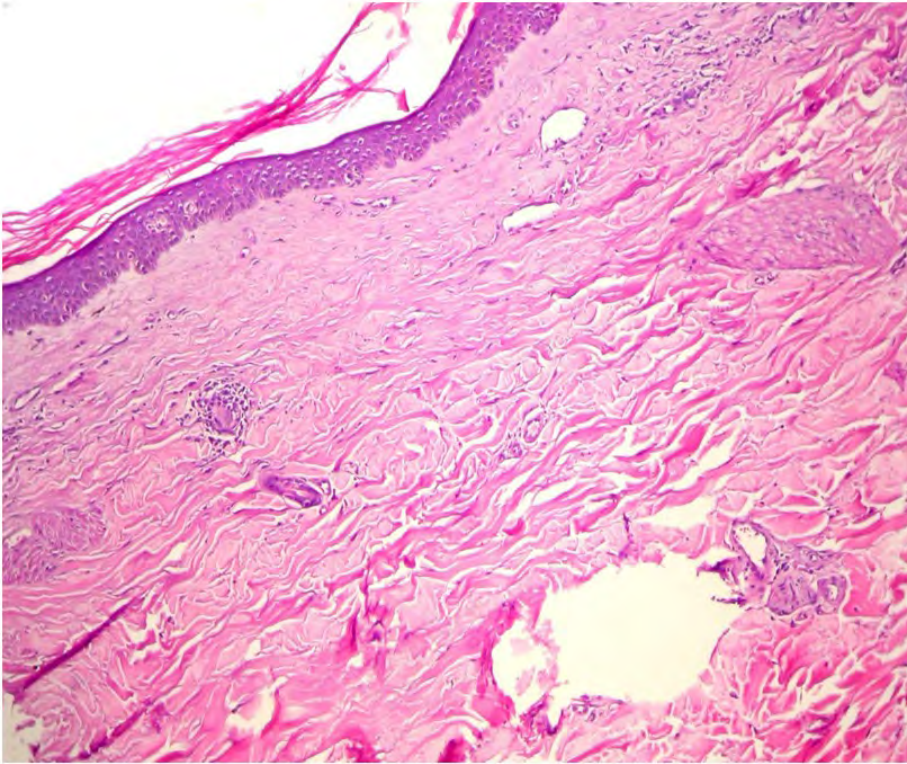


Fig. 2. Hyperkeratosis, flattening of the dermoepidermal junction, oedema in the upper dermis and occasional perivascular infiltrates (H&E, $\times 200$).

Third case is a 36-year old man who suffered from itchy papules on the scalp and body from one year. The lesions on the scalp are perifollicular and polygonal papules, which merged and formed atrophic areas. The histopathology from here showed atrophy of the epidermis, not well defined upper dermis and dermal inflammatory infiltrates. The biopsy from the lesion of the lateral part of the truncus defined mild hyperkeratosis and partial mild acanthosis, oedema, subepidermal slight hyalization and rare perivascular infiltrates (**Fig. 3**).

The patients are diagnosed with extragenital LSA based on the clinical and histopathological findings.

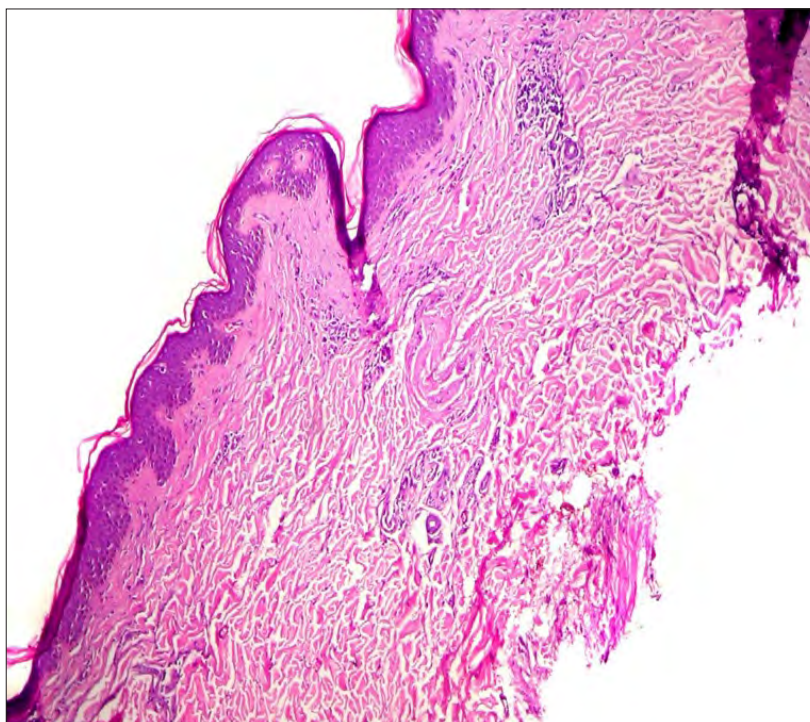


Fig.3. Mild hyperkeratosis and partial mild acanthosis, oedema, subepidermal slight hyalination and rare perivascular infiltrates (H&E, x 200).

Discussion

LSA was first described by Hallopeau in 1897 [6] and Darier reported the histological changes in 1892 [4]. They considered the disorder to be a type of lichen planus. Others thought that it was related to circumscribed scleroderma. Now, LSA is known as a separate entity because of the distinct clinical signs and pathological changes.

The cause of LSA is unknown, but most studies suggest that it is multifactorial. A genetic predisposition, based on familial clustering was observed [13]. The association of specific human leukocyte antigen (HLA) type - HLA II DQ7 and other autoimmune diseases suggests that LSA is an autoimmune process [5]. Autoimmune diseases are observed in up to 33% of women, particularly thyroid disease, alopecia areata, vitiligo, diabetes mellitus, rheumatoid arthritis, pernicious anemia, lupus erythematosus and morphea [7, 8]. Immunoreactivity to extracellular matrix protein 1 has been demonstrated in up to 74% of cases [10].

LSA may occur in skin, which is already scarred or damaged – so called Koebner phenomenon. From this point of view trauma, injury and scarring are suggested as possible triggers of symptoms in genetically predisposed people. Extragenital LSH involvement commonly develops in preexisting scars and damaged areas [11]. Lesions preferentially occurring on left side of body in most of the reported cases and has been

attributed to stronger cell-mediated immune hypersensitivity in the left side of the body in healthy young subjects. It is speculated that the cellular immune responsiveness might influence the confinement of the Blaschko-linear LSA to the left side of the body [3]. This is in contrast to our first case where lesions were on the back and on the both sides of the body and on the third case – lateral sides of the truncus and scalp. These two patients are man and late onset in the first one, which is not common for this diagnosis. The skin involvement in our second case, which is a woman was on the left side – left inguinal fold and internal part of the left thigh.

Extragenital lesions occur most often on the chest, upper back, and breasts. Cases of linear LSA have been reported along the lines of Blaschko [2]. Most often hypopigmented atrophic patches are observed, which are typically asymptomatic. However, progressive disease may cause discomfort and pruritus.

Histopathologically, these lesions were likely to show concomitant changes of lichen simplex chronicus or dermal eosinophils in one series [1]. The striking histological features in LSA is a band of hyalinization of the dermal collagen bellow the epidermis. The hyalinized tissue appears formless, oedematous and may contain sparse cells or has dilated capillaries. The epidermis shows variable thickening, hyperkeratosis and follicular plugging. Later, the epidermis could become thinner. Perivascular round cell infiltration is also present. In older lesions the lymphocytic infiltrations are more scanty and focal. Extragenital LSA showed decreased expression of the proliferation marker Ki-67 and p53 in comparison to genital LSA, which may explain in part the lack of reported malignant transformation in the extragenital subtype [12].

Conclusions

We present three patients with the rare extragenital form of LSA. The diagnosis is clinically and histopathology confirmed. All of them are followed to detect any atypical or malignant changes and no transformation of the lesions happens. Two of them are men which is not common according to the statistic of mainly women affected. All of them have disseminate lesions and one of them has scalp involvement, which is unusual localization. Histopathological finding varies depending on the evolutionary stage and localization of the investigated lesions. There are scarce perivascular infiltrates unlike those found in LSA with genital lesions. Extragenital LSA in most of the cases has no atrophy and may lead to hypertrophic epithelium.

References

1. **Carlson, J., P. Lamb, J. Malfetano, R. Ambros, M. Mihm.** Clinicopathologic comparison of vulvar and extragenital lichen sclerosus: histologic variants, evolving lesions, and etiology of 141 cases. – *Mod. Pathol.*, **11**, 1998, 844-854.
2. **Choi, S., J. Yang, H. Park, C. Kim.** A case of extragenital lichen sclerosus following Blaschko's lines. – *J. Am. Acad. Dermatol.*, **43**, 2000, 903-904.
3. **Dane, S., T. Erdem, K. Gümüştekin.** Cell-mediated immune hypersensitivity is stronger in the left side of the body than the right in healthy young subjects. – *Percept Mot. Skills*, **93**, 2001, 329–332.
4. **Darier, J.** Lichen plan scléreux. – *Ann. Dermatol. Syphiligr. (Paris)*, **23**, 1892, 833-837.

5. **Gao, X., M. Barnardo, S. Winsey, T. Ahmad, J. Cook, J. Agudelo, N. Zhai, J. Powell, S. Fuggle, F. Wojnarowska.** The association between HLA DR, DQ antigens, and vulval lichen sclerosus in the UK. – *J. Invest. Dermatol.*, **125**, 2005, 895-899.
6. **Hallopeau, H.** Lichen plan sclereux. – *Ann. Dermatol. Syphilol.*, **10**, 1889, 447.
7. **Harrington, C., I. Dunsmore.** An investigation into the incidence of auto-immune disorders in patients with lichen sclerosus and atrophicus. – *Br. J. Dermatol.*, **104**, 1981, 563-566.
8. **Kar, B., K. Dash.** Co-existence of lichen sclerosus et atrophicus and morphoea along lines of blaschko. – *Indian J. Dermatol.*, **59**, 2014, 77-79.
9. **Nair, P.** Vulvar lichen sclerosus et atrophicus. – *J. Midlife Health.*, **8**, 2017, 55-62.
10. **Oyama, N., I. Chan, S. Neill, T. Hamada, A. South, V. Wessagowit, F. Wojnarowska, D. D'Cruz, G. Hughes, M. Black, J. McGrath.** Autoantibodies to extracellular matrix protein 1 in lichen sclerosus. – *Lancet.*, **362**, 2003, 118–123.
11. **Powell, J., F. Wojnarowska.** Lichen sclerosus. – *Lancet.*, **353**, 1999, 1777-1783.
12. **Scurry, J., J. Whitehead, M. Healey.** Histology of lichen sclerosus varies according to site and proximity to carcinoma. – *Am. J. Dermatopathol.*, **23**, 2001, 413-418.
13. **Sherman, V., T. McPherson, M. Baldo, A. Salim, X. Gao, F. Wojnarowska.** The high rate of familial lichen sclerosus suggests a genetic contribution: An observational cohort study. – *J. Eur. Acad. Dermatol. Venereol.*, **24**, 2010, 1031-1034.

Mast Cells Distribution in the Domestic Swine Urinary Bladder's Wall

Angel Vodenicharov¹, Ivaylo Stefanov^{2,3}, Nikolay Tsandev¹, Genadi Kostadinov¹

¹Department of Veterinary Anatomy, Histology and Embryology, Faculty of Veterinary Medicine, Trakia University, Stara Zagora, Bulgaria

²Department of Anatomy, Faculty of Medicine, Trakia University, Stara Zagora, Bulgaria,

³Department of Anatomy, Histology and Cytology, Pathology, Faculty of Medicine, University „Prof. Assen Zlatarov”, Bourgas, Bulgaria

The localization and density of toluidine blue (TB) stained mast cells (MCs) in *lamina propria mucosae* and muscular tunic of pig's urinary bladder in order to elucidate their role in organ function, were studied. It was established that in *propria*, the MCs were localized predominantly close to vessels of microcirculatory bed. Their number was highest in *trigonum* – 4.00 ± 0.84 and *corpus* – 3.44 ± 0.51 ($P < 0.001$), followed by *apex* – 2.56 ± 0.51 and *collum vesicae* – 1.17 ± 0.38 ($P < 0.001$). In the muscular tunic, the MCs were localized near the capillaries' basal lamina, in the adventitia of arteries and veins and between the muscle bundles. The highest MCs density was detected in the muscular tunic of *collum* (16.50 ± 0.51) – and *trigonum* – 16.61 ± 0.50 ($P < 0.001$), followed by *apex* – 15.89 ± 0.83 , and *corpus* – 12.33 ± 0.48 ($P < 0.001$) *vesicae*. In conclusion the higher number of MCs in muscular tunic than *propria* ($P < 0.001$) allowed to suggest their significant role in the regulation of smooth muscle contractility.

Key words: Mast cells, urinary bladder, domestic swine

Introduction

Urine storage and urination depend on the coordinated activity of the two organs – the bladder and urethra [1]. The bladder receives and stores incoming urine, and the urethra ensures its retention of the urinary reflex [7].

In the last 20 years and more, the domestic pig has been an extremely suitable animal model for human research [2, 3]. In this regard, studies related to immunohistochemical detection of biologically active substances in the sensory neurons of the lumbar and sacral spinal ganglia into the bladder wall in pigs are of interest [5, 8]. Having in mind these finding with clinical importance, the presence of mast cells in the bladder wall in domestic pigs is of particular interest. Enzyme – and immunohistochemical studies

on mast cells in the ureter, the male urethra, and renal blood vessels in pig have shown expression of several their substances [4, 10, 11]. The lack of data on the distribution of mast cells in the bladder wall in domestic pigs, related to motility of organ's smooth muscle cells gave motivation for the present study.

Materials and Methods

The material was taken from four areas of the bladder – triangle, tip, body and neck, immediately after slaughter of twelve, 6 month pigs – 6 males and 6 females (Landrace × Bulgarian White) at 90 – 100 kg/b.w. The animals were slaughtered for meat consumption in full compliance with national legislation.

The sections of about 1 cm² from the wall of four areas were placed for immersion fixation in Carnoy fluid for 4 hours, dehydrated in ascending ethanol series, cleared in xylene and embedded in paraffin. Serial 5 µm sections were prepared, and were stained with 0.1% toluidine blue in Mc Ilvane buffer, pH 3.

Statistical analysis

The number of mast cells with clearly visible nuclei was recorded on serial sections. The density of the observed cells was determined by Leica DM 1000 light microscope, digital camera Leica DFC 290 and software LAS V4.10.0 2016, as the number of microscopic fields (×200). The analysis was performed using GraphPadPrism 6 for Windows, one-way ANOVA and Tukey-Kramer test. Significance of the difference in mast cell count was reported at P<0.05 using one-way ANOVA.

Results

Light microscopic observations showed the presence of mast cells in all four sections of the bladder wall examined. In the mucosal layer, the mast cells were unevenly distributed, and they were located mainly near to arterioles, capillaries and venules. The number of mast cells in the propia varied from region to region. The highest density of mast cells was found in the *trigonum vesicae* and in the *corpus vesicae* – (P<0.001), followed by their density in the *apex vesicae* and that in the *collum vesicae* (P< 0.001), (Table 1).

Table 1. Density of mast cells in microscopic fields (×200) of the propria and musculature in the different areas of urinary bladder

<div>Area \ Layer</div>	<i>Lamina propria</i>	<i>Tunica muscularis</i>
<i>Apex vesicae</i>	2.56±0.51	15.89±0.83
<i>Corpus vesicae</i>	3.44±0.51	12.33±0.48
<i>Trigonum vesicae</i>	4.00±0.84	16.61±0.50
<i>Collum vesicae</i>	1.17±0.38	16.50±0.51

Between and next to the smooth muscle bundles in the middle shell of the bladder wall, mast cells were located mainly near the basement membrane of capillary endothelial cells, in the adventitia of arteries and veins, and in the connective tissue between bundles formed by smooth muscle cells. The highest density of mast cells was observed in the muscular coat of the *collum vesicae* – and the *trigonum vesicae* – ($P < 0.001$), followed by that at the *apex vesicae* – and in *corpus vesicae* – ($P < 0.001$), of the bladder (**Table 1**).

The percentage of mast cells localized in the propria was as follows: top – 22.91%; body – 30.8%, triangle – 35.81% and neck – 10.47%, and for the muscular sheet, respectively: top – 25.9%, body – 20.1%, triangle – 27.1% and neck – 26.9%.

Discussion

Of particular note of this original data is the percentage of toluidine-positive mast cells in the propria and the muscular layer of the bladder. The highest percentages found in the „boundary zone“ between the ureter and the bladder, namely the triangle, could be explained by the important role that mast cells play through the release of biologically active substances, both in maintaining the local microenvironment (homeostasis) and in the motility of smooth muscle cells.

It is quite logical to assume that the role of smooth muscle cells in this narrowed compared to the broad lumen of the body of the bladder, in the passage of urine to the beginning of the urethra after dilatation of *m. urethralis*, is indisputable. Of course, the involvement of mast cells in influencing the motility of smooth muscle cells in the apex and body also deserves attention.

The hypothesis proposed more than 15 years ago [10] for the participation of mast cells not only in maintaining local homeostasis (microenvironment) of the porcine ureter, but also in the motility of smooth muscle cells on its wall was recently confirmed by [6].

Conclusion

The original data obtained supplement the lack of knowledge about mast cells in the bladder wall. Along with what is known about them in the ureter, ureterovesical junction [9] and urethra, a clearer and more complete picture of the presence and role of mast cells in the extrarenal part of the urinary tract in domestic pigs is obtained.

References

1. Birder, L., M. Drake, W. C. De Groat, C. Fowler, E. Mayer, J. Morrison, J. Paton, D. Griffiths, I. W. Mills, K. Thor. Neural control. – In: *Incontinence*, (Eds. P. Abrams, L. Cardozo, S. Khoury, A. Wein, 4th edn.) 2009, Paris, Health Publications Ltd, pp. 167-254.
2. Gutierrez, K., N. Dicks, W. G. Glanzner, L. B. Agellon, V. Bordinon. Efficacy of the porcine species in biomedical research. – *Front. Genet.*, **6**, 2015, 293.
3. Iwase, H., T. Kobayashi. Current status of pig kidney xenotransplantation. – In: *J. Surg.*, **23**, 2015, 229-233.

4. **Kostadinov, G., A. Vodenicharov, A. Bozhilova-Pastirova.** Alcian blue-and tyrosine hydroxylase- positive mast cells in the pig's pelvic urethra. – *Compt. Rend. Acad. Bulg. Sci.*, **67**, 2014, 1171-1174.
5. **Kozłowska, A., A. Mikołajczyk, M. Majewski.** Distribution and neurochemistry of porcine urinary bladder-projecting sensory neurons in subdomains of the dorsal root ganglia: A quantitative analysis. – *Ann. Anat.*, **216**, 2018, 36-51.
6. **Lim, I., R. Chess-Williams, D. Sellers.** 5-HT_{2A} receptor is the predominant receptor mediating contraction of the isolated porcine distal ureter to 5-HT in young and old animals. – *Eur. J. Pharmacol.*, **818**, 2018, 328-334.
7. **Morrison, J. F. B.** Reflex control of the lower urinary tract. – In: *The physiology of the lower urinary tract*. (Eds. M. Torrens, J.F.B. Morrison), 1987, London. Springer, pp. 193-235,
8. **Pidsudko, Z.** Immunohistochemical characteristics and distribution of sensory dorsal root ganglia neurons supplying the urinary bladder in the male pig. – *J. Mol. Neurosci.*, **52**, 2014, 71-81.
9. **Tsandev, N., A. Vodenicharov, G. Kostadinov, I. Stefanov.** Mast cell distribution in the terminal part of porcine ureter. – *Acta Morphol. Anthropol.*, **26** (1-2), 2019, 52-55.
10. **Vodenicharov, A., R. Leiser, M. Gulubova, T. Vlaykova.** Morphological and immunocytochemical investigations on mast cells in porcine ureter. – *Anat. Histol. Embryol.*, **34**, 2005, 343-349.
11. **Vodenicharov, A.** Morphological studies on the role of mast cells mediators, on other vasoactive substances and the glomerular arterioles in the renal hemodynamics of domestic swine. *Doctor of Science dissertation*, 2008, Trakia University, Stara Zagora.

Quality of Intact and Artificially Collapsed Human Blastocysts after Vitrification

Galina Nenkova^{1}, Galina Yaneva¹, Tsonka Dimitrova¹, Emil Kovachev³,
Simona Anzhe², Dobri Ivanov¹*

¹ Department of Biology, Medical University, Varna, Bulgaria

² Medical Center for Assisted Reproduction, Varna, Bulgaria

³ Department of Obstetrics and Gynecology, Medical University, Varna, Bulgaria

* Corresponding author e-mail: g_alina_n@abv.bg

It is well known that the survival rate of embryos after vitrification depends on their expansion stage. We aimed to compare behavior of early (n=31) and expanded blastocysts (n=83) after vitrification. Expanded Day 5 embryos were divided into two groups – artificially collapsed (n=38) and intact (n=45). All blastocysts selected for vitrification were Day 5, classified into three groups – excellent, good and average quality. Thawed blastocysts were cultivated for at least 3 hours before embryo transfer. Assessment of their vitality and re-expansion was conducted every hour. Our study showed that mechanical collapse of blastocoele through micropipette puncture has a positive effect on embryo survival rate. The greatest survival rate (96.8%) and the fastest re-expansion were observed in early blastocysts. 35 (92.1%) survived thawing in the group of deflated blastocysts, while 39 embryos (86.6%) survived in the group of untreated before vitrification.

Key words: blastocyst, vitrification, artificial collapse

Introduction

Embryo cryopreservation has multiple benefits and is a routine procedure in most in vitro fertilization programs. Compared to slow freezing vitrification provides minimal embryo damage and higher survival rates. Cryopreservation prevents discard of surplus embryos and makes it possible to store them for future use [6].

It is well known that the efficiency of blastocyst vitrification depends on the expansion stage of fluid-filled cavity [1, 2, 3, 7]. While expanded blastocysts are more vulnerable to ice formation, early blastocysts have better post thaw survival rate due to the small amount of blastocoele fluid [5]. For that reason we decided to compare behavior of early and expanded blastocysts after vitrification.

Material and Methods

Couples who took part in this research were patients of Medical Center for Assisted Reproduction – Varna. They were diagnosed with male factor infertility, unexplained infertility or female factor infertility. The age range varied between 27-43 years for men and between 28-39 years for women. All participants in the research provided informed consent.

The semen samples were obtained through masturbation after 3-5 days of ejaculatory. Concentration, motility and morphology were evaluated in accordance with the WHO's 2010 requirements. Ejaculates were prepared by density gradient centrifugation.

To stimulate follicle development, gonadotropin releasing hormone antagonists were administered. Follicle punctures were conducted under short-term anaesthesia and ultrasound guidance. Oocytes were fertilized by conventional in vitro fertilization or intracytoplasmic sperm injection. Embryos were cultivated in culture medium prior to vitrification. Blastocysts behaviour after thawing was assessed according to the degree of their cavity expansion. Early (n=31) and expanded (n=83) blastocysts were examined. Expanded Day 5 embryos were divided into two groups – artificially collapsed (n=38) and intact (n=45). Blastocyst collapse was performed by micropipetting in buffered medium. All blastocysts selected for vitrification were Day 5, and were classified into three groups – excellent, good and average quality.

Only one embryo per cryotop was loaded. After thawing blastocysts were cultivated for at least 3 hours. Assessment of their vitality and re-expansion was conducted every hour. Single embryo transfer was performed in all cases. Blood pregnancy tests were conducted 10 days after embryo replacement. Pregnancy confirmation ultrasound scan was performed two weeks later.

Results

Table 1 reveals the outcomes after thawing of early, expanded and artificially collapsed blastocysts. The greatest survival rate (96.8%, 30/31) and the fastest re-expansion were observed in early blastocysts ($p=0.01$). The survival rate in artificially collapsed and intact Day 5 embryos after thawing was 92.1% (35/38) and 86.6% (39/45) respectively. We didn't notice any significant difference in time needed for blastocoele re-expansion between artificially collapsed and intact Day 5 embryos. Blastocysts which failed to re-expand were 7.9% (3/38) in the deflated group and 13.34% (6/45) in the group of untreated expanded blastocysts ($p<0.001$). Clinical pregnancy rate did not differ between the three groups.

We do not report miscarriage rate and live birth rate because most of the pregnancies are still ongoing.

Table 1. Comparison of outcomes after thawing of early, expanded and artificially collapsed blastocysts.

	Early blastocysts n (%)	Artificially collapsed blastocysts n (%)	Intact expanded blastocysts n (%)
Embryos	31	38	45
IVF	9 (29,03%)	11 (28.95%)	10 (22.22%)
ICSI	22 (70,97%)	27 (71.05)	35 (77.78)
Survival rate after thawing	30 (96.8%)	35 (92.1%)	39 (86.6%)
1st hour re-expansion,	21 (67.74%)	17 (44.74%)	19 (42.22%)
2nd hour re-expansion	10 (32.26%)	17 (44.74%)	20 (44.44%)
3rd hour re-expansion	0 (0%)	1 (2.62%)	0 (0%)
lack of re-expansion	0 (0%)	3 (7.9%)	6 (13.34%)
Clinical pregnancy rate	14 (45.16%)	17 (44.74%)	20 (44.44%)

Discussion

The blastocyst expansion stage affects embryo quality after vitrification. Unlike early D5 embryos, expanded blastocysts contain a greater amount of liquid. This prolongs their exposure in cryoprotectants and increases the risk of ice crystals formation.

In this study it was found that early blastocysts had the highest survival rate after thawing. When blastocysts were fully expanded artificial collapse before freezing improved their chances of survival. Lower survival rate in the group of intact expanded blastocysts can be attributed to the fact that excessive amount of water led to the formation of ice crystals and embryo damage.

Raju et al. also reported that compared to deflated expanded blastocysts early blastocysts have better survival rate after thawing [5].

Our findings lend further support to the proposition by Mitsuata et al. [4] that artificially collapsed blastocysts have a significantly higher survival rate when compared to those which did not undergo microsuction. However in contrast to us, Mitsuata et al. [4] also reported higher implantation and live birth rates in the deflated group than in the group of intact expanded blastocysts. But according to them these differences were not statistically significant [4].

We didn't find any difference in clinical pregnancy rate between the three groups but this can be attributed to the small sample size of our research.

We can conclude that artificial collapse by micropipetting before vitrification benefits the survival rate of expanded blastocysts.

References

1. **Fields, R. A., H. Werland, J. Nguyen, K. R. Sieren, T. G. Turner, K. M. Silverberg.** Laser collapsing of blastocysts prior to vitrification leads to better embryonic survival and improved overall IVF cycle outcome. – *Fertil. Steril.*, **100(3)**, 2013, S106.
2. **Kader, A. A., A. Choi, Y. Orief, A. Agarwal.** Factors affecting the outcome of human blastocyst vitrification. – *Reprod. Biol. Endocrinol.*, **7(1)**, 2009, 99.
3. **Menezo, Y.** Cryopreservation of IVF embryos: which stage? – *Eur. J. of Obs. & Gyn.*, **113**, 2004, 28–32.
4. **Mitsuata, S., Y. Endo, M. Hayashi, Y. Fujii, H. Motoyama.** Effect on clinical and neonatal outcomes of blastocelic microsuction prior to vitrification. – *Reprod. Med. Biol.*, **18**, 2019, 284–289.
5. **Raju, G. R., G. J. Prakash, K. M. Krishna, K. Madan.** Vitrification of human early cavitating and deflated expanded blastocysts: clinical outcome of 474 cycles. – *J. Assist. Reprod. Genet.*, **26**, 2009, 523–529.
6. **Rienzi, L., C. Gracia, R. Maggiulli, A. R. LaBarbera, D. J. Kaser, F. M. Ubaldi, S. Vanderpoel, C. Racowsky.** Oocyte, embryo and blastocyst cryopreservation in ART: systematic review and meta-analysis comparing slow-freezing versus vitrification to produce evidence for the development of global guidance – *Hum. Reprod. Update*, **23** 2017, 139–155
7. **Vanderzwalmen, P., D. Connan, L. Grobet, B. Wirleitner, B. Remy.** Lower intracellular concentration of cryoprotectants after vitrification than after slow freezing despite exposure to higher concentration of cryoprotectant solutions. – *Hum. Reprod.*, **28(8)**, 2013, 2101–2110.

Thermal Changes in Human Bone Following Osteotomy by Three Different Devices – a Histological Analysis Using Different Staining Protocols

Bistra Blagova^{1*}, Dimo Krastev^{2,3}, Lina Malinova⁴

¹ Maxillofacial Surgery Division, University Multiprofile Hospital for Active Treatment and Emergency Medicine N. I. Pirogov, Sofia, Bulgaria;

² Medical College “Jordanka Filaretova”, Medical University of Sofia, Sofia, Bulgaria;

³ Faculty of Public Health, Health Care and Sport, South-West University “Neofit Rilski”, Blagoevgrad, Bulgaria;

⁴ Department of Anatomy, histology and embryology, Medical University of Sofia, Sofia, Bulgaria

*Corresponding author e-mail: dr_blagova@abv.bg

Osteotomy is a common step in surgery. Chisels, drills and ultrasound machines are commonly used. Recently, high-energy lasers have been introduced. Heat and related mechanical damage during osteotomy can impair bone healing. Therefore, thermal osteonecrosis greatly affects the postoperative outcome. So, the **aim** of our study was to compare the thermal changes occurring in human bone after *in vivo* bone cutting using three different devices. Well-defined histological signs of thermal changes were demonstrated in all samples. Based on the observed results, it can be concluded that despite cooling systems, it is not completely possible to prevent thermal changes in human bone by its *in vivo* osteotomy.

Key words: drilling, Er:YAG laser, human bone, piezosurgery, thermal changes

Introduction

Osteotomy is a common step in surgery. Motorized rotary and oscillating cutting tools have been developed, allowing precise and direct cutting. However, conventional osteotomies have several drawbacks: the requirement for relatively high open exposure, the risk of tissue overheating, leading to possible thermal necrosis [10]. Heat and thermal osteonecrosis greatly affect patients' postoperative outcome, possibly causing infections [8], implant loss and delayed healing [2]. To reduce these complications, laser- and ultrasound-based osteotomy have been developed. Several *ex vivo* studies on animal bone [11] have recently focused on the heat production during osteotomy. However, conflicting conclusions regarding the effect of temperature on bone tissue

can be seen by comparing *in vivo* and *ex vivo* studies [14]. Wächter et al. [14] revealed lower bone temperature in *in vivo* samples because bleeding can evacuate more heat energy than in *ex vivo* settings. Researchers have concluded that *in vivo* studies are essential for understanding how bone healing occurs after osteotomy and how blood flow and biological factors fit together [11].

In our opinion, the results of *ex vivo* animal models cannot be transferred mechanically to clinical practice. There are many similarities and differences regarding bone parameters concerning animal species and between animals and humans [1]. Thus, the **aim** of our study was to compare the direct thermal impact of three different cutting devices on human bone.

Material and Methods

Human bone biopsies for analyses of thermal changes following conventional drilling, laser and ultrasound osteotomy were taken during surgical removing of mandible third molars. Patients who were taking bone morphology affecting drugs or antibiotics for current acute local infection at the time of operation or who had chronic bone disease were excluded. All patients were informed about surgery, postoperative time and possible complications. The research has been carried out in accordance with Declaration of Helsinki. The research design was approved by an ethical committee. All participants signed an informed consent.

The following instruments were evaluated in the study: an Er:YAG laser (2.94 µm LiteTouch, Light Instruments®, Israel), an ultrasound unit (Woodpecker Ultrasurgery®, China) and a conventional drilling device (W & H Surgical Handpiece®, Austria). A standard setup for bone manipulations were used according to the manufacturer's instructions. All biopsies were obtained by the same oral surgeon. Bone fragments were placed in 10% buffered formalin solution. Following decalcification, 5 µm thick sections were stained with Hematoxylin – Eosin and Toluidine Blue and examined under an optical microscope.

Results

Although all examined osteotomes were fitted with a cooling system, histology signs of thermal changes were observed in all samples. Sections obtained by traditional drilling showed poor peripheral carbonization and a low-grade thermal damage was clearly visible on all staining methods. Piezosurgery bone biopsies demonstrated bone incisions with minimal thermal damage established on the specimens stained with Toluidine Blue in contrast to the Hematoxylin - Eosin staining. Bone fragments obtained with an Er:YAG laser showed also peripheral thermal changes, but no melting was observed at the edges of the incisions; even osteocytes near the incision were unchanged (**Fig. 1**).

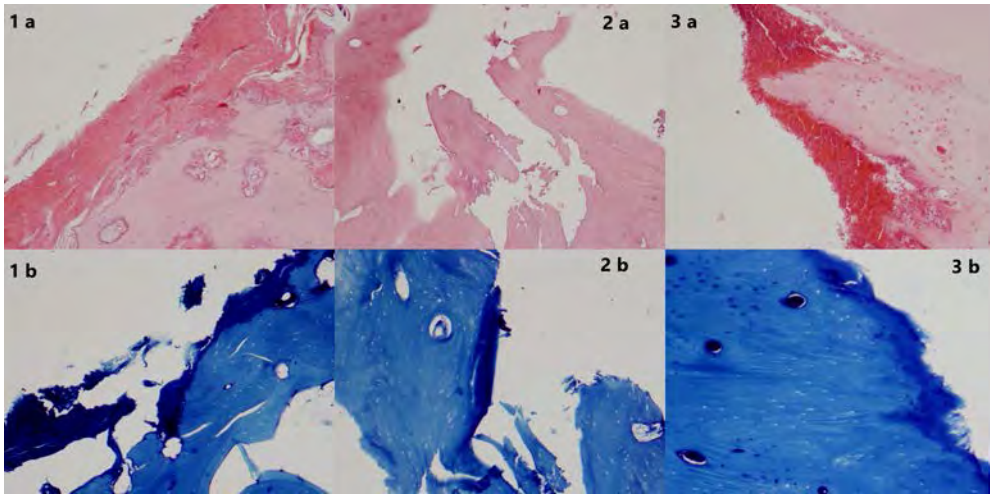


Fig. 1. Images of human bone specimens ($\times 10$): **1** – a conventional drilling device; **2** – an ultrasound unit; **3** – an Er:YAG laser; **a** – Hematoxylin - Eosin; **b** – Toluidine Blue.

Discussion

To date, histology is the gold standard for study of heat-related bone necrosis, as it allows *in situ* analysis of the cells [7]. The temperature effects on bone tissue have been studied and it was found that heat stress inhibited osteoblast regeneration and caused bone resorption and adipocyte conversion, thus inhibiting bone healing [6]. The excessive frictional heat generated during osteotomy could impair the turnover activity of bone tissue by causing hyperemia, necrosis, fibrosis, osteocytic degeneration and increased osteoclastic activity [13].

Traditionally, rotating instruments, such as burs, have been used for osteotomy. However, disadvantages are related to the use of these traditional systems, including bone overheating and damage to adjacent tissues [10]. The absence of certain thermal alterations of tissue caused by the conventional rotary device used in our study was probably due to the low speed and constant irrigation, as explained in a study by de Mello et al. [5].

In presented trial, the overheating of bone samples with the ultrasound device compared to the other two osteotomes was an unexpected finding, established not by the conventional Hematoxylin-Eosin, but by Toluidine Blue staining. Previous findings by Szalma [12] on bone overheating with ultrasound devices were questioned by Zheng [15] in an additional *ex vivo* model. He found that the temperature of the cortical bone during ultrasound-assisted osteotomy was lower than during rotational drilling [11, 15].

Laser osteotomy is a heat-induced cavitation effect creating cavitation-bubbles. Once the water in bone tissue is consumed, the heat energy cannot be transformed into kinetic energy anymore and thus leads to carbonization and necrosis of the adjacent bone layers [4]. It has been suggested that the Er:YAG laser is probably the least destructive of the bone cutting lasers because it generates light at an energy level

that is readily absorbed by water and thus minimizes carbonation and adjacent tissue necrosis [3]. The microanalysis of the surface of bone following laser ablation showed little evidence of thermal damage and any char layer appeared to be restricted to a minimal micrometric zone [9].

Conclusion

Our study proved that despite the evolution of bone cutting devices bone trauma is ever-present. The verified direct changes in human bone could be used as a set point for further research comparing bone healing dynamics and the quality of new bone formation in humans following bone surgery.

References

1. Anesi, A., M. Di Bartolomeo, A. Pellacani, M. Ferretti, F. Cavani, R. Salvatori, R. Nocini, C. Palumbo, L. Chiarini. Bone healing evaluation following different osteotomic techniques in animal models: a suitable method for clinical insights. – *Appl. Sci.*, **10**, 2020, 7165.
2. Augustin, G., S. Davila, K. Mihoci, T. Udiljak, D. S. Vedrina, A. Antabak. Thermal osteonecrosis and bone drilling parameters revisited. – *Arch. Orthop. Trauma Surg.*, **128**, 2008, 71-77.
3. Bornstein, E. S. Why wavelength and delivery systems are the most important factors in using a dental hard-tissue laser: a literature review. – *Compend. Contin. Educ. Dent.*, **24**(11), 2003, 837-848.
4. Colucci, V., F. L. do Amaral, J. D. Pecora, R. G. Palma-Dibb, S. A. Corona. Water flow on erbium: yttrium–aluminum–garnet laser irradiation: effects on dental tissues. – *Lasers Med Sci.*, **24**, 2009, 811-818.
5. de Mello, E. D., R. M. Pagnoncelli, E. Munin, M. S. Filho, G. P. de Mello, E. A. Arisawa. Comparative histological analysis of bone healing of standardized bone defects performed with the Er:YAG laser and steel burs. – *Lasers Med Sci.*, **23**, 2008, 253-260.
6. Eriksson, R. A., T. Albrektsson, B. Magnusson. Assessment of bone viability after heat trauma. A histological, histochemical and vital microscopic study in the rabbit. – *Scand. J. Plast. Reconstr. Surg.*, **18**, 1984, 18, 261-268.
7. Iwaniec, U. T., T. J. Wronski, R. T. Turner. Histological analysis of bone. – *Methods Mol. Biol.*, **447**, 2008, 325-341.
8. Mediouni, M., T. Kucklick, S. Poncet, R. Madiouni, A. Abouaomar, H. Madry, M. Cucchiari, B. Chopko, N. Vaughan, M. Arora. An overview of thermal necrosis: Present and future. – *Curr. Med. Res. Opin.*, **35**, 2019, 1555-1562.
9. Panduric, D. G., I. Bago, D. Katanec, J. Žabkar, I. Miletić, I. Anić. Comparison of Er:YAG laser and surgical drill for osteotomy in oral surgery: an experimental study. – *J. Oral Maxillofac. Surg.*, **70**, 2012, 2515-2521.
10. Queiroz, T. P., F. A. Souza, R. Okamoto, R. Margonar, V. A. Pereira-Filho, I. R. Garcia Jr., E. H. Vieira. Evaluation of immediate bone-cell viability and of drill wear after implant osteotomies: immunohistochemistry and scanning electron microscopy analysis. – *J. Oral Maxillofac. Surg.*, **66**, 2008, 1233-1240.
11. Rashad, A., P. Sadr-Eshkevari, M. Heiland, R. Smeets, H. Hanken, A. Gröbe, A. T. Assaf, R. H. Köhnke, P. Mehyar, B. Reicke, J. Wikner. Intraosseous heat generation during sonic, ultrasonic and conventional osteotomy. – *J. Cranio Maxillofac. Surg.*, **43**, 2015, 1072-1077.

12. **Szalma, J., L. Vajta, E. Lempel, A. Tóth, S. Jeges, L. Olasz.** Intracanal temperature changes during bone preparations close to and penetrating the inferior alveolar canal: drills versus piezosurgery. – *J. Craniomaxillofac. Surg.*, **45**, 2017, 1622-1631.
13. **Tehemar, S. H.** Factors affecting heat generation during implant site preparation: a review of biologic observations and future considerations. – *Int. J. Oral Maxillofac. Implants.*, **14**, 1999, 127-136.
14. **Wächter, R., P. Stoll.** Increase of temperature during osteotomy. In vitro and in vivo investigations. – *Int. J. Oral Maxillofac Surg.*, **20**, 1991, 245-249.
15. **Zheng, Q., L. Xia, X. Zhang, C. Zhang, Y. Hu.** Reduction thermal damage to cortical bone using ultrasonically-assisted drilling. – *Technol. Health Care*, **26**, 2018, 843-856.

Can Serum IgG Antiganglioside Antibodies to GM1, GM3 and GD1a be Used as Markers in Patients with Ischemic Stroke?

Vera Kolyovska^{1*}, Desislava Drenska², Dimitar Maslarov^{2,3}

¹ Dept. Experimental Morphology, Institute of Experimental Morphology, Pathology and Anthropology with Museum, Bulgarian Academy of Sciences, Sofia, Bulgaria

² Neurology Clinic, University First MHAT-Sofia, "St. John Krastitel", Sofia, Bulgaria

³ Medical University of Sofia, Medical College "Y. Filaretova", Sofia, Bulgaria

*Corresponding author e-mail: verakol@abv.bg

Our aim is to verify whether serum IgG antiganglioside antibodies (anti-GM1, anti-GD1a and anti-GM3) can be used as markers for patients with ischemic stroke. We showed the results of the antibody titer obtained by ELISA technique. There were 21 sera from patients under 75 years of age with ischemic strokes received between 2017-2020 from University First MHAT – Sofia, "St. John Krastitel". Three patients had a very weak indication for demyelination. Five had indication that correlates with possible metabolic abnormalities. The conclusion that could be drawn was that the antiganglioside antibodies titer was not decisive and could not be used as biomarker in stroke patients, and did not directly correlate with stroke severity, size of the ischemic area (reported by computed tomography data), and likely recovery prognosis. In ischemic strokes none of the patients had an indication of neuronal damage, as in the case with severe attacks of multiple sclerosis or Alzheimer's disease.

Key words: serum antiganglioside antibodies, biomarkers, ischemic stroke, ELISA

Introduction

The expression patterns of gangliosides vary in different tissues, during different life periods, as well as in various pathologies [1, 9, 11, 12]. The antiganglioside antibodies (AGAs) have the potential to be suitable diagnostic and therapeutic biomarkers for many brain abnormalities [14]. The ganglioside composition is related with a certain disorder [14]. Our team has been working with multiple sclerosis (MS), Alzheimer's disease (AD) and aging people for many years [7, 8, 16].

The aim of the present study was to examine whether serum IgG antiganglioside (anti-GM1, anti-GD1a and anti-GM3) antibodies could be used as markers for patients with ischemic stroke. To investigate whether and to what extent higher titers of these

antiganglioside antibodies correlate with stroke severity, ischemic area size (reported by computer tomography data), and whether they are associated with reversal of symptoms.

Materials and Methods

We had 21 sera from patients under 75 years of age with ischemic strokes received from the University First MHAT – Sofia “St. John Krastitel” from 2017 to 2020. All sera were taken before any therapy or immune intervention and they were analyzed in series. All participants agreed to be included in research studies and signed informed consent according to the Declaration of Helsinki. Statistical assay by Student’s t-test using statistical package was performed. The results were reported as mean values \pm SEM (Standard Error of the Mean) of three independent experiments. Differences were regarded as significant at $p < 0.05$. In our work we applied our modification on enzyme-linked immunosorbent assay (ELISA technique). The optical density was detected by ELISA reader Sunrise. The experiments were in triplicate [7, 8].

Results and Discussion

Here we present data from analysis of IgG antibodies against GM1, GD1a and GM3 in patients with stroke (**Table 1**).

Three patients had high titer of anti-GM1 antibodies (a weak indication for demyelination). Five patients showed increased levels of anti-GM3 antibodies-indication that is related with possible metabolic abnormalities (for example diabetes) and/or with possible problems with endothelium. None of the patients had any elevations of anti-GD1a antibodies, which is indicative for neuronal damage, such as severe MS attack and/or AD. Interestingly, in three of the patients, an increased titer of two of the antibodies was observed at the same time, and this demonstrates the dynamic of the gangliosides ratio. The results show that neurons were not damaged enough to be detected by the titer of antibodies to GD1a, as it is in the case of severe attack of MS and in AD. These data suggest that antibodies titers did not directly correlate with stroke severity. From our previous research, it has been concluded that there is a correlation between brain and serum antibodies in various neurological diseases (such as MS) due to disruption of the integrity of the blood-brain barrier (BBB) [7, 8, 16].

There are data showing that anti-GT1b and anti-GM1 (IgM and IgG) antibodies can transiently increase after stroke, but their titers are not associated with late post-apoplectic epilepsy [5]. On the other hand, an elevated titer of anti-GD1b antibodies was observed in patient diagnosed with acute motor axonal neuropathy [2]. Anti-GQ1b ganglioside antibodies are a serological marker of the Miller Fisher syndrome (MFS), a variant of Guillian-Barre syndrome (GBS) and are believed to be the principal pathogenic mediators of the disease [4, 6].

Diseases as epilepsy, Parkinson’s disease, Huntington’s disease, and melanoma may include impaired ganglioside metabolism [8, 9, 12]. The accumulation of GM2 and GM3 ganglioside types has been proposed as indicative of a mechanism of interactions between stroke, AD and other neurodegenerative diseases and disorders *in vitro* and in rat

Table 1. Titers of anti-GD1a, anti-GM1 and anti-GM3 antibodies in sera from stroke patients

Stroke patients			Anti GD1a antibodies titers	Anti GM1 antibodies titers	Anti GM3 antibodies titers
A	66 years old	female	-	+ 1:40	+ 1:200
B	70 years old	female	-	-	-
C	52 years old	male	-	-	-
D	72 years old	female	-	-	-
E	70 years old	female	-	-	-
F	71 years old	male	-	+ 1:40	+ 1:100
G	70 years old	female	-	-	+ 1:200
H	71 years old	female	-	-	-
I	75 years old	female	-	-	-
J	75 years old	female	-	-	-
K	71 years old	female	-	-	-
L	64 years old	male	-	-	-
M	72 years old	male	-	-	-
N	66 years old	female	-	-	-
O	70 years old	female	-	-	-
P	52 years old	male	-	-	-
Q	72 years old	female	-	-	-
R	70 years old	female	-	-	-
S	71 years old	male	-	-	+ 1:100
T	70 years old	female	-	-	-
U	71 years old	female	-	+ 1:40	+ 1:400

models [1]. The protective role of GM1 ganglioside against brain hypoxia-ischemia was established in animal model [13] and the increased levels of gangliosides in damaged cortex have proposed protection against ischemic damage [10, 15].

In an animal model of MS, we have shown high content of GD1a and increased titer of antibodies against this ganglioside in a blood test, just before the onset of signs of the disease. Thus, serum GD1a may be suggested as a biomarker of axonal BBB disruption, which provides an impetus to initiate early therapy [16]. Therefore, if screening is done and early therapy is started, the development of the disease can be prevented.

AGAs can target immune attack against neuronal cells and to neutralize their complement inhibitory activity. AGAs are important especially in acquired demyelinating immune-mediate neuropathies, like MS, GBS and its variant, the MFS [3, 6].

Conclusion

The conclusion is that the titer of antiganglioside antibodies to GM1, GM3 and GD1a is not decisive and cannot be used as biomarker in ischemic stroke patients. Higher titers of these anti-ganglioside antibodies did not directly correlate with stroke severity, size of the ischemic area (reported by computed tomography data), and likely recovery prognosis.

References

1. Caughlin, S., J. D. Hepburn, D. H. Park, K. Jurcic, K. K.-C. Yeung, D. F. Cechetto, S. N. Whitehead. Increased expression of simple ganglioside species GM2 and GM3 detected by MALDI imaging mass spectrometry in a combined rat model of A β toxicity and stroke. – *PLoS One*, **10**(6), 2015, e0130364.
2. Chi, M. S., S. H. Ng, L. Y. Chan. Asymmetric acute motor axonal neuropathy with unilateral tongue swelling mimicking stroke. – *Neurologist*, **21**(6), 2016, 106-108.
3. de Castillo, L. L. C., J. D. B. Diestro, K. H. D. Ignacio, P. M. D. Pasco. A rare mimic of acute stroke: rapidly progressing Miller-Fisher syndrome to acute motor and sensory axonal neuropathy variant of Guillain-Barre syndrome. – *B.M.J. Case Rep.*, **12**, 2019, e228220.
4. Halstead, S. K., F. M. P. Zitman, P. D. Humphreys, K. Greenshields, J. J. Verschuuren, B. C. Jacobs, R. P. Rother, J. J. Plomp, H. J. Willison. Eculizumab prevents anti-ganglioside antibody-mediated neuropathy in a murine model. – *Brain*, **131**(5), 2008, 1197-1208.
5. Hsieh, P. F., M. T. Liu, K. C. Jeng. Anti-GT1b and anti-GM1 antibodies can increase after stroke but neither is associated with late post-apoplectic epilepsy. – *Kaohsiung J. Med. Sci.*, **14**(2), 1998, 68-75.
6. Koga, M., M. Takahashi, K. Yokoyama, T. Kanda. Ambiguous value of anti-ganglioside IgM autoantibodies in Guillain-Barré syndrome and its variants. – *J. Neurol.*, **262**(8), 2015, 1954-1960.
7. Kolyovska, V. Serum IgG antibodies to GD1a and GM1 gangliosides in elderly people. – *Biomed. Khim.*, **62**(1), 2016, 93-95.
8. Kolyovska, V., S. Ivanova. Neurodegenerative changes and demyelination in serum IgG antibodies to GM1, GD1a and GM3 gangliosides in patients with secondary progressive multiple sclerosis – preliminary results. – *Compt. Rend. Acad. Bulg. Sci.*, **72**(1), 2019, 115-122.
9. Kolyovska, V., S. Ivanova, D. Drenska, D. Maslarov, R. Toshkova. Role of GM3 ganglioside in the pathology of some progressive human diseases and prognostic importance of serum anti-GM3 antibodies. – *Biocell*, **45**(6), 2021, 1485-1494.
10. Kwak, D. H., S. M. Kim, D. H. Lee, J. S. Kim, S. M. Kim, S. U. Lee, K. Y. Jung, B. B. Seo, Y. K. Choo. Differential expression patterns of gangliosides in the ischemic cerebral cortex produced by middle cerebral artery occlusions. – *Mol. Cells*, **20**(3), 2005, 354-360.
11. Lucki, N. C., M. B. Sewer. Nuclear sphingolipid metabolism. – *Ann. Rev.*, **74**, 2012, 131-151.
12. Ohmi, Y., M. Kambe, Y. Ohkawa, K. Hamamura, O. Tajima, R. Takeuchi, K. Furukawa, K. Furukawa. Differential roles of gangliosides in malignant properties of melanomas. – *PLoS One*, **13**(11), 2018, e0206881.
13. Rong, X., W. Zhou, C. Xiao-Wen, L. Tao, J. Tang. Ganglioside GM1 reduces white matter damage in neonatal rats. – *Acta Neurobiol. Exp. (Wars)*, **73**(3), 2013, 379-386.
14. Sarbu, M., R. Ica, A.D. Zamfir. Gangliosides as biomarkers of human brain diseases: Trends in discovery and characterization by high-performance mass spectrometry. – *Int. J. Mol. Sci.*, 2022, **23**, 693.
15. Whitehead, S. N., K. H. N. Chan, S. Gangaraju, J. Slinn, J. Li, S. T. Hou. Imaging mass spectrometry detection of gangliosides species in the mouse brain following transient focal cerebral ischemia and long-term recovery. – *PLoS One*, **6**(2), 2011, e20808.
16. Zaprianova, E., D. Deleva, V. Kolyovska, B. Sultanov. Elevated IgM titers of serum anti-GD1a antibodies in relapsing-remitting multiple sclerosis: correlation with neuronal damage. – *Medical Data*, **3**(2), 2011, 127-129.

Profile of Manganese Accumulation in the Host-Parasite (Rattus norvegicus-Fasciola hepatica) System after Manganese Salt Treatment

Veselin Nanev^{1*}, Ivelin Vladov¹, Elitza Dencheva¹, Margarita Gabrashanska¹, Katya Georgieva²

¹ Department of Experimental Parasitology, Institute of Experimental Morphology, Pathology and Anthropology with Museum, Bulgarian Academy of Sciences, Sofia, Bulgaria

² Department of Animal Diversity and Resources, Institute of Biodiversity and Ecosystem Research, Bulgarian Academy of Sciences, Sofia, Bulgaria

*Corresponding author e-mail: veselinnanev@gmail.com

The aim of our study was to evaluate the combined effect of manganese salt ($\text{MnCl}_2 \cdot \text{H}_2\text{O}$) and experimental *Fasciola hepatica* infection on the Mn-concentration in the system rat/ *F. hepatica*. Mn concentration was determined in the liver, kidney and the musculature of the host and as well as in *F. hepatica*, using ICP method. Results: the treated non-infected rats showed a significantly increased Mn level in the kidney and musculature, and slightly higher in the liver. In the infected rats, Mn-concentration in the liver was reduced, increased – in the musculature and non-changed in the kidney in comparison to those observed in the non-infected host. The *F. hepatica* isolated from the Mn treated rats showed double increased Mn concentration than that in the *F. hepatica* found in non-treated hosts. Conclusion: Mn homeostasis may play an important role at the rat/ *F. hepatica* interaction.

Key words: host-parasite system, Mn, bioaccumulation

Introduction

Manganese (Mn) is one of several first-order transition elements involved in many metabolic processes in animal organisms. This metal is involved in different biological activities dependent on multiple Mn-dependent enzymes [1]. Mn-enzymes have an important role in protecting cells from damage caused by free radicals and determined the oxidative status of animals. Infection with endoparasites affects the trace element balance due to redistribution among host tissues [3, 4].

Data from targeted studies on the effects of parasitic infection on host Mn homeostasis are scarce. This comparative study was conducted to determinate the Mn levels in the host (*Rattus norvegicus*) tissues and in the parasite (*F. hepatica*).

Material and Methods

Rat and parasite. The Wistar rats (*Rattus norvegicus*) used were aged 30 days, male and weighed 100 ± 10 g each. *Fasciola hepatica* used were obtained from laboratory maintained life cycle of the parasite, using *Galba truncatula* snails as intermediate host, and male Wistar rats as definitive host [2].

All animal experiments were carried out in accordance with the U.K. Animals (Scientific procedures) Act, 1986 and the associated guidelines EU Directive 2010/ 63/ EU for animal experiments, or the National Institutes of Health guide for the care and use of Laboratory animals (NIH Publications No, 8023, revised 1978).

Experimental design. At the beginning of the experiment (day 0) rats ($n = 40$) were divided into 4 groups with 10 animals each ($n = 10$): 1st – control, uninfected, untreated; 2nd – uninfected, treated with $MnCl_2 \cdot 4H_2O$, (Sigma-Aldrich US); 3rd – untreated, experimentally infected with *Fasciola hepatica*; 4th – infected with *F. hepatica* and treated with Mn salt. On day 0, each rat in groups 3 and 4 was experimentally infected orally with 15 viable *F. hepatica* metacercariae. All rats in groups 2 and 4 were treated with Mn salt solution through drinking water at a concentration of 0.323 mg Mn/animal/day for 2 weeks before the end of experiment (day 60).

Sampling and analytical procedure. After exposure, rats (400 ± 20 g each) were anesthetized, slaughtered and dissected. Samples of liver, kidney and muscle (pectoralis major) as well as parasites, removed from the rats, were used to determine the concentration of Mn using Inductively coupled plasma-optical emission spectrometry (ICP – OES, VISTA MPX CCD Simultaneous VARIAN). The statistical analysis was carried out on the Prism 6 program. Variation analysis was used for determining the mean values, the standard deviation (SD) and the significance criterion (P). The comparison of the mean values of parameters was carried out using the one-way analysis of variance, Dunnett's Multiple Comparison Test. The results from these comparisons were also statistically significant: * ($p \leq 0.05$), ** ($p \leq 0.01$).

Results

The Mn content of host (Wistar rat) and parasite (*F. hepatica*) tissues after experimental exposure to Mn salt is presented in **Table 1**.

The content of Mn in the liver of all rats was the highest, compared to that of the other organs. The lowest concentration was found in the muscles. Treatment of control, non-infested rats with Mn salt increased the level of Mn significantly in the kidney and muscle, and insignificantly in the liver. The concentration of Mn in the liver of the invaded rats was decreased, in the kidney – unchanged, and increased in the muscle significantly compared to the control levels. The Mn content in the tissues of the infected rats was close to that of the controls, except for a twofold increase in Mn in the muscles. The concentration of Mn in the parasites isolated from the untreated rats was slightly increased compared to that in the parasitized liver. Parasites from treated rats showed a two-fold increase in Mn concentration compared to untreated rats. The concentration of Mn does not exceed the permissible concentrations in animals.

Table 1. Mn concentration values ($\mu\text{g/g d.m.}$) in host (Wistar rat) and parasite (*Fasciola hepatica*) tissues after treatment with $\text{MnCl}_2 \cdot 4\text{H}_2\text{O}$.

Tissue Groups	Liver	Kidney	Muscles	<i>F. hepatica</i>
1 st gr. – control, untreated, non-infected	2.6 (± 0.8)	1.3 (± 0.4)	0.25 (± 0.01)	
2 nd gr. – treated, non-infected	3.0 (± 0.11)	2.5* (± 1.2)	0.56* (± 0.04)	
3 rd gr. – infected	1.15* (± 0.06)	1.33 (± 0.15)	0.42* (± 0.07)	1.49 (± 0.18)
4 th gr. – infected and treated	2.71 (± 1.1)	1.62 (± 0.28)	0.5* (± 0.06)	2.9** (± 0.94)

Data were presented as means \pm standard deviation. * Significant differences between tissues of rats in control and other groups ($p < 0.05$). ** Significant differences between *F. hepatica* tissues in 3rd and 4th group ($p < 0.01$).

Discussion

This study investigates the content of Mn in the rat tissues (liver, kidney and muscle) affected by *F. hepatica* and supplied with Mn salts. Different concentrations of Mn were detected in the test samples. Comparing its content in the tissues of healthy rats, it is observed the higher concentration of Mn in the rat livers than that of rat kidneys and muscles. The highest level of Mn was measured in the parasite. Our results clearly show that liver fluke infection affects the host's metabolism by redistribution of Mn content among its tissues and accumulating Mn in the helminth tissues. In the present study, the experimental exposure to Mn salt to uninfected rats shows identified kidney and muscle as organs for Mn accumulation. Our results show a slight increase in the level of Mn in rat liver tissue, although the liver is considered to be the site that accumulates the highest metal content in organisms [1]. Comparing the Mn content in the tissues of healthy and *F. hepatica* – infected rats, an imbalance was found in the presence of parasite. The liver fluke infection induces the significant reduction of Mn in liver and enhancement in muscle tissues of its host. *F. hepatica* and the liver accumulate Mn^{2+} in similar extend. It shows that Mn^{2+} is involved in the metabolic processes in the parasite.

Conclusion

Rats chronically treated with Mn salt and infected with *F. hepatica* showed bio-redistribution of Mn among internal organs accompanied with Mn accumulation in the infected livers. The livers accumulated Mn regardless in the presence of the infection. Mn homeostasis may play an important role at the rat/ *F. hepatica* interaction.

References

1. Avila, D. S., R. L. Puntel, M. Aschner. Manganese in Health and Disease. – *Met. Ions Life Sci.*, **13**, 2013, 199-227.
2. Georgieva, K., S. Georgieva, Y. Mizinska, SR. Stoitsova. *Fasciola hepatica* miracidia: lectin binding and stimulation of in vitro miracidium to sporocyst transformation. – *Acta Parasitol.*, **57**(1), 2012; 46-52.
3. Jankovic, A., M. Vucetic, A. Stancic, V. Otasevic, B. Buzadzic. Antioxidant defense in rat tissues after supplementation with organic form of manganese. – *Hr. I Ishrana (Beograd)*, **22**, 2014, 1, 13-18.
4. Nanev, V., M. Gabrashanska, K. Georgieva, I. Vladov, O. Kandil, N. Tsocheva-Gaytandzhieva. Trace element contents in rat tissues after experimentally induced *Fasciola hepatica* infection. – *Compt. Rend. Acad. Bulg. Sci.*, **71**, 2018, 10, 1324-1330.

Effect of *Nosema apis* and *N. ceranae* on honey bee *Apis mellifera* queen development

Sigmar Naudi¹, Risto Raimets¹, Margret Jürison¹, Egle S. Liiskmann¹,
Marika Mänd¹, Delka Salkova², Reet Karise¹

¹ Chair of Plant Health, Institute of Agricultural and Environmental Sciences, Estonian University of Life Sciences, Tartu, Estonia

² Department of Experimental Parasitology, Institute of Experimental Morphology, Pathology and Anthropology with Museum, Bulgarian Academy of Sciences, Sofia, Bulgaria

*Corresponding author e-mail: Sigmar.Naudi@emu.ee

Nosema apis and *N. ceranae* are agents causing the disease called nosemosis in honey bee workers and queens. Few is known about the impacts of it on honey bee development. The royal jelly in queen cells was infected with *Nosema* spores to see whether and how it affects the development of honey bee queens. Seven groups of grafted honey bee larvae were established, and treated as follows: high and low concentrations of *N. ceranae* and *N. apis*, mixes of both species in both concentrations, and untreated control. After allowing nurse bees to fill the queen cells with royal jelly, an injection of 50 000 spores or 10 000 spores was added into the royal jelly. We found that only *N. apis* decreased the hatching rate of honey bee queens both in single and mixed treatment at high dosages, but we did not detect any morphological deviations in unhatched pupae.

Key words: honey bee *Apis mellifera*, *Nosema* spp., honey bee queen breeding, queen quality

Introduction

Honey bees (*Apis mellifera* L.) are suffering from high colony mortality rates in Europe [11]. There are several reasons for that and pathogens are considered as most important causes [3]. One of the most damaging diseases, nosemosis is caused by microsporids *N. apis* Zander [7] and *N. ceranae* Fries [8], which can also co-exist in the same colony.

Nosemosis has been under scientific interest for a long time whereas most of the work has been conducted on honey bee workers. The queens, however, can also be susceptible to nosemosis. *Nosema*-infected queens have been seen to produce a higher amount of queen mandibular pheromone, which refers to the poorer quality of the queen [1]. Nosemosis is often linked to changing vitellogenin titers in worker and

queen bees, although, the effects can be different [2]. Changes in vitellogenin amount affect the queen's hormonal balance, oxidative stress, and longevity [5]. Still, only a few studies consider the effects of nosemosis on honey bee queen development, and to our knowledge, there are none considering the developmental success due to manipulative infection. While nosemosis is detected not only the intestine but also hypopharyngeal glands of honey bees, the royal jelly produced by nurse bees can be infected with *Nosema* spp. spores [4].

The aim of this study was to explore i) whether *Nosema* spp. spores can be transferred from royal jelly to emerged queens and ii) whether the infection causes any morphological deviations.

Materials and Methods

The study was conducted in the summer of 2021. New queens (*A. mellifera ligustica*) were bred from one-day-old larvae originating from a single queen. Colonies used for nursing (royal jelly producing, cell building) were repeatedly checked for three weeks prior to the experiment to ensure that there was no infection present.

To obtain fresh *N. apis* and *N. ceranae* spores, infected honey bee colonies were used. From those, infected worker bees were collected and the spores were separated by homogenization. The *Nosema* species were identified by a multiplex PCR (M-PCR) assay [10]. Once the species was known, a centrifugation protocol [9] was used to purify the spores, which enabled about 85% purity. In order to separate the last precipitate, the resulting suspension was cleaned with a 10-micron filter. A flow cytometer (BD Accuri C6) was used to determine the number of spores [10].

The queen cell cups were made of organic bees wax (purchased from a local producer) to reduce the risk of pesticide contamination, which could affect the outcome of the experiment. The one-day-old larvae were grafted into the cups. A total of seven treatment groups were created with ten larvae for each: *N. apis* low (10000 spores), *N. apis* high (50.000 spores); *N. ceranae* low, *N. ceranae* high; Mix low, Mix high; Control.

After grafting the cell builder colony was checked regularly until the cups were sealed by worker bees. If a cup was sealed, an injection of 2 µL of suspension was added through the wax walls of the cup into the royal jelly (ddH₂O and nosemosis agents). Larvae were located, directing (a strong) light through the wax cell, and the suspension was injected underneath the larvae. On the tenth day after the grafting, queen cups were isolated (using Nicot's queen cages) and taken into an incubator (at 35°C and 65% humidity) until hatching.

Results and Discussion

The hatching rate of honey bee queens was affected by the treatment (**Fig. 1**). Interestingly, with *N. apis* high spore load treatment, the hatching rate was zero, while it was not affected by the same spore load of *N. ceranae*. The dissection of sealed queen cells showed variable developmental deviations in this group (*N. apis* high), most of these queens had ended their development at the larval stage and didn't reach the metamorphosis. Only a couple of individuals started the pupation but stopped suddenly before finishing it as shown in **Fig. 2**. Similarly, a low hatching rate was observed in the mixed high concentration group. We suggest that *N. apis* caused this.

The hatching rate of other treatment groups was relatively normal. Usually, beekeepers aim to achieve a hatching rate of over 80% when breeding the queens. *N. apis* has been considered problematic for honey bees during the early season [7], but our study reveals yet another threat – honey bee breeding success can be seriously harmed when the nursing colonies are infected and not checked for this disease. There are no clear symptoms of nosemosis and only laboratory analyses of bee samples allow a correct diagnosis of this disease.

Some papers indicate that nosemosis agents are able to transfer through the metamorphosis process in worker bees [2, 6, 12], although, we could not confirm this in queen bees – we did not detect any infection from the adult newborn queens.

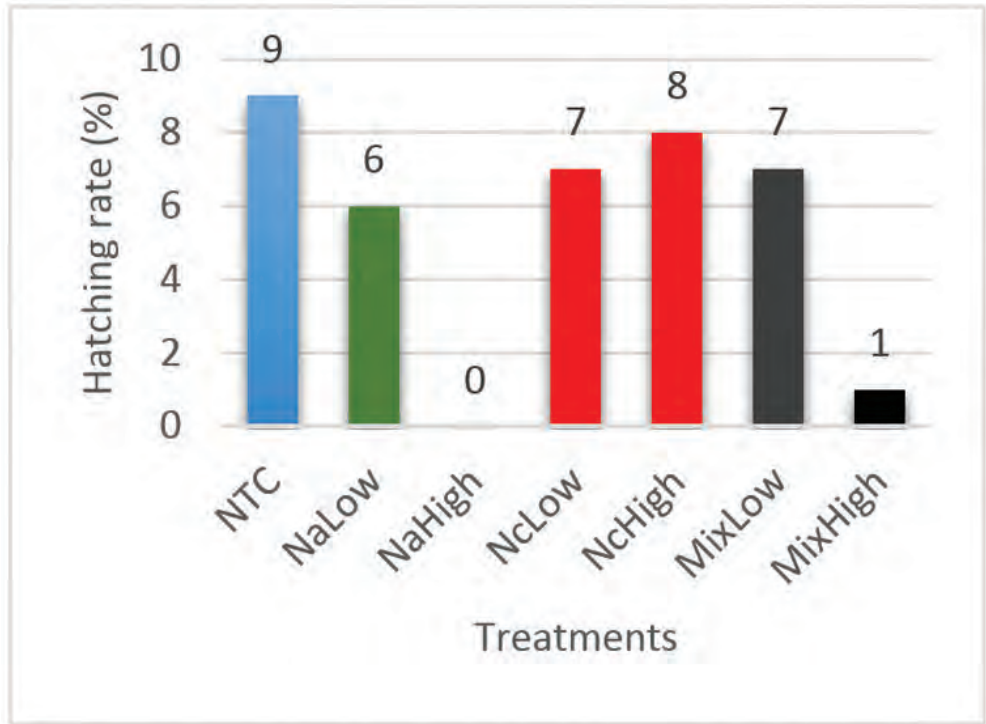


Fig. 1. The hatching rate of the treatment groups. NTC-no treatment control. Na –*N. apis*, Nc –*N. ceranae*, Mix – Na + Nc, low – 10 000 spores, high – 50 000 spores injected into royal jelly in queen cells.

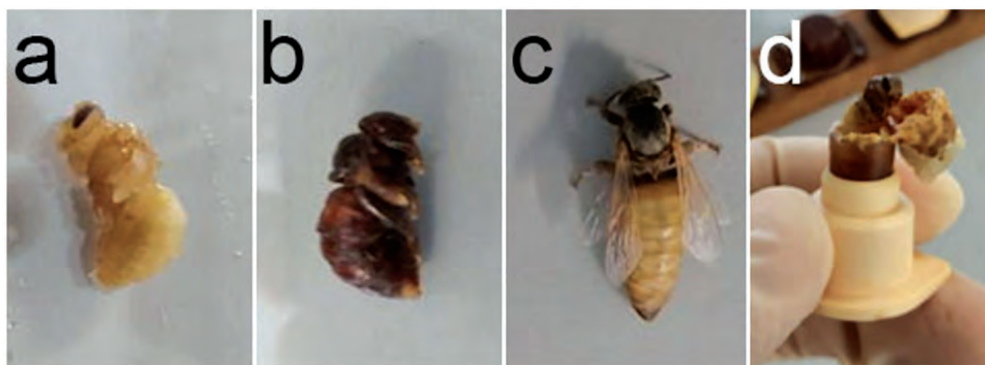


Fig. 2. High doses of *N. apis* both as pure treatment (a and b) or in mix with *N. ceranae* (c and d) caused disruption of metamorphosis at different developmental timepoints (Photos by S. Naudi)

Conclusions

Our study showed that royal jelly contamination with high concentrations of *N. apis* can cause honey bee queen mortality during breeding. This first study on *Nosema* affecting queen development through contamination of royal jelly is indicating the need for more targeted research on this topic and is really important for the honey bee queen breeding system.

Acknowledgements: The study was financed by: EMU project: P200192PKTE; by the European Regional Development Fund and executed by the Education and Youth Authority (former Archimedes Foundation), project: L220007PKTE; by the Estonian Professional Beekeepers Association, and Estonian-Bulgarian joint research project: “Field and experimental studies of actual diseases of honey bees (*Apis mellifera* L.) from Bulgaria and Estonia.” P.43/14.12.2021.

References

1. Alaux, C., M. Folschweiller, C. McDonnell, D. Beslay, M. Cousin, C. Dussaubat, J.-L. Brunet, Y. L. Conte. Pathological effects of the microsporidium *nosema ceranae* on honey bee queen physiology (*Apis Mellifera*). – *Journal of Invertebrate Pathology*, **106** (3), 2011, 380-385.
2. BenVau, L. R., J. C. Nieh. Larval honey bees infected with *nosema ceranae* have increased vitellogenin titers as young adults. – *Scientific Reports*, **7** (1), 2017, 14144.
3. Collison, E., H. Hird, J. Cresswell, C. Tyler. Interactive effects of pesticide exposure and pathogen infection on bee health – a critical analysis. – *Biological Reviews*, **91** (4), 2016, 1006-1019.
4. Copley, T. R., S. H. Jabaji. Honeybee glands as possible infection reservoirs of *nosema ceranae* and *nosema apis* in naturally infected forager bees. – *Journal of Applied Microbiology* **112** (1), 2012, 15-24.
5. Corona, M., R. A. Velarde, S. Remolina, A. M-Lauter, Y. Wang, K. A. Hughes, G. E. Robinson. Vitellogenin, juvenile hormone, insulin signaling, and queen honey bee longevity. – *Proceedings of the National Academy of Sciences*, **104** (17), 2007, 7128-7133.

6. **Eiri, D. M., G. Suwannapong, M. Endler, J. C. Nieh.** Nosema ceranae can infect honey bee larvae and reduces subsequent adult longevity. Edited by Guido Favia. – *PLOS ONE*, **10** (5), 2015, e0126330.
7. **Fries, I.** Nosema apis – a parasite in the honey bee colony. – *Bee World*, **74**, 2015, 5-19.
8. **Fries, I., F. Feng, A. da Silva, S. B. Slemenda, N. J. Pieniazek.** Nosema ceranae n. sp. (Microspora, Nosematidae), morphological and molecular characterization of a microsporidian parasite of the asian honey bee apis cerana (Hymenoptera, Apidae). – *Eur. J. Protistol.*, **32** (3), 1996, 356-365.
9. **Fries, E., J. H. Dekiff, J. Willmeyer, M-T. Nuelle, M. Ebertc, D. Remy.** Identification of polymer types and additives in marine microplastic particles using pyrolysis-GC/MS and scanning electron microscopy. – *Environ. Sci.: Processes Impacts* **15** (10), 2013, 1949-1956
10. **Naudi, S., J. Šteiselis, M. Jürison, R. Raimets, L. Tummeleht, K. Praakle, A. Raie, R. Karise.** Variation in the distribution of nosema species in honeybees (Apis Mellifera Linnaeus) between the neighboring countries Estonia and Latvia. – *Vet. Sci.*, **8** (4), 2021, 58.
11. **Osterman, J., M. A. Aizen, J. C. Biesmeijer, J. Bosch, B. G. Howlett, D. W. Inouye, C. Jung.** Global trends in the number and diversity of managed pollinator species. – *Agriculture, Ecosystems & Environment*, **322**, 2021, 107653.
12. **Traver, B. E., R. D. Fell.** Low natural levels of nosema ceranae in apis mellifera queens. – *Journal of Invertebrate Pathology*, SIP Symposium on Resistance to BtCrops., **110** (3), 2012, 408–410.

Age at Menarche in Sofia Girls /2014-2018/

*Racho Stoev, Zorka Mitova**

Institute of Experimental Morphology, Pathology and Anthropology with Museum, Bulgarian Academy of Sciences, Sofia, Bulgaria

*Corresponding author e-mail: zorkamitova@gmail.com

The aim of this study was to determine the age of menarche in city girls in modern conditions and to compare it with data for former periods. The comparison shows that in the beginning of 21st century the mean age at menarche (calculated by probit analysis) in Sofia girls remains on the same level as in 1980s – 12.7-12.9 years. Its standard deviation is on the level of 1.3-1.4 years, typical for socially heterogeneous samples. The available data do not allow determining whether there was variation of the timing of puberty under the changes of social conditions in the periods between these three researches.

Key words: age at menarche, probit analysis, transversal study, pubertal development, Sofia

Introduction

The appearance of the first menstruation (menarche, Me) is used in auxology and related disciplines as a relatively easily researched and objective indicator of puberty in girls. In addition, it is very sensitive to the influence of the environment, especially social conditions, and therefore it is widely used to assess the biological well-being of the reference group [3, 10]. It is most accurately calculated in cross-sectional studies by probit or logit analysis. The data of retrospective studies of adult women can also be used for comparisons with some caveats [10]. The aim of the present study is to assess the age at menarche in Sofia girls at the present time and to compare the results of three cross-sectional studies on the age at menarche in Sofia.

Materials and Methods

Material: Individual data of 306 school girls from Sofia city, aged 10 to 14 years, for presence or absence of menstruation. The data were collected during the period 2014-2018.

The work has been carried out in accordance with The Code of Ethics of the World Medical Association (Declaration of Helsinki) [12].

Method: Status quo (transversal) study, combined with probit analysis (probit transformation and least squares method) for evaluating the mean age at menarche. Probit analysis is based on the probit function, which transforms a normal accumulation curve into straight line (**Fig.1** and **Fig. 2**).

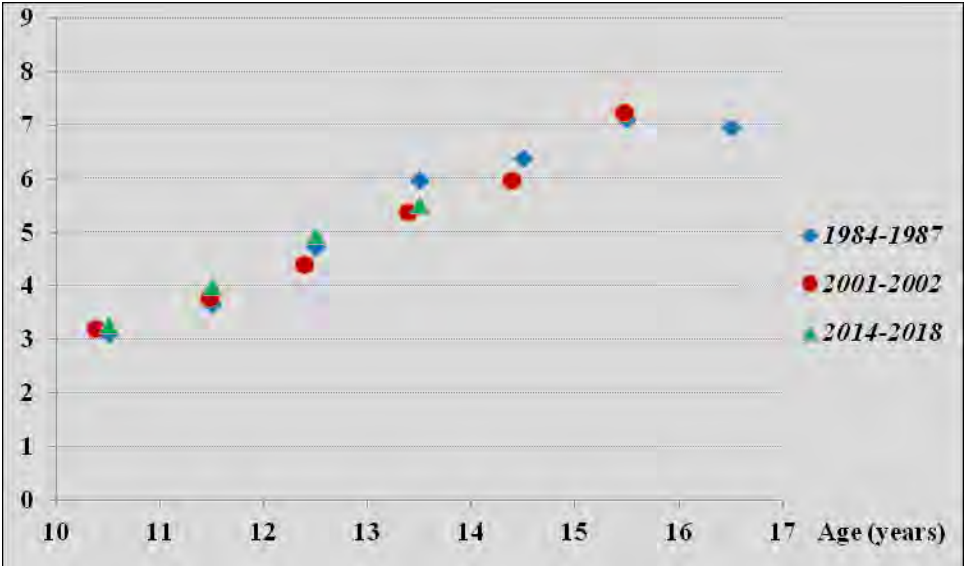


Fig. 1. Proportion of girls post menarche by age in three successive studies in Sofia.

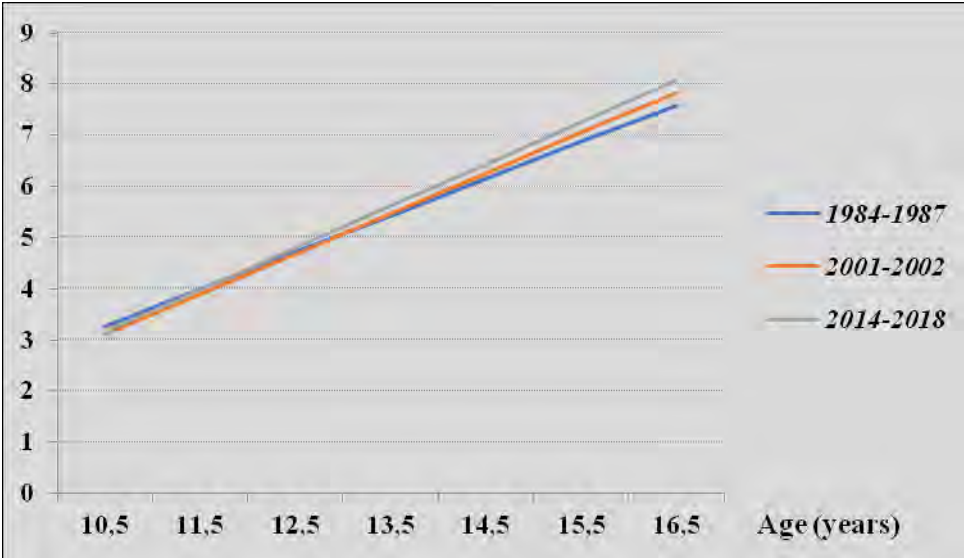


Fig. 2. Probit transformation of the proportion of girls post menarche by age in three successive studies in Sofia – lines calculated by least square method.

The data of other authors for comparison were used, where they could be checked by recalculating the age of menarche by probit analysis. When this was impossible (in some oldest works) the average age of menarche was recalculated from the distribution of retrospective data by age.

Results

The mean age at menarche, calculated by the data, is 12.74 ± 0.10 years. This is a value typical for urban populations of developed countries. Its standard deviation is 1.22 ± 0.07 years. This value is typical for socially heterogeneous populations [10].

The earliest data about age at menarche in Sofia girls were collected by Academician St. Vatev in women giving birth around 1905 [11] (**Fig. 3**). As the average age at childbirth at the beginning of the 20th century was 30 years these data with an average age at menarche of 14.5 years, reflect the period around 1890. In the next years the age of menarche quickly decreases until the 1960s: about 13.9 years by 1915 – probit analysis, data from Noikov and Katsarov [7]; 13.5 years to 1935 – a probit analysis, data from Mateev [4]; 13.3 years at the beginning of the 1950's – probit analysis, data from Seizov [8]; 13.0 years at the beginning of the 1960s – probit analysis, data from Seizov [9] and 12.7 years at the end of the 1960s – probit analysis, data from Damyanova and Georgiev [1, 2]. Retrospective data collected by Stoev in the 1980s give slightly higher values – 13.7 years in the late 1940s, 13.4 years in the 1950s, 13.0 years in the 1960s and in the 1970s [10]. The small number of data for the 1940s and the differences in the method do not allow us to say whether there was an increase in the age of menarche during the Second World War and the related difficulties in supplies (card system).

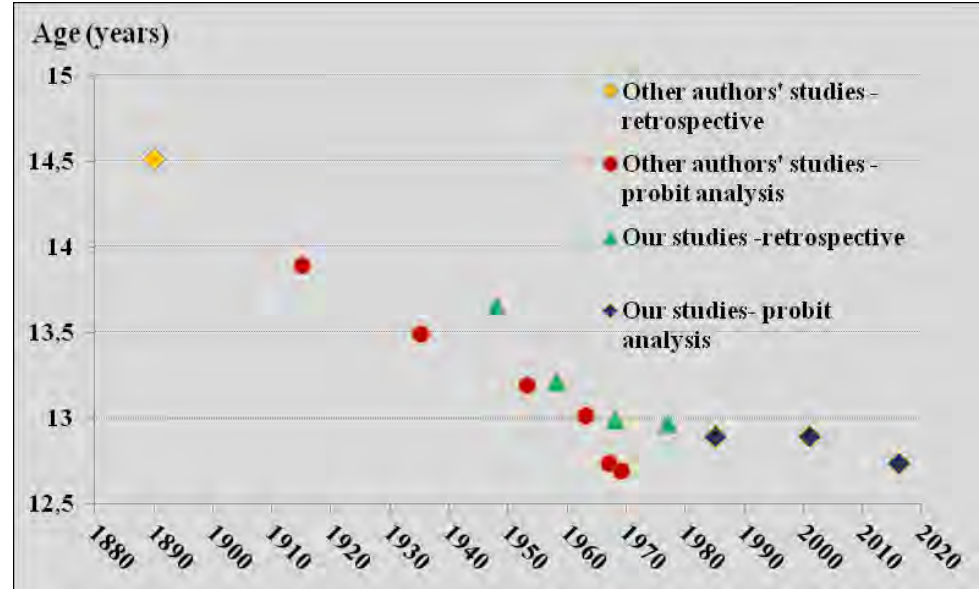


Fig. 3. Changes of age at menarche in Sofia girls from the Liberation until present.

Materials collected by Stoev in the years 1984 – 1987 show that the menarche age of Sofia girls at the 1980s was 12.90 ± 0.12 years ($SD = 1.39$) [10]. The standard deviation is quite large, because in the study, significant differences in the timing of puberty were found depending on the income, education of the parents, housing conditions, type of household and number of children in the family. According to the materials collected by Mitova in 2001 – 2002, practically the same menarcheal age can be traced – 12.92 ± 0.09 years ($SD = 1.28$) [5].

Unfortunately, there is a lack of materials for the analysis of the movements of age at menarche during the period of economic difficulties in the 1990s. At that time, a longitudinal study of the growth and development of Sofia children and adolescents was conducted, but it gave an unrealistically low age of menarche – 12.4 years, apparently due to the specific social composition of the sample (in the 1980s, such an age of menarche was observed in schoolgirls in prestigious neighborhood of Sofia). At the same time, the survey data of 15-16-year-old girls in the same schools where the longitudinal study was conducted (all but one menstruating) give an average age of menarche again of 12.9 years, i.e. six months older. Since they were examined in 2001, this may mean that there was some delay in the age of menarche during the most difficult period of 1991 and 1997 [6].

Conclusion

The acceleration of the menarche age in Sofia stopped at the end of the 1960s. Since then, the age of menarche in Sofia girls has stabilized, or rather, fluctuated at the level of 12.7 – 13.0 years (differences are unreliable). Insufficient data on social differentiation and lack of data for the subsequent period give grounds for new research.

References

1. **Damyanova, Tsv.** Indicators of normal puberty in girls. – *PhD thesis*, Sofia, 1974, 238 p. (in Bulgarian).
2. **Georgiev, B.** Peculiarities in the development of children and adolescents in longitudinal study. – *PhD thesis*, Sofia, 1974, 295 p. (in Bulgarian).
3. **Godina, E. Z.** Human auxology – a science of the 21st century: problems and prospects. – In: *Anthropology on the threshold of the III millennium* (Eds. Balanovskaya, E.V., Godina, E. Z., Dubova, N.A.), **EAA**, Russian branch, Moscow, **2**, 2003, 529-566 (in Russian).
4. **Mateev, Dr.** Report on the physical development and health status of secondary school students during the academic year 1935/36. – *School review*, XXXIV, **5-6**, 1937, 725-798 (in Bulgarian).
5. **Mitova, Z.** Anthropological characteristics of physical development, body composition and nutritional status in 9-15-year-old children and adolescents from Sofia city. – *PhD thesis*, Bulgarian Academy of Sciences, 2009, 225 p. (in Bulgarian).
6. **Mitova, Z., R. Stoev, L. Yordanova.** Changes in the age of menarche in the girls of Sofia in the twentieth century (acceleration and stabilization) – In: *Problems of modern human morphology: materials of Int. Scientific* – practical. conf., dedicated 80th anniversary of Professor B.A. Nikityuk, M., September 25-27, RGUFKSMiT, 2013, 127-129 (in Russian).
7. **Noikov, P., D. Katsarov.** Physiological manifestations of the sexual maturation of Bulgarian male and female students. – *Bulg.pr. h., Sofia*, 1919, 1-88 (in Bulgarian).

8. **Seizov, Hr.** Pubertal development according to primary and secondary sex characteristics in Sofia schoolgirls and schoolboys in 1953. – *Proceedings of IPhEdSchHealth*, Sofia, **2**, 1957, 183-207 (in Bulgarian).
9. **Seizov, Hr.** On the hastening of the pubertal development of the students in Sofia in an interval of ten years. – *Probl. Phys. cult.*, **3**, 1964, 180-183 (in Bulgarian).
10. **Stoev, R.** Anthropological characteristics of adolescents – physical development and sexual maturation in relation to family and household conditions. – *PhD thesis*, Sofia, 2007, 177 p. (in Bulgarian).
11. **Vatev, St.** The appearance of the first menstruation in Bulgarian women. – *Journal of the BAS, XXXII, Nat.-math. branch.*, **15**, 1925, 69-84 (in Bulgarian).
12. **World Medical Association.** Declaration of helsinki – Ethical principles for medical research involving human subjects. – *WMJ*, **54**(4), 2008, 122-125.

A Variation of the Third Common Palmar Digital Artery

Vasil Iliev, Lina Malinova, Lazar Jeleu*

Department of Anatomy, Histology and Embryology, Medical University of Sofia, Sofia, Bulgaria

*Corresponding author e-mail: v.iliev@medfac.mu-sofia.bg

During a standard anatomical dissection of the left upper limb of an adult female cadaver, a variation of the course of the third common palmar digital artery (CPDA III) was found. The artery was well identified only in the distal part of the fourth interosseous space, giving rise to a pair of proper palmar digital arteries. A detailed dissection revealed that the CPDA III, crossing posterior to the little finger long flexors, arose as a branch of superficial palmar arch with a significant contribution from the terminal part of the deep palmar arch. Based on its path, it is possible for the CPDA III to be compressed by the flexors' tendons. The knowledge of numerous variations in vascular architecture of hand can explain some cases of finger ischemia and might be helpful to surgeons performing microsurgical procedures of the hand and fingers.

Key words: superficial palmar arch, common palmar digital artery, proper palmar digital artery, arterial variations, upper limb

Introduction

Three common palmar digital arteries (CPDA) arise from the convexity of the superficial palmar arch (SPA) and proceed distally on the second, third, and fourth lumbrical muscles. Each receives the corresponding volar metacarpal artery and then divides into a pair of proper palmar digital arteries which run along the contiguous sides of the index, middle, ring and little fingers, behind the corresponding digital nerves. They anastomose freely in the subcutaneous tissue of the finger tips and by smaller branches near the interphalangeal joints [1]. Understanding the typical and atypical anatomy and variable relations facilitates safe surgical technique. While the most common arrangements are usually emphasized, less common patterns occur. Unrecognized, these can lead to confusion, difficulty in surgery and may potentially precipitate complications [2]. In this study, we report a variation in the origin and course of the third common palmar digital artery (CPDA III).

Materials and Methods

The variations reported were observed during routine student dissections of the left upper limb of an adult formalin-fixed female cadaver of Caucasian descent. All dissections took place at the Department of Anatomy, Histology and Embryology, Medical University of Sofia.

Results and Discussion

The present case report describes a variation in the origin and course of the CPDA III. The SPA on the left hand existed as a closed arch as the radial artery gave a thin superficial palmar branch. From the lateral side of SPA emerged two CPDA – for the second and third web spaces. The CPDA III was initially well identified only in the distal part of the fourth interosseous space, giving rise to a pair of proper palmar digital arteries. Further dissection of SPA revealed a common trunk for the ulnar proper digital artery of the little finger and another small artery that goes deeper to the flexor tendons. Complete dissection of the deep palmar structures clarified the question rising about the origin of the CPDA III. It was revealed that the aforementioned deep artery from the SPA with a significant contribution from the terminal part of DPA gave the origin of the CPDA III. This atypical artery destined to the fourth web space was found to cross posterior to the flexor tendons of the little finger. After a short course the artery received the corresponding palmar metacarpal artery from the DPA and divided into the two proper palmar digital arteries.

According to Ikeda et al., in a cadaveric study involving 220 hands using angiography and anatomic dissections, the CPDA to the second and fourth web spaces were more frequently deficient and more commonly joint the palmar metacarpal arteries [3]. In our case report the CPDA III originated from both SPA and DPA. The contributing vessel from DPA was with bigger diameter than the one from SPA. This shows that in our case the DPA is the main blood supplier of the vascular territory of the CPDA III.

SPA may present large number of variable branching patterns [3] and some of them might put the blood flow at risk [4-6]. The variations in the origin and course of the arteries to the fourth web space are associated with atypical position of the vessel posterior to the flexor tendons of the little finger [2]. This anomaly can cause pressing of the third common palmar digital artery and Raynaud syndrome. These findings call for a careful systematic approach to the vessels during surgery consistently identifying them from proximal to distal and proceeding from known to unknown [6].

References

1. **Birch, A.** Section 6. Pectoral girdle and upper limb. – In *Gray's Anatomy: The anatomical basis of clinical practice* (Ed. S. Standring), 41st ed., Elsevier, 2016, 776-897.
2. **Hashem, A. M., R. W. Knackstedt, S. Bernard, M. Hendrickson, J. M. McBride, R. Djohan.** Variations in the origins and absence of the common digital arteries of the hand: a cadaveric study. – *J. Hand Surg. Eur.*, **43**, 2018, 1054-1058.
3. **Ikeda, A., A. Ugawa, Y. Kazihara, N. Hamada.** Arterial patterns in the hand based on a three-dimensional analysis of 220 cadaver hands. – *J. Hand. Surg. Am.*, **13**, 1988, 501-509.

4. **Kaneshiro, Y., N. Hidaka** Anatomical variations of the digital artery found in pollicization: a report of two cases. – *J. Hand. Surg. Eur.*, **35**, 2010, 757-758.
5. **Olinger, A.** Upper limb arteries. – In: *Bergman's Comprehensive Encyclopedia of Human Anatomic Variation* (Eds. R Shane Tubbs, M. M. Shoja, M. Loukas), Hoboken, New Jersey, Wiley Blackwell, 2016, 583–618.
6. **Ottone, N. E., N. Prum, M. Dominguez, E. Blasi, C. Medan, S. Shinzato, D. Finkelstein, V. H. Bertone.** Analysis and clinical importance of superficial arterial palmar irrigation and its variants over 86 cases. – *Int. J. Morphol.*, **28**, 2010, 157-164.

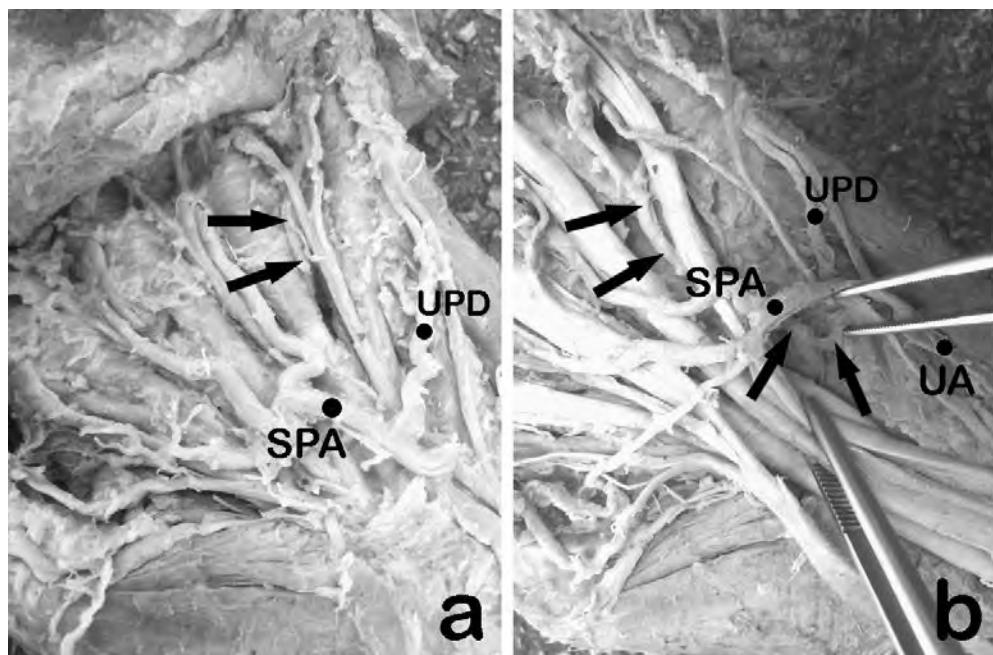


Fig. 1. Photographs of the initial (a) and further detailed dissection (b) of the cadaver's left palmar region showing the aberrant third common palmar digital artery (black arrows). Arteries: UA – ulnar artery; SPA – superficial palmar arch; UPD – ulnar proper digital artery of the little finger.

A Rare Variation of the Digastric Muscle Anterior Belly Related to False Submandibular Triangle

Albert Gradev, Nikoleta Vulova, Lazar Jelev, Lina Malinova*

Department of Anatomy, Histology and Embryology, Medical University of Sofia, Sofia, Bulgaria

*Corresponding author e-mail: a.gradev@medfac.mu-sofia.bg

In the case reported, an interesting variation of the left digastric muscle of an adult female cadaver was found during routine anatomical dissection of the anterior neck region. Additionally to the usual anterior and posterior bellies, there was a well-developed aberrant muscular slip starting from the digastric anterior belly and inserting to the inner surface of the mandibular angle in a manner nearly parallel to the posterior belly. This additional slip, together with the anterior belly and mandibular base enclosed a small but false submandibular triangle. The submandibular gland was displaced slightly posteriorly with the submandibular duct passing between the aberrant slip and the usual posterior belly.

The reported muscle variation may have importance in open surgical procedures in the neck region. Our case report provides an additional understanding of digastric muscle variations and their clinical significance.

Key words: digastric muscle, submandibular triangle, anatomical variation, cadaver

Introduction

The digastric muscle is an important landmark in the regional anatomy of the anterior neck. This muscle is composed of two bellies having different embryonic origin and nerve supply, which bellies are united by an intermediate tendon. The anterior belly is attached to the digastric fossa of the mandible and directs posteroinferiorly to the hyoid bone. The posterior belly extends from the mastoid notch and goes in a direction downward and anteriorly. The two bellies and the base of mandible enclose the submandibular triangle, also called digastric triangle, which is an important topographic region [8]. Variations of this muscle are common and can occur independently for anterior and posterior bellies. They can be classified as absence, additional heads, abnormal insertion and aberrant slips, each of them occurring uni- or bilaterally with different frequencies [4]. Several gross anatomy classifications of the digastric muscle variations exist in the literature. Mori classified them into seven

types [5] and De-Ary-Pires into thirteen types [2]. Kim and Loukas summarize the variations into twelve types in their review article [4].

In the further description we chose to follow Mori's classification.

Materials and Methods

The reported variation was observed during routine anatomical dissection of a 68-year-old formalin-fixed female cadaver of Caucasian descent. All dissections took place at the Department of Anatomy, Histology and Embryology, Medical University of Sofia.

Case report

After cutting and retracting successively the skin, platysma and investing fascial layer in the anterior neck region we revealed an interesting variation of the digastric muscle on the left side (**Fig. 1, A, B, C**). Trying to present the submandibular triangle and its content, a smaller than normal triangle, was identified at first. Following complete dissection revealed a well-developed aberrant muscular slip that mimic the usual posterior belly of digastric muscle. It was starting from the lateral side of digastric anterior belly, nearly 3 cm from the digastric fossa, and inserting to the inner surface of the mandibular angle in a manner nearly parallel to the posterior digastric belly. Thus the additional muscular slip, together with the anterior belly and mandibular base enclosed a small, but in fact false submandibular triangle being just a part of the usual one. All this unusual anatomy affects the position of the submandibular gland (**Fig. 1 asterisk**), which was displaced slightly posteriorly with the submandibular duct passing up between the aberrant slip and the usual posterior belly. On the right side (**Fig. 1 D**), the digastric muscle showed normal anatomy.

Discussion

Variations of the digastric anterior belly, existing in multiple types, are among the commonest muscle variations in human anatomy, with estimated frequency of 53.9% [5]. These variations have been described in details and summarized by several authors – Mori [5], De-Ary-Pires et al. [2], Hsiao and Chang [3] and Kim and Loukas [4]. Some differences exist between the classification systems proposed, in respect to the basic criteria used – origin and insertion, presence of additional slips or additional heads. Most commonly these muscle variations exist in the submental area and include additional slips and heads of variable directions, some of them crossing the midline, others – fusing with mylohyoid muscle [3, 6, 7, 10]. The variation reported by us corresponds to the rare Type 6 in Mori's classification – additional slips to the mandible, with a frequency of 1.1% [5]. Despite the data were collected by dissections of human cadavers of Asian descent, Mori claimed that there are no statistical racial differences. According to the same author, the only remarkable difference was higher complexity of the variations in Asians. In the classifications of other authors, our additional slip is not mentioned as a separate subtype. In De-

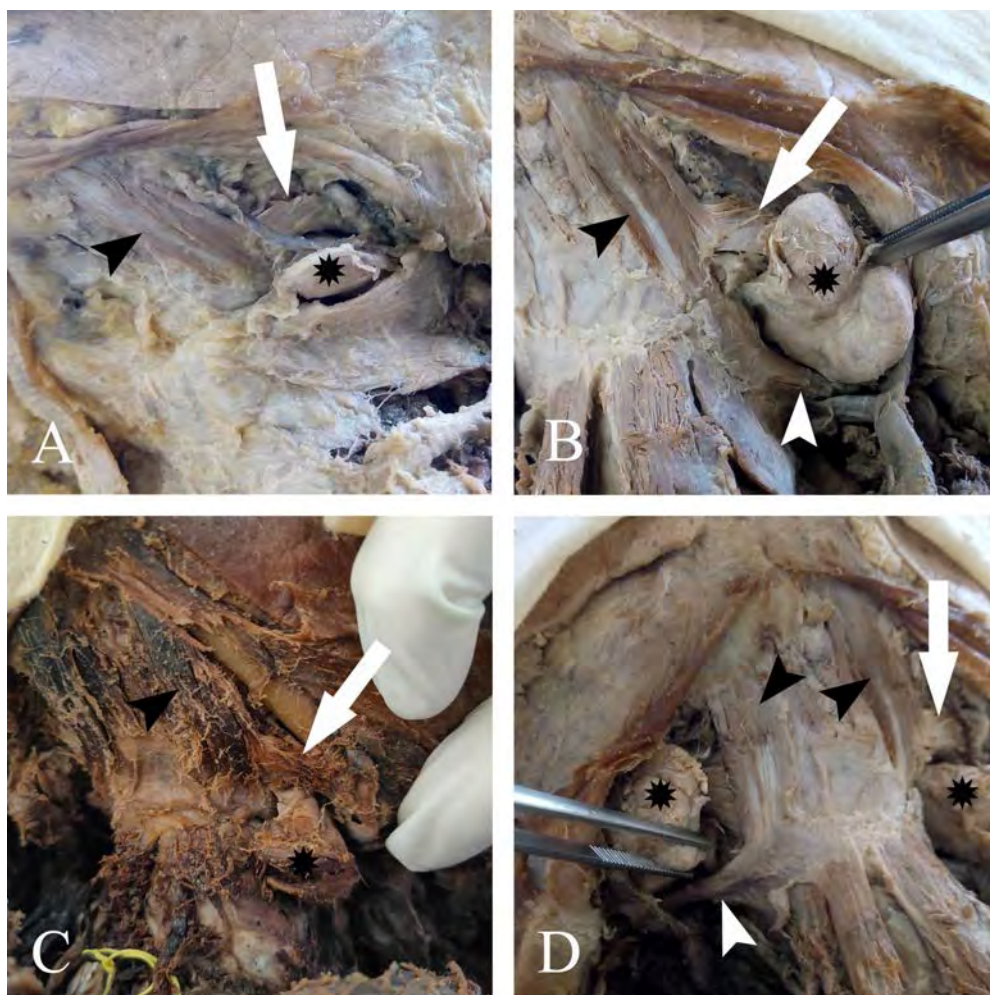


Fig. 1. Photographs of anterior neck region, on the left side (A, B, C) and on the right side (D): black arrowhead – anterior belly of digastric muscle; white arrowhead – posterior belly of digastric muscle; white arrow – aberrant muscular slip; asterisk – submandibular gland.

Ary-Pires classification [2] it can be put into Type 2 of anterior belly – two heads with additional slip to the mandible. Additionally, Kim and Loukas [4] analyzed the pertinent literature and presented a detailed reviewing table following De-Ary-Pires method, but a variation like ours is not included. Seems like in Caucasians the aberrant muscle bundle, reported here, has very low frequency. Despite rare, it may have clinical importance during open surgical dissection in the submandibular triangle because of mouth floor tumors and plastic surgical procedures. Moreover, in surgery the posterior belly can help in identifying accessory nerve, internal jugular vein, carotid arteries, and hypoglossal nerve, so it should not be missed with accessory

fascicles [9]. The anterior belly of the digastric is often included in submental flaps during facial reconstruction, as the submental vessels frequently courses deep to the muscle [1, 9].

Our case report provides an additional understanding of digastric muscle anatomical variations and their clinical significance, which should be well known by the surgical specialist working in neck region.

References

1. **Bertrand, B., C. S. Honeyman, A. Emparanza, M. McGurk, I. E. Ousmane Hamady, A. Schmidt, R. Sinna, B. Pittet-Cuénod, N. Zwetyenga, D. Martin.** Twenty-five years of experience with the submental flap in facial reconstruction: Evolution and technical refinements following 311 cases in Europe and Africa. – *Plast. Reconstr. Surg.*, **143(6)**, 2019, 1747-1758.
2. **De-Ary-Pires, B., R. Ary-Pires, M. A. Pires-Neto.** The human digastric muscle: patterns and variations with clinical and surgical correlations. – *Ann. Anat.*, **185**, 2003, 471-479.
3. **Hsiao, T. H., H. P. Chang.** Anatomical variations in the digastric muscle. – *Kaohsiung J. Med. Sci.*, **35(2)**, 2019, 83-86.
4. **Kim, S. D., M. Loukas.** Anatomy and variations of digastric muscle. – *Anat. Cell Biol.*, **52(1)**, 2019, 1-11.
5. **Mori, M.** Statistics on the musculature of Japanese. – *Okajimas Fol. Anat. Jap.*, **40**, 1964, 212-219.
6. **Ortug, G., B. Sipahi, A. Ortug, H. O. Ipsalali.** Variations of the digastric muscle and accessory bellies – A study of gross anatomic dissections. – *Morphologie*, **104(345)**, 2020, 125-132.
7. **Ozgur, Z., F. Govsa, T. Ozgur.** The cause of the difference in the submental region: aberrant muscle bundles of the anterior belly of the digastric muscle. – *J. Craniofac. Surg.*, **18(4)**, 2007, 875-881.
8. **Standring, S.** Gray's anatomy: the anatomical basis of clinical practice. – In: *Head and Neck* (Ed. M. Gleeson), 41st ed., London, Elsevier, 2016, 444-449.
9. **Tranchito, E. N., B. Bordonni.** *Anatomy, Head and Neck, Digastric Muscle*. StatPearls Publishing, 2022, Available at: <https://www.ncbi.nlm.nih.gov/books/NBK544352/>
10. **Turan-Ozdemir, S., I. H. Oygucu, I. M. Kafa.** Bilateral abnormal anterior bellies of digastric muscles. – *Anat. Sci. Int.*, **79(2)**, 2004, 95-97.

Functional Aspects of the Human Claustrum – Literary Review

Marin Kanarev^{1,2}, Nadezhda Petrova¹, Aneliya Petrova^{1,2}, Stefan Sivkov¹*

¹ *Department of Anatomy, histology and embriology, Medical Faculty, Medical University Plovdiv, Plovdiv, Bulgaria*

² *Medical Oncology Ward at MHAT Park Hospital, Plovdiv, Bulgaria*

*Corresponding author e-mail: Marin.Kanarev@mu-plovdiv.bg

The claustrum is an irregular and fine sheet of grey matter in the basolateral telencephalon present in almost all mammals. The claustrum is separated laterally from the insular cortex by the extreme capsule and medially from the lentiform nucleus by the external capsule. It has been the object of many studies using animal models and more recently in humans using neuroimaging. The claustrum has been involved in cognition and disease such as fear recognition, suppression of natural urges, multisensory integration, conceptual integration, seizures, multiple sclerosis. Nevertheless, the function of the claustrum still remains unclear. We aim to summarize the various scientific reports present in the literature regarding the structural and functional connectivity of the human claustrum using neuroimaging.

Key words: claustrum, functional connectivity, multisensory integration, relevant stimuli

Introduction

The claustrum is an anatomical structure enjoying high academic interest in the last decades due to its enigmatic role despite being anatomically described for a couple of centuries and hypothetically associated with a wide variety of functions or aspects of such in the scientific literature. In the last scientific work of Crick and Koch in 2005 [3], the idea developed that the claustrum plays a central role in consciousness and since then with the development of more precise scientific investigational methods and technology new data have accumulated regarding its anatomical connections and physiological properties. Out of all conducted research many widespread connections to all areas of the cerebral cortex and subcortical structures which suggests a role in the higher neurological functions and supports the Crick and Koch hypothesis. Due to extensive connections with the frontal cortex, a possible role for the guidance of executive functions and higher neurological functions including some aspects of

consciousness has emerged. Among them specific roles in the processing of salient stimuli and the fixation of attention stand out.

Literary review

Functional MRI (Magnetic resonance imaging) assays have provided evidence for simultaneous activation of the claustrum and different cortical zones such and subcortical structures such as frontal cortex, insula (evaluating stimuli), anterior cingulate cortex (controlling attention), thalamus in the different investigational paradigms.

Histologically in humans the structure consists like the neocortex of spiny projection neurons and aspiny interneurons. All of them can be stratified according to the expression of different peptides like parvalbumin, VIP (vasoactive intestinal polypeptide), somatostatin, neuropeptide Y and others. This expression being specific for different neuronal populations aids in specifying the embryogenesis of the claustrum. This is a contested field due to the intimate position of the structure between the putamen and the insular cortex and near the amygdaloid complex. After a 100-year debate in the scientific literature for the possible origin of the cell populations of the claustrum, the hypothesis prevails that they come from the ventrolateral dorsal pallium formed in the dorsal migratory stream from where it spreads out in the lateral pallium. As a result from over 40 years of anatomical tracer studies vast reciprocal connections with almost all parts of the cerebral cortex are observed. The most dense ones are with the frontal cortex while the ones with the sensory areas are less pronounced. The claustrum-cortical connections are topographically organized on the dorso-ventral axis of the claustrum, forming modules with the different cortical areas specific for different modalities [2]. Thus a tendency is observed that cortical areas that share cortico-claustral connections also share connections from the same claustral area through claustral neurons that send out branching axonal collaterals innervating simultaneously both cortical areas. Research shows that claustral neurons have axons that branch out extensively in many cortical areas including in the contralateral hemisphere. Another interesting aspect of the cortico-claustral and claustrum-cortical connections is their tendency to synapse more on interneurons which constructs a reciprocal antegrade inhibitory neuronal net. Apart from the cortical connections of the claustrum, its one-way afferent connections from many subcortical structures have also been observed. These subcortical structures belong to the limbic system like the basolateral amygdala, hippocampus, intralaminar thalamic nuclei and others. The claustrum also receives many neuromodulatory afferences from the basal cholinergic brain centers like the substantia innominata and from the serotonergic brain centers like the dorsal raphe nucleus as well as from the dopaminergic brain centers. These limbic and neuromodulatory afferent connections to the claustrum through its different areas can help in activating or suppressing the excitability of large efferent claustral neuronal nets.

Despite research in the last 10-15 years forming and clarifying our understanding of the different aspects of this brain structure, the claustrum continues to be associated with a wide variety of functions without an evident key one. For example, in spite of possibly not being the only area serving as the seat of consciousness as some scientist postulate, evidence shows that the claustrum plays a role in the processing and electing of salient stimuli and the guiding of attention – functions, pertaining

to the state of increased vigilance and markers of consciousness [6,7]. On the other hand, the involvement of the claustrum in modulating the cortical activeness during sleep has also been proven [4]. A possible conclusion which emerges, considering the connection of these functions with the limbic system is the role of the claustrum in integrating limbic-associated information with sensory and motor cortical areas. This is supported by its position and the observed vast connections with all cortical areas. Thus a hypothesis emerges that the claustrum is a center for associating sensory and limbic information and direct influence over attention through the frontal cortex and control of executive functions [1]. Functionally this allows the claustrum to recognize the contextual significance of a stimulus in order to guide correctly the attention and coordinate cortex activeness, directing the focus on situationally relevant stimuli. A possible mechanism through which the claustrum can accomplish this is activating of cortical interneurons which leads to antegrade inhibiting and suppressing of cortical activity to non-relevant stimuli. The role of this structure in slow-wave sleep can aid in consolidating the learned information, which is associated with relevant stimuli.

Conclusion

In conclusion, the claustrum is a highly connected brain structure hard to study due to its anatomical location and irregular form. Neuroimaging offers a powerful tool to explore its function non-invasively. The claustrum literature – including studies in animal model and in humans – has evidenced the vast anatomical connections between the claustrum and the entire cerebral cortex as well as with the subcortical structures. This helped to characterize the functional connectivity of the human claustrum, which mainly includes positive relations with insular, frontal, temporal and cingulate cortex. These findings evidence the close relationship of the claustrum with the salience network, strongly supporting its proposed role to mediate the salience value of sensory stimuli [5,8]. It has been suggested that the claustrum is central in the integration of information from multiple cortical regions into a coherent whole [3], while others have speculated that it may be central to detecting and prioritizing important external stimuli.

References

1. **Barrett, F. S., S. R. Krimmel, R. R. Griffiths, D. A. Seminowicz, B. N. Mathur.** Psilocybin acutely alters the functional connectivity of the claustrum with brain networks that support perception, memory, and attention. – *NeuroImage*, **218**, 2020, 116980.
2. **Chia, Z., G. Silberberg, G. J. Augustine.** Functional properties, topological organization and sexual dimorphism of claustrum neurons projecting to anterior cingulate cortex. – *Clastrum*, **2**, 2017, 1357412.
3. **Crick, F. C., C. Koch.** What is the function of the claustrum? – *Philos. Trans. R. Soc. Lond. B. Biol. Sci.*, **360**, 2005, 1271-1279.
4. **Jerram, M., S. Bates.** Meta-analysis of fMRI reveals role of claustrum in dissociation. Conference: Cognitive Neuroscience Society, Boston, MA, April 2014.
5. **Kavounoudias, A., J. P. Roll, J. L. Anton, B. Nazarian, M. Roth, R. Roll.** Proprio-tactile integration for kinesthetic perception: An fMRI study. – *Neuropsychologia*, **46**, 2008, 567-575.

6. **Krimmel, S. R., M. G. Whiteb, M. H. Panickerc, F. S. Barrettd, B. N. Mathurc, D. A. Seminowicz.** Resting state functional connectivity and cognitive task-related activation of the human claustrum. – *Neuroimage*, **196**, 2019, 59-67.
7. **Naghavi, H. R., J. Eriksson, A. Larsson, L. Nyberg.** The claustrum/insula region integrates conceptually related sounds and pictures. – *Neuroscience Letters*, **422** (2007), 77–80.
8. **Smith Jared B., Glenn D. R. Watson, Zhifeng Liang, Yikang Liu, Nanyin Zhang, and Kevin D. Alloway.** A role for the claustrum in salience processing. – *Frontiers in Neuroanatomy*, **13**, 2019.

Author Guidelines

Acta Morphologica et Anthropologica is an open access peer review journal published by Bulgarian Academy of Sciences, Prof. Marin Drinov Publishing House.

Corporate contributors are Bulgarian Academy of Sciences, Institute of Experimental Morphology, Pathology and Anthropology with Museum and Bulgarian Anatomical Society.

Acta Morphologica et Anthropologica is published in English, 4 issues per year.

The journal accepts manuscripts in the following **fields**: experimental morphology, cell biology and pathology, anatomy and anthropology.

Publication types: original articles, short communications, case reports, reviews, Editorial, letters to the Editors.

Acta Morphologica et Anthropologica is the continuation of *Acta cytobiologica et morphologica*

The **aim** of the Journal is to disseminate current interdisciplinary biomedical research and to provide a forum for sharing new scientific knowledge and methodology. The general editorial policy is to optimize the process of issuing and distribution of *Acta morphologica et anthropologica* in line with modern standards for scientific periodicals focusing on content, form, and function.

Scope—experimental morphology, cell biology and pathology (neurobiology, immunobiology, tumor biology, environmental biology, reproductive biology, etc.), new methods, anatomy and pathological anatomy, anthropology and paleoanthropology, medical anthropology and physical development.

Acta Morphologica et Anthropologica is published twice a year as one volume with 4 issues. For the first two issues (1-2) the deadline for manuscript submission is March 15th and for the next two issues (3-4), the deadline is September 15th. Electronic version for issues 1-2 is uploaded on the website till June 30th and for issues 3-4 – till December 30th.

Contact details and submission

Manuscript submission is electronical only. The manuscripts should be sent to the Managing Editor's e-mail address ygluhcheva@hotmail.com with copy to iempam@bas.bg

All correspondence, including notification for Editor's decision, requests for revision, is sent by e-mail.

Article structure

Manuscripts should be in English with total length not exceeding 10 standard pages, line-spacing 1.5, justified with 2.5 cm margins. The authors are advised to use Microsoft Word 97-2003, Times New Roman, 12 pt throughout the text. Pages should be numbered at the bottom right corner of the page.

The article should be arranged under the following headings: Introduction, Material and Methods, Results, Discussion, Conclusion, Acknowledgements and References.

Title page – includes:

- **Title** – concise and informative;
- **Author(s)' names and affiliations** – indicate the given name(s) and family name(s) of all authors. Present the authors' affiliation addresses below the names. Indicate all affiliations with a lower-case superscript after the author's name and in front of the appropriate address. Provide the full postal address information for each affiliation, including the country name.
- **Corresponding author** – clearly indicate who will handle the correspondence for refereeing, publication and post-publication. An e-mail should be provided.
- **Abstract** – state briefly the aim of the work, the principal results and major conclusions and should not exceed 150 words. References and uncommon, or non-standard abbreviations should be avoided.
- **Key words** – provide up to 5 key words. Avoid general, plural and multiple concepts. The key words will be used for indexing purposes.

Introduction – state the objectives of the work and provide an adequate background, avoiding a detailed literature survey or summary of the results.

Material and Methods – provide sufficient detail to allow the work to be reproduced. Methods already published should be indicated as a reference: only relevant modifications should be described.

Results – results should be clear and concise.

Discussion – should explore the significance of the results in the work, not repeat them. A combined *Results and Discussion* section is often appropriate. Avoid extensive citation and discussion of published literature.

Conclusions – the main conclusions of the study should be presented in a short section.

Acknowledgements – list here those individuals who provided help during the research and the funding sources.

Units – please use the International System of Units (SI).

Math formulae – please submit math equations as editable text, not as images.

Electronic artwork – number the tables and illustrations according to their sequence in the text. Provide captions for them on a separate page at the end of the manuscript. The proper place of each figure in the text should be indicated in the left margin of the corresponding page. **All illustrations (photos, graphs and diagrams)** should be referred to as “figures” and given in abbreviation “Fig.”, and numbered in Arabic numerals in order of its mentioning in the manuscript. They should be provided in grayscale as JPEG or TIFF format, minimum 300 dpi. The illustrations should be submitted as separate files.

References – they should be listed in alphabetical order, indicated in the text by giving the corresponding numbers in parentheses. The “References” should be typed on a separate sheet. The names of authors should be arranged alphabetically according to family names. In the reference list titles of works, published in languages other than English, should be translated, original language must be indicated at the end of reference (e.g., [in Bulgarian]). Articles

should include the name(s) of author(s), followed by the full title of the article or book cited, the standard abbreviation of the journal (according to British Union Catalogue), the volume number, the year of publication and the pages cited, for books – the city of publication and publisher. In case of more than one author, the initials of the second, third, etc. authors precede their family names. Ideally, the names of all authors should be provided, but the usage of “et al” after the fifth author in long author lists will also be accepted.

For articles: **Davidoff, M. S., R. Middendorff, G. Enikolopov, D. Riethmacher, A. F. Holstein, D. Muller.** Progenitor cells of the testosterone-producing Leydig cells revealed. – *J. Cell Biol.*, **167**, 2004, 935-944.

Book article or chapter: **Rodriguez, C. M., J. L. Kirby, B. T. Hinton.** The development of the epididymis. - In: *The Epididymis - from molecules to clinical practice* (Eds. B. Robaire, B. T. Hinton), New York, Kluwer Academic Plenum Publisher, 2002, 251-269.

Electronic books: **Gray, H.** *Anatomy of the human body* (Ed. W.H.Lewis), 20th edition, NY, 2000. Available at <http://www.Bartleby.com>.

PhD thesis: **Padberg, G.** Facioscapulohumeral diseases. *PhD thesis*, Leiden University, 1982, 130 p.

Website: National survey schoolchildren report. National Centre of Public Health and Analyses, 2014. Available at <http://ncphp.government.bg/files>

Page charges

Manuscript publication is free of charges.

Ethics in publishing

Before sending the manuscript the authors must make sure that it meets the Ethical guidelines for journal publication of *Acta morphologica et anthropologica*.

Human and animal rights

If the work involves the use of human subjects, the authors should ensure that work has been carried out in accordance with *The Code of Ethics of the World Medical Association* (Declaration of Helsinki). The authors should include a statement in the manuscript that informed consent was obtained for experimentation with human subjects. The privacy rights of human subjects must always be observed.

All animal experiments should comply with the *ARRIVE guidelines* and should be carried out in accordance with the U.K. Animals (Scientific procedures) Act, 1986 and the associated guidelines *EU Directive 2010/63/EU* for animal experiments, or the National Institutes of Health guide for the care and use of Laboratory animals (NIH Publications No. 8023, revised 1978) and the authors should clearly indicate in the manuscript that such guidelines have been followed.

Submission Details

Acta morphologica et anthropologica is published twice a year as one volume with 4 issues. For the first two issues (1-2) the deadline for manuscript submission is March 15th and for the next two issues (3-4), the deadline is September 15th. Electronic version for issues 1-2 is uploaded on the website till June 30th and for issues 3-4 – till December 30th.

Manuscript submission is electronical only.

The manuscripts should be sent to the Managing Editor email address ygluhcheva@hotmail.com with copy to iempam@bas.bg

All correspondence, including notification for Editor's decision, requests for revision, is sent by e-mail.

Submission declaration

Submission of the manuscript implies that the work described has not been published previously, is not considered under publication elsewhere, that its publication is approved by all authors, and that if accepted, it will not be published elsewhere in the same form, in English or in any other language, including electronically, without the informed consent of the copyright-holder.

Contributors

The statement that all authors approve the final article should be included in the disclosure.

Copyright

http://www.iempam.bas.bg/journals/acta/Author%20Copyright%20Agreement_last.pdf

Upon acceptance of an article, the authors will be asked to complete a “**Copyright Transfer Agreement**”.

http://www.iempam.bas.bg/journals/acta/Copyright_Transfer_Agreement_Form_AMA.doc

Peer review

Once a manuscript is submitted, the Managing Editor (or the Editor-in-Chief) briefly checks the manuscript for conformance with the journal's Focus, Scope, Policies and style requirements and decide whether it is potentially suitable for publication and can be processed for review, or rejected immediately, or returned to the author for improvement and re-submission.

Manuscripts are peer-reviewed by the Editors, Editorial Board members, and/or external experts before final decisions regarding publication are made. The entire editorial workflow is performed in the following steps:

1. The submitted manuscript is checked in the editorial office whether it is suitable to go through the normal peer review process.
2. If deemed suitable, the manuscript is sent to 2 reviewers for peer-review. The choice of reviewers depends on the subject of the manuscript, the areas of expertise of the reviewers, and their availability.
3. Each reviewer will have 2 weeks to provide evaluation of the manuscript. The Editor may recommend publication, request minor, moderate or major revision, or provide a written critique of why the manuscript should not be published (rejected).
4. In case only one reviewer suggests rejection of the manuscript, the latter is subjected to additional evaluation by a third reviewer.
5. The manuscript will be published in a revised form provided that the authors successfully answer the critics received. The Editor-in-Chief is the final authority on all editorial decisions.

Open Access

This journal provides immediate open access to its content on the principle that making research freely available to the public supports a greater global exchange of knowledge.

After acceptance**Proof correction**

The corresponding author will receive proofs by e-mail in PDF format and will be requested to return it with any corrections within two weeks.

ISSN 1311-8773 (print)

ISSN 2535-0811 (online)

